

QUANTITATIVE DETECTION OF CIRCULATING EMBOLIC MATERIALS WITH DOPPLER ULTRASOUND

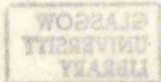
by

Yi Yang

This being a thesis submitted for the degree of
Doctor of Philosophy in the Faculty of Medicine
of the University of Glasgow

Department of Medicine
and Therapeutics
November 1995

© Y. Yang



ProQuest Number: 13832540

All rights reserved

INFORMATION TO ALL USERS

The quality of this reproduction is dependent upon the quality of the copy submitted.

In the unlikely event that the author did not send a complete manuscript and there are missing pages, these will be noted. Also, if material had to be removed, a note will indicate the deletion.



ProQuest 13832540

Published by ProQuest LLC (2019). Copyright of the Dissertation is held by the Author.

All rights reserved.

This work is protected against unauthorized copying under Title 17, United States Code
Microform Edition © ProQuest LLC.

ProQuest LLC.
789 East Eisenhower Parkway
P.O. Box 1346
Ann Arbor, MI 48106 – 1346

<u>LIST OF CONTENTS</u>	<u>Page N°</u>
ACKNOWLEDGEMENTS	i
DECLARATION	ii
LIST OF FIGURES	iii
LIST OF TABLES	vi
SUMMARY	vii
CHAPTER ONE - GENERAL INTRODUCTION	1
1. Introduction	2
1.1 Acute stroke and cerebral embolism	2
1.2 Cerebral emboli	2
1.2.1 Macroemboli and microemboli	2
1.2.2 Gaseous emboli	3
1.2.3 Solid embolism	5
A. Solid emboli from cardiac source	5
B. Solid emboli from internal carotid artery source	5
C. Fat emboli	6
D. Cholesterol crystal emboli	7
1.3 Principles of ultrasound and Doppler ultrasonography	8
1.3.1 Physical features of ultrasound	8
1.3.2 Reflection at interface of two media	9
1.3.3 Acoustic impedance	10
1.3.4 Doppler effect	10

	<u>Page N°</u>
1.3.5 Intensity of Doppler ultrasound signal	12
1.3.6 Attenuation	13
1.3.7 Transcranial Doppler ultrasonography (TCD)	14
1.4 Identification of embolus materials	15
1.4.1 Identification of embolus material using non-ultrasound techniques	15
1.4.2 Differentiation from artifact using transcranial Doppler ultrasonography	16
1.4.3 Detection of extracranial emboli with Doppler ultrasound	18
1.4.4 Detection of intracranial emboli with Transcranial Doppler ultrasonography	19
1.5 Clinical applications of TCD in detection of cerebral emboli	20
1.5.1 Small infarcts	20
1.5.2 Differentiation of emboli from haemodynamic transient ischaemic attack (TIA)	20
1.5.3 Intraoperative monitoring	21
1.5.4 Other clinical applications	22
1.6 Experimental models for characterizing, counting, and sizing emboli	23
1.6.1 Models for characterizing emboli	23
1.6.2 Models for counting and sizing emboli	24
1.6.3 Investigation of the factors affecting quantification of embolic signal	25

	<u>Page N°</u>
1.7 Aims of this study	25
CHAPTER TWO - GENERAL MATERIALS AND METHODS	30
2.1 Definition of embolic signal	31
2.2 Design of the model simulating the middle cerebral artery (MCA) and preparation of circulating materials	31
2.2.1 The MCA model	31
2.2.2 Circulating materials	32
1. 0.03 Sigmacell solution	32
2. Red blood cell (RBC) concentrate	32
3. Human whole blood	32
2.3 Doppler ultrasound equipment and off-line analysis	32
2.3.1 Doppler ultrasound equipment	33
2.3.2 Off-line analysis	33
2.4 Preparation of embolic materials	34
2.4.1 Preparation of whole blood clots	34
2.4.2 Preparation of platelet-rich thrombus	34
2.4.3 Preparation of platelet aggregate-rich plasma	35
2.4.4 Preparation of human atheromatous emboli	35
2.4.5 Preparation of microbubbles	35
2.4.6 Preparation of fat globule emboli	36
2.4.7 Preparation of cholesterol crystal emboli	36
2.5 Measurement of embolic materials	37
2.6 Data analysis	37

3.2.2 Microscopic examinations

CHAPTER THREE - QUANTITATIVE STUDY OF THE INTENSITY OF DOPPLER SIGNALS FROM MICROBUBBLES INTRODUCED INTO A CIRCULATING MODEL	42
3.1 Introduction	43
3.1.1 Microbubbles and gaseous cerebral embolism	43
3.1.2 Ultrasound detection of microbubbles	43
3.1.3 The models to detect air microemboli	44
3.1.4 Preparation of embolic materials	45
3.1.5 Aims	46
3.2 Materials and methods	46
3.2.1 The middle cerebral artery (MCA) <i>in vitro</i> model	46
3.2.2 Microscopic study of microbubbles	47
3.2.3 Microbubble preparation	47
3.2.4 Investigation of the relationship between signal intensity and the number of microbubbles	47
3.2.5 Investigation of the effect of bubble concentration on signal intensity	48
3.2.6 Analysis of Doppler signal intensity of microbubbles	49
3.2.7 Preparation of different sizes and concentrations of microbubbles in Ultravist 370	50
3.2.8 Statistical analysis	50
3.3 Results	50
3.3.1 Doppler signals produced on the MCA model	50

	<u>Page N°</u>
3.3.2 Microscopic examinations	51
3.3.3 Relation between signal intensity and the number of microbubbles	77 51
3.3.4 Effect of concentration of microbubbles on the signal intensity	51
3.3.5 Establishment of the microbubble preparation techniques	52
3.4 Discussion	53
4.2.6 TCD recording and off-line study	77
CHAPTER FOUR - QUANTITATIVE CHARACTERISATION OF TCD SIGNALS FROM DIFFERENT KINDS OF MICROEMBOLI IN A CIRCULATION MODEL	71
4.3 Results	73
4.1 Introduction	72
4.1.1 Embolic materials related to cerebral embolism	72
4.1.2 Detection of circulating emboli with Doppler ultrasound	73
4.1.3 Sizing and differentiating embolic materials with Doppler ultrasound	73
4.1.4 Aims	74
4.2 Materials and methods	75
4.2.1 The MCA model and the circulation system	75
4.2.2 Preparation of different embolic materials	75
(1) Air bubble emboli	76
(2) Rabbit whole blood emboli	76
(3) Rabbit fat globule emboli	76
(4) cholesterol crystal emboli	76
(5) Human whole blood clots	77

	<u>Page N°</u>
3.1.1 Echocardiographic 'smoke' and cardiac emboli	77
3.1.2 (6) Human atheromatous material	77
(7) Platelet-rich thrombus	77
4.2.3 Measurement of embolic materials	77
4.2.3 Injection of emboli	77
4.2.5 Relating <i>in vitro</i> data to <i>in vivo</i> recordings	77
4.2.6 TCD recording and off-line study	77
4.2.7 Statistical analysis	78
4.3 Results	78
4.3.1 The ability of TCD to detect different embolic's materials	78
4.3.2 Comparison of embolic signal intensities (mutiple emboli)	79
4.3.2 (1) Microbubbles vs. rabbit fat globules	79
(2) Rabbit whole blood clots vs. cholesterol crystals	79
4.3.3 Comparison of embolic signal intensities (single-emboli)	79
4.3.4 Relation between embolic signal intensity and the size of embolic materials	80
4.3.5 Characterisation of different embolic materials using embolic signal intensity	80
4.3.6 Relating <i>in vitro</i> data to <i>in vivo</i> recordings	80
4.4 Discussion	80
CHAPTER FIVE - IDENTIFICATION OF ECHOCARDIOGRAPHIC 'SMOKE' IN A BENCH MODEL WITH TRANSCRANIAL DOPPLER ULTRASOUND	94
5.1 Introduction	95

	<u>Page N^o</u>
5.1.1 Echocardiographic 'smoke' and cardiac emboli	95
5.1.2 Identification of determinants of the echocardiographic	100
5.1.3 'smoke' phenomenon	95
5.1.3 Haemorrhologic factors in the formation of the	101
5.1.3 echocardiographic 'smoke' phenomenon	96
5.1.4 Aims	97
5.2 Materials and methods	97
5.2.1 Definition of spontaneous contrast	97
5.2.2 <i>In vitro</i> models for the reproduction of smoke-like echoes	97
5.2.2 and TCD evaluation	97
5.2.3 Ultrasonic signal recording and off-line study	98
5.2.4 TCD detection during smoke-like echoes appearance	98
5.2.5 Preparation and injection of embolic materials	98
5.2.5 (1) Whole blood clots	98
5.2.5 (2) Platelet aggregate-rich plasma	99
5.2.5 (3) Air bubbles	99
5.2.5 (4) Degassed normal saline	99
5.2.6 Correlation of smoke-like echo with Doppler flow velocity	99
5.2.7 Investigation of the role of 'smoke' state in thrombus formation	99
5.2.8 Statistical analysis	100
5.3 Results	100
5.3.1 RBC and HCT	100
5.3.2 Reproduction of smoke-like echoes	100

	<u>Page N°</u>
5.3.3 TCD examination of smoke-like echoes at post-stenosis	100
5.3.4 Injection of embolic particles and normal saline	101
5.3.5 Correlation of smoke-like echo with Doppler velocity	101
5.3.6 Smoke-like echoes and thrombus formation	101
5.4 Discussion	102
6.3 Results	126
CHAPTER SIX - ULTRASONIC QUANTIFICATION OF TURBULENCE AND DIFFERENTIATION OF EMBOLIC SIGNALS	117
6.1 Introduction	118
6.1.1 Definition of turbulence flow	118
6.1.2 Turbulence and vessel stenosis	118
6.1.3 Detection of turbulence with Doppler ultrasound technique	118
6.1.4 Turbulence flow and cerebral embolism	120
6.1.5 Aims	120
6.2 Materials and methods	121
6.2.1 Reproduction of turbulent flow in the MCA stenosis model	121
6.2.2 The Degree of stenosis and the turbulence	121
6.2.3 Preparation and injection of embolic materials	123
CHAPTER SEVEN - EFFECT OF TRANSMITTING ULTRASONIC QUANTIFICATION OF EMBOLI IN ANIMAL	142
1.) Comparison of average signal intensity in different sample positions	124
2.) Correlation between the degree of stenosis and average	143

6.2.4	signal intensity or mean flow velocity at post-stenosis I position	124
6.2.5	3.) Comparison of the total signal intensity of turbulence with that of emboli	125
6.2.5	Statistical analysis	125
6.3	Results	126
6.3.1	Turbulence flow in different sample positions	126
6.3.2	The relationship between the turbulence and the degree of stenosis of artery	126
	1.) Turbulence and the degree of stenosis	126
	2.) Average signal intensity and the degree of stenosis	127
	3.) Mean flow velocity and the degree of stenosis	127
6.3.3	Comparison of turbulence signal with embolic signals	127
	1.) Visual comparison	127
	2.) Comparison of total signal intensity of turbulence with that of embolic signals	127
6.4	Discussion	128
	2.) Embolic signal intensity	146
CHAPTER SEVEN - EFFECT OF TRANSMITTING FREQUENCY AND FLOW VELOCITY ON ULTRASONIC QUANTIFICATION OF EMBOLI IN AN <i>IN VITRO</i> MODEL		147
7.1	Introduction	143
7.1.1	Detection of emboli with Doppler ultrasonography	143

7.1.2	Detection of intracranial emboli with transcranial Doppler ultrasonography	147
7.1.3	Effect of transmitting frequency and flow velocity on the quantification of embolic signal	143
7.1.4	Aims	144
7.2	Materials and methods	144
7.2.1	<i>In vitro</i> models	144
	1.) A model for investigation of the effect of alteration in the velocity of flow	144
	2.) A model for investigation of the effect of alteration in the transmitting frequency of Doppler	144
7.2.2	Preparation and injection of emboli	145
7.2.3	Ultrasound Doppler equipment and off-line analysis	145
7.2.4	Statistical analysis	146
7.3	Results	146
7.3.1	Alteration of flow velocity	146
	1.) Average signal intensity of flow waveform	146
	2.) Embolic signal intensity	146
	3.) Embolic signal duration	147
7.3.2	Alteration of Doppler transmitting frequency	147
	1.) Average signal intensity of flow waveform	147
	2.) Embolic signal intensity	147

	<u>Page N°</u>
3.) Emboli signal duration analysis	147
4.2.3 Statistical analysis	165
5.3 Results	166
7.3.3 Precision of repeated measurement of embolic signals	147
7.4 Discussion of studies	148
8.3.3 Relation studies	168
CHAPTER EIGHT - ULTRASOUND DETECTION OF EMBOLI IN THE MIDDLE CEREBRAL ARTERY DURING CARDIAC CATHERISATION	159
8.1 Introduction	160
8.1.1 Cardiac catheterisation and its complications	160
8.1.2 Air embolism and catheterisation	161
8.1.3 Atheromatous embolism and catheterisation	161
8.1.4 Ultrasonic detection of emboli during catheterisation	162
8.1.5 Aims	162
8.2 Methods	163
8.2.1 Human studies	164
1.) Patient's information	164
2.) Cardiac catheterisation	164
3.) TCD monitoring	164
8.2.2 Experimental study	165
1.) Study of the increased signal intensity of air bubbles, atheromatous material, and contrast medium in an <i>in vitro</i> model	165

ACKNOWLEDGEMENTS

	<u>Page N^o</u>
I would like to thank Professor John L. Reid and Dr. Kennedy R. Lees, firstly, for	
2.) Off-line Doppler signal analysis	165
allowing me to study in this Department providing me with such an excellent training	
8.2.3 Statistical analysis	165
in medical research and, secondly, for their help and encouragement with this project	
8.3 Results	166
8.3.1 Human studies	166
I am indebted to Dr. Donald G. Grosset for his invaluable supervision and advice	
8.3.2 Experimental studies	167
throughout the course of the studies undertaken for this thesis.	
8.3.3 Relation studies	168
8.4 Discussion	168

I would also like to express my gratitude to Dr. Andrew Kelman for his technical help and Ms. Kate Howie for her suggestions on statistics. I could not forget Dr. Caroline

CHAPTER NINE - GENERAL DISCUSSION AND

Hamilton who supplied a work place in her lab where most of my study has been done, Ms. Joan Kemp who kindly assisted me on computing, and Dr. Stewart Hill

CONCLUSIONS 180

9.1 General discussion 181

9.2 Conclusions 185

Reid in reference source research are also gratefully acknowledged. I also thank

appreciated the kind assistance of the secretaries in the department, who were always

PRESENTATIONS AND PUBLICATIONS CONTAINING THE WORK UNDERTAKEN FOR THIS THESIS

187

REFERENCES 188

Finally, special thanks are given to my family - my wife, Qiu Li and my son, Wangang

Yang, and my parents and sisters for their constant support and encouragement

throughout the experiment and paperwork of this thesis.

ACKNOWLEDGEMENTS

I would like to thank Professor John L. Reid and Dr. Kennedy R. Lees, firstly, for allowing me to study in this Department providing me with such an excellent training in medical research and, secondly, for their help and encouragement with this project.

I am indebted to Dr. Donald G. Grosset for his invaluable supervision and advice throughout the course of the studies undertaken for this thesis.

I would also like to express my gratitude to Dr. Andrew Kelman for his technical help and Ms. Kate Howie for her suggestions on statistics. I could not forget Dr. Carlene Hamilton who supplied a work place in her lab where most of my study has been done, Ms. Joan Kemp who kindly assisted me on computing, and Dr Stewart Hillis for assistance with cardiac catheterisation studies. The friendly help from Mrs. Randa Reid in reference source research are also gratefully acknowledged. I also highly appreciated the kind assistance of the secretaries in the department, who were always helpful beyond the call of duty.

Finally, special thanks are given to my family - my wife, Qiu Li and my son, Wangang Yang, and my parents and sisters for their constant support and encouragement throughout the experiment and paperwork of this thesis.

DECLARATION

Page 27

I declare that this thesis has been composed by myself and is a record of work performed by myself. It has not been submitted previously for a higher degree.

This research was carried out in the Department of Medicine and Therapeutics, University of Glasgow under the supervision of Dr. D.G. Grosset, Dr. K.R. Lees and Professor J.L. Reid.

Figure 2.1 - Illumination of the MCA model and circuit	38
Figure 2.2 - Diagrammatic procedure of Doppler signal intensity analysis	39
Figure 2.3 - Diagrammatic illumination of the agitation chamber	40
Figure 2.4 - Diagrammatic illumination of the size-control set	41
CHAPTER THREE	
Figure 3.1 - Doppler signatures collected from <i>in vitro</i> and <i>in vivo</i>	60
Figure 3.2 - Frequency histogram of microbubble size in Ultravist 370	62
Figure 3.3 - Frequency histogram of microbubble size in 5% albumin solution	63
Figure 3.4 - Study of the half lives of microbubbles	64
Figure 3.5 - Correlation of Doppler signal intensity of microbubbles	65
Figure 3.6 - Effect of different concentrations of microbubbles on Doppler signal intensity	67
Figure 3.7 - The effect of concentration of microbubbles on Doppler signal intensity	68
Figure 3.8 - Effect on bubble size of changing power	69
Figure 3.9 - Effect of changing power on bubble concentration	70
Figure 3.10 - Effect of changing agitation time on microbubble size	71
Figure 3.11 - Effect of changing agitation time on microbubble concentration	72
Figure 3.12 - Effect of dilution of Ultravist 370 on microbubble size	73

Yi Yang
November, 1995

LIST OF FIGURES

	<u>Pages N°</u>
CHAPTER ONE	
Figure 1.1 - Longitudinal ultrasound wave motion	27
Figure 1.2 - The Doppler effect	28
Figure 1.3 - Two behaviours of ultrasound reflection	29
CHAPTER TWO	
Figure 2.1 - Illumination of the MCA model and circuit	38
Figure 2.2 - Diagrammatic procedure of Doppler signal intensity analysis	39
Figure 2.3 - Diagrammatic illumination of the agitation chamber	40
Figure 2.4 - Diagrammatic illumination of the size-control set	41
CHAPTER THREE	
Figure 3.1 - Doppler signatures collected from <i>in vitro</i> and <i>in vivo</i>	59
Figure 3.2 - Frequency histogram of microbubble size in Ultravist 370	60
Figure 3.3 - Frequency histogram of microbubble size in 5% albumin solution	60
Figure 3.4 - Study of the half lives of microbubbles	61
Figure 3.5 - Correlation of Doppler signal intensity and the number of microbubbles	62
Figure 3.6 - Effect of different concentrations of microbubbles on Doppler signal intensity	63
Figure 3.7 - The effect of concentration of microbubbles on Doppler signal intensity	64
Figure 3.8 - Effect on bubble size of changing power	65
Figure 3.9 - Effect of changing power on bubble concentration	66
Figure 3.10 - Effect of changing agitation time on microbubble size	67
Figure 3.11 - Effect of changing agitation time on microbubble concentration	68
Figure 3.12 - Effect of dilution of Ultravist 370 on microbubble size	69

	<u>Page N°</u>
Figure 3.13 - Effect of dilution of Ultravist 370 on microbubble concentration	112
Figure 3.6 - Intensities of injection different materials	70
CHAPTER FOUR	
Figure 4.1 - Frequency distribution of embolic particle sizes	85
Figure 4.2 - Evaluation of compatability of embolic materials in size	86
Figure 4.3 - Comparison of embolic signal intensity between air bubbles and rabbit fat globules	87
Figure 4.4 - Comparison of embolic signal intensity between cholesterol crystals and rabbit whole blood clots	88
Figure 4.5 - Comparison of embolic signal intensity between atheromatous material, human whole blood clots and human platelet-rich clots	89
Figure 4.6 - Embolic signal intensity in association with embolus size	90
Figure 4.7 - A comprehensive picture of embolic signal intensities from different sources of embolic particles in different sizes	91
Figure 4.8 - Doppler images of embolic signals from <i>in vitro</i> and <i>in vivo</i>	92
Figure 4.9 - Comparison of embolic signal between <i>in vitro</i> and <i>in vivo</i>	93
CHAPTER FIVE	
Figure 5.1 - Illustration of the circuit model for reproduction of smoke-like echo and TCD examination	106
Figure 5.2 - Flow rate and smoke-like signals	107
Figure 5.3 - Comparison of average Doppler signal intensity between the blood flow with smoke-like signal and the blood flow bypassed the chamber	110
Figure 5.4 - TCD detection of embolic materials	111
Figure 5.5 - Two-dimensional echo images of embolic materials in	115

	<u>Page N°</u>
Figure 5.4 - the chamber	112
Figure 5.6 - Average Doppler intensities of injection different materials	114
Figure 5.7 - Doppler velocity related to smoke-like echo	115
CHAPTER SIX	
Figure 6.1 - Showing the main features of the anticipated four zones distal to an asymmetric stenosis at a Reynolds's number of around 545	132
Figure 6.2 - Illustration of the MCA stenosis model and the Doppler ultrasound sample positions	133
Figure 6.3 - Photography of the different cross-sections along the stenosis aorta	134
Figure 6.4 - Doppler ultrasound waveform sampled in different positions along the stenosis aorta	135
Figure 6.5 - Average Doppler signal intensity in different sample positions along with the stenosis aorta	136
Figure 6.6 - The change of image components in Doppler velocity waveform at post-stenosis I with increasing degree of stenosis	137
Figure 6.7 - Correlation between the degree of stenosis and the average signal intensity at post-stenosis	138
Figure 6.8 - Correlation between the degree of stenosis and the mean velocity at post-stenosis	139
Figure 6.9 - The visual difference between turbulence signal and embolic signals	140
Figure 6.10 - Comparison of the total signal intensity of turbulence and those of embolic materials	141
CHAPTER SEVEN	
Figure 7.1 - Diagrammatic illustration of the model for transmitting frequency test	152
Figure 7.2 - Signal intensity related to Doppler velocity of blood flow	154
Figure 7.3 - The background flow waveform	155

	<u>Page N°</u>
Figure 7.4 - Embolic signal intensity related to Doppler velocity of blood flow	156
Figure 7.5 - The same embolus in the blood flow at different velocity	157
Figure 7.6 - Embolic signal duration related to Doppler velocity of blood flow	158
CHAPTER EIGHT	
Figure 8.1 - Embolic signal intensities and signal events relating to different phases of cardiac catheterisation	173
Figure 8.2 - The correlation of embolic signal intensity and embolic signal events	174
Figure 8.3 - Acoustic characteristics of embolic signals relating to the phase of cardiac catheterisation	175
Figure 8.4 - Comparison of embolic signal intensities at different phases of cardiac catheterisation	176
Figure 8.5 - Comparison of embolic signal duration in different cardiac catheterisation	177
Figure 8.6 - Doppler signal intensities relating to injection of different materials	178
Figure 8.7 - Correlation of embolic signal intensities <i>in vitro</i> with those <i>in vivo</i>	179

LIST OF TABLES

Table 7.1 - Effect of alteration of transmitting frequency on ultrasonic quantification of Doppler signals 153

intensity analysis was used as a major measurement method to quantify the Doppler signals in this study. The validity of this method was also supported in experimental and clinical settings.

2. In an MCA *in vitro* model, the ability of TCD at different frequencies was evaluated. Two sizes of microbubbles (5 μ m and 30 μ m diameter) were used. The 370 (a contrast medium) and 5% albumin respectively. TCD was able to detect microbubbles as small as 5 μ m in diameter. The signal intensity and the number of microbubbles were proportional to the concentrations of microbubbles with signal intensity proportional to the volume of microbubbles present in the Doppler sample volume. The signal intensity tended to weaken at higher concentrations of microbubbles.

3. In the same model, the relationship between embolic signal intensity and the emboli of different sources was examined and the signal intensity caused by embolic materials were compared. Seven types of embolic materials were studied in this test. A quantitative relationship existed between the embolic signal intensity and the size of all the types of emboli tested. Air bubble emboli caused higher signal intensity than that caused by any solid embolic materials. Among the solid emboli at an average size of 100 μ m, platelet-rich thrombus produced the highest signal intensity. Further, the suitability of using total embolic signal intensity to differentiate the different sources of embolic was studied. It was found that an assigned embolic signal intensity could be produced by a small but highly reflective type of embolus or a larger but less reflective type of embolus.

SUMMARY

1. Detection, quantification and differentiation of circulating embolic materials and other related hemodynamic phenomena was performed in middle cerebral artery (MCA) *in vitro* models using transcranial Doppler (TCD) ultrasonography. Signal intensity analysis was used as a major measurement method to quantify the Doppler signals in this study. The validity of this method was also examined in experimental and clinical settings

2. In an MCA *in vitro* model, the ability of TCD to detect microbubbles was initially evaluated. Two sizes of microbubbles (5 μm and 30 μm) were prepared in Ultravist 370 (a contrast medium) and 5% albumin respectively. TCD proved to be sensitive to detect microbubbles as small as 5 μm in diameter. The correlation between embolic signal intensity and the number of microbubbles was investigated in two concentrations of microbubbles with signal intensity analysis. It was found that embolic signal intensity was proportional to the increase in the number of microbubbles present in the Doppler sample volume. However, this relationship tended to weaken at higher concentrations of microbubbles.

3. In the same model, the relationship between embolic signal intensity and the size of emboli of different sources was examined and the signal intensities caused by different embolic materials were compared. Seven types of embolic material were prepared and studied in this test. A quantitative relationship existed between the embolic signal intensity and the size of all the types of emboli tested. Air bubble emboli caused higher signal intensity than that caused by any solid embolic materials. Among the solid emboli at an average size of 100 μm , platelet-rich thrombin produced the highest signal intensity. Further, the suitability of using total embolic signal intensity to differentiate the different sources of embolic was studied. It was found that an assigned embolic signal intensity could be produced by a small but highly reflective type of embolus or a larger but less reflective type of embolus.

4. In an modified MCA model, spontaneous contrast echo was reproduced in a expansion chamber under low flow conditions. With a two-dimensional cardiosonography system and TCD, the differentiation of spontaneous contrast from emboli was carried out by both visual observation of the echo images and Doppler signal intensity analysis. Spontaneous contrast was distinct from emboli (whole blood clots, platelet-rich thrombin, and microbubbles) in echographic appearances and Doppler signal intensity.

5. The relationship between average signal intensity and the degree of stenosis of the MCA and the differentiation of turbulence from embolic signals were examined in a stenotic *in vitro* MCA model. A series of short, asymmetric stenoses were prepared in this test. Transition of turbulence from the laminar flow began to occur at a moderate degree of stenosis (55%) but became dump at the high degrees of stenoses (75% and 85%). Turbulence caused a significant increase in Doppler signal intensity. However, The degree of stenosis was not associated with signal intensity at the region of the turbulence but was related to the mean flow velocity through the narrowed region. Air bubbles (30 μm) and platelet-rich clots (100 μm) had a significantly higher signal intensity than the signal intensity through areas of turbulence. All the tested embolic signals showed different Doppler characteristics from the signals associated with turbulent flow.

6. The effect of transmitting frequency and flow velocity on ultrasonic quantification of emboli was investigated in an modified MCA model. A measured platelet-rich clot (2 x 2 x 2 mm for flow velocity test and 1 x 1 x 1 mm for transmitting frequency test) was repeatedly introduced into the model at different settings (23 cm/sec and 40 cm/sec for mean velocity settings; 2 MHz, 4 MHz, and 8 MHz for transmitting frequency settings). An embolus floating at a high flow velocity had a lower increase in total signal intensity and shorter duration of passage than an embolus passing at low flow velocity. The intensity of embolic signals recorded from a probe with lower transmitting frequency was significantly higher than that by a probe with higher frequency. Similarly, the duration of embolic signal was inversely proportional to the transmitting frequency of the probe.

7. Quantitative detection of cerebral emboli from the MCA was studied in 16 patients undergoing cardiac catheterisation. A continuous TCD recording was made throughout the procedure and the occurrence and intensity of embolic signals were examined in relation to different steps of the catheterisation. Embolic signal intensity was also correlated to the *in vitro* findings. In descending order of frequency, ventriculogram, change of the catheter guidewire, and catheter manipulation contributed to the highest incidence of cerebral emboli and to the highest embolic signal intensities. Embolic signals occurring during catheter insertion and catheter manipulation often showed lower intensities compared to those generated by the injection of normal saline at the level of the ascending aorta or within the left ventricle. The intensities from the former were equal to the intensities caused by atheroma materials (100 μm) *in vitro* and the intensities from the latter were similar to the intensities produced by microbubbles (30 μm) *in vitro*.

1. INTRODUCTION

1.1. Acute Stroke and Cerebral Embolism

Stroke is a principal cause of death and chronic disability in all developed countries. It has been estimated that strokes cause about 10 deaths per 100,000 population per annum in Europe and USA in those aged 40 years, rising to 1,000 per 100,000 per annum at 75 years (Kumar et al, 1990). The outcome of stroke in terms of morbidity and mortality is dead 31%, independent 58%, dependent 21% and recurrence 10% (Danford, 1990).

CHAPTER ONE

GENERAL INTRODUCTION

Vascular stroke has two main types: cerebral ischaemia and cerebral haemorrhage. In cerebral ischaemia the signs and symptoms of stroke result from interference with the circulation to the brain owing to a generalised or localized reduction of blood flow (Barnett, 1991). Cerebral infarction from thromboembolism usually produces a stroke, but small infarcts may present as transient ischaemic attacks (TIAs) which are symptomless. In an aetiological investigation of young stroke patients it has been reported that embolism is the most important cause (18.1%) associated with cerebral ischaemia (Lisovsky and Rousseaux, 1991). However, there is a need for new non-invasive methods that can be routinely used to detect cerebral emboli. At present it remains difficult to differentiate cerebral thrombosis from cerebral embolism on a clinical basis.

1.2. Cerebral Emboli

1.2.1. Macroemboli and microemboli

Emboli are divided into macroemboli and microemboli in terms of size (Brass and Fayed, 1993). Macroemboli are defined as emboli of size over 25 to 40 μm . Microemboli, less than 25 to 40 μm in size, have recently gained increased attention due to the following factors: 1. macroembolic complications have been reduced as preventive methods have improved; 2. imaging technology, in particular TCD

1. INTRODUCTION

1.1. Acute Stroke and Cerebral Embolism

Stroke is a principal cause of death and chronic disability in all developed countries. It has been estimated that strokes cause about 10 deaths per 100,000 population per annum in Europe and USA in those aged 40 years, rising to 1,000 per 100,000 per annum at 75 years (Kumar et al, 1990). The outcome of stroke in terms of morbidity and mortality is dead 31%, independent 38%, dependent 21% and reoccurrence 10% (Bamford, 1990).

Vascular stroke has two major causes: ischaemia and haemorrhage. In cerebral ischaemia the signs and symptoms of stroke result from interference with the circulation to the brain owing to a generalized or localized reduction of blood flow (Barnett, 1991). Cerebral infarction from thromboembolism typically produces a stroke, but small infarcts may present as transient ischaemic attacks (TIAs) or even be symptomless. In an aetiological investigation of young stroke patients, it has been reported that embolism is the most important cause (38.3%) accounted for cerebral ischaemia (Lisovoski and Rousseaux, 1991). However, there is a lack of investigative methods that can be routinely used to detect cerebral emboli (Russell, 1992) and it remains difficult to differentiate cerebral thrombosis from cerebral embolism on a clinical basis.

1.2. Cerebral Emboli

1.2.1. Macroemboli and microemboli

Emboli are divided into macroemboli and microemboli in terms of size (Brass and Fayad, 1993). Macroemboli are defined as emboli of size over 25 to 40 μm . Microemboli, less than 25 to 40 μm in size, have recently gained increased attention due to the following factors: 1. macroembolic complications have been reduced as preventive methods have improved; 2. imaging technology, in particular TCD

ultrasonography, has advanced such that it can detect microemboli. Emboli which are often encountered clinically are composed of a wide variety of materials including gaseous bubbles, calcified material or atheroma from the ascending aorta, clotted blood components, fat globules, cholesterol crystals, and so on. However, in the practice of ultrasound monitoring, emboli is often conveniently classified as either gaseous emboli or solid emboli according to their constitution.

1.2.2. Gaseous Emboli

Problems associated with the introduction of gaseous microemboli into the circulation have been documented since the mid 17th century (Boyle, 1670a and 1670b). It is generally recognized that cerebral gaseous emboli are often involved in open-heart surgery (Spencer et al, 1969b), decompression (Spencer et al, 1968), carotid endarterectomy (Naylor et al, 1991), and cerebral angiography (Markus et al, 1993a).

Air embolism was considered as a potential complication of open-heart operation as early as the beginning of this century. From initial retrospective investigation of complications of cardiopulmonary bypass (Coffee et al, 1983), the incidence of the postoperative neurological deficits was only 3%. Recently prospective studies with full neuropsychological assessment have shown that significant neuropsychologic impairment occurs in 79% of patients after surgery (Shaw et al, 1986). Many deficits were minor and resolved without specific therapy, but 37% still had significant abnormalities at 8 weeks (Treasure et al, 1989). Although it has been suggested that the neurological deficits were also associated with other factors such as older age, concomitant disease, poor perfusion, longer pump time, previous stroke, and atherosclerosis of the ascending aorta (Shaw et al, 1986, 1987), the accumulated evidence indicates that microemboli, particularly gaseous emboli, may play an important role (Taylor, 1986 and Blauth et al, 1988, 1990).

The principal source of gas bubbles in a heart-lung machine is the oxygenator, or artificial lung, component (Richardson, 1985). Most circuits for extracorporeal circulation are built to trap any large bubbles. However, small bubbles can be carried

by the blood stream for long distances in tubing and can then pass into the circulation of a patient. An increased awareness of the frequency of neurological complications has led to an emphasis on intraoperative monitoring with ultrasound instruments (Brass and Fayad, 1993).

Rapid return to the surface from deep ocean dives results in differences of the pressure between the inside and outside of body, which can form gas bubbles, mainly nitrogen or helium, in the circulation and in multiple organs. Gaseous emboli were previously documented in animal and then in humans suffering decompression sickness (Spencer et al, 1968, 1969a, 1972a). There is a recent report of cerebral gaseous embolism relating to decompression sickness caused by submarine escape training (Dutka et al, 1992). Although hyperbaric treatment could relieve symptoms of air embolism immediately in most cases of decompression sickness, it was reported that some of these victims with initial recovery will develop 'late' or 'secondary' deterioration such as headache, visual changes, and worsening of the original focal deficit (Pearson and Goad, 1982).

Embolic signals relating to air bubbles were recorded from the MCA of patients undergoing carotid endarterectomy (CEA) with TCD ultrasonography (Padayachee et al, 1986 and Berger et al, 1990). These embolic signals happened more frequently during CEA with the procedure of shunting than in those without shunting. In a similar investigation, signals representing gaseous emboli were documented upon release of common carotid artery crossclamps (Spencer et al, 1990). However, in these cases, air emboli did not immediately produce any obvious symptoms.

An additional clinical source of cerebral air emboli is in intracranial neurosurgical procedures (Edmonds-Seal and Maroon, 1969 and Maroon and Edmonds-Seal, 1969).

Air bubbles in the body can become trapped in the microcirculation, leading to interference with the transport of nutrients and oxygen to dependent tissue. Air bubbles reaching the small arteries pass rapidly into the arterioles, where they cause

an immediate but temporary block, which leads to dilation of vessels associated with marked stasis and occasionally with small perivascular haemorrhage by diapedesis (Chase, 1934 and Fazio and Sacchi, 1954). It has been suggested that the dilation following gaseous emboli is not related to reactive hyperaemia but a response to the direct injury of the lining of the blood vessels involved (Duft et al, 1954). In pathological investigation of cerebral embolism, it was demonstrated that injection of approximately 1 ml of air per Kg. of body weight via the carotid arteries over a period of 30 to 60 seconds could kill almost half of the experimental dogs (Fries et al, 1957).

1.2.3. Solid Embolism

A. Solid emboli from cardiac source

Intracardiac pathology resulting in embolic phenomena is a well-recognized cause of cerebral ischaemia and infarction. Previous studies suggested that 6-23% of all cerebral ischaemic events had a cardiac origin (Mohr et al, 1978, Weinfeld et al, 1981, Wolf et al, 1983 and Caplan, 1982). Further, it has been recently suggested that at least 5 per cent of patients with a myocardial infarction have clinical evidence of cerebral embolisation (Barnett, 1991). Emboli from a cardiac source may cause lacunar infarction by occlusion of small, penetrating cerebral arteries (Cacciatore and Russo, 1991). Factors relating to cardiac emboli include left atrial enlargement, spontaneous left atrial echo contrast, atrial septal aneurysm, interatrial shunts, atrial fibrillation, valvular disease (including rheumatic disease, endocarditis, mitral valve prolapse, mitral valvular calcification, and prosthetic valves), and abnormal ventricular wall motion (including aneurysm and globally reduced left ventricular function resulting from myocardial infarction or cardiomyopathy) (Caplan et al, 1986, Erbel et al, 1986, Lechat et al, 1988, Furlan et al, 1984 and Nishide et al, 1983). Platelet aggregates, thrombus clot and atheromatous materials are also often implicated in the above situations (Philp et al, 1972, Pugsley et al, 1990, Spencer et al, 1990 and Spencer, 1992).

B. Solid emboli from internal carotid artery source

It has been suggested that atherosclerotic plaque in the carotid arteries can produce emboli by two mechanisms: by the rupture of its contents into the bloodstream and by the breaking off of a thrombus formed on an ulcerated surface or in the bloodstream when flow distal to the plaque is slowed (Spencer et al, 1990). Emboli in the internal carotid artery territory which dislodge and block an ascending artery in brain are classified as artery to artery embolisation. This has been proved during operation and postmortem examination in which surgeons have observed both types of emboli lodging in the operative field of the exposed cortex in patients known to have irregular and ulcerative atheroma of the internal carotid or middle cerebral arteries and pathologists have identified atheromatous debris lodged in thrombi obstructing cortical and deep arteries and arterioles (Barnett, 1991). It was evident that these emboli came from the internal carotid artery (ICA) territory but not from heart. These emboli were considered as a common cause of both transient ischaemic attacks and stroke (Cunning et al, 1964 and Millikan et al, 1987).

Real time but indirect evidence of solid emboli was collected from the middle cerebral arteries in patients undergoing carotid endarterectomy by means of TCD ultrasonography. The authors indicated that embolic signals representing 'formed-element emboli' recorded before, during, and after surgical dissection, were associated with intraluminal platelet thrombus and ulceration (Spencer et al, 1990).

C. Fat emboli

It has been reported that fat emboli occur in most (more than 90 %) patients with traumatic injury and the fat embolism syndrome (FES), a serious manifestation of the phenomenon of fat emboli, occurs in 3-4 per cent of patients with long bone fractures (Levy, 1990). The major clinical features of FES include hypoxia, pulmonary oedema, central nervous system (CNS) depression and subconjunctival petechiae. However, the FES is not confined to trauma, and has also been described in many non-traumatic conditions such as burns, diabetes mellitus, severe infection, inhalation anaesthesia, chronic pancreatitis, chronic alcoholism, osteomyelitis, blood transfusion, sickle-cell anaemia, renal transplantation, steroid-induced fatty liver, acute decompression sickness, total arthroplasty, intramedullary nailing, liposuction, parenteral lipid

infusion, and cardiopulmonary bypass (Caguin et al, 1963, Moylan et al, 1976 and Levy, 1990). The mortality of FES is reportedly up to 10-20 per cent (Gourd et al, 1970). This has been proved with the finding of fat droplets within the vessels of the cerebrum and other organs in the necropsy observation of suspected FES patients (Lequire et al, 1959).

The cerebral features of FES include headache, irritability, delirium, stupor, convulsions, and coma, which occur in as many as 80 per cent patients with FES (Fabian et al, 1990). The pathophysiological mechanism accounting for the presence of cerebral symptoms of FES was explained as fat droplets which were released from the disrupted fat cells in the marrow of fractured bones or in adipose tissue, passing through the lungs either via the alveolar capillaries or through precapillary shunts and result in fat droplets blocking small vessels in brain and other organs (Besouw et al, 1989). It was also found that cholesterol crystals co-existed in blocked vessels in fat embolism but the role of cholesterol crystals in the clinical syndrome is not clear (Lequire et al, 1959).

D. Cholesterol crystal emboli

Cholesterol crystal embolisation is an infrequent but serious disorder that is often an unrecognized medical problem. It may occur spontaneously from eroded atherosclerotic plaques or most frequently following procedures such as angiography, angioplasty, cardiac catheterisation, anticoagulant therapy and aortic surgery (Colt et al, 1988, Hendel et al, 1989 and Pizzolitto et al, 1991). The mortality may be up to 81% due to multiorgan failure. The natural history of this syndrome remains unclear because of the difficulty of establishing an antemortem diagnosis (Pizzolitto et al, 1991).

Moreover, haematological disorders such as sickle cell anaemia have been suggested to contribute to the aetiology of cerebral ischaemia. In these cases, coagulation and/or platelet abnormalities have been implicated in the genesis of embolism (Kalendovsky et al, 1975 and Hess et al, 1991).

1.3. Principles of Ultrasound and Doppler Ultrasonography

1.3.1. Physical Features of Ultrasound

Ultrasound is a form of energy which consists of mechanical vibrations, the frequencies of which are so high that they are above the range of human hearing. Most diagnostic applications of ultrasound employ frequencies in the range 1-15 MHz (Wells, 1983).

Ultrasonic energy travels through a medium in the form of a wave. Although a number of different wave modes are possible, almost all diagnostic applications involve the use of longitudinal waves. The particles of which the medium is composed vibrate backwards and forwards about their mean positions, so that energy is transferred through the medium in a direction parallel to that of the oscillations of the particles (Figure 1.1).

The wavelength, l , is the distance in the medium between consecutive particles where the displacement amplitudes are identical; the wave period, T , is the time which is required for the wave to move forward through a distance, l , in the medium. The frequency, f , of the wave is equal to the number of cycles which pass a given point in the medium in unit time (usually one second). Thus:

$$f=1/T$$

The wavelength and the frequency are related to the propagation speed, c , by the equation:

$$c=fl$$

For example, at a frequency of 1 MHz the wavelength in water ($c=1500$ m/s) is 1.5 mm.

These relationships apply only to continuous waves of constant amplitude. They are more complicated for pulsed waves which are not associated with single frequency and so l and T are not constants (Wells, 1983).

The speed at which the energy is transferred through the medium is determined by the delay which occurs between the movements of neighbouring particles. This depends upon the elasticity, K (because this controls the force for a given displacement in the medium) and the density, P , (which controls the acceleration for a given force within the medium) according to the equation:

$$c = \sqrt{k / p}$$

The speeds in different soft tissues are closely similar. The speed in bone is higher (2,700-4,100 m/s), whilst that in lung is lower (650-1,160 m/s).

1.3.2. Reflection at Interface of Two Media

The characters of ultrasound mentioned above are subject to conditions in which the sound beam travels in a uniform, or homogeneous medium. When the medium is not uniform, that is, heterogeneous, waves may not be propagated with equal facility in all directions. If the medium is a mixture of materials with varying densities and velocities of propagation, then another process occurs called reflection. Reflection takes place at interfaces when the interface is larger than the wave length of sound source and where a portion of the incident wave energy is reflected back. However, the scattered wave is emitted in all directions (nonspecular reflection) when the wave length of sound source is larger than the interface (Figure 1.2).

When a wave meets the interface between two mediums at normal incidence, it is propagated without deviation into the second medium. At an oblique incidence, the wave is deviated by refraction unless the speeds in the two media are equal. The relationship is:

$$(\sin q_i) / (\sin q_r) = c_1 / c_2$$

however, results in a compression of the wavelength of the reflected wave, and vice versa where θ_i =incident angle; θ_r =refraction angle; c_1 =propagation speed of medium 1; c_2 =propagation speed of medium 2.

1.3.3. Acoustic Impedance

Acoustic impedance, z , is a measure of the resistance to sound passing through a medium and is the product of density, ρ , times velocity, c , i.e. $z=\rho c$. High density materials have high velocities and therefore high acoustic impedance. Similarly, low-density materials such as gases have low acoustic impedance. If there is a difference in acoustic impedance between an embolus in the bloodstream and the blood, a high proportion of ultrasound will be reflected at the interface. The more the acoustic impedance, the more ultrasound beam reflection and then, the higher signal intensity. This relationship is described by a reflection coefficient, a_R , which is expressed in the following equation:

$$a_R = [(Z_2 - Z_1) / (Z_2 + Z_1)]^2$$

where a_R =reflection coefficient; Z_1 =acoustic impedance of medium 1; Z_2 =acoustic impedance in medium 2.

If $Z_1=Z_2$, $R=0$: thus, there is no reflection at a boundary between media of equal characteristic impedance. On the other hand, if $Z_2 \ll Z_1$, then $R=1$, corresponding to almost complete reflection.

The equation also suggests that it does not matter which impedance is the larger or smaller for the two materials. Thus, the same proportion of reflection will occur at an interface whether going from a high acoustic impedance to a lower acoustic impedance, or vice versa.

1.3.4. Doppler Effect

The frequencies of the transmitted and the reflected waves are equal if the reflecting boundary is stationary. Movement of the reflecting boundary towards the source,

however, results in a compression of the wavelength of the reflected wave, and vice versa. Since the velocity of propagation is constant, these changes in wavelength produce corresponding changes in frequency. The phenomenon is called the Doppler effect (Figure 1.3). This theory was first introduced by the Austrian physicist Christian Doppler (1842) and further experimentally verified by a Dutch physicist three years later (Ballot, 1845). The calculation of frequency shift is based on the following principles.

At normal incidence if f is the frequency of the incident wave, and v is the velocity of the reflecting boundary towards the source, the Doppler shift in frequency f_D which occurs in the reflected wave ($f_D = f' - f$, where f' is the received frequency) is given by:

$$f_D = 2vf/c$$

provided that $v \ll c$, as is generally the case in diagnostic applications. In these applications, it often happens that the direction of the motion of the reflecting boundary is at an angle g with the incident wave, although the incident and reflected waves are effectively coincident. Then:

$$f_D = 2v(\cos g)f/c$$

This Doppler shift can be heard in the earphones of the Doppler instrument and seen on the spectrum analyzer. A velocity of 1 m/sec will produce a shift of about 2.5 KHz when transmitted Doppler ultrasound frequency is 2 MHz and 5 KHz if the original frequency is 4 MHz (Aaslid 1992).

It is via the Doppler effect that ultrasound is able to provide information on blood flow velocity. The velocity of blood flow can be calculated by the difference between the frequency of transmitted ultrasound from a transducer and that reflected from the blood cells, acting as a moving reflector, received by the same transducer. This technology is now widely used in several branches of medical application.

1.3.5. Intensity of Doppler Ultrasound Signal

For the application of ultrasound Doppler technique to estimate blood velocity, no use is made of the intensity of the returned signal. But this parameter provides information on the material that the ultrasound beam meets, and theoretically it could be used to detect circulating emboli (Markus and Brown, 1993b).
Ultrasound intensity is equal to the quantity of energy flowing through unit area in unit time. The amount of intensity of the returned ultrasound depends on the proportion of the transmitted beam that is reflected. This in turn is associated with the type of tissue through which the ultrasound beams pass. As mentioned above, the ratio of ultrasound reflected at the interface between two different media, for instance, between blood and an embolus, is dependent upon the difference in acoustic impedance of the two materials. Acoustic impedance itself depends on density; therefore, the greater the difference in density between the two media, the greater the amount of ultrasound reflected, and the greater the intensity of the received signal. For particles with a size equal to or smaller than the wavelength of the transmitted ultrasound (0.77 mm for a standard 2-MHz transcranial Doppler probe), the amount of ultrasound reflected is governed by Rayleigh scattering (Rayleigh, 1945). Assisted by a spectral analyzer, the Doppler spectrum not only contains the velocity reading but also has information on signal power or intensity that is reflected. This means that not only the frequency of the sound that is returning to the Doppler transducer is available but also the amount (Russell, 1992).

1.3.6. Attenuation

In addition to the above factor, the amount of sound is also related to the size of the reflecting surface. There are two behaviours of sound reflection: scattering or nonspecular reflection and specular reflection. The former happens when the interfaces are smaller than one wavelength of the incident ultrasound. Each individual interface then acts as a new separate sound source, and sound is reflected in all directions. As a result, the signal intensity of reflected sound which is received from the transducer is low. Against the 0.77 mm wavelength of ultrasound at a frequency of 2 MHz, the diameter of red blood cells (RBC) is 7-10 μm . Therefore scattering by

blood cells is the main determinant of signal intensity which is recorded in the blood velocity waveform.

The size of the interface is the other factor which determines signal intensity (Russell, 1992). Since emboli are usually larger than the wavelength of 2 MHz ultrasound, the reflected ultrasound at the interface may act as a specular reflector. The intensity of the ultrasound returning to the Doppler transducer will be determined mainly by reflection rather than scattering which causes reflected sound loss. Combining the two factors, different acoustic impedance at the interface and specular reflection from larger interface, embolic signals would be expected on theoretical grounds to have a distinctively higher signal intensity than those caused by flowing blood cells.

Regarding measurement of signal intensity, it has been suggested that the absolute value of ultrasonic intensity is an important consideration in relation to possible biological effects, and to the ability of a system to detect an ultrasonic wave in the presence of noise. It is frequently very convenient, however, to measure the ratios between pairs of intensities, particularly if the level of one of these is taken as a reference for comparison with others (Wells, 1983). In the use of TCD ultrasonography to measure blood velocity, it has been noted that the intensity of returned signal is proportional to the number of blood cells having this velocity component in the insonation area (Aaslid, 1992).

1.3.6. Attenuation

There are two processes by which the intensity of an ultrasonic wave may be attenuated during its propagation. Firstly, the wave may diverge from a parallel beam, or it may be scattered by small discontinuities in characteristic impedance, so that the ultrasonic power flows through an increased area (convergence of the beam results in an increase in intensity towards the focus). Secondly, the wave may be absorbed, ultrasonic energy being converted into heat.

The mechanisms by which ultrasound may be attenuated depend upon the properties of the material in which the wave is propagated. Attenuation is proportional to the

acoustic impedance of the medium and also increases with rising frequency (Wells, 1983).

1.3.7. Transcranial Doppler Ultrasonography (TCD)

The mechanism behind TCD ultrasonography to image flowing blood in intracranial arteries is that ultrasound frequency used in transcranial Doppler is lower (2 MHz) than those used in duplex ultrasound devices (7 to 10 MHz) and this thereby achieves enough penetration through a weaker (thinner) part of skull to insonate the arteries of the circle of Willis deep within the cranial vault. Unfortunately, this fact seems to have been realized early but the practice was hampered by a 'more psychological than physical' barrier, which resulted in a delay in wider application of this technique in the field of cerebral circulation (Aaslid, 1992). The anatomically thinner parts of the skull which allow ultrasound signal to pass through are called 'transcranial windows'. The commonly used 'windows' for TCD investigation are composed of the transtemporal, transorbital and suboccipital windows. Additionally, because transcranial Doppler technology incorporates a range-gated pulsed ultrasound signal, instead of a continuous signal, the depth of insonation can be adjusted by changing the time between the emission and the reception of the signal by the probe (Aaslid, 1986). This is applied when assessing the flow velocity at different points in arteries along their intracranial course.

Doppler ultrasound has long been used to demonstrate the presence, direction, velocity, and characteristics of blood flow (Berger and Tegeler, 1993). As a non-invasive velocity measurement method, this technique has been conventionally used in quantification of haemodynamics in the cardiovascular field. However, this technique was not used to evaluate the intracranial circulation until an earlier type of Doppler instrument with a 2 MHz probe was introduced by Aaslid and his colleagues (1982). Since then, the further development of a simple, small, microprocessor-controlled TCD instrument with analog/digital output of velocity waveform facilitated the use of this technique for monitoring of cerebral haemodynamics (Lundar et al, 1985 and Ringelstein et al, 1985). For instance, by measuring the alteration of blood flow velocity in cerebral basal arteries, transcranial Doppler ultrasonography may help in

the diagnosis of vasospasm following subarachnoid haemorrhage (Harders et al, 1987, Sloan et al, 1989, and Grosset et al, 1992, 1993a), head injury and cerebral circulatory arrest (Hassler et al, 1988 and Saunders et al, 1988), intracranial artery stenosis (Spencer et al, 1986) intracranial arteriovenous malformations (Petty et al, 1990), and vascular dementia (Provinciali et al, 1990) and estimation of regional cerebral blood flow when combined with other neuroimaging methods (Sorteberg et al, 1989), assessment of cerebral autoregulation dynamics (Aaslid et al, 1991), and investigation of cerebrovascular responses to pharmacological agents (Dahl et al, 1989). Increasing evidence shows that TCD monitoring is of diagnostic value in a variety of clinical fields since the data obtained with TCD may influence the approach to management and treatment of the patient. Finally, this method has been successfully used to detect cerebral emboli.

1.4. Identification of Embolus Materials

1.4.1. Identification of Embolus Materials Using Non-ultrasound Techniques

In addition to ultrasound techniques, methods for investigating gas emboli in blood include timed collection of a sample of blood, with subsequent gravitational separation of bubbles or measurement of bulk compressibility; and examination of small samples (usually taken as slipstreams) by optical or electric impedance devices (Richardson, 1985). However, these methods are not convenient to handle and not reliable since the reproducibility of the samples examined is a problem.

Several different approaches have been made to collect evidence for the existence of solid emboli. Numerous autopsy studies of patients who had received large quantities of intravenous fluids during life have shown cotton fibres and cellulose granulomas in the lungs (Bruning, 1955, Sarrat et al, 1960 and Garvan et al, 1964). Swank (1961) used a screen filtration pressure device to identify the presence of blood cell aggregates in stored human blood containing either heparin or acid-citrate-dextrose. Autopsy was also used to reveal gas embolisation. Following demonstration of the existence of cerebral gaseous emboli in goats during cardiopulmonary bypass more than two decades ago by Simmons et al (1972), more neuropathological findings of

air embolism in human autopsy after open heart surgery were accumulated (Aguilar et al, 1971 and Pearson et al, 1981). Most recently, microemboli occurring in cardiopulmonary bypass were imaged with a retinal fluorescein angiography technique (Blauth et al, 1990). In their study, retinal fluorescein angiograms were performed in the patients preoperatively and five minutes before the end of bypass. Indirect evidence of microembolisation was obtained through identification of the perfusion defects by digital subtraction of preoperative and end-bypass angiograms. Moreover, angiography was also employed by Moody and coworkers (1990) to identify gaseous or fat emboli by showing empty, 'sausage-like' dilatation of medium-sized cerebral arterioles in patients and experimental dogs during cardiac surgery or aortography.

It is generally recognised that computer used tomography (CT) cannot tell whether cerebral ischaemia is due to embolism or thrombosis although it can conveniently exclude cerebral haemorrhage from ischaemic stroke. Moreover, the CT appearance of ischaemia changes. In the acute phase as many as 40 per cent of definite cerebral infarcts will not be visible (Bamford, 1990). Magnetic resonance imaging (MRI) may shorten the diagnostic period, but is still unable to distinguish embolism from thrombolism. Some indication of an embolic source may come from CT or MRI studies in the presence of multiple bilateral ischaemic areas.

It is obvious that all these non-ultrasound manoeuvres mentioned above have such limitations that they can only collect the evidence after the embolic event or just detect the potential source of embolism while ultrasonic device monitoring may supply continuous and accurate time information about the occurrence of microemboli (Clark, 1985).

1.4.2 Differentiation from Artifact using Transcranial Doppler Ultrasonography

As ultrasonography itself is very sensitive, discrimination of a signal caused by an embolus from that by an artifact due to probe or head motion becomes essential. Generally, embolic signals with high intensity are easy to visualise when they are

superimposed on an intensity-color-coded blood flow waveform which is contributed by each moving part of the blood within the sample volume.

The features of a typical embolic signal and those of an artifact or noise transient signal have been clearly outlined by Spencer (1992), in which Doppler emboli are described as: 1. short transients, less than 0.1 sec ranging 3 to 60 dB above the background Doppler blood velocity spectrum; 2. unidirectional within either the advancing or receding velocity spectrum. 3. duration in the spectrum is inversely proportional to their velocity; 4. random in occurrence in the cardiac cycle; 5. change of frequency/velocity as they pass through the sample volume; 6. sound to the ear like harmonic chirps, whistles, or clicks, depending on their velocity. By contrast, the major features of artifact signals are defined as bi-directional signals with frequencies spread away from the zero frequency reference, with a noisy sound quality and coincident with probe impacts, sudden motion, or electrical switching transients and sounds with a noisy quality, without the tonal quality of embolic signals. Although it is not difficult to exclude artifacts according to the above indicators, a very stable fixation of the probe and a good signal-to-noise ratio are essential in clinical application of TCD (Aaslid, 1992).

Early automatic detection devices recorded a sudden rise in intensity of the returned signal but did not differentiate an artifact from an embolus (Abts et al, 1978). More recently, this situation was been improved by Brucher et al (1993) who introduced an automated on-line embolus recognition program which gives a probability score for a possible embolic signal according to the characteristics of embolic signal described above. The programme is designed to assign a low or negative score to the bi-directional intensity increase caused by artifact but positive score to a typical unidirectional signal resulted from an embolus; the higher the score, the more likely the signal is to represent an embolic signal. The sensitivity and specificity of this programme was further studied and confirmed later in an experimental sheep model and in patients with carotid artery stenosis by Markus et al (1993c). There was a high sensitivity (98.7 %) and a high specificity (98.0 %) in embolus detection in their study

of solid materials, but this automated on-line embolus recognition program has not been tested in the detection of gaseous emboli.

1.4.3. Detection of Extracranial Emboli with Doppler Ultrasound

The difference in acoustic impedance of embolic material, as compared to the surrounding blood, produces identifiable differences in the intensity of the returning Doppler signal. Detection of intravascular microemboli with Doppler ultrasound began from detecting gas emboli or particulate matter in the arterial line during cardiopulmonary bypass (Austen and Howry, 1965) and, later, gas emboli in the vena cava and aorta of sheep (Spencer et al, 1968) and swine (Gillis et al, 1968) following decompression from exposure to hyperbaric air, which was followed by Kessler and Patterson (1970) who employed a pulsed-echo system to examine microemboli produced by blood oxygenators during bypass. With the application of the ultrasonic Doppler prototypes, Austen and Howry (1965) and Kessler and Patterson (1970) observed that solids were detected poorly by Doppler, and the pulsed-echo system was inaccurate since particles were counted more than once within the chamber, while no detection was possible for particles located near the walls. This technique was extended to detect decompression venous gas emboli in the peripheral veins and in the pulmonary artery in human volunteers (Spencer et al, 1972a, 1972b) and the embolus data was used to develop safer decompression tables (Spencer et al, 1976). In 1972, ultrasound was used to detect fat emboli in the venous effluent of fractured extremities of dogs and humans (Kelly et al, 1972). In this study, abnormal Doppler ultrasound signals were noted (the animal model involved in this experiment will be described later in section of 1.6. in this Chapter). Similar application and findings were reported by Herndon et al (1975) during total hip replacement.

Prior work has shown that the ultrasound emboli detector registered the passage of particles as small as 50 μm and the number of returned embolic signals was proportional to the concentration of microemboli in the blood (Brennan et al, 1971).

In an attempt to improve the ability of the Doppler ultrasound device to image emboli during cardiopulmonary bypass surgery, Dietz et al (1974) constructed a continuous-

wave ultrasonic microembolus detector using transmission ultrasonic spectrometry. The system used an ultrasonic resonator assembly consisting of two piezoelectric transducers mounted opposite each other to produce a standing ultrasonic wave in the blood passing between the two transducers. This resonator field enhanced the sensitivity of microembolus detection. It was reported that this system was able to detect more than 95 % of 100 μm fibrin and glass microspheres.

However, the constitution of emboli signals remains assumed but not proven in the clinical setting.

The special embolus-detecting system was helpful in evaluating the efficiency of filters used in the extracorporeal circulatory tubing. In 1987, Pearson et al (1987) compared the ability of three different ultrasonic microbubble detectors to document air bubbles in flowing blood and related microbubble occurrence to the course of the cardiopulmonary bypass operation.

1.5.1 Small Infarcts

Equipped with ultrasound techniques, the increased awareness of the importance of microemboli has led to a marked improvement in all of the devices in the bypass circuit and in diving decompression in order to minimize the formation of microemboli.

and on anatomic features, and the patient may not experience symptoms if the infarct is located in a clinically silent area of the brain (Fisher, 1963, Petersen,

1.4.4. Detection of Intracranial Emboli with Transcranial Doppler Ultrasonography

After intracranial emboli were first detected in patients during cardiopulmonary bypass using TCD ultrasonography (Padayachee et al, 1987), this application has been widely developed in both operative monitoring such as detection of microemboli during carotid endarterectomy (Spencer et al, 1990) and cerebral angiography (Markus et al, 1993a) and non-operative detection of microemboli such as in patients with prosthetic aortic valves (Berger et al, 1990) and with atrial fibrillation (Tegeler et al, 1990). Most recently, the TCD technique was employed to investigate clinically silent intracranial embolism in patients with symptomatic extracranial carotid artery disease (Siebler et al, 1992 and Grosset et al, 1993b). In these circumstances, low gain settings were usually chosen to facilitate visualization of the embolic signals superimposed on the blood flow waveform. Monitoring of patients with potential embolic sources may allow identification of high-risk patients who can then be

selected for prophylactic treatment. Such an application needs to be followed by an analysis of prognostic implications of the method.

As intracranial microemboli are detected using TCD ultrasonography in a variety of clinical settings, it has been generally agreed that the ability of transcranial Doppler ultrasound to record the passage of emboli is very promising. However, the constitution of emboli signals remains assumed but not proven in the clinical setting. This issue needed to be examined by evaluating the ability of transcranial Doppler method in counting, sizing, and characterizing microemboli.

1.5. Clinical Applications of TCD in Detection of Cerebral Emboli

1.5.1 Small Infarcts

It has been suggested that small emboli may cause small cortical or subcortical infarcts by blocking the penetrating arteries (diameters 0.1 to 0.4 mm) in human brain (Stehbens, 1972 and Fisher, 1978). The clinical effects of such small infarcts in humans depend on anatomic features, and the patient may not experience symptoms if the infarct is located in a clinically silent area of the brain (Fisher, 1965, Petersen, 1987, Kempster, 1988 and Kase, 1989). However, it has been reported that the small size infarcts may have a cumulative detrimental effect on neuropsychological function, especially in aged patients (Ratcliffe, 1985). TCD may act as a sensitive and non-invasive method in diagnosis of asymptomatic cerebral embolism and, furthermore, be of potential prognostic and therapeutic significance in patients with a potential embolic source, for instance, by identifying a subgroup of patients with a greater risk for embolic stroke (Russell, 1992). Conversely, identification of a sub-group of patients with 'lone atrial fibrillation' without the complication of cerebral embolism may prevent the risks of long-term anticoagulation in such patients (Cujec et al, 1991).

1.5.2. Differentiation of Embolic from Haemodynamic Transient Ischaemic Attack

(TIA)

Long-term Doppler ultrasound detection for cerebral emboli may help in resolving the controversy regarding the pathogenesis of TIA. Doppler information has important implications for both the management of individual patients and the assessment of new therapies, since a treatment that improves blood flow will not necessarily benefit patients without thromboembolic events and vice versa.

1.5.3. Intraoperative Monitoring

A main example of TCD intraoperative monitoring is detection of microemboli during cardiopulmonary bypass operation although this technique is also used in other surgical procedures such as carotid endarterectomy (Spencer et al, 1990) and craniotomy (Giller et al, 1990, 1993). Extracorporeal circuits have been in use for dialysis and in cardiopulmonary bypass surgery for many years. The brain damage involved in cardiopulmonary bypass surgery remains a major concern. Thus a method for assessing and quantifying neurological damage during and after bypass is urgently needed (Henriksen et al, 1983). Before TCD ultrasonography was available, early ultrasound detectors were placed in the arterial line of a bypass device or in the carotid artery to monitor the passage of microemboli and/or check the efficiency of the filter (Brennan et al, 1971 and Pearson et al, 1987). Recently, Harrison and associates (1990) applied TCD ultrasonography to record intracranial emboli in two groups of patients undergoing coronary artery bypass surgery: one group with an extra filter and the other one without. It was found that patients in the filtered group had less recordable microemboli and were less likely to show postoperative deterioration in performance on a neuropsychological test battery. This result accorded with a view that the consistently detectable neuropsychological deterioration in a proportion of patients after coronary artery bypass surgery is due at least in part to cerebral embolism (Smith et al, 1986). A similar result was reported earlier by Padayachee and his colleagues (1987, 1988). Continuous TCD measurement was also used to identify the occurrence and the timing of cerebral emboli during bypass (van der Linden and Casimir-Ahn, 1991). TCD monitoring in this field has played an important role in improving the surgical techniques as well as extracorporeal circulation facilities to reduce the risk of the operation.

Intraoperative monitoring of the MCA or internal carotid artery during invasive cardiovascular surgery such as open-heart surgery and carotid endarterectomy, in which cerebral emboli are a major cause of neurological and neuropsychological dysfunction (Pugsley 1990, Smith, 1986, 1988 and Shaw, 1987), may alert the surgical team that emboli are entering the cerebral circulation, so that immediate preventive or therapeutic measures may be undertaken (1977). It remains difficult to

differentiate cerebral embolism from a toxic reaction to contrast agent, dehydration,

1.5.4. Other Clinical Applications monitoring may be helpful in identification of the

Paradoxical embolisation via a patent atrial foramen ovale is suspected as a cause of embolic stroke or transient ischaemic attacks, especially in young adult patients (Lechat et al, 1988 and Webster et al, 1988). Transcranial Doppler ultrasound, a sensitive method for detecting circulating emboli, has also been used to identify patients with right-left cardiac or pulmonary shunts by venous injection of microbubble contrast (Teague et al, 1991 and Chimowitz, 1991). In a clinical investigation of right-to-left vascular shunting in patients with stroke, transient neurological defect, or a possible atrial septal defect, two-dimensional echocardiography and transcranial Doppler were simultaneously performed (Teague et al, 1991). It was observed that the transcranial Doppler technique had a higher sensitivity in right-to-left shunt detection and a good accordance with echocardiographic findings. More importantly, TCD can supply unambiguous information about target organ (brain) involvement. The authors cited that cardiac catheterisation appeared far less sensitive to the presence of patent foramen ovale than the two ultrasonic techniques. Thus, along with two-dimensional echocardiography, transcranial Doppler ultrasonography is a sensitive technique to demonstrate a potential cardiac source of cerebral embolism due to the right-to-left shunt after venous contrast delivery. mit the reliability when relating the experimental

data to clinical findings. In 1993, Markus and Brown (1993b) included this variable in

The returned signal power of a particular Doppler frequency is proportional to the number of blood cells having this velocity component (Aaslid, 1992) and the number of blood cells within the sample volume is proportional to the cross-section of the artery in TCD measurements (Arts et al, 1972). Therefore, this principle may be

mm) platelet emboli resulted in a lower maximum amplitude than did the other

theoretically used to estimate the cross-section alteration of the cerebral artery if blood velocity remains unchanged.

Symptomatic cerebral disorders are a serious complication of cardiac catheterisation although the incidence is fortunately not high (1.5-3.4 per cent) (Clements and Gatlin, 1991, Lockwood et al, 1983 and Dawson and Fischer 1977). It remains difficult to differentiate cerebral embolism from a toxic reaction to contrast agent, dehydration, or hypotension. Continuous TCD monitoring may be helpful in identification of the emboli during this practice.

1.6. Experimental Models for Characterizing, Counting and Sizing Emboli

1.6.1. Models for Characterizing Emboli

Earlier studies of embolus detection concentrated on confirmation of diagnostic ability of the ultrasound technique in detection of emboli (Austen and Howry, 1965 and Spencer et al, 1969a), and the composition and exact size of emboli based on Doppler characteristics were not considered (Berger and Tegeler, 1993).

More recent work done by Russell et al (1991) attempted to characterize different embolic materials. Embolic materials including air bubbles, fat, platelet aggregates, and atheroma were introduced into a rabbit aorta and monitored with a TCD instrument. Although air and fat produced stronger Doppler embolic signals, accurate characterization of the type of embolus was not possible.

The above study in an extracranial artery did not account for the attenuation of ultrasound by the skull. This may limit the reliability when relating the experimental data to clinical findings. In 1993, Markus and Brown (1993b) included this variable in a model with an acoustic skull window. The amplitude of emboli signals was compared with embolus size in an extracorporeal circuit filled with a saline/Tween solution and driven by a peristaltic pump. It was found that large (>2 mm) emboli of all materials caused a similar maximum amplitude signal but for smaller emboli (<1.5 mm) platelet emboli resulted in a lower maximum amplitude than did the other

materials. However, the size of different of emboli was not standardized in their comparison.

1.6.2. Models for Counting and Sizing Emboli

Estimation of bubble numbers using pulsed ultrasound techniques are based on echo counts. Sizing of emboli is possible with ultrasonic techniques which depend on the measurement of ultrasound perturbation produced by the presence of an embolus in the field of insonation.

In an attempt to evaluate the validity and reliability of ultrasound technique in detection of artery emboli, Stump et al (1991) used a 5-MHz CW Doppler system with an automatic counting capability to detect polystyrene spheres. They observed that the spheres could be accurately counted using the automated counter when they passed through the sample volume.

Russell et al (1991), in their *in vitro* model of embolus detection, noted a linear relationship between the maximal amplitude of the Doppler signal caused by the emboli and embolus size. This result, along with data from an *in vitro* experiment in which peak amplitude of embolic signals caused by air bubbles was calibrated using glass beads of known size (Pearson et al, 1987), implies that TCD ultrasonography may be used to size emboli according to their Doppler signatures.

Another experimental correlation between air embolus volume and embolic signal power was undertaken by Bunegin et al (1991). In this study, air was injected into a bench model of MCA with a pneumatic pump at different volumes of 0, 0.5, 0.75, 1.0, 2.0, 5.0, 10.0 and 20.0 ml. Assisted with Fast Fourier Transform (FFT) analysis of audio segments, it was reported that there was a linear relationship between emboli volume and the integrated value of the power spectrum up to 20 ml ($r^2=0.923$). This result is of direct interest in any study of cerebral air embolism using TCD. However, bubble size was not considered, and since the size of bubbles is likely to influence clinical evidence of embolism, this is a significant limitation to the study.

1.6.3. Investigation of the Factors Affecting Quantification of Embolic Signal

In 1975 Hills and Grulke applied two CW Doppler units (5 and 2.2 MHz) to detect air bubbles of sizes ranging from 40 to 2,500 μm at different velocities (20 to 55 cm/sec). Bubbles in size of over 150 μm were easily detected with either instrument and at all velocities settings. Conversely, bubbles less than 70 μm were undetectable by either device at any velocity. However, intermediate-size bubbles were detected only at higher velocities or when presented in a cluster or a cloud. This result suggested that the acoustic behaviour of bubbles changed according to the surrounding characteristics, including the fluid medium.

1.7. Aims of This Study

As a sensitive, convenient, and non-invasive diagnostic method, embolus detection with Doppler ultrasound offers the possibility of a new understanding of stroke and cerebral embolism and may have many important potential clinical applications. The localization of embolic source using Doppler ultrasound, and an examination of methods to size emboli and characterize their nature were principal aims of this study. As ultrasonic embolus detection is a relatively new technique verification of the ability and reliability of Doppler ultrasound in detection of circulating microemboli has already been recognized as important, and the evidence and failings of prior *in vitro* and *in vivo* models were taken into account.

The aim of this study was to improve our understanding of Doppler ultrasound techniques, in particular transcranial Doppler ultrasonography, in detection and differentiation of emboli by further evaluating the ability and reliability for sizing and characterizing embolic signals in an *in vitro* MCA model in a quantitative fashion.

Principally there was a need for assessing quantitative estimation of embolic signals in a model comparable to human detection in intracranial arteries. We chose and built a bench model to simulate the middle cerebral artery condition because the middle cerebral artery territory is the most common site for cerebral embolism (Barnett, 1991). It is the middle cerebral artery which is mostly frequently insonated by transcranial Doppler. On this basis, signal intensity analysis software was employed to

quantify the embolic signals produced by introduction of different types of embolic materials into this circuit. A wide range of embolic materials such as air bubbles, blood thrombus clot, platelet aggregate, atheroma, fat globules, and cholesterol crystals, which are assumed to be often involved in the cause of cerebral embolism, were ultrasonically examined in this setting.

Importantly, accompanied with a microscopic observation of embolus size, we made efforts to develop a method to standardize the size of different kinds of emboli, on which comparison of the signature characteristics among each types of emboli in terms of relative intensity unit and signal duration become realistic. By this means, the possibility of TCD ultrasonography for sizing and differentiating different emboli are evaluated.

It is an unanswered question whether or not Doppler ultrasound embolus detection can prove the origin of emboli in clinical situations (Russell et al, 1991). In this study, we also explored the potential to correlate experimental information to the clinical findings from patients undergoing cardiac catheterisation. In this study, we attempted to repeat clinical settings in the *in vitro* model and compare the embolic signals found *in vitro* and *in vivo* according to the intensity and duration of embolic signals.

Furthermore, an effort was also made to differentiate embolic signals with pathological flow phenomena such as spontaneous contrast echo and turbulence since the later have been reported to be commonly encountered in clinic and to co-exist with embolic incident in clinical situations.

Finally, it was important to examine several factors which may affect the embolus detection and quantification. This may enhance our understanding of embolus detection with Doppler ultrasound and help in interpretation of the results in this area.

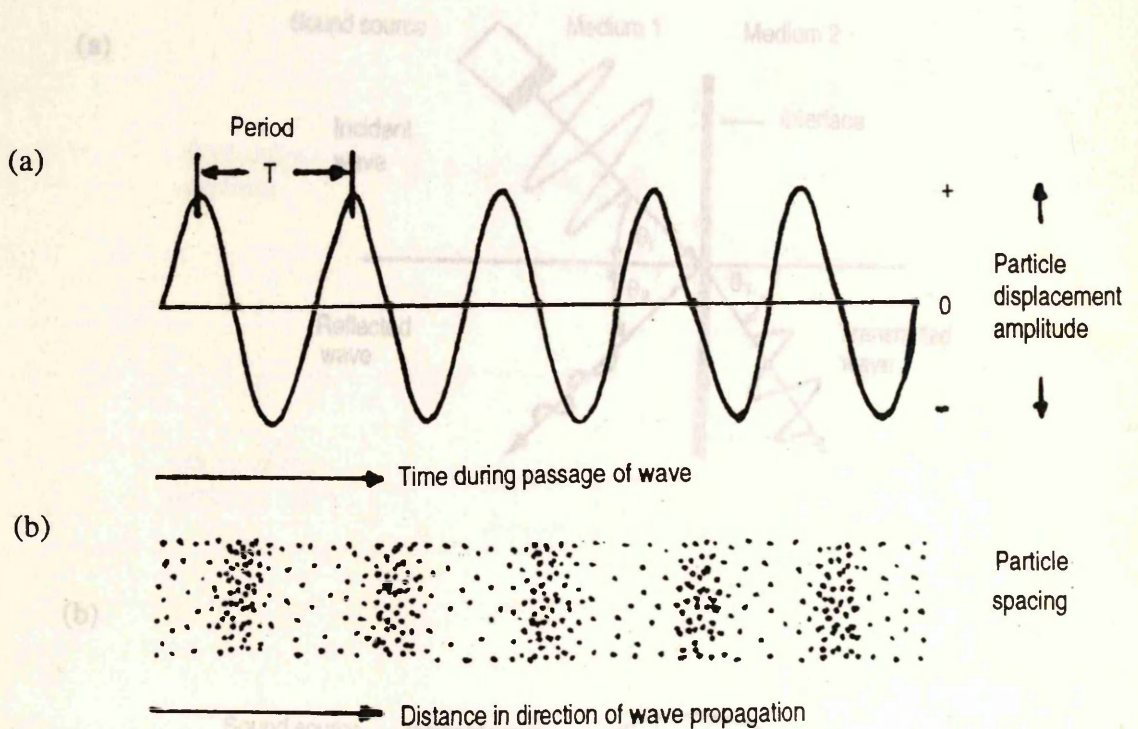


Figure 1.1 Longitudinal ultrasound wave motion. Diagrams illustrating displacement amplitude and particle spacing at a particular point in the ultrasonic field; (a) the distribution of wave in time; (b) the distribution of wave in space.

Adapted partly from Wells (1983).

Fig. 1.2. Reflection and refraction: (a) An ultrasound beam at a regular interface between two media is partly transmitted and reflected at the same angle of incidence (specular reflection); (b) the scattered wave is emitted in all directions (nonspecular reflection) when the wave length of sound source is larger than the interface.

θ_i : incident angle; θ_r : reflected angle; θ_t : transmitted angle.

Modified from Russell (1992).

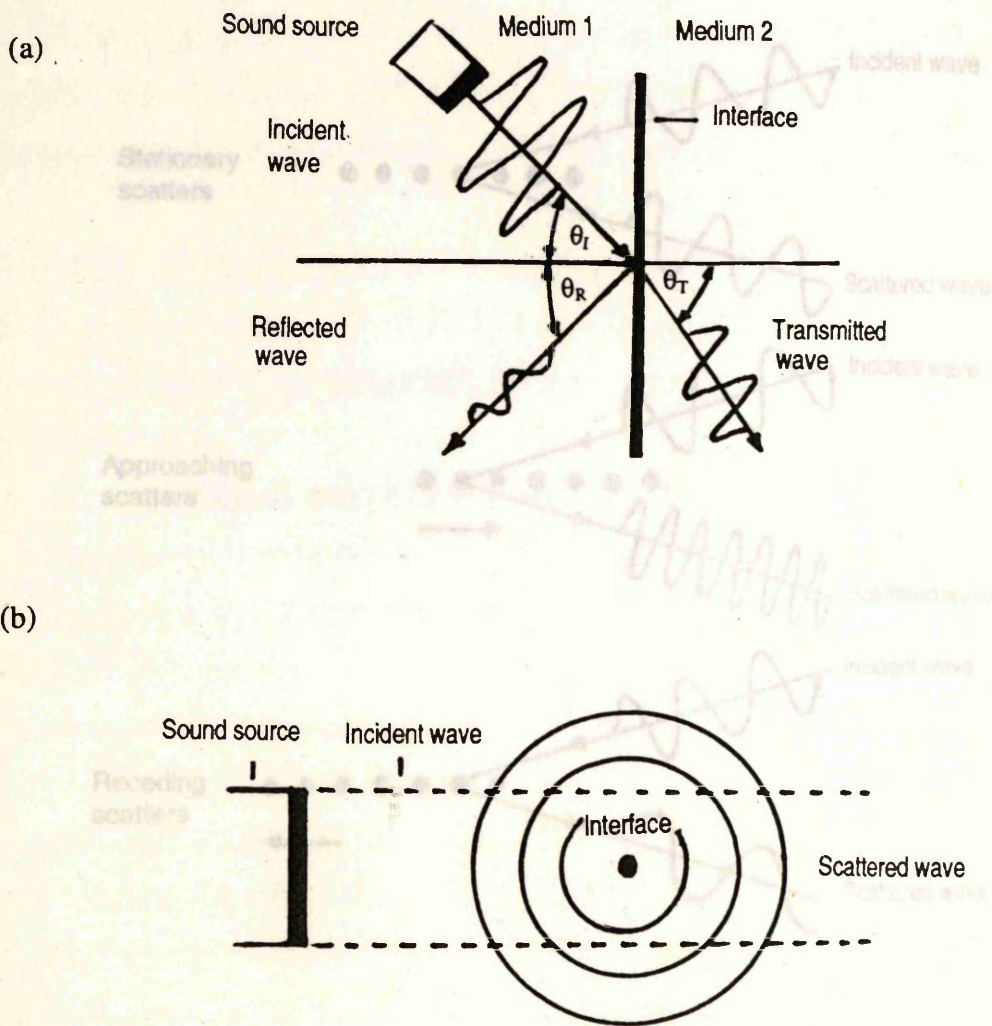


Figure 1.2 Two behaviors of ultrasound reflection. (a) An ultrasound beam at a regular interface between two media is partly transmitted and reflected at the same angle of incidence (specular reflection); (b) the scattered wave is emitted in all directions (nonspecular reflection) when the wave length of sound source is larger than the interface.

θ_I : incident angle; θ_R : reflected angle; θ_T : transmitted angle.

Modified from Russell (1992).

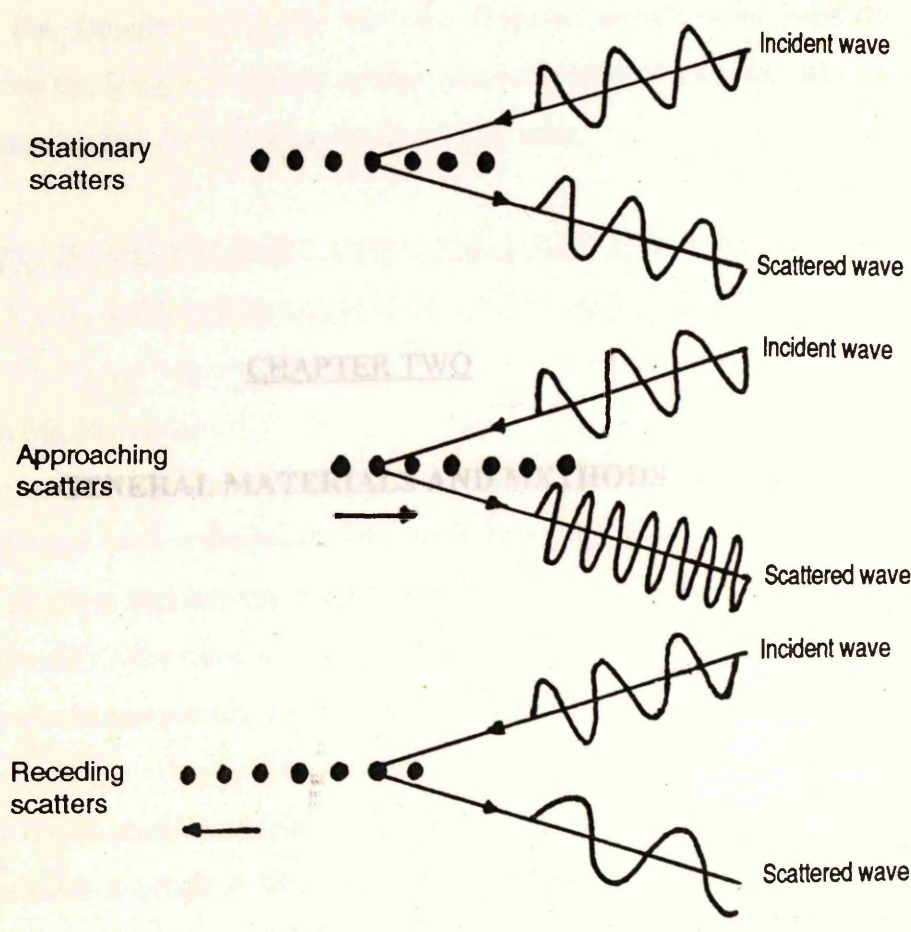


Figure 1.3 The Doppler effect. Diagrams illustrating the Doppler shift in frequency due to the motion of an ensemble of scatters.

Adapted from Wells (1983).

2.1 DEFINITION OF EMBOLIC SIGNAL

In this study, an embolic Doppler signal was defined as an embolus event-relevant, unidirectional Doppler signal with an increased intensity on a small band of frequencies in the Doppler spectrum. Embolic Doppler signals were carefully distinguished from the Doppler signal of artifact according to their different acoustic characteristics (see Section 1.4.2 of Chapter One for details).

2.2 DESIGN OF THE MODEL SIMULATING THE MIDDLE CEREBRAL ARTERY (MCA) AND PREPARATION OF CIRCULATING MATERIALS

2.2.1 The MCA Model

To quantify the embolic signals and evaluate the ability to characterise different types of embolic materials with transcranial Doppler ultrasonography, we developed a simple in vitro model to simulate the middle cerebral artery, into which different kinds but the same size of or the same source but different sizes of emboli materials were introduced, circulated and monitored.

The model, as shown diagrammatically in Figure 2.1, was constructed with a plastic box (length x width x height = 30 x 16 x 12 cm) inlaid with a piece of human temporal bone (average 1.5 mm in thickness) along the length of a side wall. A section of plastic tube or artery with an internal diameter of 4.5 mm, which falls within the normal range of the human middle cerebral artery dimensions (van der Linden and Casimir-Ahn, 1991), obliquely passed through the two walls of this box so that the angle between the direction of flow in the tube and the Doppler ultrasound beam from the probe positioned outside of the temporal bone was 30 degrees. The box was filled with normal saline. Two pumps, one constant flow pump (Model-C16.c., Charles Austin Pumps, UK) and one pulsed pump (H.R. flow inducer, Type-MHRE/72, Watson-Marlow, UK), were connected to the model in series. Thus a flow in pulsed fashion with an adjustable flow rate from 20 to 180 ml/min was available. Flow rate in the circulation was continually monitored with an in-line magnetic flow meter which was initially calibrated by repeated measurement of flow

rate using a glass measuring cylinder before use. At beginning of every test the circulation system was gently cleaned with normal saline to excluded gas bubbles trapped in tubing dead space.

2.2.2. Circulating Materials

Three kinds of circulating materials were used throughout the studies:

1. *0.3% Sigmacell Solution*

This was prepared by adding 3 grams of Sigmacell (Cellulose, type 20, SIGMA, USA) to 1000 ml normal saline which was previously degassed in a sonicator basin (Transsonic T890/H, CAMLAB, UK) for 15 minutes. This solution was stored in a 1000 ml glass reservoir and a magnetic stirrer hotplate was used to distribute the sigmacell evenly.

2. *Red Blood Cell (RBC) Concentrate*

Permission to use expired red blood cells was obtained from the local blood transfusion council. Red blood cell concentrate was diluted with degassed normal saline at a ratio of 3:2 (red blood cell concentrate : normal saline in volume) so that a similar red blood cell count as well as haematocrit (HCT) with those of whole blood was achieved.

3. *Human whole blood*

Human whole blood was obtained from the same source as above but used without dilution.

When using whole blood or diluted red blood concentrate as the circulating fluid, red blood cell concentration and haematocrit were measured throughout the study with Sysmex NE 8000 (TOA Medical Electronic, Japan).

2.3 DOPPLER ULTRASOUND EQUIPMENT AND OFF-LINE ANALYSIS

2.3.1 Doppler Ultrasound Equipment

Continuous Doppler monitoring was performed during each study using a TC2000 Transcranial Doppler Device (TCD) with a 2-MHz probe (Nicolet/EME, Warwick, UK). All TCD parameters and settings such as power, gain, sampling depth, sweep speed were kept constant throughout each study. The Doppler probe was held in place by a clamp which was mounted on calipers thereby allowing the probe to be precisely aligned with respect to the tube/artery. The ultrasound probe was coupled to the outside of the temporal bone with acoustic gel, and the angle between the transmitted ultrasound beam and forward flow in the tube inside the model was maintained at 30 degrees.

2.3.2 Off-line Analysis

Doppler signal analysis employs a 128-point Fast Fourier Transform (FFT). This mathematical approach can convert a complex waveform pulse wave into a series of sine waves characterised by amplitude (intensity), phase, and time period (Njemanze et al, 1991). Fourier analysis is based on the expression:

$$f(x) = \sum_{n=0}^{\infty} (a_n \cos nx + b_n \sin nx)$$

where
$$a_n = \frac{1}{\pi} \int_0^{2\pi} f(x) \cdot \cos nx \cdot dx$$

and
$$b_n = \frac{1}{\pi} \int_0^{2\pi} f(x) \cdot \sin nx \cdot dx$$

$f(x)$ = a periodic waveform defined in the interval $0 \leq x \leq 2\pi$ and satisfying the condition that $f(x)$ and its first derivative are piecewise continuous; n = harmonic number; nx = frequency of $f(x)$; a_n = amplitude of frequency of $\cos n$; b_n = amplitude of frequency of $\sin n$.

When such a waveform is analysed, then a series of components corresponding to $n = 1, 2, 3, \dots$, are obtained, whose intensities are given by

minutes. Platelet-rich thrombus was then formed, containing >99% platelets (Russell et al, 1991). The methods for sizing were the same as mentioned in Section 2.4.1 of

In this study, embolic signal intensity was calculated by analysis of digital spectral information as described by Muller et al (1991); each Fourier spectrum is described by a series of amplitude components, $A(i)$. As a measure of total reflected energy, the sum of the squared amplitude components is calculated and divided by the resolution to give an average intensity per spectral component, expressed as relative intensity units, i.e. mean intensity = $A^2(i) / \text{resolution}$. The total intensity of each embolic signal was calculated by summing of the average intensity per spectral line over which the embolus was visible (Figure 2.2).

2.4 PREPARATION OF EMBOLIC MATERIALS

2.4.1 Preparation of Whole Blood Clots

1 ml 0.2 M CaCl_2 solution was added to 10 ml whole blood obtained from a donor and then gently shaken. This blood was incubated at 37°C for 24 hours to clot. One gram of whole blood clot was then sliced with a McIlwain tissue chopper (Mickle Laboratory Engineering, UK) set at a cutting distance of $350\ \mu\text{m}$. Chopping was performed in four 90 degree directions. Clots were further agitated to reduce in size with a polytron (Type-PCU-2, Kinematica, Sweden) at a power of 4 watts for 3 seconds to produce microemboli. In some portions of the study larger clots were studied and in this instance small cubes were prepared by manually slicing instead of agitation with the polytron. Prepared clots were stored in 10 ml Dulbecco's phosphate buffer.

2.4.2 Preparation of Platelet-rich Thrombus

The method of making platelet-rich thrombus has been described by Russell et al (1991). 10 ml whole blood from a donor was anticoagulated with 0.5 ml 0.1 M citrate anticoagulant and centrifuged with a refrigerated centrifuge (Sorvall RT6000B, Refrigerated Centrifuge, Du Pont, Stevenage, UK) at $100 \times G$ for 15 minutes to prepare platelet-rich plasma. One ml of platelet-rich plasma was added to 2 ml of 10 units/ml bovine thrombus (Sigma Chemical Co., USA) and stored at 20°C for 30

minutes. Platelet-rich thrombus was then formed, containing >99% platelets (Russell et al, 1991). The methods for sizing were the same as mentioned in Section 2.4.1 of this Chapter.

2.4.3 Preparation of Platelet Aggregate-rich Plasma

20 ml of human blood was collected from a donor, transferred into a Universal container containing 2 ml of sodium citrate and centrifuged in an MSE Mistral 2L at 970 r.p.m. at 20⁰ C for 10 minutes to obtain platelet-rich plasma (PRP). After centrifugation, the PRP obtained was pipetted off to a tube and capped tightly to be isolated from air outside. A platelet count was obtained using a Sysmex NE-8000.

One ml (containing 0.5 mM) of ADP ascorbic acid/saline solution was added to 6 ml PRP and incubated at 37⁰ C for 10 minutes to commence aggregation. Once aggregation was initiated, visible platelet aggregates could be observed. Then the platelet aggregate-rich plasma was counted again to determine the percentage of the platelets which were aggregated.

2.4.4 Preparation of Human Atheromatous Emboli

Human atheromatous material was obtained from patients undergoing carotid endarterectomy and sliced into small cubes (size range of 50-180 μ m) with a surgical blade. Atheromatous emboli were used within eight hours of surgical dissection.

2.4.5 Preparation of Microbubbles

15 ml of Ultravist 370, a non-ionic contrast medium (Schering Health Care Ltd., Germany) was drawn into an agitation chamber, which composed of a plastic cylinder with height of 15 cm and 2.5 cm in diameter and a side port (see Figure 2.3). The horn of the polytron was placed 0.5 cm from the bottom of the chamber and used to generate microbubbles by stirring for 40 seconds with power set at 10 watts. Microbubbles with a diameter of approximately 30 μ m were generated. Smaller microbubbles with an average diameter of 5 μ m were produced with 5% bovine albumin solution (diluted in normal saline) instead of Ultravist 370 and was agitated with the polytron at power of 3 watts for 15 seconds.

calculated by microscopic examination and adjusted by dilution with 25 ml 99%

The size of prepared microbubbles was further controlled by transferring into a size-control set. This set was constructed with a 20 ml plastic syringe which was inlaid by two micro-filter membranes, the first one with the pore size of 40 μm (AF-10250, arterial blood filter, Baxter Healthcare, USA) and the second with the pore size of 30 μm (AN 3H, Millipore, UK). A side-port was located between the two micro-filter membranes. Once the agitated bubble-rich medium was transferred into the set through the bottom of the syringe, certain prompting pressure was given manually. This allowed microbubbles with the diameter over 40 μm to stay outside the first filter and those with the diameter below 30 μm to pass through the second filter. Thus, the filtrate containing microbubbles with a diameter ranging from 30 μm to 40 μm stayed between the two micro-filters and were obtained through a side-port of this set (see Figure 2.4).

100 μl of whole blood clots or cholesterol crystals was sampled with a pipette and

2.4.6 Preparation of Fat Globule Emboli and measurement.

Two grams of subcutaneous fat tissue taken from the lower rabbit abdomen was chopped with a McIlwain tissue chopper described in Section 2.3.1 of this Chapter. Chopped fat tissue was put into the agitating chamber with 10 ml normal saline at 30 $^{\circ}\text{C}$ and agitated with the polytron at power of 3 watts for 6 seconds. The agitated fat tissue was pulled into the size-control set (previously described in Section 2.4.5 of this Chapter) for double filtration. Finally the filtrate between two filter membranes was withdrawn with a 10 ml plastic syringe through a side-port of this set. Fat globules in the range of 30 - 40 μm were ready for further measurement as well as injection.

Specific statistical techniques appreciated in the individual study are described as

2.4.7 Preparation of Cholesterol Crystal Emboli

One gram of cholesterol fine powder (C-8503, Sigma, USA) was added to 50 ml 99% ethanol in a 200 ml glass container. Manual agitation was carried out for 40 minutes when this mixture was bathed at 50 $^{\circ}\text{C}$ to dissolve. Then, the cholesterol ethanol solution was evaporated in a water bath at a temperature of 100 $^{\circ}\text{C}$ for 50 minutes until cholesterol crystals formed. The concentration of the crystals was

calculated by microscopic examination and adjusted by dilution with 25 ml 99% ethanol.

2.5 MEASUREMENT OF EMBOLIC MATERIALS

Air bubbles and fat globules were sampled from the central part of their solutions immediately after preparation and dropped onto a blood chamber. The concentration of bubbles or globules was determined microscopically by counting the number of the emboli in four separate blocks with a volume of 1 mm^3 . The size of bubbles or globules was measured with a net reticule eye piece. To size solid embolus materials, the longest and the shortest edges were measured, and the average length [(the longest edge + the shortest edge) / 2] calculated.

100 μl of whole blood clots or cholesterol crystals was sampled with a pipette and dropped onto a glass slide for counting and measurement.

To determine the mean size of each kind of embolic materials when injecting them in multiple fashion, 50 embolic particles were measured for each sample.

2.6 DATA ANALYSIS

All data in this study were expressed as mean \pm 1SD. Student *t*-testing was used to investigate the differences between two groups and one way ANOVA was used for comparison among more than two groups. Correlation coefficients and regression were calculated to test the relationship between the variables and their responses. Specific statistical techniques appreciated in the individual study are described as appropriately. All the data analysis was performed on a computer using the Minitab Data analysis software (version 7.1) (Minitab, Inc, USA, 1989).

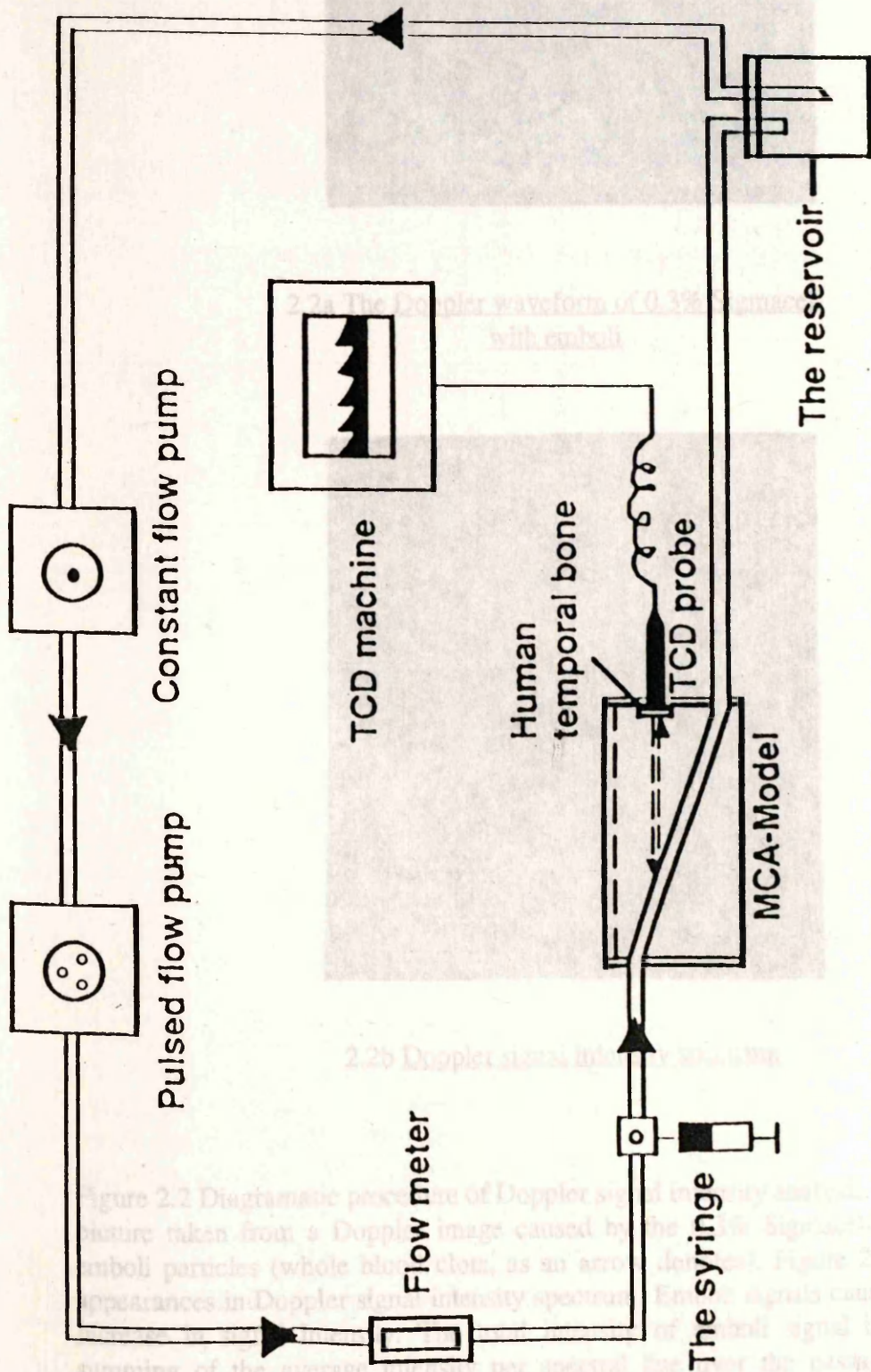
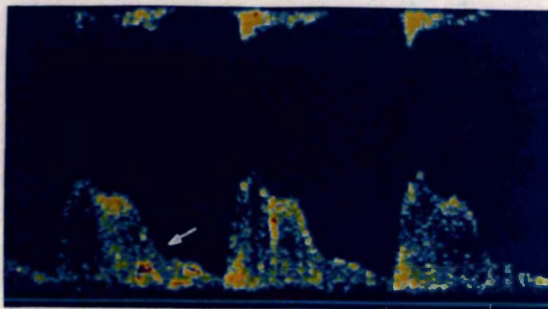
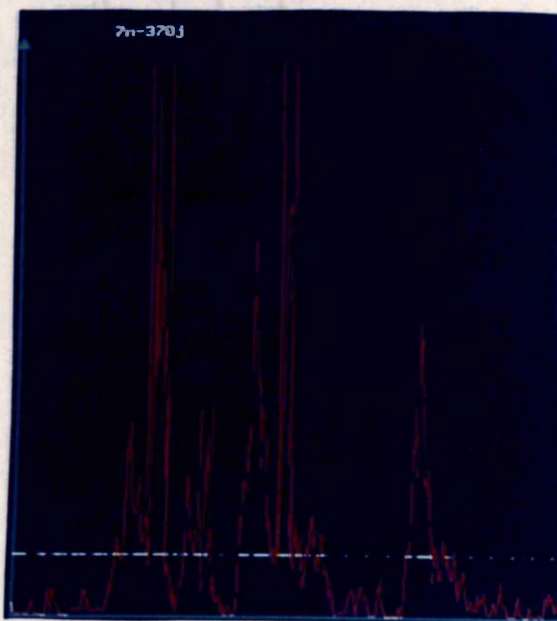


Figure 2.1 Illumination of the MCA model and circuit. Circulating material was pumped into the MCA model in pulsed fashion by two pumps and the emboli were injected via the side port. Embolic Doppler signals as well as flowing velocity waveform were continuously recorded from the ultrasound probe which was coupled with the outside of temporal bone.



2.2a The Doppler waveform of 0.3% Sigmacell with emboli



2.2b Doppler signal intensity spectrum

Figure 2.2 Diagrammatic procedure of Doppler signal intensity analysis. Figure 2.2a is a picture taken from a Doppler image caused by the 0.3% Sigmacell flow with two emboli particles (whole blood clots, as an arrow denotes). Figure 2.2b shows their appearances in Doppler signal intensity spectrum. Emboli signals caused a significant increase in signal intensity. The total intensity of emboli signal is calculated by summing of the average intensity per spectral line over the passage duration (as arrows denote).

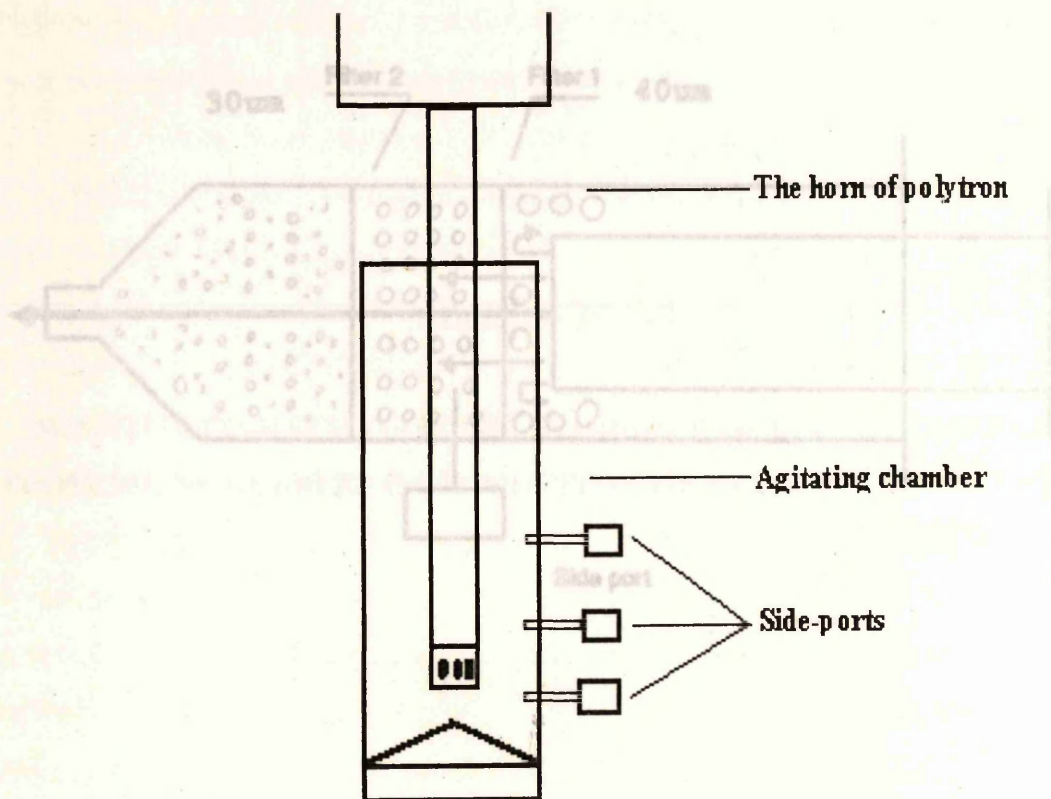


Figure 2.4 Diagrammatic illumination of the size-control set. The size-control set was constructed with two micro-filter membranes, filter 1 with pore size of 40 μm .

Figure 2.3 Diagrammatic illumination of the agitation chamber. 10 - 15 ml bubble-carrier solution was agitated with the horn of the polytron, which was placed 0.5 cm from the bottom of the chamber, to generate microbubbles. The agitation speed and period can be adjusted. The microbubble-rich solution was withdrawn from the side-port of the chamber for injection as well as for measurements.

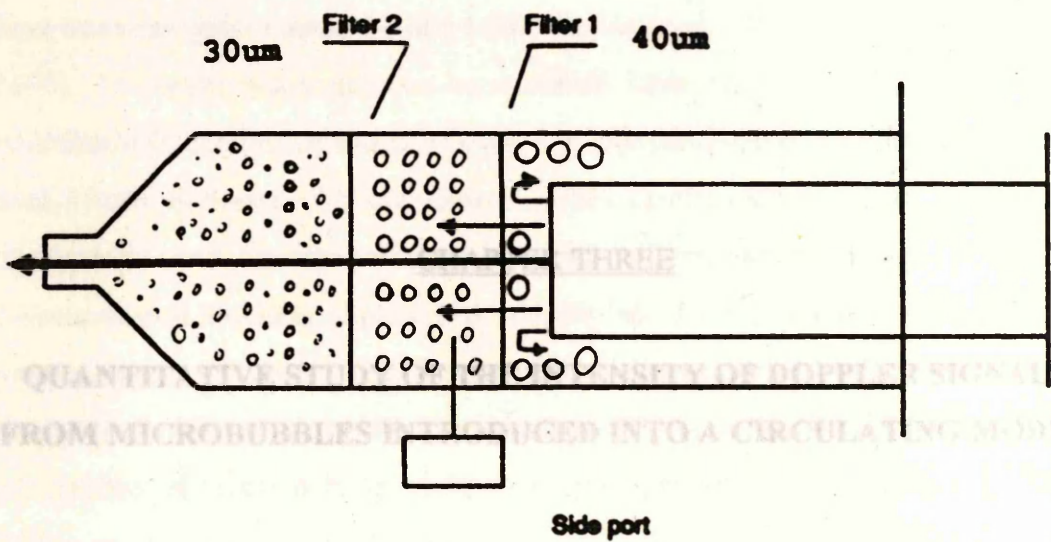


Figure 2.4 Diagrammatic illumination of the size-control set. The size-control set was constructed with two micro-filter membranes, filter 1 with pore size of 40 µm and filter 2 with pore size of 30µm. The filtrate containing particles with the size ranging from 30 to 40 µm was obtained from the side port of this set.

3.1 INTRODUCTION

3.1.1 Microbubbles and Gaseous Cerebral Embolism

Problems associated with the introduction of gaseous microemboli into the circulation have been recognised since the mid 1600s (Davis et al, 1970 and Butler and Kurisa, 1985). In recent years gaseous microemboli have been considered as a major contributor to cerebral dysfunction occurring after cardiopulmonary bypass (Spencer et al, 1969b; Editorial, 1975 and Gilston, 1986), carotid endarterectomy (Padayachee et al, 1986 and Spencer et al, 1986) and decompression sickness (Spencer et al, 1969a). Although major strokes due to

CHAPTER THREE

QUANTITATIVE STUDY OF THE INTENSITY OF DOPPLER SIGNALS FROM MICROBUBBLES INTRODUCED INTO A CIRCULATING MODEL

of intellectual function in up to 70 % of such patients (Padayachee et al, 1986). Although the aetiology of this cerebral dysfunction is likely to be multifactorial, gaseous embolism is considered to be a major source. A study of the cerebral effects of cardiopulmonary bypass by the USA Food and Drug Administration (Mortensen et al, 1981) concluded that 'it appears likely that some degree of embolisation of microbubbles was inherent in most CPB perfusions and if not excessive, is probably acceptable under current technology.' However, despite a lack of methods of quantifying emboli there has been an available technique for defining excessive embolisation until recently.

3.1.2 Ultrasound Detection of Microbubbles

It seems possible that ultrasound techniques which have been applied since 1965 to detect abnormally high amplitude signals attributable to microbubbles could be refined to develop a method of quantifying emboli. In particular, the technique of transcranial Doppler (TCD) introduced in 1982 may be preferable in studying neurological complications of bypass surgery since it allows continuous detection of gaseous microemboli in major cerebral vessels.

With this non-invasive technique, bubble embolic signals have been detected in the middle cerebral artery (MCA) in patients during CPB (Padayachee et al, 1987a, b, 1990). In an animal model study, it was found that the intensity of signals produced by bubbles and fat emboli was greater than signals

3.1 INTRODUCTION

3.1.1 Microbubbles and Gaseous Cerebral Embolism

Problems associated with the introduction of gaseous microemboli into the circulation have been recognised since the mid 1600s (Davis et al, 1970 and Butler and Kurusz, 1985). In recent years gaseous microemboli have been considered as a major contributor to cerebral dysfunction occurring after cardiopulmonary bypass (Spencer et al, 1969b, Editorial, 1975 and Gilston, 1986), carotid endarterectomy (Padayachee et al, 1986 and Spencer et al, 1990), hip arthroplasty (Svartling, 1988), and decompression sickness (Spencer et al, 1969a). Although major stroke due to cardiopulmonary bypass (CPB) is rare and most patients recover without residual disability (Pugsley et al, 1990), neuropsychological tests revealed minor impairment of intellectual function in up to 70 % of such patients (Padayachee et al, 1988). Although the aetiology of this cerebral dysfunction is likely to be multifactorial, gaseous embolism is considered to be a major source. A study of the overall safety of cardiopulmonary bypass by the USA Food and Drug Administration in 1981 (Mortensen et al, 1981) concluded that 'It appears likely that some degree of embolisation of microbubbles was inherent in most CPB perfusions, and if not excessive, is probably acceptable under current technology.' However, in the absence of methods of quantifying emboli there has been no available technique for defining excessive embolisation until recently.

3.1.2 Ultrasound Detection of Microbubbles

It seems possible that ultrasound techniques which have been applied since 1965 to detect abnormally high amplitude signals attributable to microbubbles could be refined to develop a method of quantifying emboli. In particular, the technique of transcranial Doppler (TCD) introduced in 1982 may be preferable in studying neurological complications of bypass surgery since it allows continuous detection of gaseous microemboli in major cerebral vessels.

With this non-invasive technique, bubble embolic signals have been detected in the middle cerebral artery (MCA) in patients during CPB (Padayachee et al, 1987a, 1987b and Harrison et al, 1990). In an animal model study, it was found that the intensity of signals produced by bubbles and fat emboli was greater than signals arising from platelets and blood clots (Russell et al, 1991). In an MCA model there was no difference in the high-amplitude signals produced by bubble injection when compared with those seen in the patients during bypass (Pugsley et al, 1990). In this study, however, the size and the number of bubbles injected was not specified. Quantification of numbers of high-amplitude signals produced by gaseous microemboli has been used in a clinical study of cardiopulmonary bypass but not of signal intensity (van der Linden and Casimir-Ahn, 1991). Thus previous reports have not satisfactorily documented a quantitative relationship between the intensity of microbubble signals and the number and/or type of microbubbles introduced, which may yield vital information correlating total numbers of bubbles passing into the brain and patient outcome after cardiopulmonary bypass.

signals was logarithmically proportional to the sizes of emboli. However, these studies

3.1.3 The Models to Detect Air Microemboli

In order to qualify and quantify the proposed embolic Doppler signals and furthermore, to correlate the embolic signal with the size of embolic materials of certain source, a circulating model is needed.

3.1.4 Preparation of Embolic Materials

Initially, Russell et al (1991) developed an animal model to test the ability of transcranial Doppler ultrasound to detect arterial embolic composed of materials that are often involved in cerebral embolism. In his study, the aorta and left renal artery were cannulated in an anaesthetised rabbit. Doppler signals caused by injection of embolic materials were obtained with a 2-MHz probe which was clamped in position over the abdomen aorta at an angle of 45 degrees and 7 cm caudal to the left renal artery when emboli were introduced into the rabbit aorta via the left renal artery. The results of this experiment demonstrated that TCD may detect different kinds of emboli in a range of sizes. However, this approach may overestimate the sensitivity of embolus detection when compared to the human cranial circulation since the intensity of ultrasonic signals reflected from flowing blood or circulating emboli can be

remarkably reduced by skull bone due to its big acoustic impedance. More representative models were employed for this purpose by Pugsley et al (1990) and Markus et al (1993b). In their studies, a short segment of vein (Pugsley et al) or plastic tube (Markus et al, 1993b) with internal diameter of 5 mm, which is almost equal to the internal diameter of the middle cerebral artery (2.4 - 4.6 mm) (Gibo et al, 1981), was positioned to approximate the course of the MCA in a human skull surrounded and filled by acoustic coupling gel. A probe was then placed on the outside of the skull, just above the zygomatic arch so that circulating flow could be insonated via the transtemporal window of the skull at a depth of 5 cm. Blood (in the former study) or saline mixed with a 0.001% solution of Tween 80 (in the latter study) was used as circulating fluid and was prompted through the extracorporeal circuit by a pump. With such a model, Pugsley et al (1990) reported that the high-amplitude flow disturbance signal related to introduction of microbubbles in the circuit were similar to those found in the patients undergoing cardiopulmonary bypass. Markus et al (1993b) observed that the maximum amplitude of embolic signals was logarithmically proportional to the sizes of emboli. However, these models produced some technical difficulty such as in positioning 'the middle cerebral via the carotid canal' (Markus et al, 1993b), so that visual information about the emboli passing through the ultrasound sampling volume was limited.

3.1.4 Preparation of Embolic Materials

Methods of preparing different kinds of embolic materials such as clotted whole blood, platelets-rich thrombus, atheromatous materials, fat tissue and air bubble emboli have been well documented (Russell et al, 1991, Pugsley et al, 1990, Markus et al, 1993b). However, soluble fat globules rather than solid fat tissue may be involved in cerebral embolism due to cardiopulmonary bypass and trauma (Caguin and Carter, 1963 and Muller et al, 1992). Little work has been done to test the ability of TCD to detect fat globules as embolic material. Additionally, the size and the number of air bubbles introduced in previous studies were poorly controlled.

Finally, proper measurement of embolic material size is a precondition to establishing the quantitative relationship between Doppler signal and embolus size. However, it is

difficult to measure the size of prepared microemboli because of their irregular shapes and their softness and/or friability on handling. In Russell et al's (1991) study, embolus size was indirectly estimated from the weight of embolus and its gravity. This calculation is quite rough due to the uncertain shape of emboli. Markus and colleague (1993) improved the methodology by measuring the maximum length of the longest edge and the maximum cross-sectional area for each embolus. However, it is clear that the length of shortest edge should not be overlooked since an embolus may reflect ultrasonic beams with the shortest edge when passing the sampling volume.

3.1.5 Aims

There were three targets in this study. First, we developed a simple method to prepare stable microbubbles of a controlled size and concentration. Because air microbubbles are by their nature effervescent and therefore changing with time, we also observed the half life of the microbubbles prepared in two different solutions. Secondly, we aimed to demonstrate the utility of transcranial Doppler ultrasound using ultrasound signal intensity to quantify microbubbles. The hypothesis was of an increase in intensity of Doppler ultrasound signal on the introduction of microbubbles and a change of signal intensity corresponding to the number of microemboli introduced. For this an *in vitro* flow system was used, which consisted of a MCA model and allowed careful control of the ultrasonic monitoring equipment, volumetric flow, and microbubble injection. Finally, we also examined the quantification according to air bubble concentration.

3.2 MATERIALS AND METHODS

3.2.1 The Middle Cerebral Artery (MCA) In Vitro Model.

The *in vitro* model used in this study to simulate the MCA is described in detail at Section 2.2.1 of Chapter Two and illustrated in Figure 2.1. 0.3% Sigmacell (Cellulose, type 20, SIGMA, USA) solution was used as circulating fluid. This circulating fluid was prepared by dilution with distilled normal saline and then degassed for 15 minutes in the basin of a sonicator (Transsonic T890/H, CAMLAB,

UK). After degassing, it was gently transferred into a 1000 ml glass container and circulated through a plastic tube with an internal diameter of 4.5 mm [representing the upper limit human MCA diameter (van der Linden and Casimir-Ahn, 1991)]. The Sigmacell solution was not recirculated. Adjustments to the on-line magnetic flow meter, and two pumps were made to maintain the pulsed flow at 15 to 20 ml/sec.

In order to distribute the Sigmacell evenly in the circulation, a magnetic stirrer hotplate was placed under the bottom of the glass container and operated throughout the experiment.

3.2.2 Microscopic Study of Microbubbles

Determination of the number and the size of prepared microbubbles was described in Chapter Two. The half life ($t_{1/2}$) of microbubbles in Ultravist 370 and in 5 % bovine albumin solution was measured in repeated counts at 1 min, 2.5 min, 5 min, 7.5 min, 10 min, 15 min, 20 min, 25 min after preparation. Ten samples were tested for the half life of microbubbles in each solution. The precision of microbubble size in prepared samples was also assessed by calculation of the coefficient of variance. The temperature caused by agitation of Ultravist 370 with the polytron was also measured.

3.2.3 Microbubble Preparation

15 ml of Ultravist 370, a non-ionic contrast medium (Schering Health Care Ltd. Germany), used as a microbubble-carrier solution, was drawn into an agitation chamber with a side port (See Figure 2.2). The probe of a polytron (Type-PCU-2, Kinematica, Sweden) was placed 0.5 cm from the bottom of the chamber and used to generate bubbles by stirring in the medium for 40 seconds with the power setting at 10 W.. Then the bubble-rich medium was obtained through a side-port and taken away for microscopic examination immediately. In the same way, five samples of microbubbles in 5 % bovine albumin solution were also prepared.

3.2.4 Investigation of the Relationship between Signal Intensity and the Number of Microbubbles

(I/B) which was calculated as total bubble intensity produced following each injection volume divided by the total number of bubbles in that

The quantitative relationship between signal intensity and microbubbles was tested at two different microbubble concentrations. Each concentration test further consisted of a range of bubble number injections, which was done by injecting microbubble-rich contrast medium at that concentration in different volumes, 0.1, 0.2, 0.4, 0.6, and 0.8 ml.

To prepare different concentrations of microbubbles, 0.1 or 1 ml microbubble-rich medium was sampled from the chamber with a pipette and diluted with 9.9 ml or 9.0 ml Ultravist 370 contrast medium. The diluted solution was then gently stirred for 10 seconds to distribute the microbubbles evenly. Thus, 1 % and 10 % microbubble solutions were prepared. The concentration of the two diluted microbubble-rich medium was determined by immediate microscopic examination (described in Section 2.5 of Chapter Two). For each concentration, 0.1, 0.2, 0.4, 0.6, 0.8 ml of the microbubble solution was then injected into the MCA circulation model. Thereby the number of microbubbles introduced into the circuit for each injection can be estimated by the following equation: the concentration of microbubbles x the volume of microbubble medium injected. Each sample was repeated eight times. In order to offset the order-effect due to bubble decay during injections, the order of injections was reversed for the second half of the samples and as a consequence, eight data of Doppler signal intensity in each injection volume were obtained. The same volume of Ultravist 370 without bubbles was injected into the circulation system as control.

Each above injection was completed within 0.5 second. This infusion rate was much lower than the overall volumetric flow rate within the system, and therefore had no significant effect on the overall volumetric flow rate or velocity of flow.

3.2.5 Investigation of the Effect of Bubble Concentration on Signal Intensity

The effect of different concentrations of bubbles on Doppler embolic signal intensity was studied using three approaches. Firstly the relationship between the two concentrations of microbubbles was assessed. Secondly, we examined the signal intensity per bubble (I/B) which was calculated as total bubble intensity produced following each injection volume divided by the total number of bubbles in that

injection. Finally, we injected the same number of microbubbles in different concentrations. This was done by immediately diluting the prepared microbubble-rich contrast medium to 1:40, 1:60, 1:80 to 1:200 and injecting the same volume (1 ml) of microbubble-rich medium in different dilution ratios into the circuit. The Doppler signal intensity for the same number of bubbles in different dilution ratios was estimated by using the product of signal intensity of each dilution and its times of dilution [Estimated Doppler signal intensity = signal intensity (1 ml sample) x the denominator of dilution ratio]. Four samples were repeatedly injected for each dilution ratio.

3.2.6 Analysis of Doppler Signal Intensity of Microbubbles

A 2 MHz-probe of transcranial Doppler was put on the temporal bone coupling with acoustic gel (Figure 2.1.). TCD parameters of frequency, gain, power and depth of insonation of TCD were fixed throughout the study. Firstly, six screens of the background signals produced by circulating Sigmacell were continually recorded. Then the Doppler signals due to injection of degassed medium (control) and embolic Doppler signals relating to microbubble-rich medium injected in different volumes were recorded separately. The intensities of signals were quantitatively processed off-line with the intensity analysis software described in Chapter Two. For quantification of embolic signals, the resulting data were represented as the total Doppler signal intensity over the duration of its passage. To exclude the signal intensity increased by contrast medium used as the microbubble-carrier solution, the intensities of signals produced purely by microbubbles (in each different injection volume) were obtained by employing the equation:

$$I_E = I_M - I_C$$

3.3 RESULTS

where, I_E = Embolic signal intensity (signal intensity purely due to introduction of embolic microbubbles); I_M = Signal intensity due to injection of microbubble-rich medium; I_C = Signal intensity due to injection contrast medium only.

3.1b) in terms of shape and background intensity although there was a higher
3.2.7 Preparation of Different Sizes and Concentrations of Microbubbles in

Ultravist 370

In order to verify the potential utility of the method applied in this study to prepare microbubbles, we also processed microbubbles under the following conditions: (1) The power of polytron was adjusted to 2, 4, 6, 8, and 10 W., with an agitation time of 40 seconds; (2) The agitation time was set at 10, 20, 40, 60, and 90 seconds separately to produce bubbles in Ultravist 370 (power 8 W. during each preparation); (3) Ultravist 370 contrast medium was diluted with normal saline in different ratios: Ult.370 : N.S.=10:0, 9:1, 3:1, 1:1 and 1:3 (power 8 W., agitation 40 seconds); (4) 0.5, 1.5, 3 ml of 2.5 per cent albumin solution were added into 9.5, 8.5, 7 ml of Ultravist 370 contrast medium to form 1:19, 3:17, and 3:7 mixture solutions (power 8 W., agitation 40 seconds). Each condition of preparation of microbubbles was repeated five times and the mean bubble size and bubble concentration were measured as described in Chapter Two.

3.2.8 Statistical Analysis.

The correlation coefficient and linear regression was calculated from the quantitative study of relationship between TCD intensity and the number of microbubbles. In the observation of the effect of different concentrations of microbubbles on the signal intensity, *t*-testing was used to compare signal intensities among different dilution ratios with appropriate correction for multiple comparison. Results were considered significant if $p < 0.05$. Results of size and the concentration were expressed as mean \pm 1SD.

3.3 RESULTS

3.3.1 Doppler Signals Produced on the MCA model

Satisfactory Doppler velocity waveform was obtained by 0.3% Sigmacell solution circulating in the MCA model (Figure 3.1a). This *in vitro* Doppler signal was matchable to that collected from human MCA (with the same TCD settings) (Figure

3.1b) in terms of shape and background intensity although there was a higher pulsatility in the bench circuit. Introduction of pure Ultravist 370 contrast produced a general increase in reflected signal intensity within the flow waveform, while microbubble-rich contrast medium produced an even higher reflected signal which was less homogeneous, consisting of stripes of increased signal intensity which could extend beyond the maximum velocity envelope of the Doppler waveform.

3.3.2 Microscopic Examinations

The mean size of microbubbles prepared in Ultravist 370 contrast medium for signal intensity quantification in this study was $34.3 \pm 9.2 \mu\text{m}$ (Figure 3.2). The mean size of the microbubbles produced in 5% bovine albumin solution with a polytron was $5.6 \pm 1.9 \mu\text{m}$ (Figure 3.3). The bubble concentration was 1.4×10^5 bubbles/ml for dilution ratio 1:10 and 1.4×10^4 bubbles/ml for dilution ratio 1:100. The $t_{1/2}$ of microbubbles in the two bubble-carrier solutions is shown in Figure 3.4. The $t_{1/2}$ of microbubbles in Ultravist 370 (5.25 ± 0.89 min.) was two times longer than that in 5% albumin solution (2.6 ± 0.43 min.) ($p < 0.05$). The precision of bubble size for microbubbles in Ultravist 370 contrast medium was 4.7%. The mean temperature increased $10.24 \pm 0.06^\circ\text{C}$ (from $18.6 \pm 0.27^\circ\text{C}$ to $28.9 \pm 0.27^\circ\text{C}$) immediately after agitation of bubbles ($p < 0.01$).

3.3.3 Relation between Signal Intensity and the Number of Microbubbles

There was a linear relationship between Doppler intensity and the number of microbubbles in both concentrations (Figure 3.5). Signal intensity was proportional to the number of microbubbles introduced. The correlation coefficient (r) of the relationship is 0.90 ($p < 0.001$) either for the higher bubble concentration with dilution ratio 1:10 (1.4×10^5 bubbles/ml) or for the lower bubble concentration with dilution ratio 1:100 (1.4×10^4 bubbles/ml).

3.3.4 Effect of Concentration of Microbubbles on the Signal Intensity

Although an increase in microbubble numbers produced higher Doppler signal intensity (Figure 3.5) the relationship was not directly proportional. For example, for the 1:10 dilution, a doubling of the injected number of bubbles (from 0.1 ml to 0.2 ml

in volume) increased signal intensity from 1×10^5 to 1.55×10^5 units. Also the Doppler signal intensity from higher microbubble concentration (1.4×10^5 bubbles/ml) was only 2.5 times more than that from low microbubble concentrations (1.4×10^4 bubbles/ml) although the dilution was by a factor of ten.

The results illustrated in Figure 3.6 show a higher signal intensity per bubble for greater dilution (1:100 versus 1:10) and lower volumes of injection. This inverse relationship was in sharp contrast to that for Figure 3.5. It is apparent that the volume of intensity per bubble decreased with an increase in the number of air bubbles injected into the model.

The data from the observation of injection of the same number of microbubbles in different concentrations is summarised in Figure 3.7. The bubble concentration without dilution was 1.4×10^5 bubbles/ml. Injections of microbubbles higher bubble concentrations, e.g. 1:40 and 1:60, tended to produce less Doppler signal intensity than those at lower bubble concentrations but the overall difference other than for 1:40 ($p < 0.05$) was not significant.

3.3.5 Establishment of the Microbubble Preparation Techniques

The effect of alteration in polytron power on bubble size is summarised in Figure 3.8. Increasing the power from 2 to 4 Watts increased bubble size remarkably but no evident difference of bubble size was found when the power was changed from 4 to 10 Watts. The data from Figure 3.9. indicated that the power set at 2 Watts obtained few bubbles but the bubble concentration was sharply increased as soon as power was changed to 4 Watts or more.

Shorter periods of agitation produced larger microbubbles of variable size whereas longer agitation introduced smaller but more uniform microbubbles (Figure 3.10). Moreover, there was a relatively steady bubble size between 20 and 40 seconds of agitation. There was an inverse correlation between agitation period and bubble concentration (Figure 3.11).

Dilution of bubble-carrier solution (Ultravist 370) did not change bubble size (Figure 3.12) but reduced bubble concentration significantly according to the dilution ratio (Figure 3.13).

After the mixture of Ultravist 370 and 5 % bovine albumin was agitated with the polytron, microbubbles with two distinguished diameters (average of 5 μm and 34 μm respectively) were found to co-exist in the mixing solution.

3.4 DISCUSSION

We successfully proved that the simple MCA model used in this study can match the required standards: a pulsed-fashion waveform was satisfactorily obtained with a 2-MHz TCD probe, and off-line signal intensity analysis could be carried out. Sigmacell solution at the concentration of 0.03 % supplied a good acoustic imaging in which embolic signals were easily identified. Application of Sigmacell solution instead of blood as a circulating material may not be only more economical but also can avoid possible contamination.

A marked increase was observed in Doppler signal intensity which appeared as a high-amplitude TCD signal after introduction of microbubble-rich contrast medium into the MCA model. This is in keeping with previous observations both in experimental models (Pugsley et al, 1990 and Russell et al, 1991) and in clinical studies (Gilston, 1986 and Padayachee et al, 1988). Such ultrasonic properties of bubbles are due to highly different acoustic impedance Z ($\text{gm}/\text{cm}^2 \times \text{sec}$) between air ($Z = 0.0043 \times 10^5$) and blood plasma ($Z = 1.4 \times 10^5$) (Nishi, 1972 and Shimon et al, 1989). In contrast, in blood cells ($Z = 1.5 \times 10^5$) and other soft tissues (brain, $Z = 1.56 \times 10^5$), the impedance Z does not differ so much. The same principle also explains the increase in Doppler intensity produced by pure contrast medium against a background waveform from 0.03% Sigmacell circulatory solution.

We have identified a quantitative relationship between Doppler signal intensity and the numbers of microbubbles, which is in accord with the experimental observation by

Schwarz et al (1993) using a higher frequency transducer and smaller microbubbles but which has not been documented in previous transcranial Doppler studies. Also a quantitative correlation from two concentrations of microbubbles was defined. Although it is difficult to calibrate Doppler intensity for clinical application establishment of criteria for excessive embolisation may be possible.

Second, the intensity of scattered ultrasound from any microscopic target

In this quantitative study, we also found that although there was close correlation between Doppler intensity and the number of microbubbles at both dilution ratios the increment of Doppler intensity was not directly proportional at a ratio of 1:1 to the increment of microbubbles injected. We preliminary analysed these results and found that signal intensity increased per bubble (intensity/bubble) from higher concentration was evidently less than that from lower concentration. It seems that the more bubbles injected, the less signal intensity per bubble is achieved for both concentrations of microbubbles introduced in our study. This observation was further confirmed by our result of injections of the same number of bubbles at different bubble concentrations. These findings are in agreement with a previous experimental phenomenon exploited by Keller et al (1987) with a two-dimension ultrasonic instrument, in which a linear relationship between bubble concentration and ultrasound backscatter held only at low bubble concentrations. There are several possible factors which may be responsible for this observation.

and Doppler signal intensity may not apply at high concentration because bubbles in

Firstly, the quantification of Doppler signal intensity may be influenced by a high-pass filter which is used in almost all clinical Doppler units to remove the large signals (50 - 70 dB) scattered or reflected from stationary and slow moving objects such as the vessel wall (Bascom, et al, 1990). This high-pass filter may start to cut down the incoming signal intensity when the concentration of microbubbles is high enough to produce the large signal that exceeds the threshold. Thus, the relationship between Doppler signal intensity and the microbubble number becomes non-linear at the higher bubble concentration. This was supported by Wilson et al (1993) who reported in which the quantitative relationship between the magnitude of the backscatter and the concentration of microbubbles injected in coronary artery was examined using two-dimensional echocardiography. The concentration of microbubbles used in their study

ranged from $1 \times 10^8/\text{ml}$ to $3 \times 10^8/\text{ml}$. It was observed that, above certain microbubble concentrations, a further increase in the concentration no longer resulted in a corresponding increase in the grey level. Non-linear signal processing which was commonly used in commercial scanners was considered as a reason for this.

Second, the intensity of scattered ultrasound from any microscopic target (microparticle or microbubble) is dependent on the incident ultrasound intensity and the scattering cross-section of the target (Ophir and Parker 1989 and Tuthill et al, 1991). In the case of microbubbles, which may oscillate or resonate at particular frequencies, the scattering cross-section may be many-fold larger than the actual geometric cross-section of the scatter. This feature of microbubble is one of the most important reasons for their high scattering efficiency. If there are multiple scatters, the effective scattering cross-section is equal to the number of scatters multiplied by the scattering cross-section of one scatter. The number of scatters, therefore, should correspond to the scattered ultrasound intensity. But the number of microbubbles may change with time or after exposure to pressure (Schwarz et al, 1993). The above correspondence may not exist if the microbubble decay is related to bubble concentration.

Finally, the theoretical proportional relationship between the number of microbubbles and Doppler signal intensity may not apply at high concentration because bubbles in close proximity may not all receive the ultrasound signal equally: as a consequence, 'sheltering' of bubbles in the central part of a zone of high bubble concentration may happen.

Recently, in order to overcome the limitations inherent to TCD applications during low flow situations such in high-grade cerebrovascular spasm and subtotal stenosis, air microbubbles of defined diameter and properties have been used as a signal enhancer for TCD detection in animal experiments (Ries et al, 1988 and 1991). Furthermore, microbubble echo enhancement has also been suggested to be useful in indicator-dilution blood flow analysis (Rovai et al, 1987). However, quantitative blood flow analysis using indicator-dilution principles has been limited because the

relationship between echo contrast concentration and the degree of ultrasound signal enhancement is poorly understood, especially for Doppler ultrasound (Schwarz et al, 1993). Our results have increased the understanding of the quantitative relationship and may suggest that such an application may extend to quantify cerebral blood flow when stable microbubbles are used at a lower concentration.

Although many bubbles that enter the brain circulation may pass through the arterioles and capillary beds and do not obstruct blood flow, such bubbles could still disrupt brain function (Helps et al, 1990). In five open-brain rabbits done by Helps and his colleagues (1990), 25 μ l or more of air can cause occlusion of the exposed vessels, including dilatation of the affected pial arterioles (mean increase after 15 minutes of 27%), significant and progressive reduction of cerebral blood flow and neural function changes measured with cortical somatosensory evoked response. The microbubbles (with mean diameter of 34.3 μ m) used for Doppler intensity quantification in the study are large enough to occlude the arterioles and capillaries in the brain since entrapment of an embolus in a cerebral arteriole depends on the size of the bubble, the perfusion pressure and the diameter of the arteriole (Halliday et al, 1994). The bubble size that we studied should be pathological and therefore of potential clinical significance.

We have established a simple method to produce relatively large microbubbles of controlled concentration and size. Microbubbles have been used as acoustic agents since 1968, when agitated indocyanine green dye was used as a contrast agent during echocardiography (Feinstein, 1991). Smaller erythrocyte-sized microbubbles have been used to diagnose myocardial perfusion defects (Ten Cate et al, 1984 and Armstrong et al, 1982) and have the advantage of not being entrapped in the microcirculation (Feinstein et al, 1984 and Keller and Feinstein, 1986). However, our study concentrated on developing a method to prepare relatively large microbubbles which may cause pathological changes, for example during CPB. Hand-agitated microbubbles of a smaller size (mean size 16 μ m) occlude flow through the microvessels (Ten Cate et al, 1984).

However, hand-agitation is limited because controlling the bubble size and concentration is difficult. An alternative technique is possible, by which gas is forced through a needle of internal diameter 25 to 70 μm , into a solution containing a surfactant, and generates bubbles of 10 to 400 μm in diameter (Grulke et al, 1973) but this method also produces bubbles of variable size and is complicated. In our current study, bubble size and concentration are relatively well controlled. The half life of microbubbles in Ultravist 370 (5.25 min.) is very similar to those of microbubbles prepared with sonication techniques (5 min.) (Ten Cate et al, 1984), which allow for adequate time for injection and analysis of microbubbles.

The size of microbubbles produced in 5 % bovine albumin solution in our study using polytron agitation is in accordance with previous reports using the sonication method (Keller and Feinstein, 1987, Feinstein et al, 1988, Keller et al, 1988 and Shimon et al, 1989). However, the half life of the microbubbles in our study was much shorter than those produced by sonication. It should be emphasised that the solution temperature immediately after agitation of albumin solution with a polytron rose to only 28.9 °C in our study, but the solution temperature was up to 65°C immediately after sonication (Keller et al, 1988). This finding may supply good evidence to support a hypothesis that the long half-life of microbubbles produced with sonication is due to the denatured albumin 'shell' caused by heat. It is also not surprising that the half life of microbubbles (mean diameter = 5.6 μm) in 5 % albumin is still shorter than that of microbubbles (mean diameter = 34.3 μm) in Ultravist 370 because, for a bubble of a soluble gas in a liquid, the time required for absorption of the bubble by a unsaturated solution is proportional to the square of the radius of the bubble (Richardson, 1985).

Change of polytron power or agitation time or dilution ratio of carrier solution caused different effects on bubble size and concentration. Combining the results of change of power and change of agitation time, the greatest stability of size and concentration of microbubbles may be obtained at a polytron power between 8 and 10 Watts and an agitation time between 20 and 40 seconds. A change of the dilution ratio of Ultravist 370 may produce different bubble concentrations. Agitation of the mixture of Ultravist 370 and 5 per cent albumin yielded microbubbles in two different sizes. This

interesting finding strongly implied that bubble size was predominantly determined by the property of carrier solution. Hence, different bubble size may be theoretically obtained by choosing a proper carrier solution.

A limitation in the study was the manual injection of microbubble-carrier solutions because the force of injection is difficult to standardise. Automatic injection devices, as used in clinical medical practice, may be useful to reduce this variability.

In conclusion, this study illustrated a simple method to prepare relatively large, uniform and stable microbubbles and identified the quantitative correlation between Doppler intensity and the number of microbubbles injected. This quantification may be affected by the concentration of microbubbles existing in the sample volume. The linear relationship between Doppler signal intensity and the number of air bubbles can be held only at lower bubble concentrations.

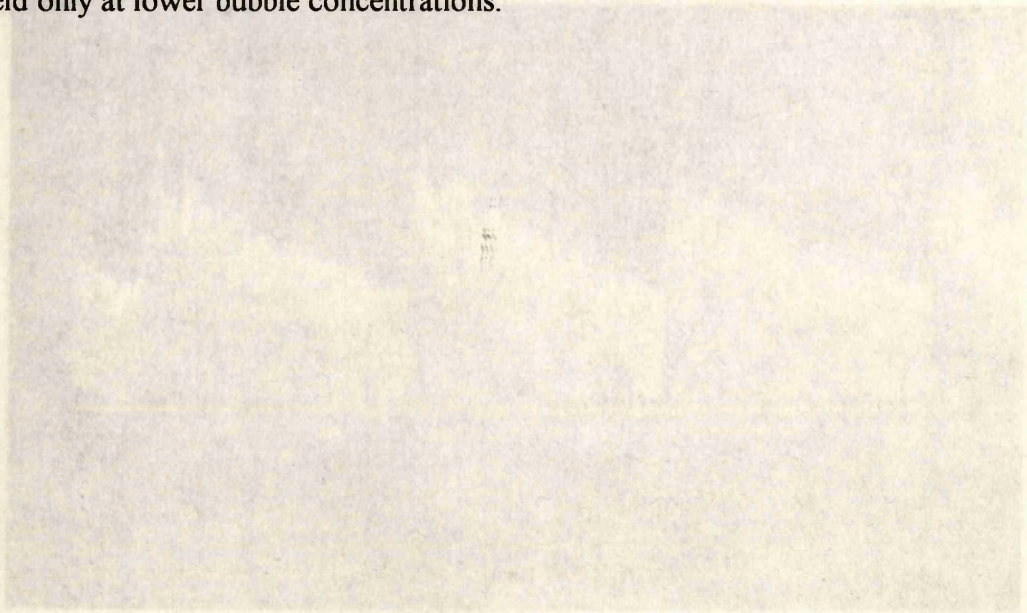
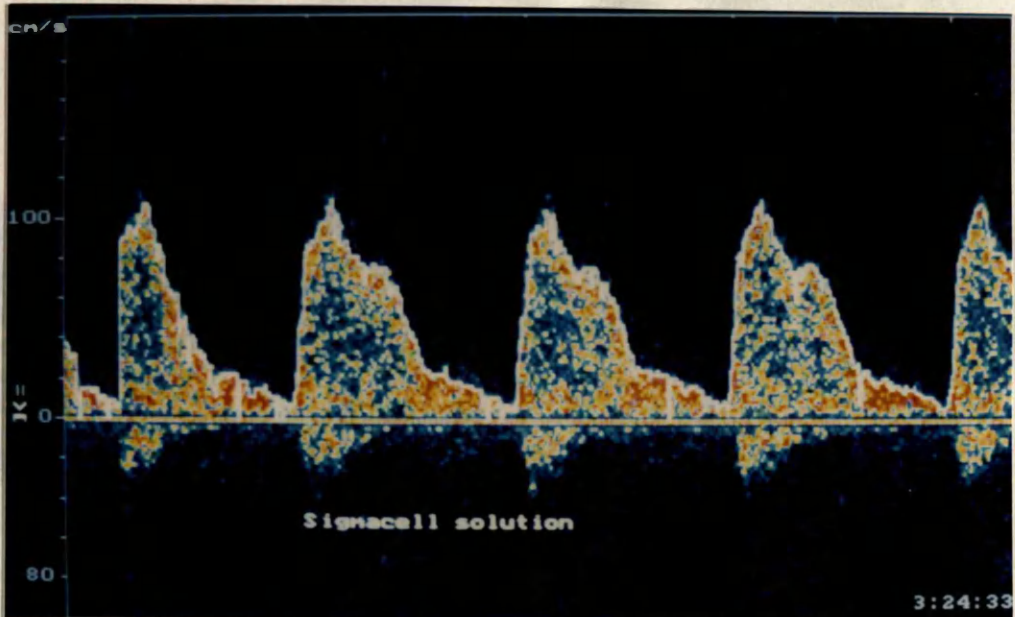
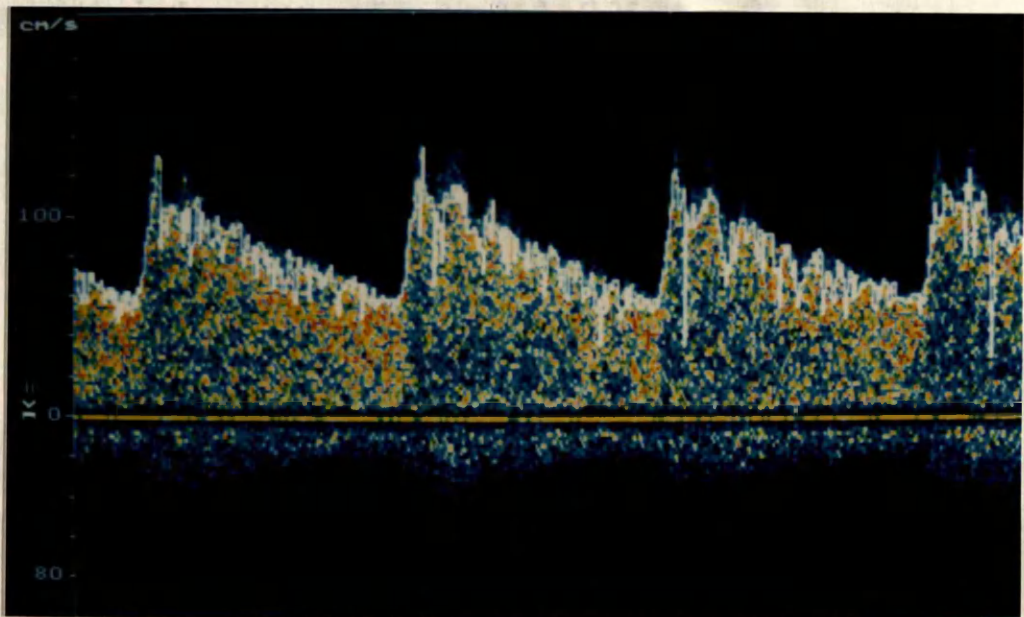


Figure 3.1 Doppler signatures collected from *in vitro* test by using 0.3% Signacell solution presented a satisfactory pulsed fashion Doppler waveform at the MCA medial (3.4). It showed a similar acoustic reflecting effect and wave-form with those collected from the blood flow in human MCA (3.2b) using the same 0.3% solution.



a) 0.3% Sigmacell Solution



b) Blood Flow in the MCA

Figure 3.1 Doppler signatures collected from *in vitro* and *in vivo*. 0.3% Sigmacell solution presented a satisfactory pulsed-fashion Doppler waveform in the MCA model (3.1a). It showed a similar acoustic reflecting effect and waveform with those collected from the blood flow in human MCA (3.1b) using the same TCD settings.

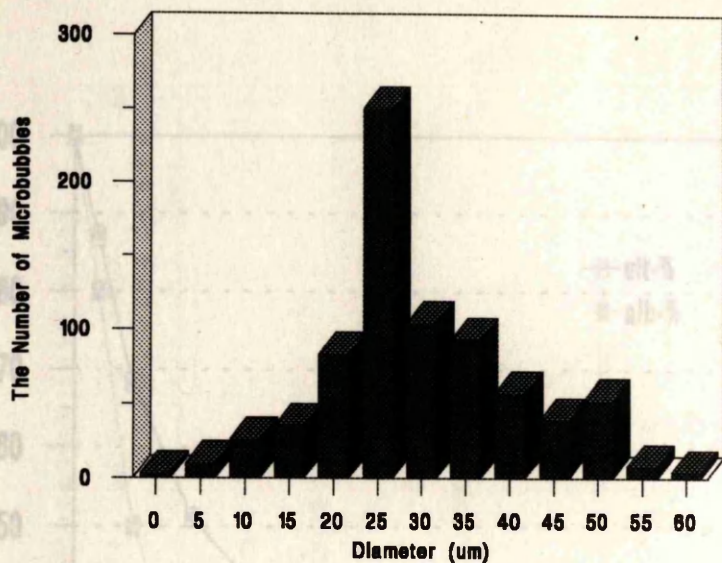


Figure 3.2 Frequency histogram of microbubble size in Ultravist 370. Mean diameter of microbubbles in the contrast medium was $34.3 \pm 9.25 \mu\text{m}$.

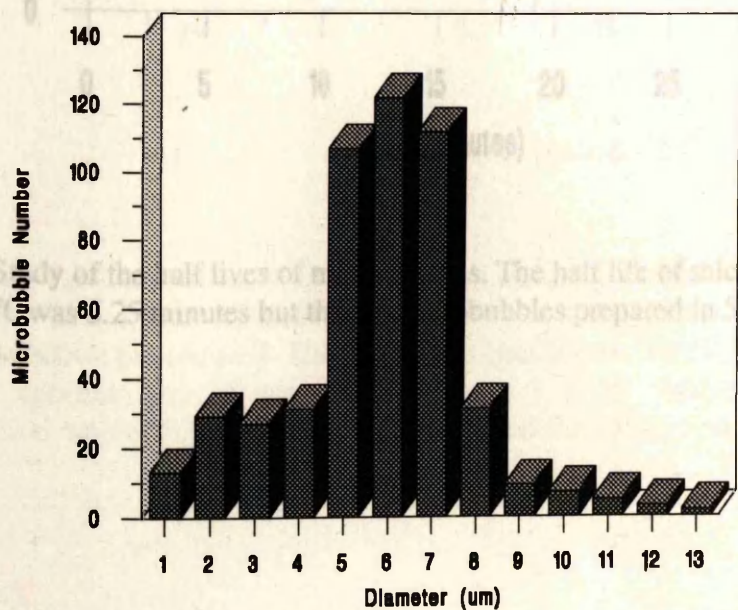


Figure 3.3 Frequency histogram of microbubble size in 5% albumin solution. Mean diameter of microbubbles in 5% albumin solution was $5.6 \pm 1.9 \mu\text{m}$.

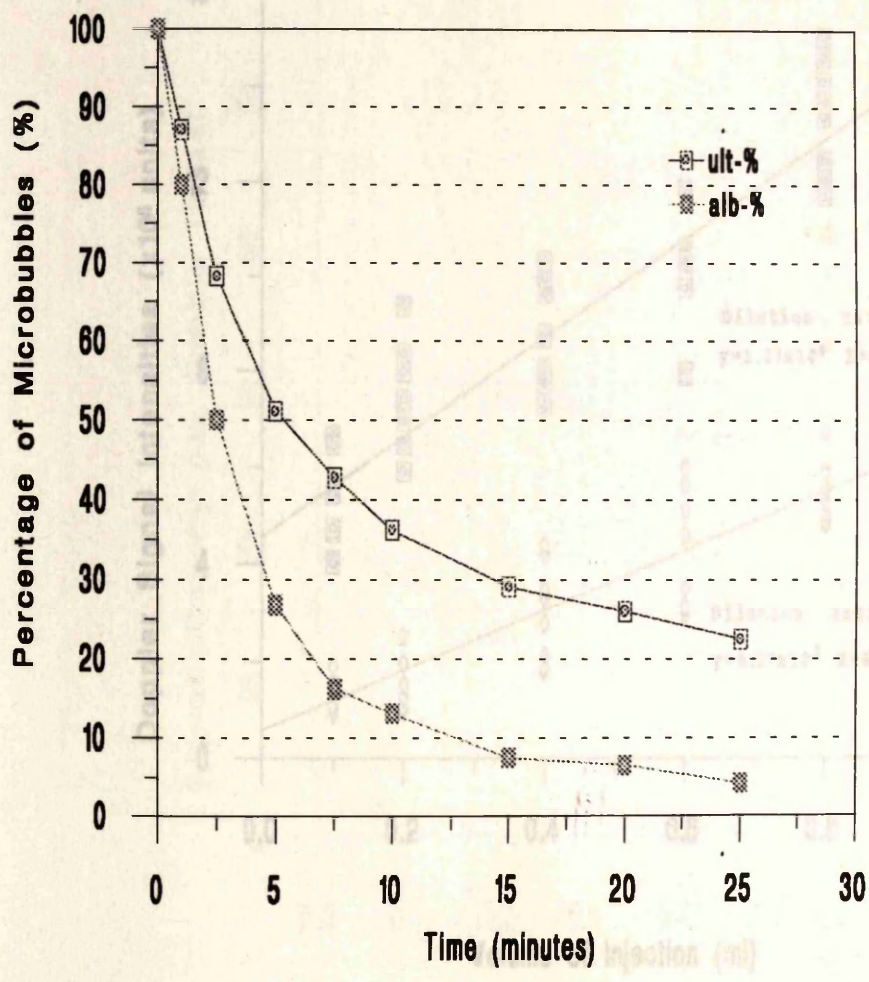


Figure 3.4 Study of the half lives of microbubbles. The half life of microbubbles prepared in Ultravist 370 was 5.25 minutes but that of microbubbles prepared in 5% albumin solution was 2.6 minutes.

The concentration of microbubbles was 1.4×10^6 bubbles/ml for dilution/ml for dilution ratio of 1:10 and 1.4×10^5 bubbles/ml for dilution ratio of 1:100.

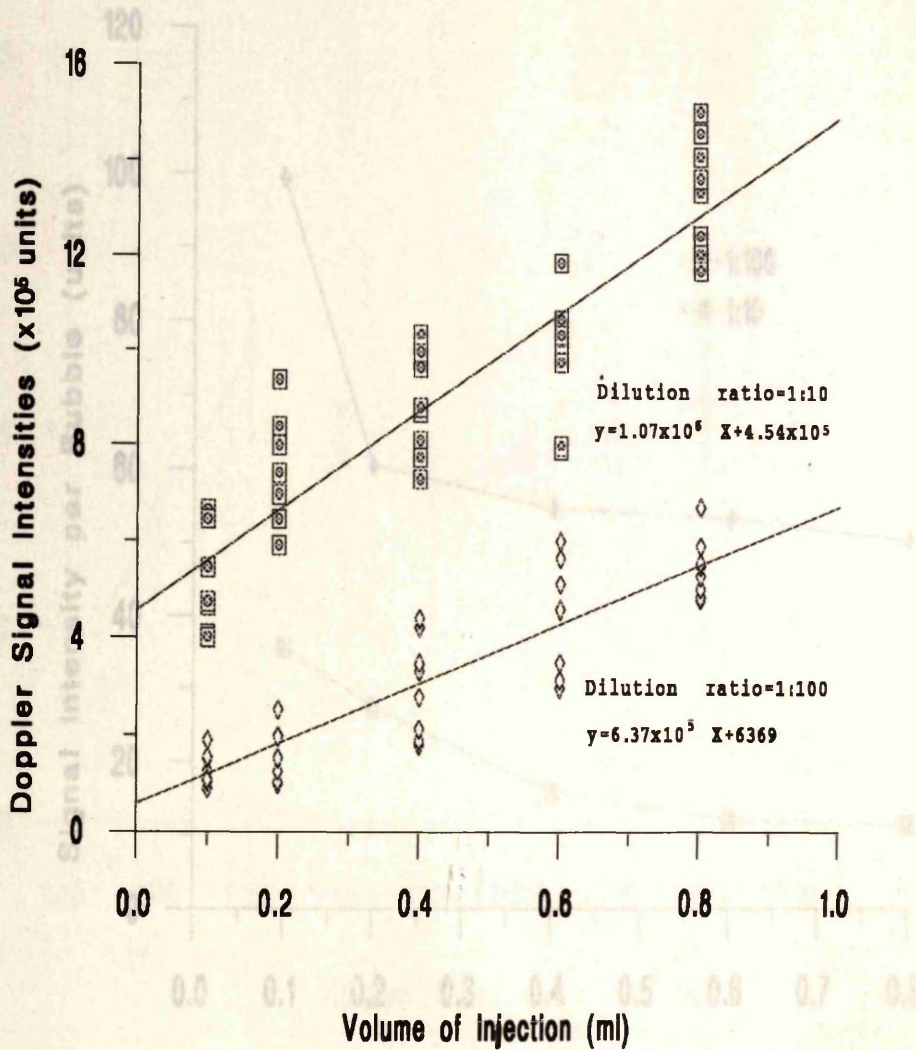


Figure 3.5 Correlation of Doppler signal intensity and the number of microbubbles. There is a linear relationship between the signal intensity and the number of microbubbles introduced. The correlation coefficients for the two lines were both 0.90. The concentration of microbubbles was 1.4×10^5 bubbles/ml for dilution ratio of 1:10 and 1.4×10^4 bubbles/ml for dilution ratio of 1:100.

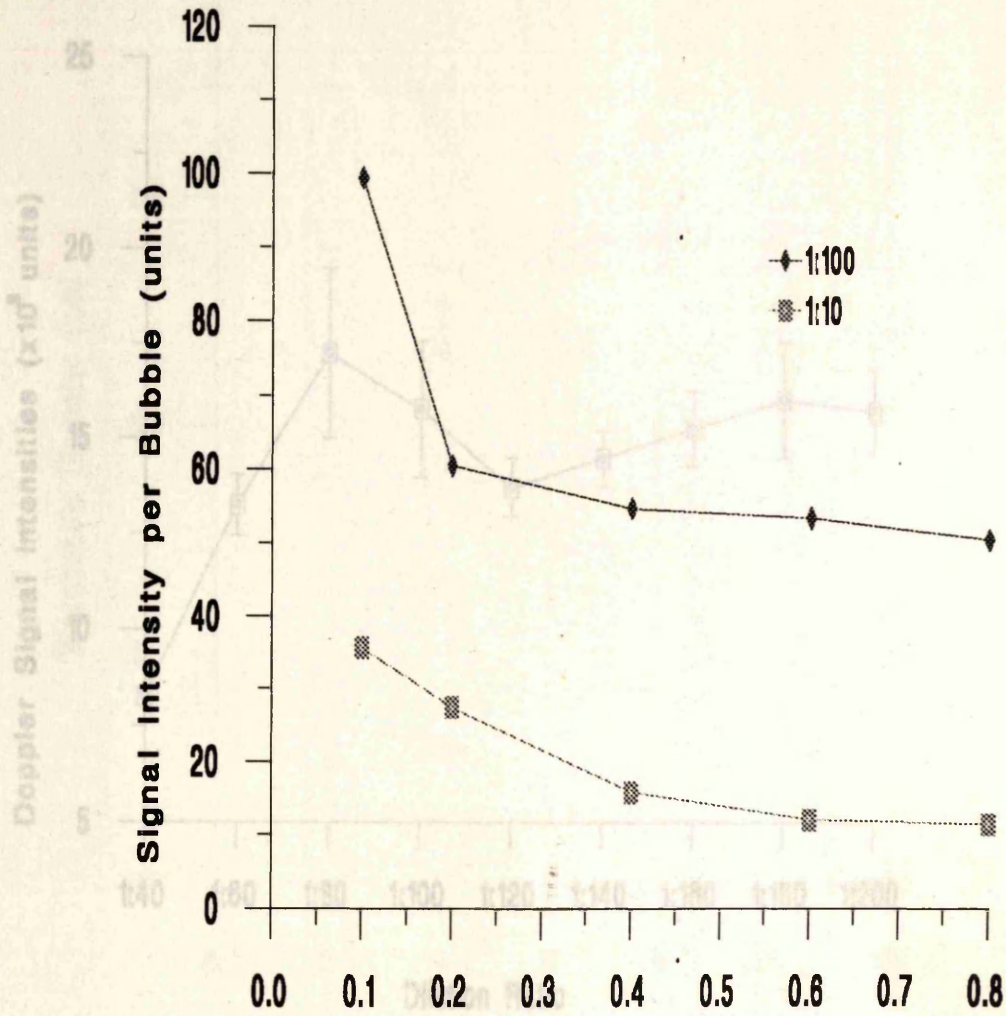


Figure 3.7 The effect of concentration of microbubbles on Doppler signal intensity. The same number of microbubbles at different concentrations were injected into the *in vitro* model. Injection of microbubbles at higher concentration (dilution ratios of 1:40) was associated with a lower Doppler signal intensity, but there was no significant difference at other dilution.

Figure 3.6 Effect of different concentrations of microbubbles on Doppler signal intensity. Introduction of microbubbles at lower concentration (dilution ratio 1:100) held higher signal intensity/bubble than injection of microbubbles at higher concentration (dilution ratio 1:10).

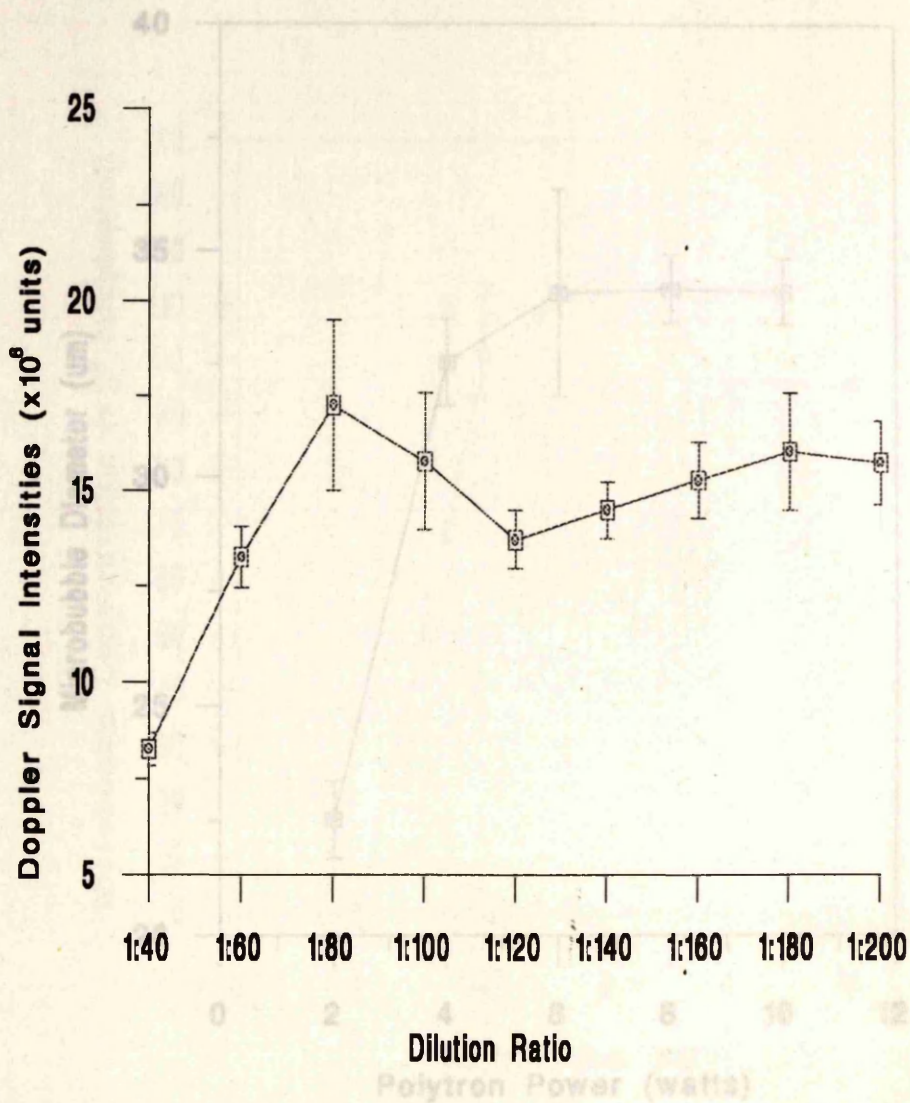


Figure 3.7 The effect of concentration of microbubbles on Doppler signal intensity. The same number of microbubbles at different concentrations was introduced into the *in vitro* model. Injection of microbubbles at higher concentration (dilution ratios of 1:40) was associated with a lower Doppler signal intensity, but there was no significant difference at other dilution.

Figure 3.8 Effect on bubble size of changing power. An increase of polytron power from two to four watts increased bubble size but no evident difference of bubble size was found when the power was changed between four and ten watts.

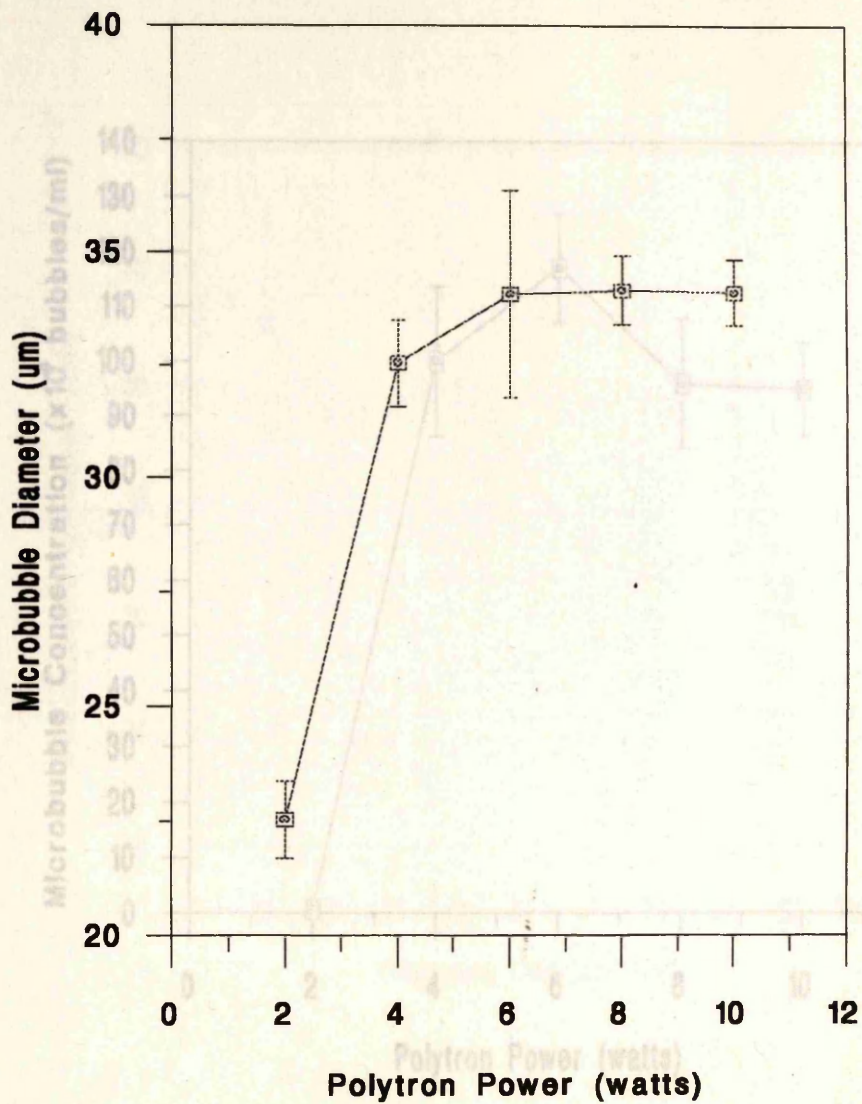


Figure 3.9 Effect of changing power on bubble concentration. Setting polytron power at two watts produced very few microbubbles. The bubble concentration was relatively constant between four and ten watts.

Figure 3.8 Effect on bubble size of changing power. An increase of polytron power from two to four watts increased bubble size but no evident difference of bubble size was found when the power was changed between four and ten watts.

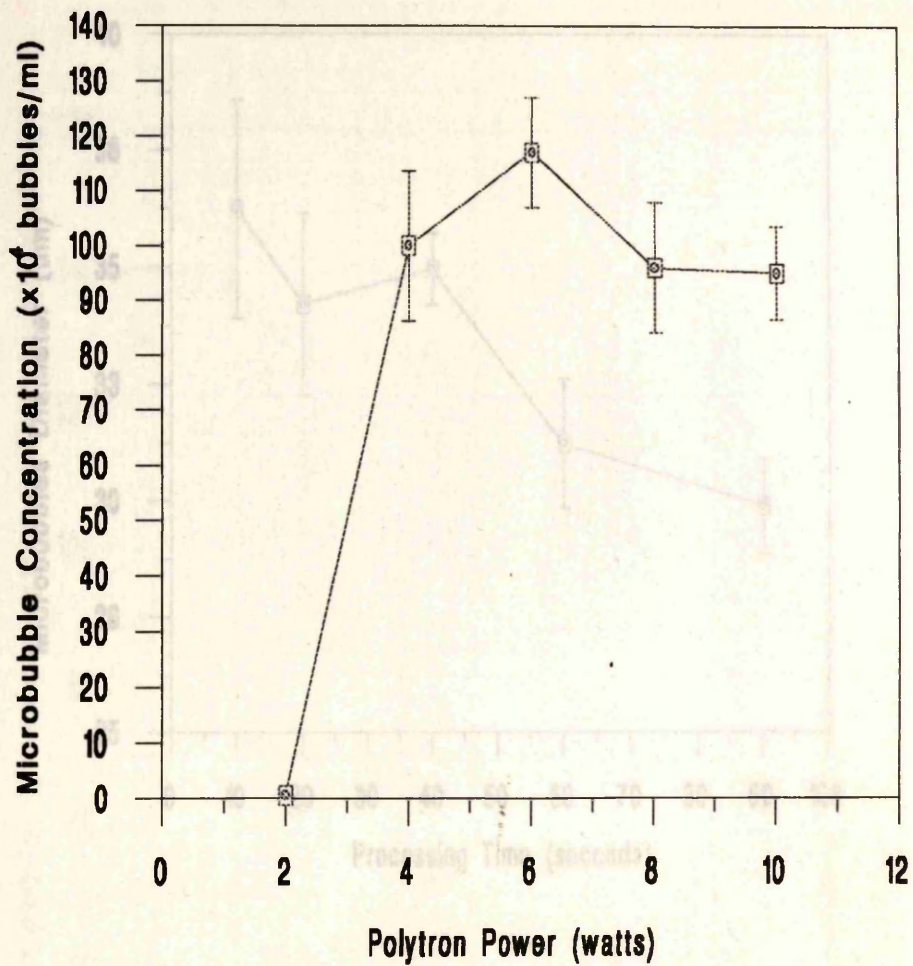


Figure 3.9 Effect of changing power on bubble concentration. Setting polytron power at two watts produced very few microbubbles. The bubble concentration was relatively constant between four and ten watts.

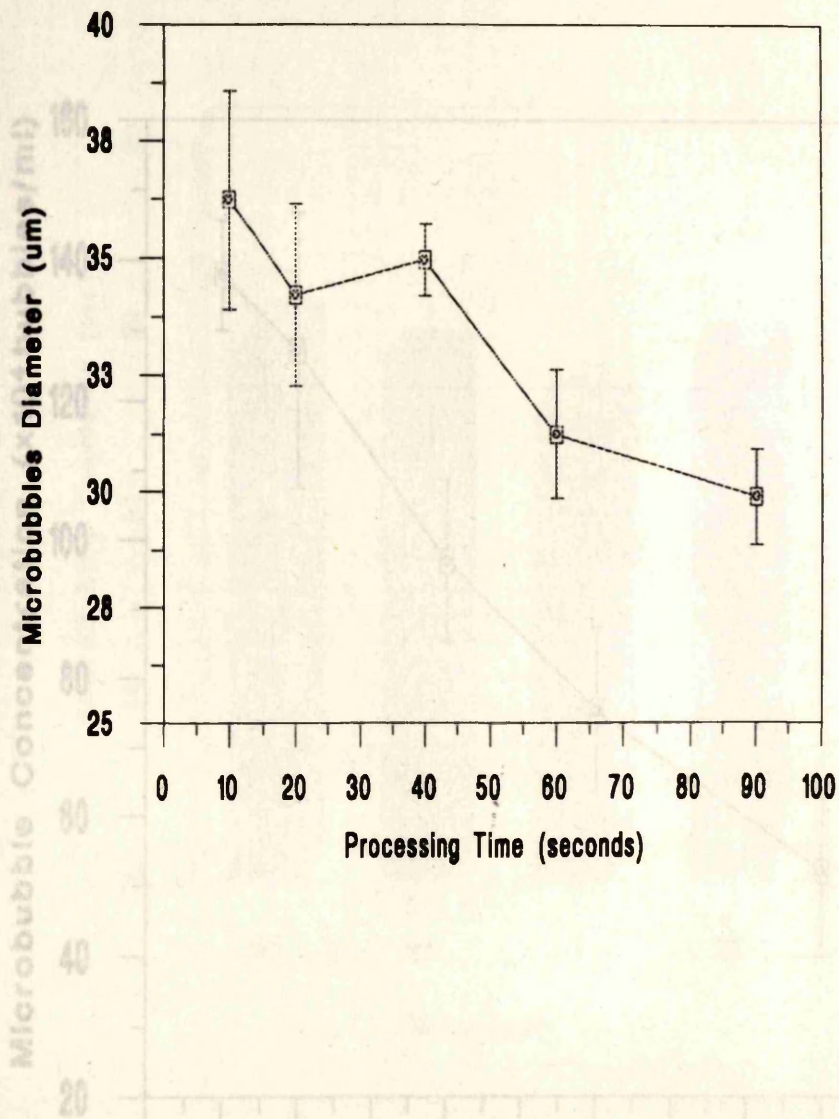


Figure 3.10 Effect of changing agitation time on microbubble size. Within the period of agitation shown in the figure, shorter agitation produced bigger bubbles with larger standard deviation whereas longer agitation produced small bubbles with smaller standard deviation.

Figure 3.11 Effect of changing agitation time on microbubble concentration. There was an inverse relationship between processing period and microbubble concentration.

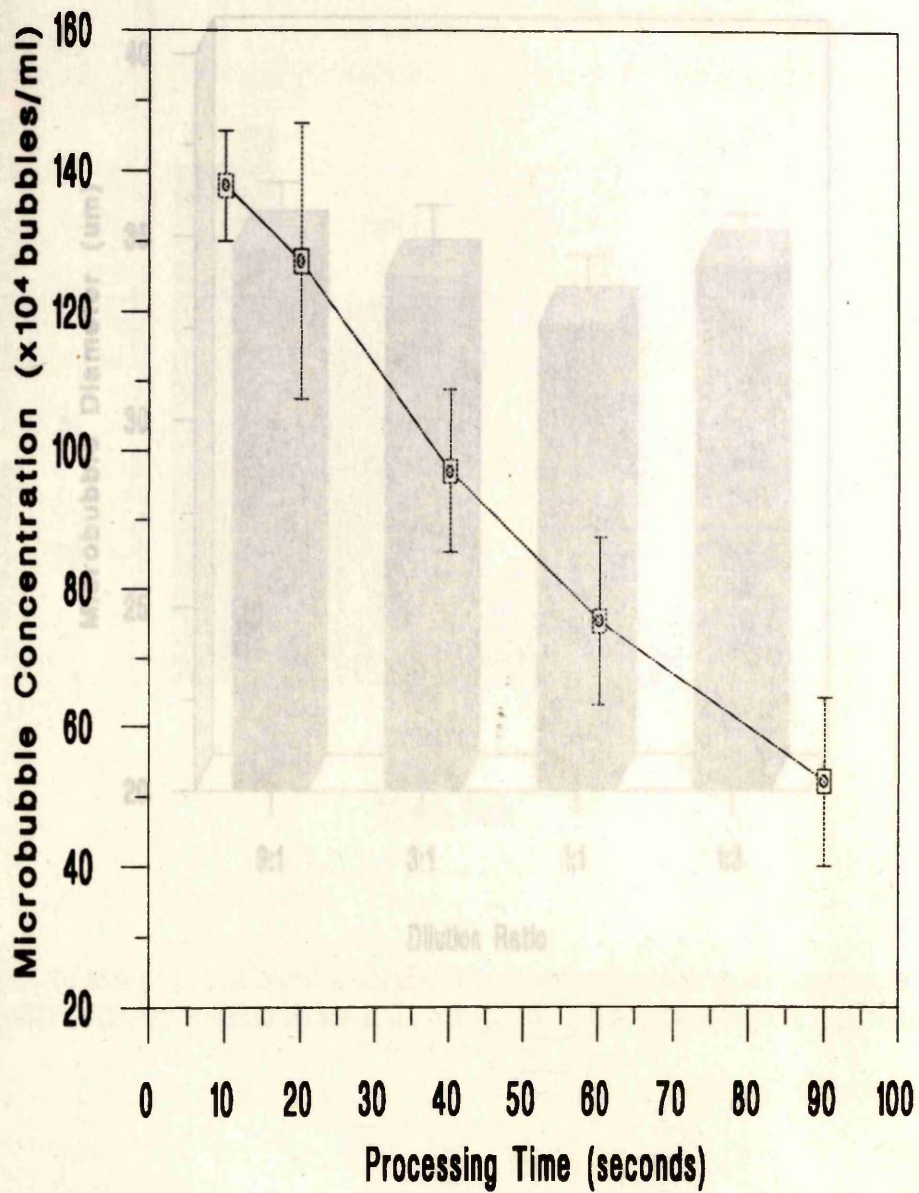


Figure 3.12 Effect of dilution of Ultravist 370 on microbubble size. Dilution of Ultravist 370 with normal saline did not alter microbubble size. The diameter of Figure 3.11 Effect of changing agitation time on microbubble concentration. There was an inverse relationship between processing period and microbubble concentration.

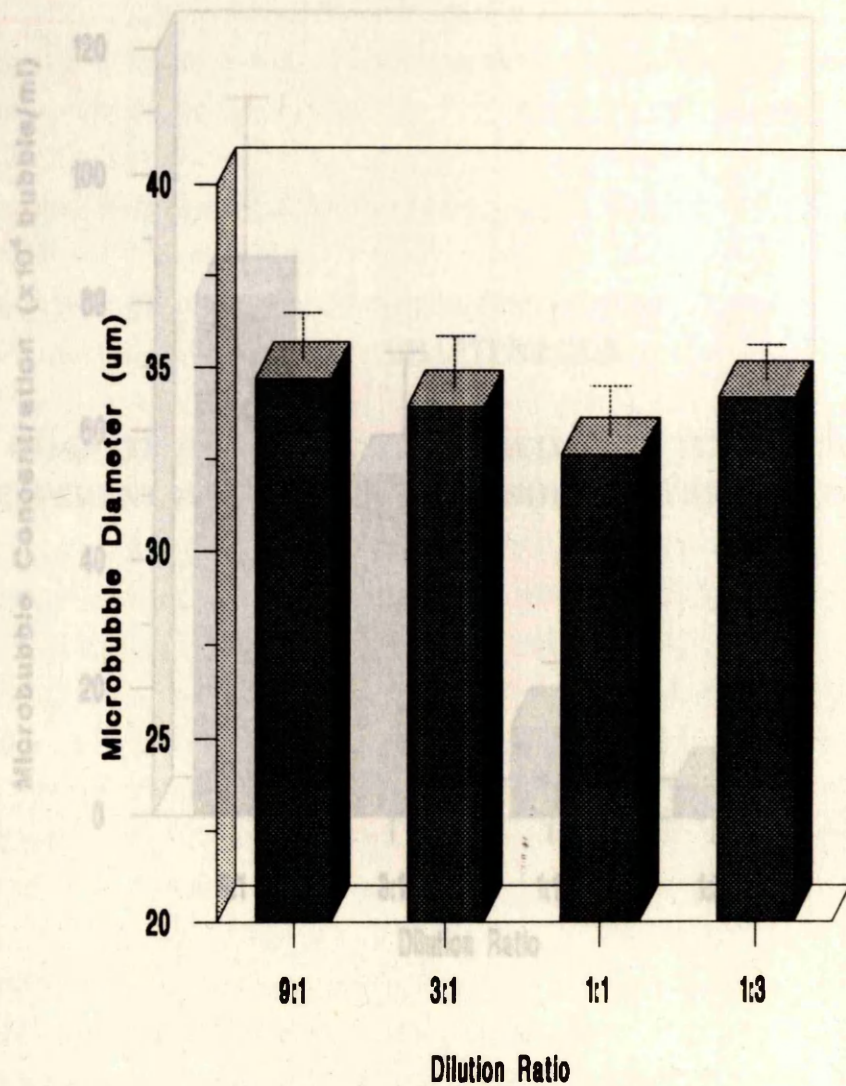


Figure 3.13 Effect of dilution of Ultravist 370 on microbubble concentration. Dilution of Ultravist 370 with normal saline reduced microbubble concentration significantly.

Figure 3.12 Effect of dilution of Ultravist 370 on microbubble size. Dilution of Ultravist 370 with normal saline did not alter microbubble size. The diameter of microbubbles ranged 32.6 to 34.6 µm in different dilution ratios.

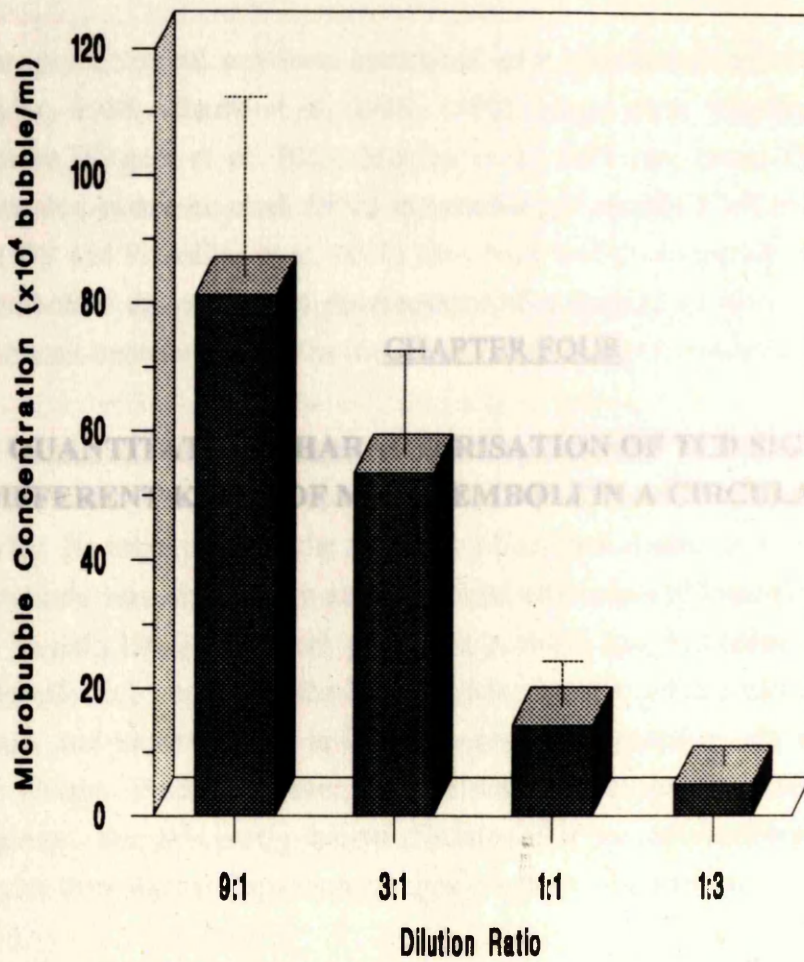


Figure 3.13 Effect of dilution of Ultravist 370 on microbubble concentration. Dilution of Ultravist 370 with normal saline reduced microbubble concentration significantly.

4.1 INTRODUCTION

Neuropsychological problems associated with microemboli such as gaseous bubbles (Taylor, 1986, Blauth et al, 1988, 1990), blood clots (Pugsley et al, 1996), fat globules (Caguin et al, 1963, Moylan et al, 1976 and Levy, 1990), atheromatous materials (Amarenco et al, 1992) and cholesterol crystals (Coff et al, 1988, Hendel et al, 1989 and Pizzolitto et al, 1991) have been well documented. However, detection of emboli is difficult. The development of a method to identify emboli may have significant benefits in both the diagnosis and treatment of patients.

CHAPTER FOUR

4.1 QUANTITATIVE CHARACTERISATION OF TCD SIGNALS FROM A DIFFERENT KINDS OF MICROEMBOLI IN A CIRCULATION MODEL

(1969a); Its importance in the aetiology of cerebral dysfunction following open-heart operations was also widely acknowledged afterwards (Richardson, 1985 and Brass and Fayad, 1993). In recent years this problem has decreased, probably owing to more effective venting of the left ventricle, filtration of the cardiopulmonary bypass circuit, and improvements in the intra- and post-operative care of patients (Fabian and Wright, 1985). However, a finite neurological deficit remains and it has been suggested that this partly due to the release of gas microbubbles into the patient's arteries from the cardiopulmonary bypass system (Richardson, 1988).

In addition to gaseous emboli, the following pathological materials have been found to act as the causes of cerebral embolism. It has been reported that brainstem stroke was caused by dislodged blood clots during internal jugular vein catheterisation (Sloan et al, 1991). Results from an experimental model study have related platelet microemboli to transient cerebral ischaemic events (Kestler et al, 1992). Fat embolism often happens in patients with traumatic injury (Levy, 1990), especially in bone fractures, but it also can occur as a complication in other situations (Caguin et al, 1963, Moylan et al, 1976 and Levy, 1990). It has been reported that among the patients who developed fat embolism syndrome, as many as 80 % of them were neurologically relevant (Fabian et al, 1990). This may be caused by fat droplets causing obstruction within the vessels of the cerebrum (Lequire et al, 1959). Atheromatous embolisation has been suggested as a principal cause of stroke after cardiac operations (Wareing et al, 1992). Blauth et al (1992) analysed the autopsy findings in 221 patients who underwent cardiac surgery and found that 16.3% of

these patients had evidence of cerebral atheroembolism which was considered to have been due to dislodgement of atheromatous material from the ascending aorta.

4.1 INTRODUCTION

Furthermore, cholesterol emboli, which also come from the same aortic lesions as the Neuropsychological problems associated with microemboli such as gaseous bubbles (Taylor, 1986, Blauth et al, 1988, 1990), blood clots (Pugsley et al, 1990), fat globules (Caguin et al, 1963, Moylan et al, 1976 and Levy, 1990), atheromatous materials (Amarenco et al, 1992) and cholesterol crystals (Colt et al, 1988, Hendel et al, 1989 and Pizzolitto et al, 1991) have been well documented. However, detection of emboli is difficult. The development of a method to identify emboli may have significant benefits in both the diagnosis and treatment of patients.

Previously limited until ultrasonic techniques became available. These techniques depend on the measurement

4.1.1 Embolitic Materials Related to Cerebral Embolism

Air embolism was initially reported by Boyle (1670a, 1670b) and Spencer et al (1968, 1969a). Its importance in the aetiology of cerebral dysfunction following open-heart operations was also widely acknowledged afterwards (Richardson, 1985 and Brass and Fayad, 1993). In recent years this problem has decreased, probably owing to more effective venting of the left ventricle, filtration of the cardiopulmonary bypass circuit, and improvements in the intra- and post-operative care of patients (Furness and Wright, 1985). However, a finite neurological deficit remains and it has been suggested that this partly due to the release of gas microbubbles into the patient's arteries from the cardiopulmonary bypass system (Richardson, 1985).

(Woods et al, 1990)

In addition to gaseous emboli, the following pathological materials have been found to act as the causes of cerebral embolism. It has been reported that brainstem stroke was caused by dislodged blood clots during internal jugular vein catheterisation (Sloan et al, 1991). Results from an experimental model study have related platelet microemboli to transient cerebral ischaemic events (Kessler et al, 1992). Fat embolism often happens in patients with traumatic injury (Levy, 1990), especially in bone fracture, but it also can occur as a complication in other situations (Caguin et al, 1963, Moylan et al, 1976 and Levy, 1990). It has been reported that among the patients who developed fat embolism syndrome, as many as 80 % of them were neurologically relevant (Fabian et al, 1990). This may be caused by fat droplets causing obstruction within the vessels of the cerebrum (Lequire et al, 1959). Atheromatous embolisation has been suggested as a principal cause of stroke after cardiac operations (Wareing et al, 1992). Blauth et al (1992) analysed the autopsy findings in 221 patients who underwent cardiac surgery and found that 16.3% of

due to the fact that the brain may tolerate small amounts of air bubbles, declining in

these patients had evidence of cerebral atheroembolism which was considered to have been due to dislodgement of atheromatous material from the ascending aorta.

Furthermore, cholesterol emboli, which also come from the same aortic lesions in the ascending aorta and arch, have been considered as a possible source of cerebral embolism of unknown cause (Amarenco et al, 1992). Cholesterol emboli occur spontaneously but more frequently after invasive aortic procedures such as diagnostic angiography or cardiovascular surgery (Colt et al, 1988).

4.1.2 Detection of Circulating Emboli with Doppler Ultrasound

Techniques for detecting of circulating microemboli were severely limited until ultrasonic techniques became available. These techniques depend on the measurement of ultrasound perturbation produced by the presence of embolic materials in a field of insonation.

In 1965, Austen and Howry (1965) used a 2.0 MHz Doppler probe in dogs to demonstrate that it was possible to detect microbubbles when the detector was placed in the cardiopulmonary bypass circuit. Doppler signals thought to be produced by air emboli were reported in divers with decompression sickness and patients during open heart surgery (Spencer et al, 1969a, 1969b) and by fat globules in patients following fractures of the tibia or femur (Kelly et al, 1972). More recently, fat emboli have been visualised in the right heart by transesophageal echocardiography (Wenda et al, 1990).

The visible and audible high amplitude embolic signal was considered to be due to the Doppler beams reflected from the fluid-embolus interface. The transcranial Doppler (TCD) has the capacity to measure the velocity of flow in intracranial and extracranial blood vessels non-invasively via a cranial window and, recently, to detect cerebral emboli, e.g. detecting of air bubbles in patients undergoing cardiopulmonary bypass (Thiel et al, 1988), carotid endarterectomy (Spencer et al, 1990), and non-air emboli in patients with prosthetic heart valves in patients (Cowburn et al, 1992) and in animal models of transient focal cerebral ischaemia (Kessler et al, 1992).

4.1.3 Sizing and Differentiating Embolic Materials with Doppler Ultrasound

Recently, it was reported that changes in the 6-week postoperative neuropsychological status of coronary artery bypass graft patients could not be statistically correlated to incidences of air embolism (Mitzel et al, 1991). This may be due to the fact that the brain may tolerate small amount of air bubbles, declining in

function only after the entrainment of a threshold volume (Fries et al, 1957). Thus, estimation of the size of emboli may be more useful than incidence information regarding a cause and effect relation between neuropsychological dysfunction and cerebral air embolism. Although Doppler ultrasound devices have been proved to have value to detect some kinds of circulating microemboli in the above instances, most previous embolic detection with Doppler instrument lacked an accurate and reliable quantitative technique to get information about the size of emboli. It would be more helpful for the diagnosis and treatment if the type of microemboli can be distinguished by Doppler technology especially when more than one type of microemboli is simultaneously involved in the same patient. Previous such experimental studies are limited in terms of comparability. Further, there still remain other types of emboli which have not been investigated with TCD but which are assumed to be often encountered in clinical situations, such as cholesterol crystals and fat globules.

Theoretically, TCD ultrasound may also differentiate between different embolic materials according to the intensity or amplitude of reflected signals. Recent studies suggest that this technique might be useful in differentiating between different types of embolic materials (Russell et al, 1991 and Markus et al, 1993b). Albin et al (1989) reported an experimental study with TCD, in which air was sequentially injected into the left internal jugular at the volumes from 0.8 to 100 μl and latex microspheres of 1.0 and 25.0 μm diameter in three anaesthetised rhesus monkeys. It was found that injection of air at 0.8 μl produced more brightness (higher amplitude Doppler return signal) than injection of microspheres of 1.0 μm diameter. This suggested that the TCD can differentially image and detect small volumes of air and solid microaggregates. However, the limitation for this study is that it is only a semi-quantitative estimation and such a comparison between air bubble and solid microsphere is less meaningful because the size of the compared embolic materials is not equal.

4.1.4 Aims

As mentioned in Chapter 1.3.5, the returned signal intensity of embolic material principally depends on the geometrical cross-sectional area at the reflection interface and the difference in ultrasonic impedance at the associated interface between two different media (Furness and Wright, 1985, Russell, 1992). The greater the reflection area, the greater the reflected signal intensity. Similarly, the greater the difference in density between the two media, the greater the amount of ultrasound reflected, and

the greater the intensity of the received signal. By the use of this theory, it may be possible to identify a useful relationship between embolus size and embolic Doppler signal intensity and to differentiate the types of embolic materials when the suspending medium (0.3% Sigmacell solution in this study) and other measuring components are kept unchanged.

In the present study, we estimated Doppler signal intensity from the embolic signals produced by injection of embolic materials into the MCA circulating model. With this quantitative method, in a circulating model, we aimed to evaluate the ability of TCD 1) in detecting and sizing different embolic materials; 2) in differentiating different embolic materials according to their Doppler signal intensity from the reflected embolic signals; 3) finally, we compared *in vitro* data to *in vivo* recordings.

4.2 MATERIALS AND METHODS

4.2.1 The MCA model and the Circulation System

The middle cerebral artery-model used for this study has been described in 2.2.1 of Chapter Two and pictured in Figure 2.1. However, for this study, a section of rabbit's thoracic aorta (with an internal diameter of 3.8 mm), instead of a plastic tube, was used as a middle cerebral artery. Expired human red blood cell (RBC) concentrate was used as a circulatory fluid. 300 ml red blood cell concentrate was diluted with 200 ml normal saline (dilution ratio 3:2 in volume) and degassed in a sonicating basin (Transsonic T890/H, CAMLAB, UK) for 15 minutes before use. To avoid any air bubble trap, degassed RBC concentrate was gently transferred onto a 1 litre glass container and circulated through a plastic tube with an internal diameter of 4.5 mm. Pulsed flow was maintained at 15 to 20 ml/sec..

In order to distribute the red blood cells evenly in the circulation, a magnetic stirrer hotplate was placed under the bottom of the glass container and operated throughout the experiment. A 2-fold gauze was fixed on the outlet of the circulation to prevent the re-circulation of embolic materials.

4.2.2 Preparation of Different Embolic Materials

(5) *Human whole blood clots* 10 ml fresh human whole blood was withdrawn from a

(1) *Air bubble emboli* 15 ml ultravist 370 (Schering Health Care Ltd., Germany), held in an agitating chamber (Figure 2.2, Chapter 2), was agitated by a polytron with power at 10 watts for 40 seconds. The prepared microbubble solution was transferred into a size-controlled set Chapter 2.4.5, Figure 2.3) to obtain microbubbles of sizes ranging from 30 to 40 μm .

(2) *Rabbit whole blood emboli* Four New Zealand White rabbits weighing 2-3 kg were sacrificed. 20 ml whole blood was taken from the heart with a 20 ml syringe and transferred into four 5 ml containers and incubated in a 37°C bath for 36 hours to clot. After incubation, the clotted rabbit's blood (weight 1.5 g) was chopped and agitated to further reduce the size (Chapter 2.4.1). Then, the agitated blood clots were filtered with a 2-fold gauze swab and the filtrate was stored in 10 ml Dulbecco's phosphate buffer waiting for measurement and injection. Whole blood emboli were injected within two hours of preparation.

(3) *Rabbit fat globule emboli* 10 gram subcutaneous fat tissue was taken from the lower rabbit abdomen and stored in a refrigerator at 4°C for making fat embolus within four hours. 2 gram rabbit's fat tissue was sliced with a tissue chopper and then agitated (Chapter 2.4.6). The agitated fat tissue was pulled into the size-controlled set for double filtration. Finally, fat globules with a size ranging from 30 to 40 μm between the two filter membranes were withdrawn with a 10 ml plastic syringe through a side-port for measurement and injection.

(4) *Cholesterol crystal emboli* The method for preparation of cholesterol crystal emboli was described in Chapter 2.4.7. In the present study, the prepared cholesterol crystals were further diluted with 25 ml 99% ethanol to make a suspension of embolic particles with a similar concentration to the other kinds of embolic materials under study.

Because of technical difficulty in making a single particle, the above four kinds of embolic materials were injected into the circulating model as multiple particles but in the similar size and same concentration for each pair (e.g., air bubbles vs. fat globules, close to 400 particles/ml, and cholesterol crystals vs. rabbit blood clots, 100 particles/ml). The following types of embolic materials were however available to be injected singly and they could therefore be compared individually with other types of emboli.

(5) *Human whole blood clots* 10 ml fresh human whole blood was withdrawn from a donor and prepared to form blood clots in the same way as for preparation of rabbit blood. Blood clots were sliced into small cubes with a wide range (35-180 μm) using a razor blade. The prepared blood embolic material was stored in Dulbecco's phosphate-buffered saline. A total of sixteen human whole blood embolic particles were separately injected.

(6) *Human atheromatous material* Human atheromatous material was obtained from a human carotid endarterectomy specimen and sliced into small cubes of size range 50-180 μm . Twenty nine atheromatous embolic particles with different size were tested in this study. Atheromatous material was used within 8 hours after surgical dissection.

(7) *Platelet-rich thrombus* 10 ml human whole blood was used to prepare platelet-rich thrombus using a method mentioned in 2.4.2 of Chapter Two. Once the platelet-rich thrombus, which contained >99% platelets, was formed, it was sliced into small particles with different sizes. A total of 25 platelet-rich embolic particles with a size ranging from 45 -135 μm were injected in this study. Platelet-rich thrombus was used within 2 hours after preparation.

4.2.3 Measurement of Embolic Materials

The measurement included size and, for multiple emboli, concentration. The methods of measurement are described in 2.5 of Chapter Two.

4.2.4 Injection of Emboli

The different kinds of emboli were injected into the MCA-model through a side-port. A volume of 1 ml was injected over 3 seconds. Before introduction of emboli, the same volume of carrier-solution was injected as a control.

4.2.5 Relating In Vitro Data to In Vivo recordings

Five whole blood clots with an average size of 100 μm were injected individually into the model. Their embolic signal intensities as well as the appearance in the Doppler waveform were compared with those of the embolic signals ($n = 8$) recorded in patient with prosthetic heart valves.

4.2.6 TCD Recording and Off-line Study

A 2-MHz probe of Transcranial Doppler ultrasonography was coupled with acoustic gel with the MCA model and the returned signal was continuously. The Doppler

signal was saved as embolic signals occurred. The same TCD settings (Doppler ultrasound frequency, gain, power, screen speed, and depth of insonation of TCD, were maintained throughout the study.

4.3.2 Comparison of Embolic Signal Intensities (Multiple Emboli)

Signal intensity was analysed off-line with the intensity-analysis software package described in 2.3.2 of Chapter Two. The total embolic signal intensity (the signal intensities over the whole passage of embolic material) was calculated with the following equation:

Total embolic signal intensity = Intensity produced by injection of embolic material - Intensity produced by control injection

4.2.7 Statistical Analysis

Firstly, the mean size of each type of material injected as multiple emboli was analysed using histography. The embolic signal intensities of these four kinds of embolic materials was compared in two pairs, i.e., the rabbit fat globules vs. microbubbles, the cholesterol crystals vs. the rabbit blood clots when their concentrations were equal within a pair. This comparison was made because the size of rabbit fat globules and cholesterol crystals was determined by their nature and seemed not adjustable, but the size of the other two embolic materials (the microbubbles and the rabbit blood clots) could be adjusted in a certain range. For such comparisons, *t*-testing was employed. Before carrying out the comparison, the comparability of each paired embolic materials was evaluated in terms of size. To do this, the significant difference between the two mean sizes of the compared embolic materials were tested. The comparison of embolic signal intensities caused by individual embolus injection (human platelet rich clots, human whole blood clots and human atheromatous materials), was made by one way ANOVA. To investigate the relationship between embolic signal intensity and embolus size, the correlation coefficient was also calculated and its significance was tested. All data in this study were expressed as mean \pm 1SD.

4.3 RESULTS

4.3.1 The Ability of TCD to Detect Different Embolic Materials

Injection of carrier solution of embolic materials did not significantly alter the signal intensity. However, all the kinds of embolic materials used in this study significantly caused a rise in signal intensity and were sensitively detected by TCD with a 2-MHz

probe as a result. This device detected embolic materials with a wide range from 8 to 180 μm .

4.3.2 Comparison of Embolic Signal Intensities (Multiple Emboli)

Comparison between different materials injected as multiple emboli was made in two pairs:

(1) *Microbubbles vs. rabbit fat globules*

The mean diameter of microbubbles after filtration was $29.7 \pm 9.1 \mu\text{m}$ (range sizes 8 to 55 μm)(figure 4.1 A). The mean diameter of fat globules was $29.2 \pm 8.6 \mu\text{m}$ (ranged from 7 to 50 μm)(Figure 4.1 B). There was no significant difference between the two sizes ($p = 0.57$) (Figure 4.2). The concentration of the two different embolic materials was equally 350 particles/ml. The embolic signal intensities increased by injection of microbubbles ($31.0 \times 10^5 \pm 1.9 \times 10^5$ units) was 300 times higher than that caused by injection of fat globules ($8.5 \times 10^3 \pm 4.5 \times 10^3$ units) of a similar size and concentration ($p < 0.001$) (Figure 4.3).

(2) *Rabbit whole blood clots vs. cholesterol crystals*

The mean size of rabbit whole blood clots was $169.3 \pm 44.8 \mu\text{m}$ (Figure 4.1 C). The mean size of cholesterol crystals was $166.7 \pm 41.23 \mu\text{m}$ (Figure 4.1 D), which was not significantly different from that of whole blood clots ($p = 0.40$) (Figure 4.2). Both embolic materials had the same concentration of 500 particles/ml. However, the embolic signal intensity of cholesterol crystals ($8.2 \times 10^4 \pm 2.2 \times 10^4$ units) was higher than that produced by injection of blood clots ($2,723 \pm 1,123$ units) ($p < 0.01$) (Figure 4.4).

4.4 DISCUSSION

4.3.3 Comparison of Embolic Signal Intensities (Single emboli)

A comparison was made between different embolic materials injected individually considering only emboli of similar length. In this group, there were 6 human platelet-rich clots, 8 human atheromatous materials, and 5 human whole blood clots which had an average length around 100 μm . There was no significant difference between the sizes of different embolic materials. Injection of human platelet-rich clot produced higher signal intensity ($16.5 \times 10^3 \pm 9 \times 10^3$ units) than injection of human atheromatous material ($5 \times 10^3 \pm 3 \times 10^3$ units) ($p = 0.01$) and whole blood clot ($6 \times 10^3 \pm 2 \times 10^3$ units) ($p = 0.02$) (Figure 4.5). However, there was no significant difference between the embolic signal intensities from human atheromatous material and human whole blood clot.

4.3.4 Relation between Embolic Signal Intensity and the Size of Embolic

Materials We used a size-control device to narrow the size range of embolic materials. There was a positive correlation between the embolic signal intensity and embolus size for all embolic materials injected singly, including human atheromatous material ($r = 0.758$, $p < 0.002$), human whole blood clots ($r = 0.618$, $p < 0.01$), and human platelet-rich clots ($r = 0.725$, $p < 0.002$) (Figure 4.6 a, b, c).

4.3.5 Characterisation of Different Embolic Materials using Embolic Signal Intensity

Figure 4.7 shows a combined graph of embolic signal intensities from injection of the above three kinds of embolic materials (human platelet-rich clots, human atheromatous materials, and human whole blood clots) of different sizes. It was found that a given signal intensity may be produced by injection of different embolic materials in different sizes. For example, in Figure 4.7, injection of whole blood clot in the size of 35 μm , or injection of platelet-rich clot in the size of 50 μm , or injection of atheromatous material in the size of 120 μm caused a similar rise in signal intensity (around 7×10^3 units).

4.3.6 Relating In Vitro Data to In Vivo Recordings

The embolic signal (Figure 4.8 A) in patient with prosthetic heart valves was similar to that from injection of a 100 μm whole blood clot in the MCA model (Figure 4.8 B). Mean signal intensity from eight clinical embolic signals (5763 ± 863 units) was also similar to the mean signal intensity from five whole blood clots in this model (6244 ± 1125 units) ($p = 0.75$) (Figure 4.9).

4.4 DISCUSSION

Six types of embolic materials have been quantitatively analysed with TCD ultrasonography in this study. Especially, we first evaluated the ability of TCD to detect the circulating cholesterol crystals. This may imply a potential use of TCD of detecting cholesterol emboli in the high-risk patients. Our data demonstrate that transcranial Doppler ultrasound is capable of detecting different embolic materials existing in the blood circulation. The technique also proved to be sensitive to detect emboli in all range of sizes used in this *in vitro* study. The minimum size of embolus we used in this study was approximately 30 μm , which is big enough to block capillaries (internal diameter = 7-9 μm) in the human brain. This indicates that TCD may have an ability to detect pathogenic embolic particles in a wide range of sizes which may be encountered clinically.

We have employed a size-control device to narrow the size range of embolic particles. Thus a reasonable comparison of embolic signal intensity can be made. This method by which prepared air bubbles were further uniformed to a size range of 30 - 40 μm has not been previously reported although there has been an established method to prepare lipid-coated microbubbles with a relatively standardised size (99% are less than 4.5 μm in diameter) and usually used as a ultrasound contrast agent or imaging enhancer (D'Arrigo et al, 1991). In this study, we emphasised evaluation of Doppler signal intensity of air bubbles which are big enough to block the capillary beds. This method was also used to standardise the size of fat globules. Early study showed that free fat globules with size of 30 - 40 μm had a clinical relevance (Wright et al, 1963).

Unfortunately, we could not compare the all kinds of embolic materials used in the present study on the basis of equal size, due to the natural origin of embolic materials or technical limitations or both. For instance, human or rabbit whole blood clots could not be made less than 35 μm . Moreover, we also had technical difficulty introducing air bubbles or fat globules into the circuit as individual emboli. Most recently, Bunegin and co-workers (1994) confirmed that the intensity of returned Doppler signals was proportional to the volume of air bubbles by introducing the single air bubbles into an *in vitro* model.

This study shows that, among all the emboli in this study, air bubble emboli are most powerful in increasing signal intensity. For signal intensity comparison from embolic materials injected singly, platelet clots cause higher signal intensity than other ones. These results are partly in accord with a previous study done by Russell et al (1991) but different from the recent report from Markus et al (1993b). In Russell's study, emboli composed of air or fat produced stronger signals than those of clotted whole blood, platelets, or atheromatous material. Markus et al (1993b) reported that atheromatous material caused higher signal amplitude (intensity) than that from fat tissue or platelet clot. It is perhaps relevant that sliced fat tissue but not fat globules were used in both these studies. Obviously, solid fat tissue should have different acoustic reflective properties than fluid fat globules. Free fat globules used in the present study may have more clinical importance because they have been microscopically visualised in the blood and in plasma samples in the patients undergoing extracorporeal circulation (Wright et al, 1963) and also considered as a key role in development of fat embolism syndrome in which neurological involvement may be the primary cause of death (Sevitt 1977 and Besouw and Hinds, 1989).

TCD would be an ideal non-invasive diagnostic device in the stroke field if it can

The relationship between embolic signal intensity and embolus size has been quantitatively evaluated in this study. The result demonstrates that a positive relationship between signal intensity and embolus size exists in different embolic materials studied. This positive relationship was previously reported by Markus et al (1993b). The current results show a correlation which is more linear than that described by Markus, however. There may be two reasons for such a difference: 1). In their study, maximum signal amplitude (intensity) increased by introduction of embolic materials and embolus passage duration within a sample volume were separately considered. According to our experience, different sizes of embolic materials take different times (duration) to pass through the sample volume. The larger the embolus size, the longer it takes to pass through the sample volume. It is not surprising that Markus and co-workers (1993) observed that the relation with total duration of the high-amplitude signal was stronger than that with maximum amplitude of the Doppler signal for all embolic materials. Estimation of embolic signals only based on maximal signal amplitude may omit useful Doppler signal information however. In the present study, the total signal intensities over the entire duration of embolus passage duration were calculated for each embolus injection. 2). The maximal size of embolic materials used in their study is larger (range of maximum dimension, 0.5 - 5.0 mm) than those used in this study. It must be easier for a larger embolus to cause signal overloading than a smaller one. This may also interrupt accuracy in an interpretation of the relationship between embolic signal intensity and embolus size. To minimise this problem, we made and used smaller size of embolic materials in this study. By considering the two factors of maximum embolic signal intensity and embolic signal duration together, we established a more linear correlation between embolic signal intensity and embolus size. This result implicates that, addition to identification of emboli in circulation, transcranial Doppler ultrasonography may also be used to estimate embolus size using the total intensity of embolic signal. However, this requires an understanding of which type of embolic material is expected. We first used TCD to detect free fat globules and cholesterol crystals. The results show that TCD is a sensitive device to detect different embolic

Additionally, we also noted that some sizes of embolic materials used in this study were smaller than or of the order of the wavelength of the ultrasound (0.77 mm for 2 MHz) and thereby Rayleigh scattering may play a role in association with the Doppler signal. However, it seems that this did not affect the quantitative correlation between the embolic signal intensity and embolus size. whole blood clot and platelet clots.

Quantitative analysis of TCD signal intensity produced by emboli in the MCA model may help in discriminating between gas and other embolic materials but not between

TCD would be an ideal non-invasive diagnostic device in the stroke field if it can differentiate different source of embolic materials. However, after we put all the embolic signal intensity readings associated with different types of embolic materials with different sizes together, it is clear that an equal embolic signal intensity can be produced by more than one type of embolic material in different sizes. That is to say, a given signal intensity may be related to a small whole blood clot or a big atheromatous particle. This suggests that Doppler signal intensity alone cannot be used to identify the nature of formed element microemboli signals. Furthermore, only particulate emboli of a known type can be sized, and some types of emboli can be distinguished when their size is already known. Most recently, with fast-Fourier transform analysis of audio segments, it was observed that introduction of air emboli not only increased Doppler signal intensity but also increased the Doppler frequency (Bunegin et al, 1994). However, whether this criterion can be used to help differentiation of different embolic materials is still to be evaluated.

It is possible to correlate the signal intensity produced by emboli from *in vitro* and *in vivo* based on an assumption that the embolus source is same. As a result, information about embolic size may be obtained.

In this study, embolic signals in clinical TCD recording was related to the results from the *in vitro* model. In addition to the resemblance in signal appearance in the Doppler waveform, it has been found that the intensity of embolic signals from *in vivo* is similar with that of embolic signals from injection of the known source of embolic material in given size. This implies that it is possible to roughly size an embolic signal *in vivo* according to its signal intensity if the source of the involved emboli is known and both TCD settings in *in vitro* and *in vivo* are equivalent. However, this should need a lot of clinical data for this calibration.

In conclusion, six kinds of different embolic materials have been prepared and tested in this *in vitro* study. We first used TCD to detect free fat globules and cholesterol crystals. The results show that TCD is a sensitive device to detect different embolic materials in a wide range of sizes and introduction of different embolic materials increased different Doppler signal intensities. Embolic signal intensity increased by introduction of air bubbles is the highest among the embolic materials used in this study. There is a positive correlation between embolic signal intensity and embolic particle size for human atheromatous material, whole blood clot and platelet clots. Quantitative analysis of TCD signal intensity produced by emboli in the MCA model may help in discriminating between gas and other embolic materials but not between

non-gas emboli. Further work is proposed to correlate embolic signals between the *in vitro* model and patients -- this may be useful in identifying size of embolic material *in vivo*, but this assumes that the nature of embolic material is known.

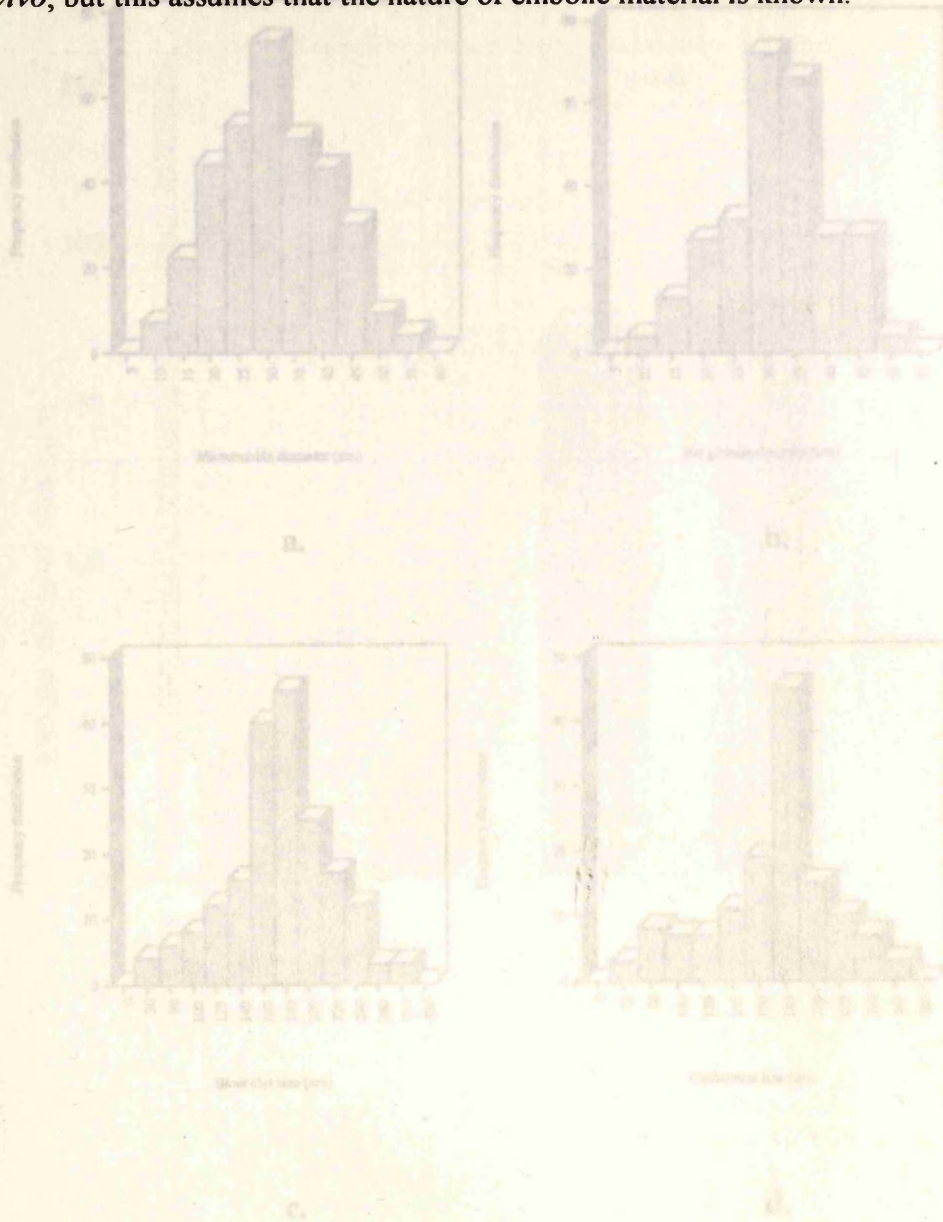
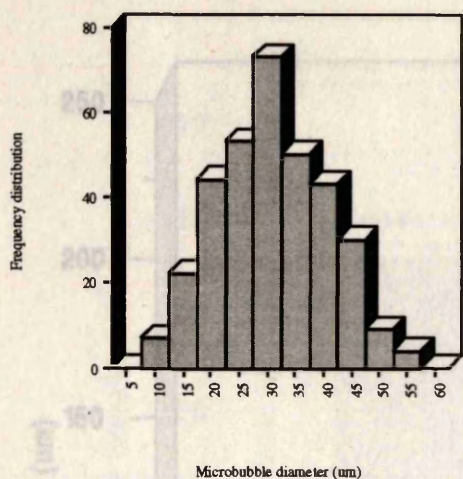
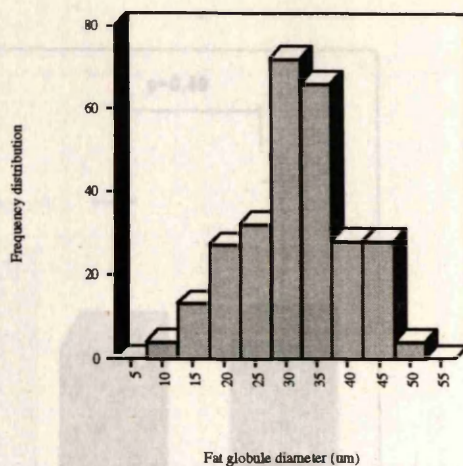


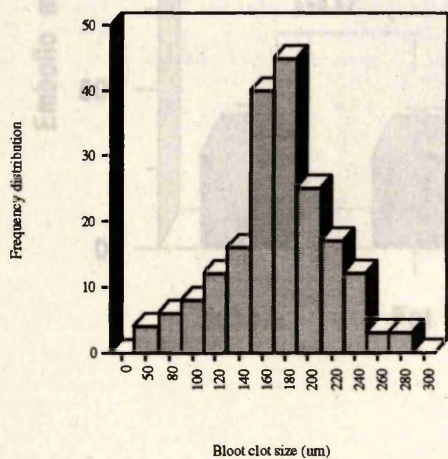
Figure 4.1 Frequency distribution of embolic particle sizes. The mean size of air bubbles, rabbit fat globules, rabbit blood clots and cholesterol crystals was 29.7 ± 9.15 (4.1 a), 29.2 ± 8.6 (4.1 b), 166.7 ± 41.2 (4.1 c), 169.4 ± 44.8 μm (4.1 d) separately. There was no significant difference in size between air bubbles and fat globules ($p = 0.57$) or between whole blood clots and cholesterol crystals ($p = 0.40$).



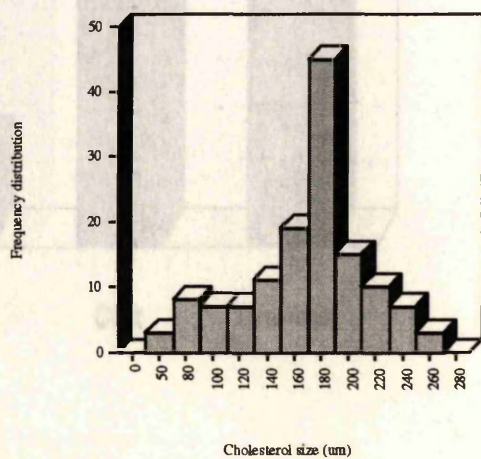
a.



b.



c.



d.

Figure 4.1 Frequency distribution of embolic particle sizes. The mean size of air bubbles, rabbit fat globules, rabbit blood clots and cholesterol crystals was 29.7 ± 9.15 (4.1 a), 29.2 ± 8.6 (4.1 b), 166.7 ± 41.2 (4.1 c), $169.4 \pm 44.8 \mu\text{m}$ (4.1 d) separately. There was no significant difference in size between air bubbles and fat globules ($p = 0.57$) or between whole blood clots and cholesterol crystals ($p = 0.40$).

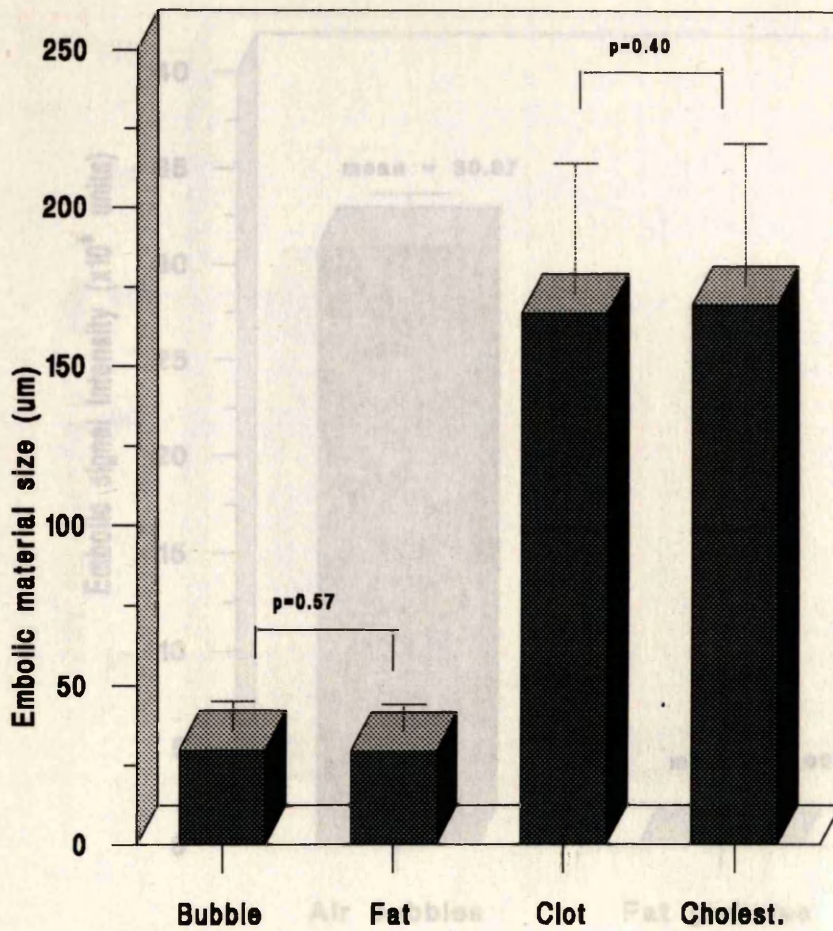


Figure 4.3 Comparison of embolic signal intensity between air bubbles and rabbit fat globules. Air bubbles were similar to rabbit fat globules in size and in concentration. However, the embolic signal intensity produced by injection of air bubbles was over 300 times higher than that caused by injection of rabbit fat globules ($p < 0.001$).

Figure 4.2 Evaluation of compatibility of embolic materials in size. There is no significant difference between microbubbles and rabbit fat globules in size ($p = 0.57$) or between rabbit whole blood clots and cholesterol crystals in size ($p = 0.40$).

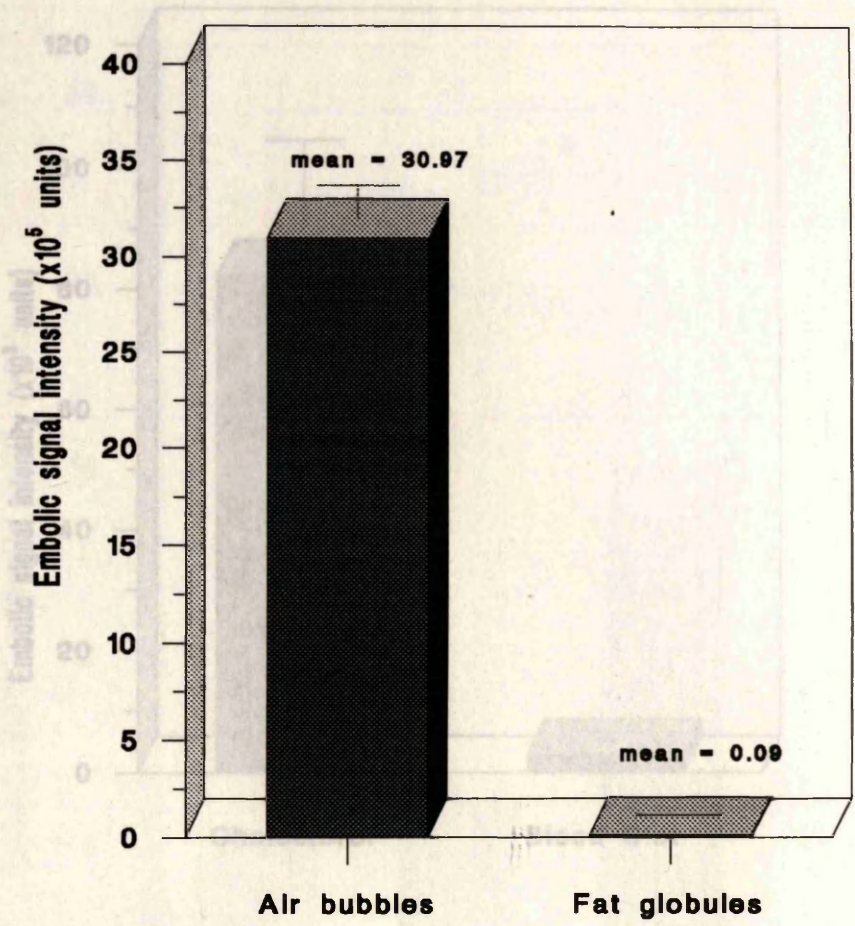


Figure 4.3 Comparison of embolic signal intensity between air bubbles and rabbit fat globules. Air bubbles were similar to rabbit fat globules in size and in concentration. However, the embolic signal intensity produced by injection of air bubbles was over 300 times higher than that caused by injection of rabbit fat globules ($p < 0.001$).

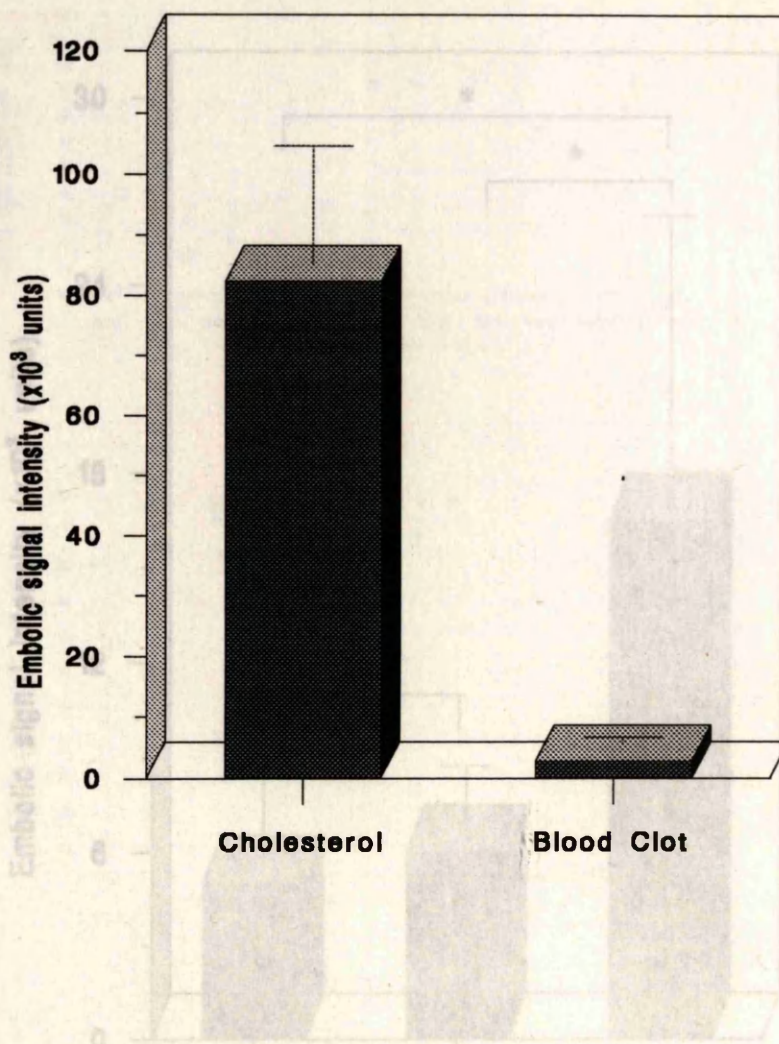


Figure 4.4 Comparison of embolic signal intensity between cholesterol crystals and rabbit whole blood clots. Cholesterol crystals were similar to rabbit whole blood clots both in size and in concentration. The embolic signal intensity produced by introduction of cholesterol crystals was much higher than that caused by injection of whole blood clots ($p < 0.01$).

Figure 4.5 Comparison of embolic signal intensity between atheromatous material, human whole blood clots, and human platelet-rich clots. All embolic particles were similar in average size (around 100 μm) and injected into the model individually. Embolic signal intensity of platelet-rich clots > that of whole blood clots > that of atheromatous material.

* $p < 0.05$

NS: no significant difference

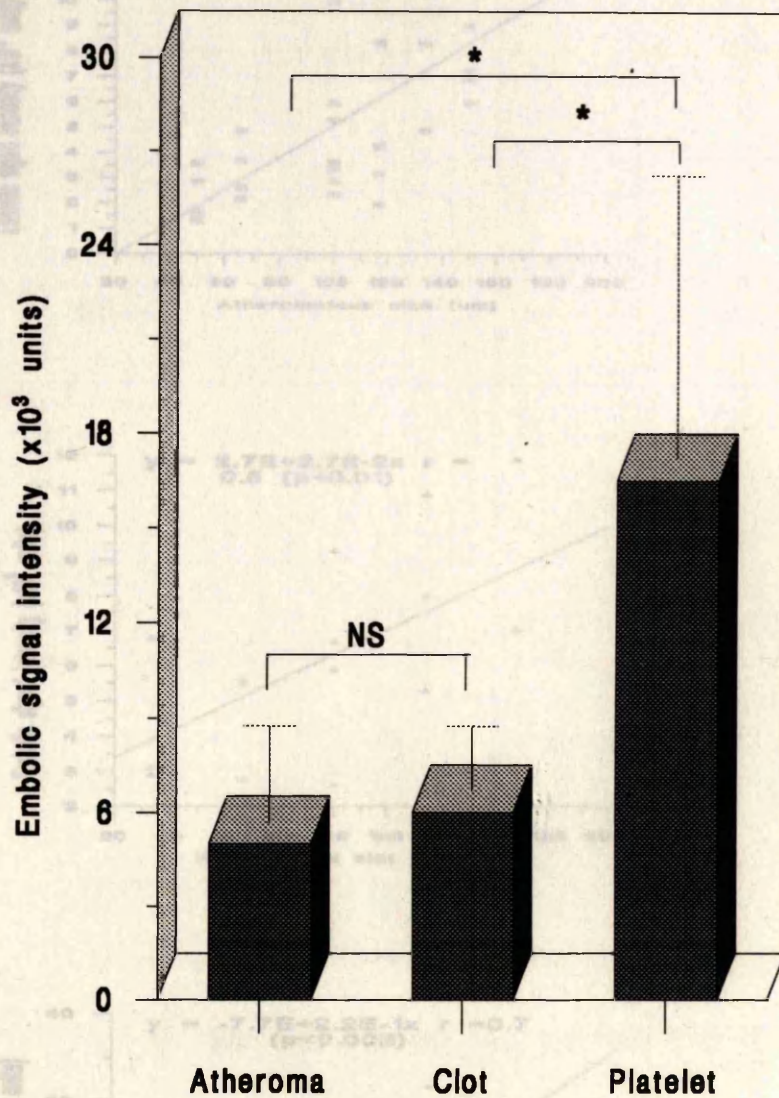


Figure 4.5 Comparison of embolic signal intensity between atheromatous material, human whole blood clots, and human platelet-rich clots. All embolic particles were similar in average size (around 100 μm) and injected into the model individually. Embolic signal intensity of platelet-rich clots > that of whole blood clots > that of atheromatous material.

* $p < 0.05$;

NS: no significant difference.

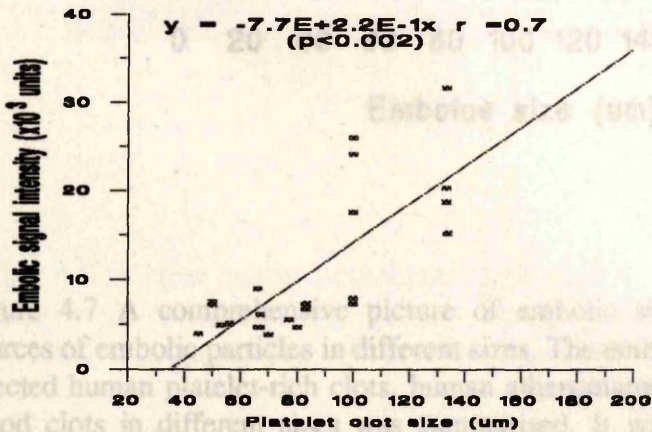
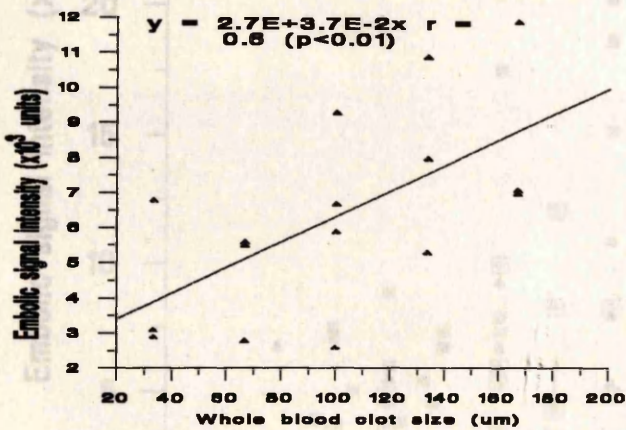
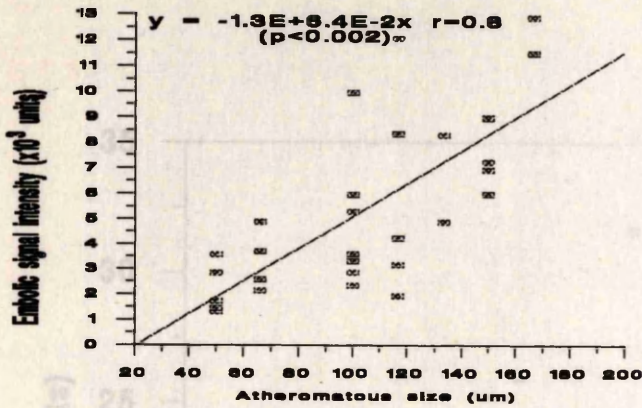


Figure 4.6 Embolic signal intensity in association with embolus size. A positive linear correlation between embolic signal intensity and embolus size was held in atheromatous material ($r = 0.8$, $p < 0.002$), human whole blood clots ($r = 0.6$, $p < 0.01$) and human platelet-rich clots ($r = 0.7$, $p < 0.002$).

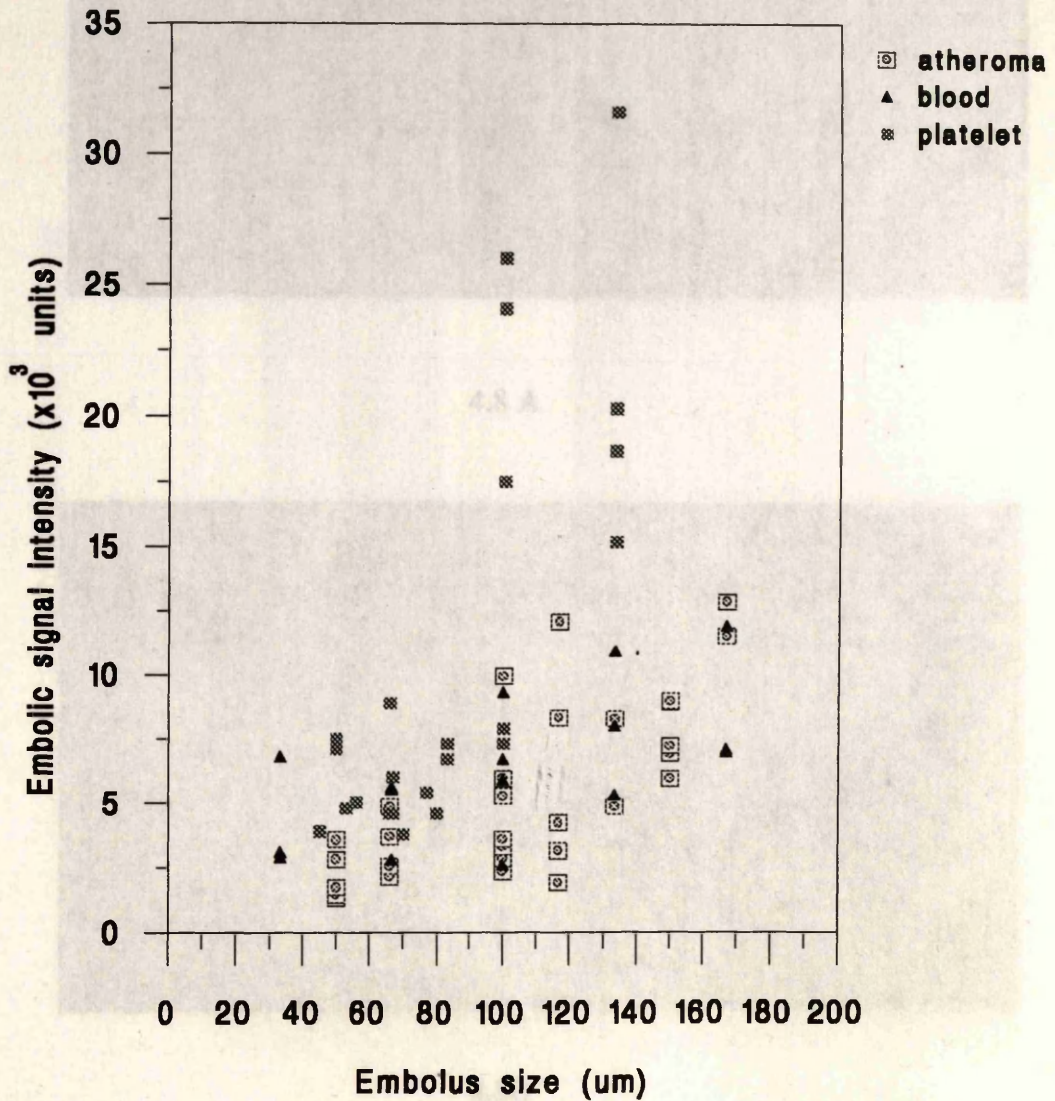
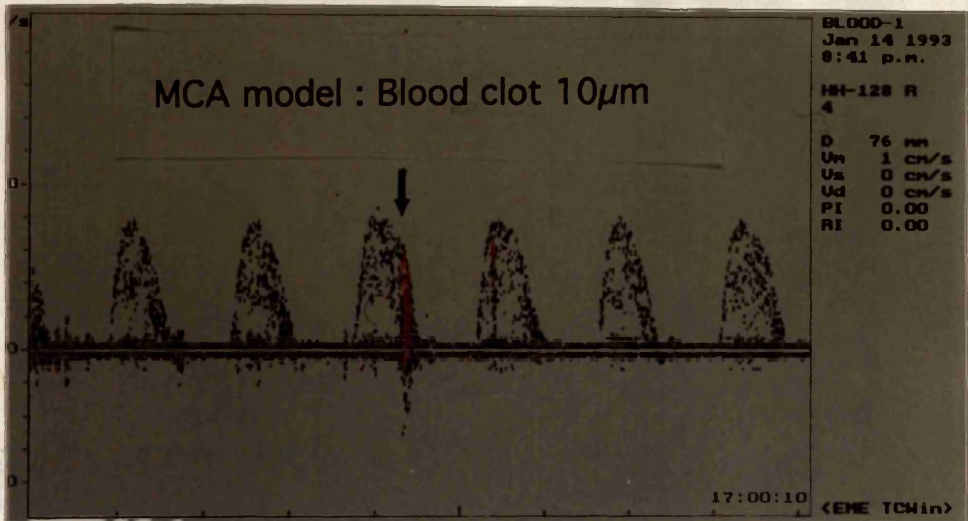
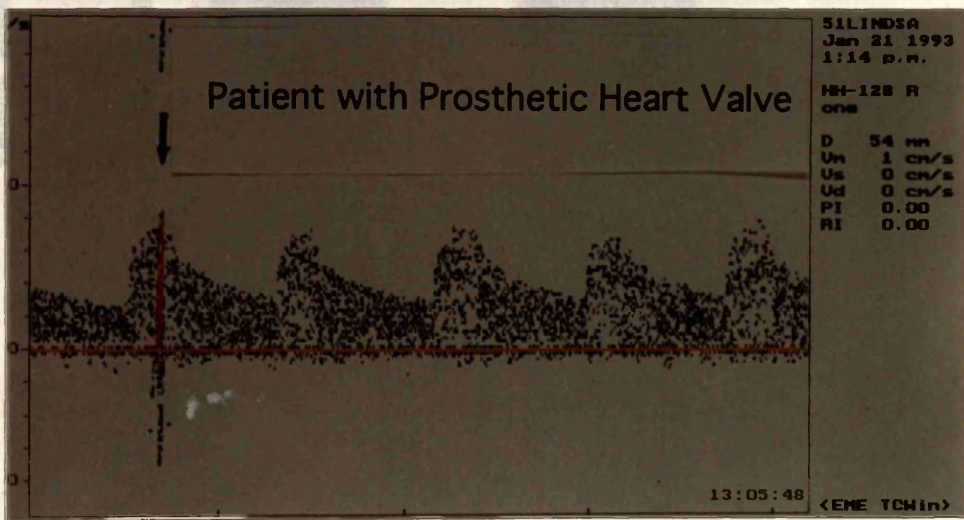


Figure 4.7 A comprehensive picture of embolic signal intensities from different sources of embolic particles in different sizes. The embolic signal intensities caused by injected human platelet-rich clots, human atheromatous materials, and human whole blood clots in different sizes was summarised. It was obvious that a given signal intensity may be presented by different embolic materials in different sizes.



4.8 A



4.8B

Figure 4.9 Comparison of embolic signal between *in vitro* and *in vivo*. The embolic signal (n=5) produced by human whole blood clots in an average size of 100 μ m was

Figure 4.8 Doppler images of embolic signals from *in vitro* and *in vivo*. Injection of a human whole blood clot showed high intensity signal (4.8A) which resembled the TCD finding in the patients with prosthetic heart valves (4.8 B).

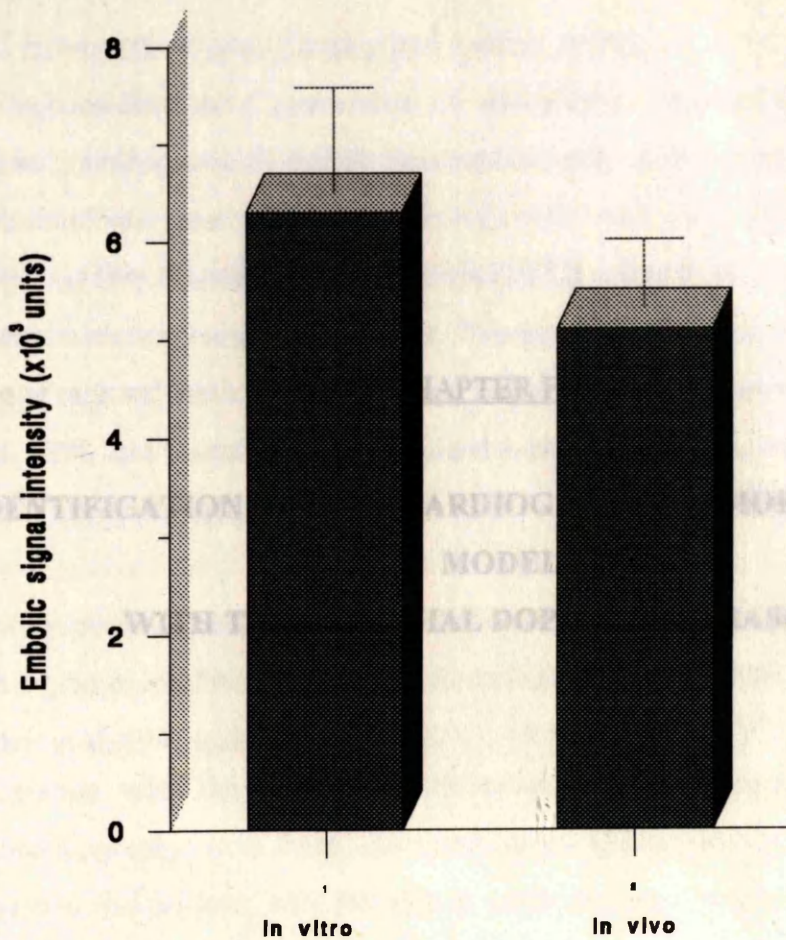


Figure 4.9 Comparison of embolic signal between *in vitro* and *in vivo*. The embolic signal (n=5) produced by human whole blood clots in an average size of 100 μm was similar with embolic signals (n=8) from a patient with prosthetic heart valves ($p>0.05$).

5.1 INTRODUCTION

5.1.1 Echocardiographic 'Smoke' and Cardiac Emboli

The echocardiographic appearance of spontaneous contrast or echocardiographic 'smoke', is recognised by mobile increased intensity of the blood within left and right heart chambers, great vessels and veins (Castello et al, 1990 and Merino et al, 1992), which was first described by Feigenbaum (1976), using M-mode echocardiography in patients with coronary artery disease. This phenomenon is occasionally noted in the state of regional stasis of blood in the left atrium or ventricle diameter (Daniel et al, 1988 and Castello et al, 1990) and it may disappear when contractility of the

IDENTIFICATION OF ECHOCARDIOGRAPHIC 'SMOKE' IN A BENCH MODEL WITH TRANSCRANIAL DOPPLER ULTRASOUND

Previous clinical studies have shown that atrial fibrillation is associated with a greater incidence of left atrial thrombi (Daniel et al, 1988, Castello et al, 1990, Archer et al, 1991 and Sadler et al, 1991). To determine the incidence of 'smoke' and its relation with the intracardiac thrombus, transoesophageal and transthoracic echocardiography have been commonly used (Fisher et al, 1991). It has been suggested that patients with left atrium and appendage 'smoke' were at higher risk for intracardiac thrombus (Fisher et al, 1991), and the latter play an important role as a cardiac source of cerebral embolism. Knowledge of the relationship between echocardiographic 'smoke' and intracardiac thrombus and the nature of the 'smoke' may help the management of patients with cerebral embolism when the need for anticoagulant or anti-platelet aggregatory agent is to be considered (Kfata et al, 1991).

5.1.2. Identification of Determinants of the Echocardiographic 'Smoke' Phenomenon

Recently, several methods have been employed to investigate the pathogenesis of spontaneous contrast (Merino et al, 1992, Mikell et al, 1982, Meltzer et al, 1980). In the previous studies, although blood stasis (Meltzer et al, 1980), platelets aggregation (Wessler et al, 1971), red blood cell coagulation (Markus and Brown, 1993) and

5.1 INTRODUCTION

5.1.1 Echocardiographic 'Smoke' and Cardiac Emboli

The echocardiographic appearance of spontaneous contrast or echocardiographic 'smoke', is recognised by mobile increased intensity of the blood within left and right heart chambers, great vessels and veins (Castello et al, 1990 and Merino et al, 1992), which was first described by Feigenbaum (1976), using M-mode echocardiography in patients with coronary artery disease. This phenomenon is occasionally noted in the state of regional stasis of blood such as larger left atrial or ventricle diameter (Daniel et al, 1988 and Castello et al, 1990) and it may disappear when contractility of the heart is improved (Mikell et al, 1982).

Previous clinical investigations have shown that the presence of 'smoke' is associated with a greater incidence of left atrial thrombi (Daniel et al, 1988, Castello et al, 1990, Archer et al, 1991 and Sadler et al, 1991). To determine the incidence of 'smoke' and its relation with the intracardiac thrombus, transoesophageal and transthoracic echocardiography have been commonly used (Fisher et al, 1991). It has been suggested that patients with left atrium and appendage 'smoke' were at higher risk for intracardiac thrombus (Fisher et al, 1991), and the latter play an important role as a cardiac source of cerebral embolism. Knowledge of the relationship between echocardiographic 'smoke' and intracardiac thrombus and the nature of the 'smoke' may help the management of patients with cerebral embolism when the need for anticoagulant or anti-platelet aggregatory agent is to be considered (Hata et al, 1991).

5.1.2. Identification of Determinants of the Echocardiographic 'Smoke'

Phenomenon

Recently, several methods have been employed to investigate the pathogenesis of spontaneous contrast (Merino et al, 1992, Mikell et al, 1982, Meltzer et al, 1980). In the previous studies, although blood stasis (Meltzer et al, 1980), platelet aggregation (Wessler et al, 1971), red blood cell coagulation (Markus and Brown, 1993) and

flow-related interaction of red blood cells and plasma have been implicated in such echogenicity, the mechanism responsible for the formation of echocardiographic 'smoke' is still not fully understood.

In order to understand the putative cellular elements responsible for spontaneous echocardiographic contrast in the blood pool, several experiments have recently been done. Turakhia et al (1991) examined the roles of blood components including packed red blood cells, plasma, washed red blood cells, and exogenous fibrinogen on a 17 mm diameter expansion chamber driven by a variable speed roller pump using a 7.5 MHz mechanical sector scanner in water at 37°C. It was found that ultrasonic echo grayscale was an exponential function of fibrinogen and haematocrit but was not influenced by leukocyte count, platelet count, or serum protein level. However, in another experimental study (Mahony et al, 1991), spontaneous contrast was imaged from the rabbit heart after administration of xylazine and ketamine while red blood cell aggregation was prevented by a photometric method. The authors concluded that the circulating platelet aggregates that are filtered incompletely by the lung were the cellular origin of the spontaneous contrast in the rabbit model.

5.1.3. Haemorrhheologic Factors in the Formation of the Echocardiographic 'Smoke' Phenomenon

In addition to the factors of pathological cellular components, the shear rate of circulating blood has been also considered as a possible contributor to the echocardiographic 'smoke'. To evaluate this assumption, a variety of models have been designed to mimic the dilated left atrium and examine spontaneous contrast at different flow rate and shear rate conditions (Merino et al, 1991). In an experiment by Merion et al (1991), ultrasound imaging was performed using a fixed 7 MHz linear probe in a tubular chamber with circulating heparinised whole blood. It was observed that characteristic swirling waves of spontaneous contrast were seen in the circulating blood at low flow rate and low shear rate.

The ability of transcranial Doppler ultrasound to detect embolic particles such as blood clots, platelet clots and air bubbles has been recently confirmed both

experimentally (Spencer et al, 1969a and Russell et al, 1993) and clinically (Spencer et al, 1969, Svartling, 1988 and Evans et al, 1989). An embolus causes a Doppler signal of increased intensity because its size and acoustic impedance are different from blood (Evans et al, 1989).

5.1.4 Aims *onic Signal Recording and Off-line Study*

In this study, using an *in vitro* model to generate spontaneous contrast, we aimed to :

1. identify whether smoke-like signals result in production of embolus signals; 2. investigate whether whole blood clots or platelet clots or microbubbles can produce smoke-like signals; 3. evaluate the effect of the 'smoke' state on the formation of thrombi.

5.2 MATERIALS AND METHODS

5.2.1 Definition of Spontaneous Contrast

Echogenic smoke was defined according to the previous description (Mikell et al, 1982 and Merino et al, 1992) of: 1) low amplitude echogenic haze; 2) slow, repetitive movement in the cavity; and 3) dissipation and disappearance of the image when blood flow increases and reappearance as flow decreases.

5.2.2 In Vitro Models for the Reproduction of Smoke-like Echoes and TCD

Evaluation

The model used to generate spontaneous contrast was introduced by Merino et al (1992). It was constructed with a 28-mm diameter plastic cylindrical chamber containing a 4-mm diameter tube. A 5-MHz linear transducer (L518, Acuson) was fixed longitudinally to the chamber. In this study, we added the same internal diameter plastic tube which bypassed the expansion chamber in order to help us to identify the nature of 'smoke'. A middle cerebral artery (MCA) model for TCD detection was formed with a plastic box filled with normal saline and inlaid with a piece of human temporal bone in one of the walls and a plastic tube with internal diameter of 4.5 mm. A 2-MHz TCD probe was placed on the temporal bone to record the Doppler signal produced by blood flow passing through the tube inside the

MCA model. The two models were connected together and whole human blood (anticoagulated with 1:7 citrate phosphate dextrose adenine) was circulated by a constant pump and the flow rate was constantly monitored with a magnetic flow meter (Figure 5.1).

5.2.3 Ultrasonic Signal Recording and Off-line Study

Two-dimensional echography was performed using an ACUSON 128 Computed Sonography system (Acuson, California, US) and the images were recorded onto videotape for subsequent examination. Continuous Doppler monitoring was performed using a TC2000 transcranial Doppler device (Nicolet, Warwick, UK). All parameters including gain, power and depth for both ultrasonic devices were maintained constant throughout. Echography and Doppler signals were synchronously recorded for 1 minute before and after each processing. TCD Signal intensity analysis software developed by ourselves was used to estimate the average waveform intensity of each chosen frame.

5.2.4 TCD Detection during Smoke-like Echoes Appearance

The TCD signal was continuously monitored for 30 minutes and ten TCD frames were stored for off-line intensity analysis during the period when typical smoke-like echoes were reproduced in the expansion chamber. Then, blood flow was allowed to travel through the bypass tube and the same TCD examination procedure was repeated.

5.2.5 Preparation and injection of embolic materials

(1) *Whole blood clots* The method for preparation of whole blood clots has been described in Section 2.4.1 of Chapter Two. 10 ml human whole blood was used to form the whole blood clots. To determine the clot size and concentration, microscopy with a calibrated eye piece was used to measure the clots dropped on the glass slide. The mean clot size was obtained by measuring 50 clots and the concentration was determined by counting the number of clots in 0.1 ml blood clot-rich saline.

(2) *Platelet aggregate-rich plasma* 9 ml fresh human blood was used for preparation of platelet aggregate-rich plasma. The procedure to do this has been detailed in Section 2.4.3 of Chapter Two. After the platelet aggregate-rich plasma was formed, the same method as that used in evaluation of blood clots was applied to determine the mean size and concentration of platelet clots. Syamex NE 8000 (TOA Medical Electronic, Japan).

We assumed that whole blood and platelet clots used in this study were cubic.

5.2.8 Statistical Analysis

(3) *Air bubbles* We used the same method which has been mentioned in Section 2.4.4 of Chapter Two to preparation of air bubbles. A blood cell count chamber was used to estimate the bubble concentration. The method to determine bubble size was the same as that for blood clots. For details please refer to Section 2.2 of Chapter Two.

(4) *Degassed normal saline* 100 ml infusion normal saline was degassed in the sonicator bath for 15 minutes before injection. 2.5 ml emboli-suspended solution or degassed normal saline was manually injected into the circuit through a three-way tap within 2 seconds.

5.2.6 Correlation of Smoke-like Echo with Doppler Flow Velocity

In addition to echographic detection of smoke-like signals, a pulsed-wave Doppler device was combined to record the Doppler flow velocity from the central part of outflow jet, the area in the presence of smoke-like echo and the area near the border of the chamber. Mean velocity was calculated from 10 peaks of the flow velocities.

5.2.7 Investigation of the role of 'smoke' state in thrombus formation

Calcium chloride solution was used to supply Ca^{2+} for whole blood to coagulate. 0.2 M CaCl_2 was added into blood at the ratio of 1:20 in volume. The time which was taken for formation of blood thrombus was recorded. We investigated the coagulation time during the following three conditions: 1) 270 ml blood flow passing through the cylindrical expansion chamber after adding 13.5 ml 0.2 M CaCl_2 ; 2) the same volume of blood flow passing through the bypass tube after adding the same amount of CaCl_2 solution; 3) 9.5 ml blood in a 25 ml glass beaker after adding 0.5 ml 0.2 M CaCl_2

solution. The formation of solid thrombus was confirmed with two dimensional echographies detected from the chamber, bypass tube and the beaker. 9 ± 6.53 units)

compared with that produced by the blood passing through the bypass tube ($49.0 \pm$ The red blood cell (RBC) concentration and haematocrit (HCT) of sampled circulating whole blood were examined with Sysmex NE 8000 (TOA Medical Electronic, Japan).

5.2.8 Statistical Analysis

Statistics Statistical analyses were performed, using unpaired *t* test. All the data in this study were expressed as mean \pm 1SD. A probability value of less than 0.05 (two sided) was considered statistically significant.

5.3 RESULTS

5.3.1 RBC and HCT

Red blood cell concentrations and haematocrits of the circulating blood used in this study ranged from 2.97 to 4.19×10^{12} /L and from 0.27 to 0.42 respectively.

5.3.2 Reproduction of Smoke-like Echoes

At a flow rate = 0 ml/min, static blood in the chamber displayed the echogenic image of grainy haze with equal intensity at all areas within the chamber (Figure 5.2 a.). At a flow rate = 30 to 60 ml/min, blood entering the chamber showed an echolucent jet stream line (Figure 5.2 b.). The typical swirling smoke-like images of flow lines appeared between the outflow jet stream and the static blood near the border of chamber when flow rates were 90 to 120 ml/min (Figure 5.2 c., d.). This spontaneous contrast also characterised as a higher echodensity than the surroundings but without definite margins. At flow rate < 60 or > 180 ml/min (Figure 5.2 e.), smoke-like echoes disappeared but reappeared when the flow rate was reduced to 90 ml/min or 120 ml/min.

5.3.3 TCD Examination of Smoke-like Echoes

During the presence of echogenic smoke, the blood passing through the chamber caused no significant difference in average TCD signal intensity (49.9 ± 6.53 units) compared with that produced by the blood passing through the bypass tube (49.0 ± 4.44) ($p = 0.71$) (Figure 5.3). Additionally, no visible embolic signals were found from TCD recordings corresponding to the appearance of smoke-like echoes as well as the flow bypassing the chamber (Figure 5.4 a., b.).

5.3.4 Injection of embolic particles and normal saline

Injection of whole blood clots (mean size 1.3 ± 0.5 mm, concentration 67 clots/ml), platelet clots (0.9 ± 0.5 mm, 47 clots/ml), microbubbles (30.2 ± 9.8 μm , 1.4×10^3 bubbles/ml) and degassed normal saline (2.5 ml) all produced flame-shaped echoes with a high echodensity when they were initially pumped into chamber. The emboli in the chamber produced a general increase in average echodensity as well as star-like high echodensity points with clear margins (Figure 5.5 b., c., d.). They floated inside the chamber and finally, were exempted from chamber with the blood flow. The echographic appearance of emboli was quite distinct from the smoke-like echoes. However, compared to the control (before injection: 15.1 ± 4.45 units), only injection of whole blood clots, platelet clots and microbubbles caused a significant increase in average Doppler signal intensity (whole blood clots: 80.6 ± 23.6 units, $p < 0.001$; platelet clots: 32.4 ± 14.4 units, $p = 0.03$; microbubbles: 2453 ± 885 units, $p = 0.001$; normal saline: 14.8 ± 0.68 units, $p = 0.19$) (Figure 5.6).

Moreover, injection of embolic materials but not normal saline (Figure 5.4 c.) produced high average signal intensity and visible embolic signals in the TCD velocity waveforms (Figure 5.4 d., e., f.). Although injection of normal saline into the chamber did not alter the TCD signal intensity, it produced smoke-like echoes inside the chamber for several seconds (Figure 5 A).

5.3.5 Correlation of Smoke-like Echo with Doppler Velocity

When smoke-like echoes occurred, mean Doppler flow velocity recorded in the middle of the outflow in the expansion chamber was higher (148.7 ± 17.9 cm/sec) than that obtained in the smoke-like echo area (32.8 ± 0.18 cm/sec) ($p < 0.01$). Both

showed bi-directional wave patterns. However, the Doppler flow velocity was near to zero in the area near the side of this chamber.

5.3.6 Smoke-like echoes and thrombus formation

After adding CaCl_2 , the time taken for thrombus formation was 4 minutes for undisturbed blood, 4.5 minutes for the blood passing through the expansion chamber with the presence of smoke-like echoes, and 6 minutes for blood passing through bypass tube at flow rate of 90 ml/min.

5.4 DISCUSSION

Two-dimensional echocardiography is a well-established technique in the assessment of left atrial spontaneous echocardiographic contrast or smoke-like echo and thrombi (Garcia-Fernandez et al, 1992, Muge et al, 1990 and Aschenberg et al, 1986). Using Yorkshire albino pig blood, Merino et al (1991, 1992) mimicked spontaneous echocardiographic contrast in an expansion chamber by pumping whole blood at a low flow velocity. This *in vitro* flow model was thought to emulate pulmonary vein flow into the left atrium or mitral flow into the left ventricle. Using a similar model and flow velocity, we used human whole blood to generate similar pattern of echoes, but produced pulsed flow because this is closer to the clinical situation.

We also noted that the mean Doppler peak velocity obtained in the smoke-like echoes area in the chamber is close to that recorded in the human left atrium with the presence of spontaneous echo contrast or/and thrombi (Jolly et al, 1992 and Pollick and Taylor, 1991). This suggests that the model is adequate to mimic the clinical situation.

In this study, we employed Doppler ultrasound, which has been proved to be very sensitive in detection of embolic materials in blood flow (Russell et al, 1991 and Markus and Brown, 1993), to investigate whether smoke-like echoes resulted in the production of embolic signals. Embolic particles produce a visibly high amplitude

signal on the Doppler waveform as well as a remarkable increase in signal intensity. However, we found that the components which caused intracavitary smoke-like echoes failed to produce any embolic Doppler signals and did not increase Doppler signal intensity compared to the signal intensity produced by blood passing through the bypass tube. This result is in accord with a previous experimental report that the components of spontaneous echo contrast are not solid but are liquid materials (Mikell et al, 1982).

Interestingly, injection of normal saline produced short-lived spontaneous contrast. Although it has been reported that spontaneous echo contrast was acoustically distinct from endocardial mural thrombus attached to the ventricular apex (Mikell et al, 1982), no previous study has attempted to differentiate echographic 'smoke' signals from the emboli. Furthermore, we have identified that the blood with 'smoke'-like signals does not produce embolic signals which are detectable with transcranial Doppler ultrasonography. We also tested the reverse situation: whether emboli caused smoke-like signals since microthrombi (Vuillien et al, 1992), red blood cells and platelet aggregates (Rohmann et al, 1992) and air bubbles (Marcus et al, 1991) have been implicated in development of smoke-like echo. We found that, as expected, these emboli produced TCD signals after they circulated within the echo chamber. However, there was no evidence that they caused smoke-echoes.

Theoretically, the blood in the presence of 'smoke'-like signal needs a shorter time to The cardiac cavity is normally echo-free on the echocardiogram because the ultrasound reflection from intracardiac blood is not dense enough to appear on the screen (Beppu et al, 1985). This was confirmed as a flow-dependent phenomenon in present study. The mechanism for the echogenicity of static blood as well as spontaneous echo contrast has been investigated by Sigel et al (1981). Whole blood suspended in plasma produces visible echoes *in vitro*. However, plasma serum or erythrocytes do not produce echoes. The echogenicity of blood components may also depend on factors related to blood flow, including rheological and biochemical properties, and changes in the physical alignment of potentially echogenic blood components. Our findings that smoke-like echoes usually occurred in the area between inflow jet with higher flow velocity and static blood located in the side of chamber without Doppler-detectable flow velocity may support this hypothesis.

Thrombus was detected more frequently in patients with reduced left ventricular global systolic function (Sadler et al, 1991). It has been suggested that shear stress, defined as the product of the velocity gradients between parallel flow lines located in the centre and the periphery of blood vessels times the blood viscosity, contributed to the echogenicity of spontaneous contrast by exerting a mechanical force to change the physical layering (Merino et al, 1992).

Interestingly, injection of normal saline produced short-lived spontaneous contrast. This phenomena has also been seen in an animal model (Mikell et al, 1982). This provides further evidence that smoke-like echo is generated by fluid components. This may result from a change in physical alignment of blood components by temporally altered regional shear force or acoustic impedance between blood and normal saline. Therefore, this lasts only for a short time before complete admixture of normal saline and blood.

How static blood with 'smoke'-like echographic signal plays a role in thrombus formation has not been understood although in previous echocardiographic investigations (Castello et al, 1990, Beppu et al, 1985, Black et al, 1991) it has been found that most left atrial thrombi were accompanied by spontaneous echo contrast. Theoretically, the blood in the presence of 'smoke'-like signal needs a shorter time to develop thrombus than the blood without 'smoke'-like signal after thrombin is added. Our study demonstrated that blood in the presence of spontaneous echo contrast needs a shorter time to form thrombi than that in the bypass but longer than that in the stationary glass. It suggests that thrombus development is inversely related to the mobility (flow velocity) of blood in that location and the blood with the presence of spontaneous echo contrast has an increased risk of thrombus formation. However, this effect does not seem to be specific because the blood with 'smoke' echo still takes a longer time to develop thrombus than that in the stationary glass.

In conclusion, this *in vitro* study suggests that smoke-like echo does not produce an increase in TCD signal intensity such as is achieved by embolic materials. The echographic appearances of whole blood clots, platelet clots and air bubbles are

distinct from smoke-like echo. These results confirm the earlier reports (Mikell, 1982 and Merino et al, 1992) that smoke-like echo is a special echo phenomenon not produced by embolic particles but by static whole blood in certain conditions of slow motion. Moreover, our results show clearly that smoke-like echo occurs at low flow situations and does not itself produce material capable of embolising into the systemic circulation. Thrombus formation is related to the low flow velocity of regional blood. Thus smoke-like echo may be helpful to predict a high risk of thrombus development.

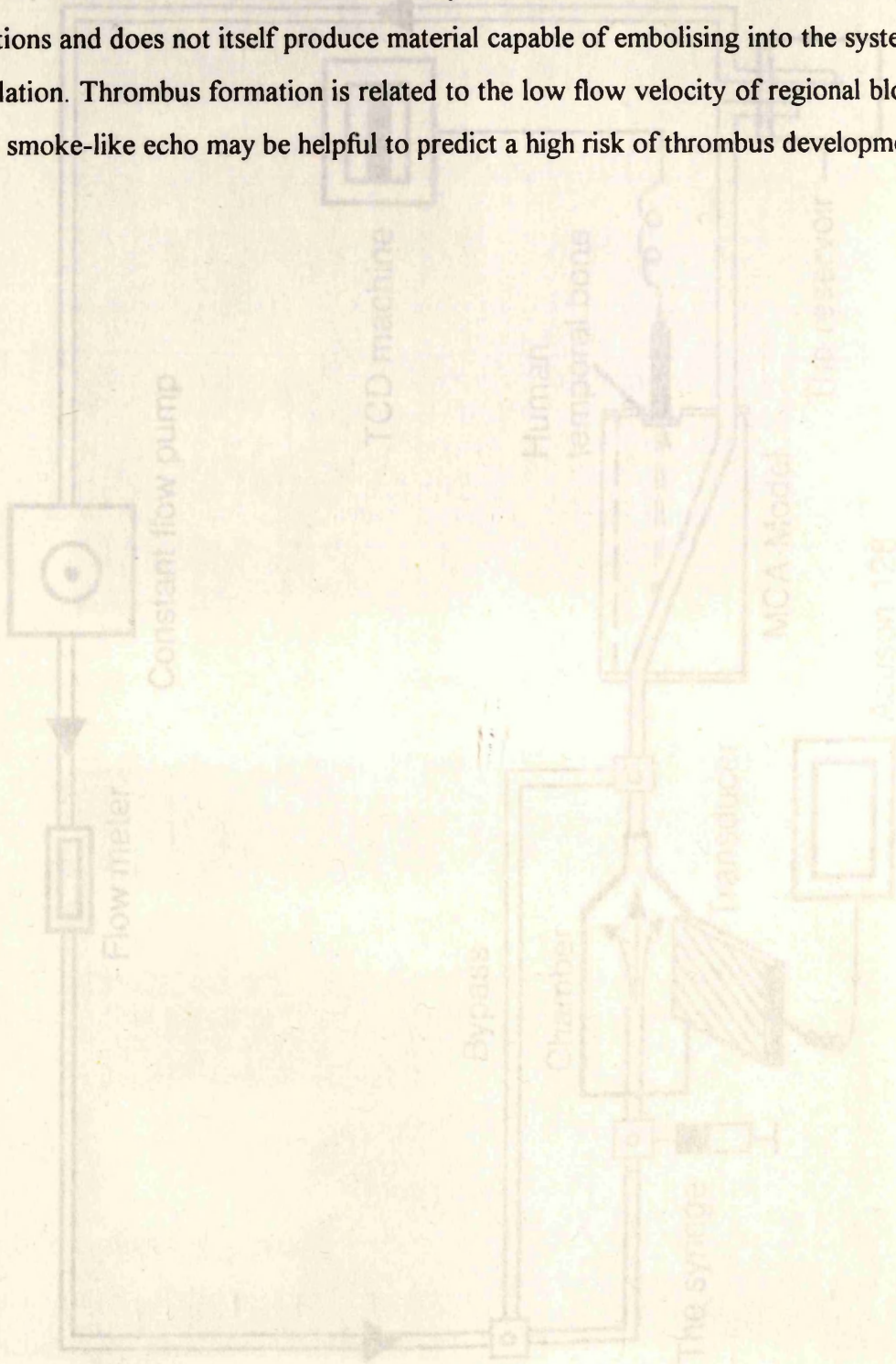


Figure 3.1 Illustration of the present model for reproduction of smoke-like echo, constant and TCD calibration.

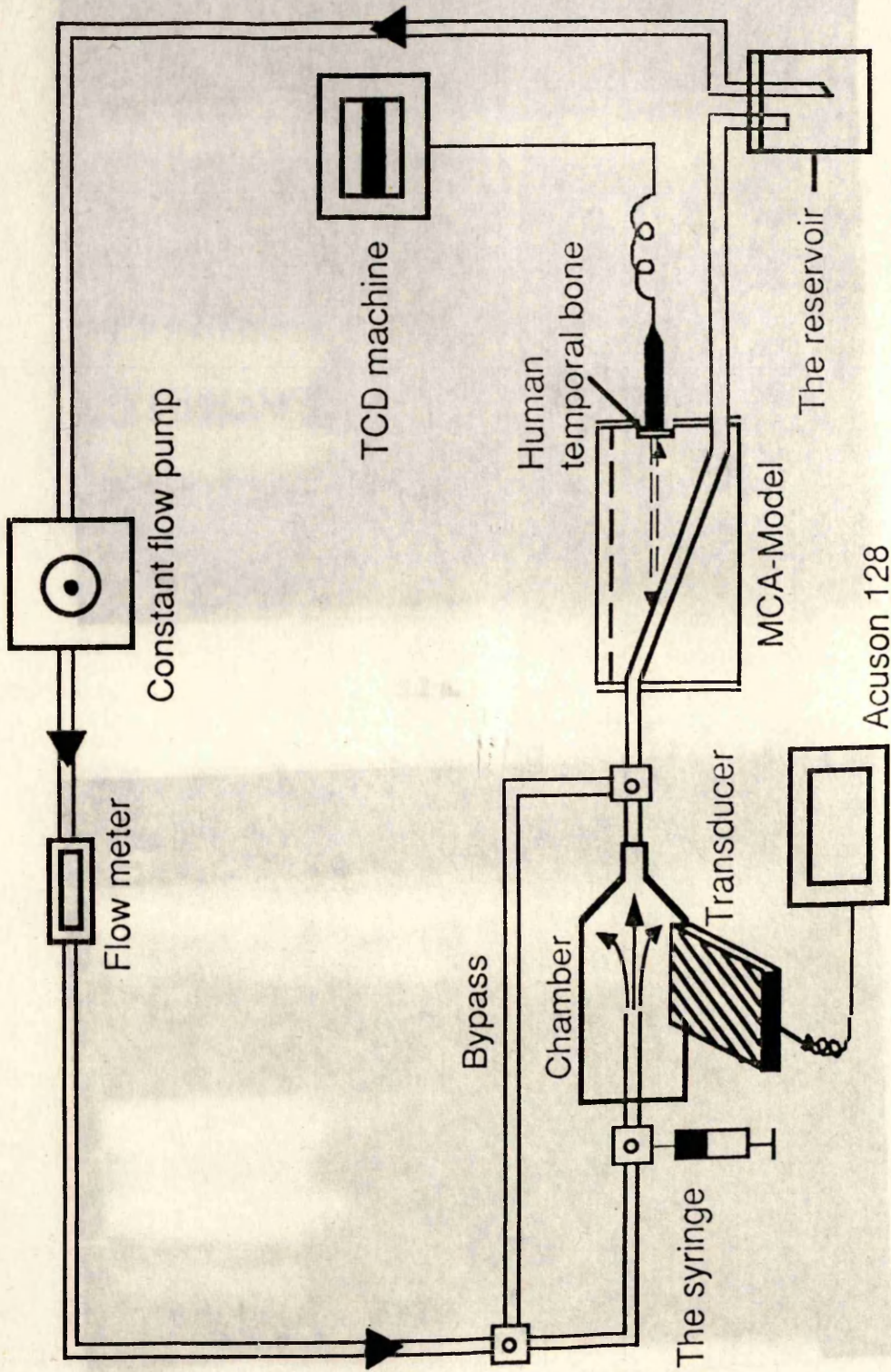
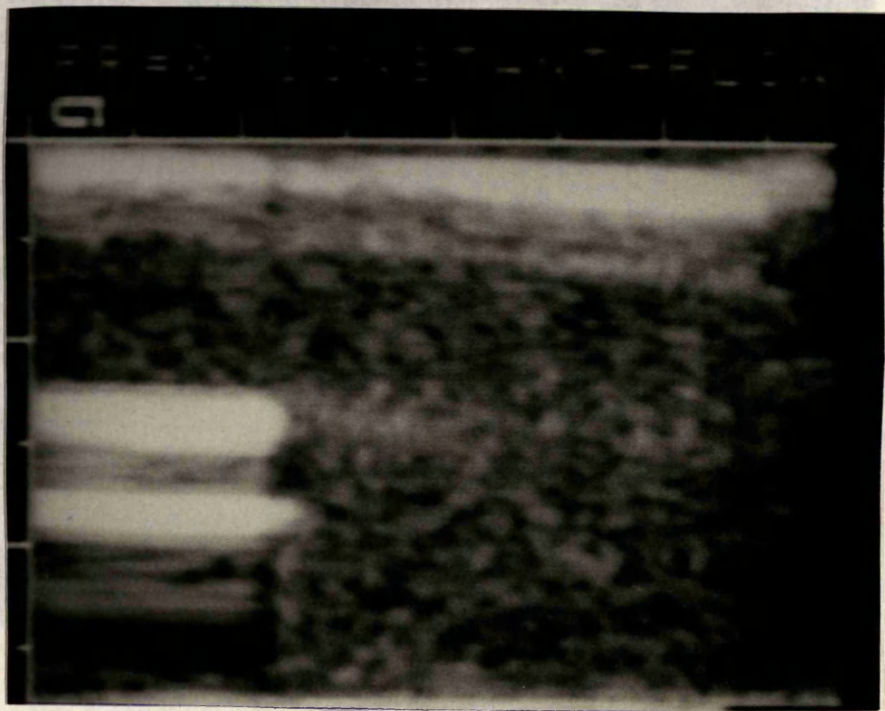
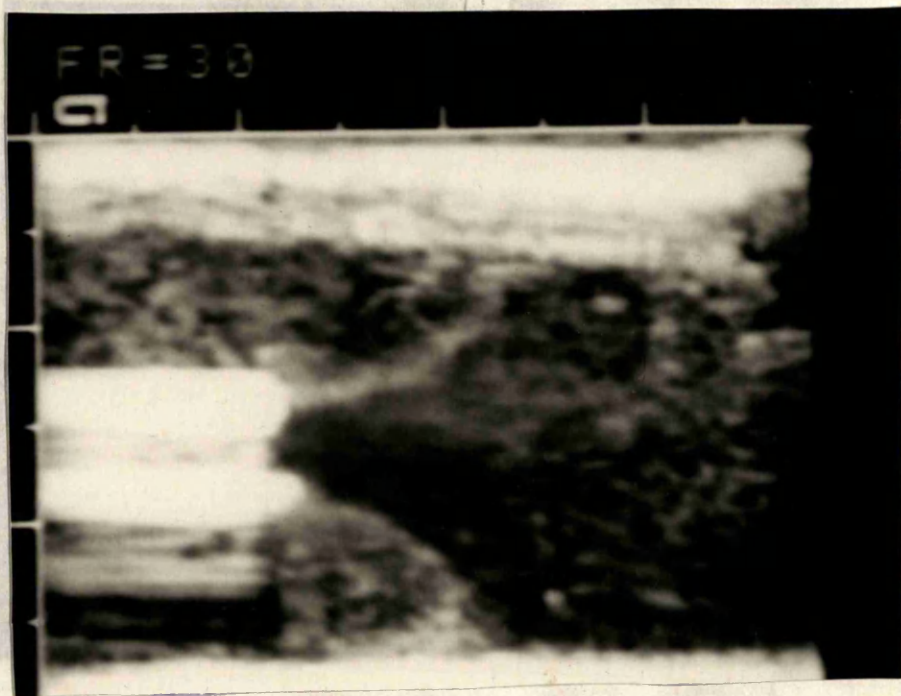


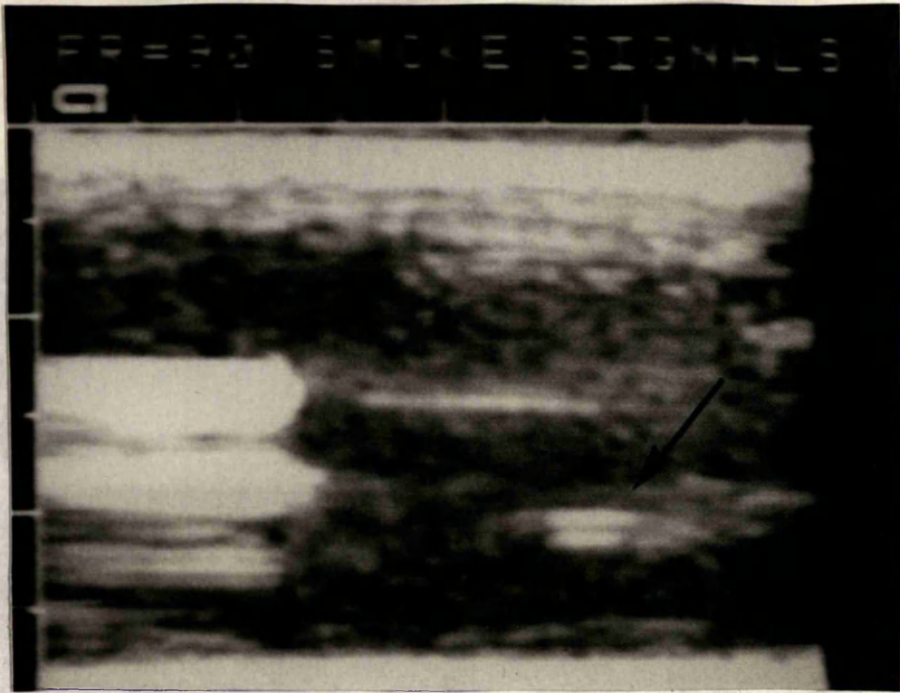
Figure 5.1 Illustration of the circuit model for reproduction of spontaneous contrast and TCD examination.



5.2 a.



5.2 b.



5.2 c.

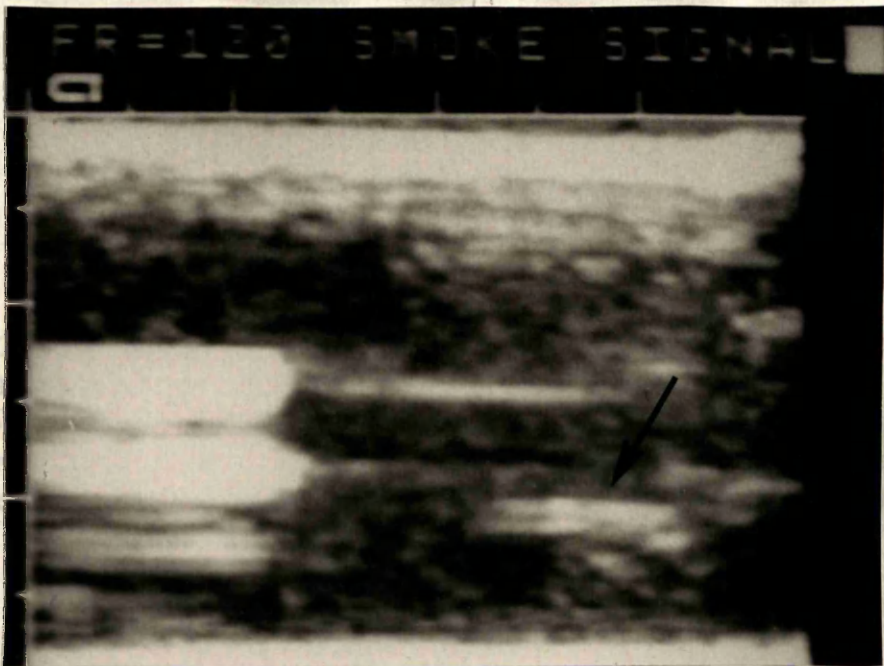
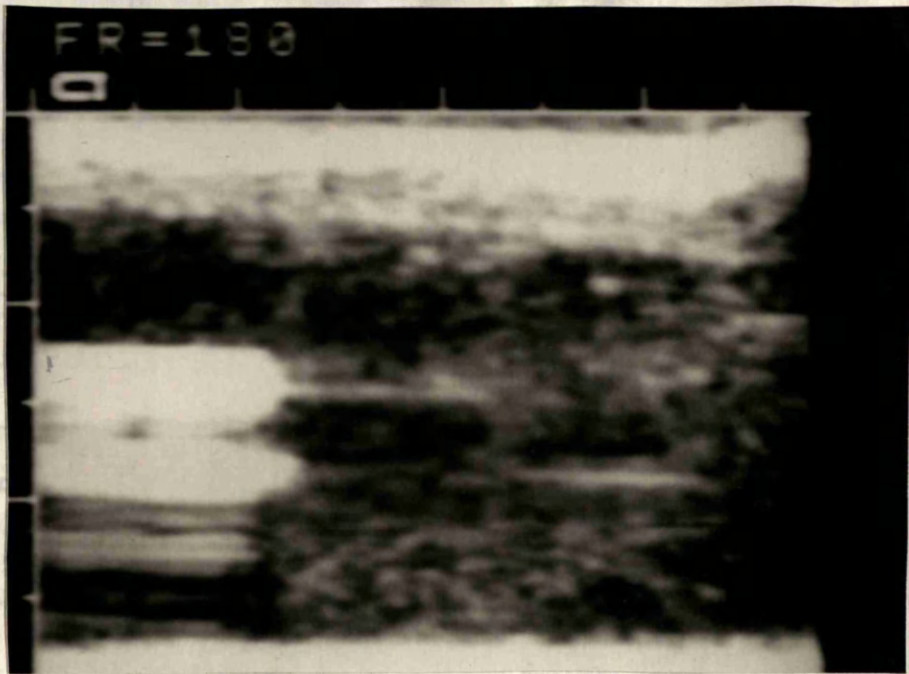


Figure 5.2
 which was
 ml/min, b
 ml/min, c
 outflow j
 e.) at 180

Figure 5.2
 ml/min, b
 ml/min, c
 outflow j
 e.) at 180

5.2 d.



5.2 e.

Figure 5.2 Flow rate and smoke-like signal. a.) At a flow rate of 0 ml/min, blood which was already in the chamber was highly echogenic; b.) at a flow rate of 30 ml/min, blood entering the chamber is echolucent; c.) and d.) at 90 ml/min and 120 ml/min, repetitively swirling smoke-like images of flow lines appeared between outflow jet stream and the static blood near the side of chamber (as arrows denoted); e.) at 180 ml/min, smoke-like signal disappeared.

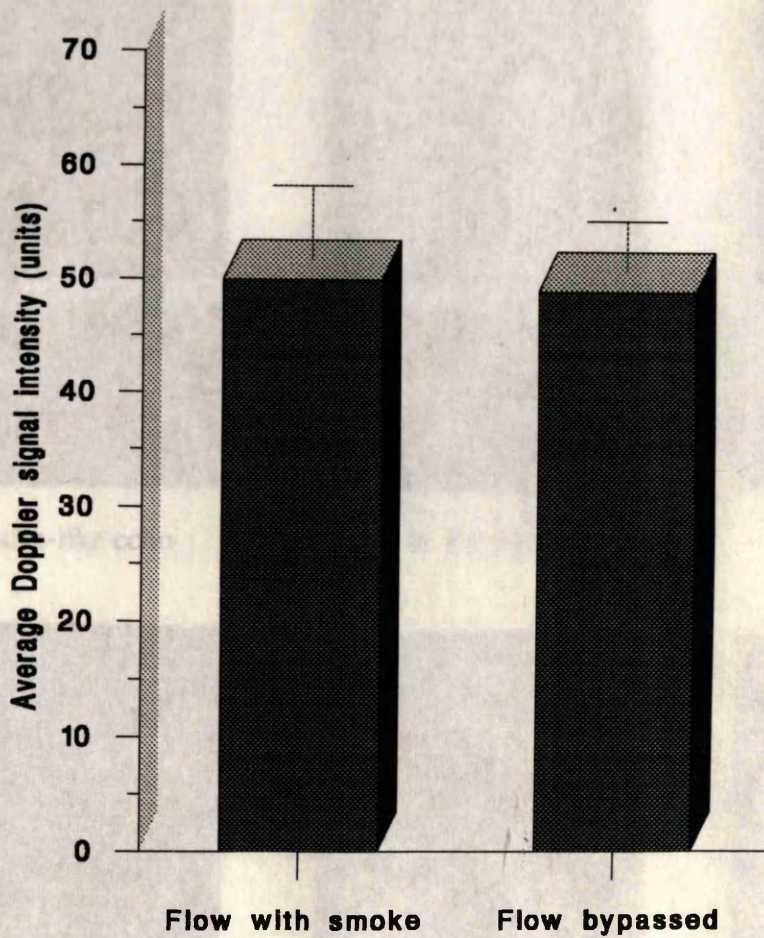
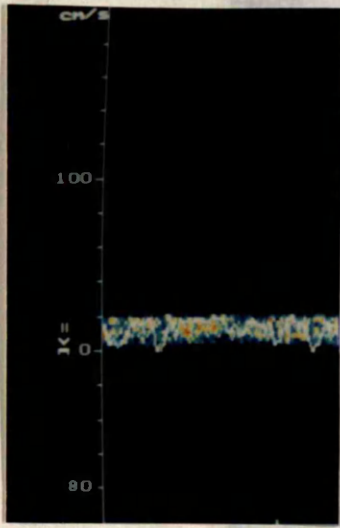
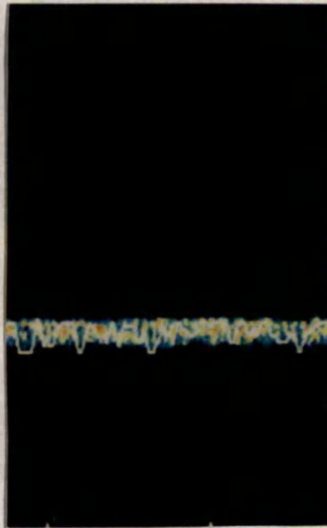


Figure 5.3 Comparison of average Doppler signal intensity between the blood flow with smoke-like signal and the blood flow bypassing the chamber. The flow which produced smoke-like signal did not significantly change average Doppler signal intensity compared with bypassing blood flow ($p = 0.71$).

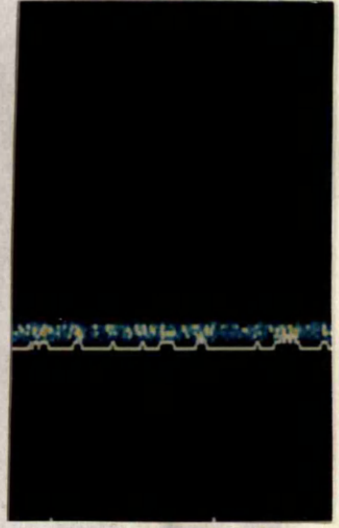
Figure 5.4 TCD detection of embolic material. The embolic signal was found from the blood flow with the presence of embolic material (a.) as well as from the blood flow bypassed (b.). Injection of normal saline at reperfusion did not change the TCD imaging (c.). However, injection of white blood clots (d.), platelet-rich clots (e.), and microbubbles (f.) produced visible embolic signals (or arrows denoted) and the signal intensity increased by several times was much higher than the other (a.).



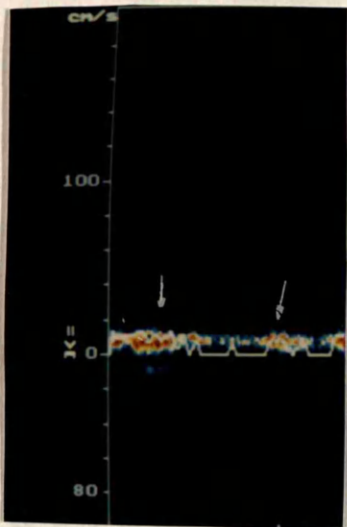
a. Smoke-like echo



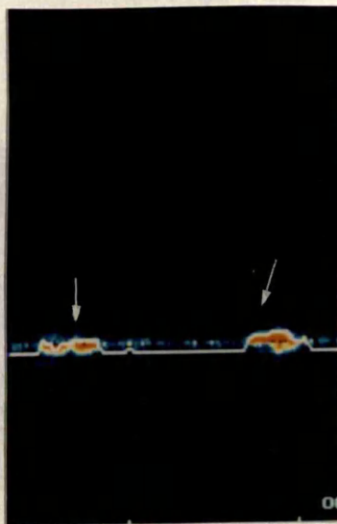
b. Bypass



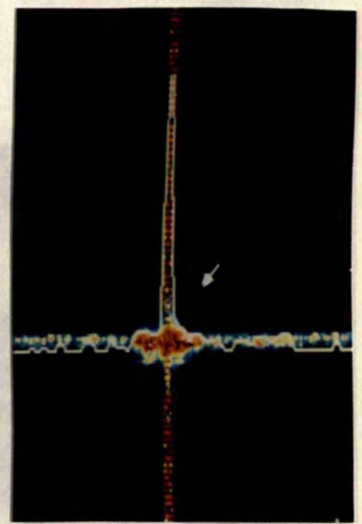
c. Normal saline



d. Blood clots



e. Platelet clots

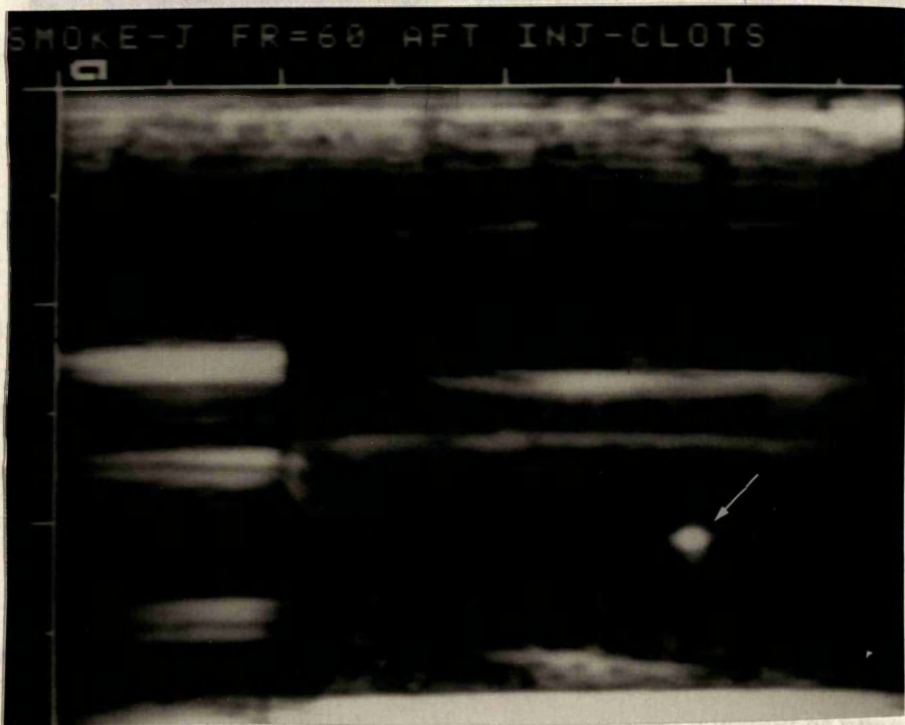


f. Microbubbles

Figure 5.4 TCD detection of embolic materials. No embolic signal was found from the blood flow with the presence of smoke-like echoes (a.) as well as from the blood flow bypassed (b.). Injection of normal saline at reported rate did not change the TCD imaging (c.). However, injection of whole blood clots (d.), platelet-rich clots (e.), and microbubbles (f.) produced visible embolic signals (as arrows denoted) and the signal intensity increased by microbubbles was much higher than the other two.

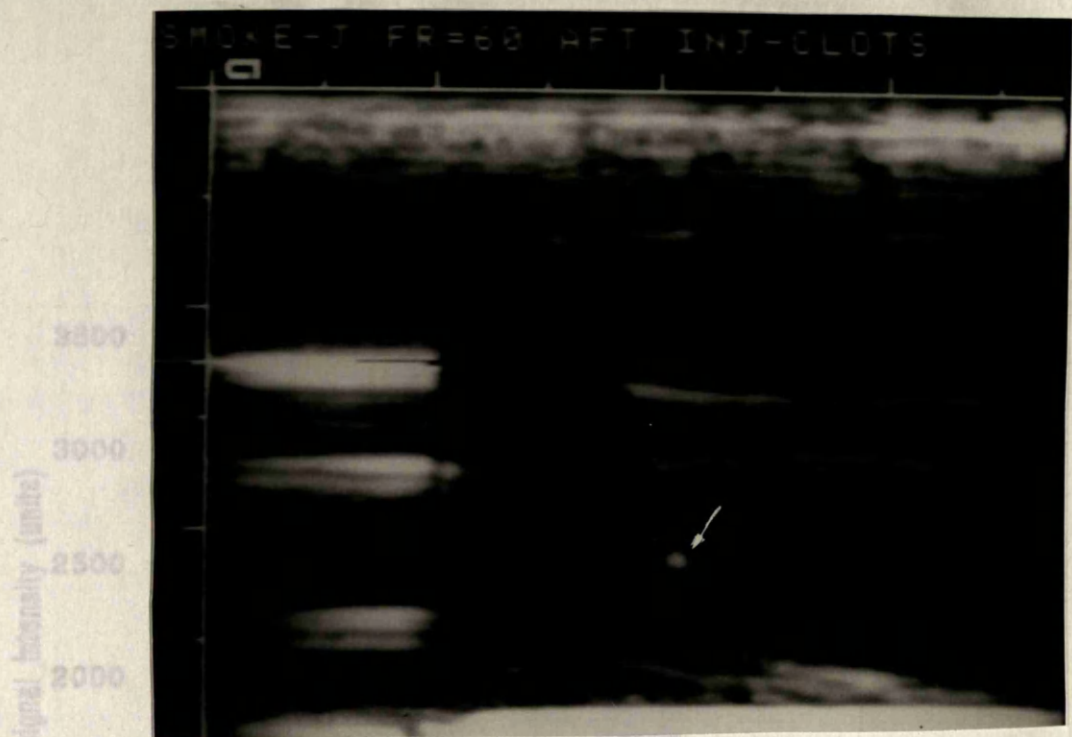


a) Normal saline

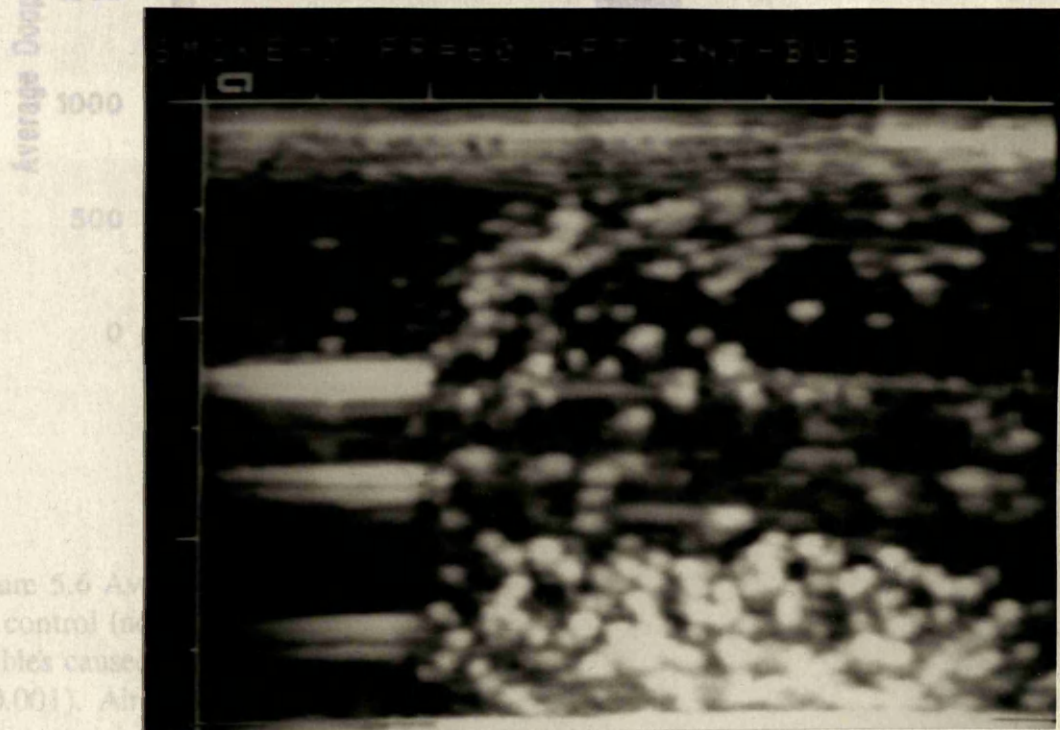


b) Whole blood clots

Figure 5.5 TV
 flow rate of
 temporarily produced smoke into the chamber. The flow rate of whole
 blood clots, platelet-rich clots, and microclots, prepared just like coagulographs (as
 arrows denoted) with clear water in the expansive chamber.



c) Platelet-rich clots



d) microbubbles

Figure 5.6 Average Doppler signal intensity of the control (no bubbles cause $p=0.001$). Air However, no intensity ($p=0.19$).

Note: * significant difference; NS no significant difference.

Figure 5.5 Two-dimensional echo images of embolic materials in the chamber. a) at flow rate of 40 ml/min (without smoke-like echo), injection of normal saline temporarily produced smoke-like imaging (as arrow denoted); b-d) injection of whole blood clots, platelet-rich clots, and microbubbles generated star-like echographies (as arrows denoted) with clear margins and floated in the expansion chamber.

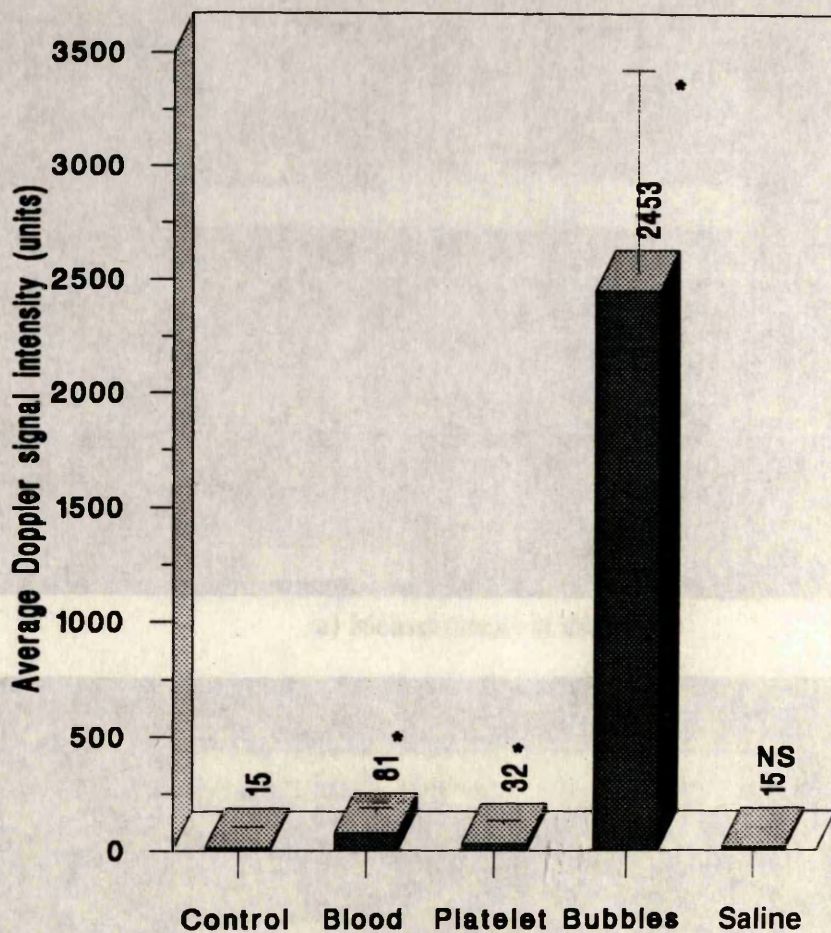
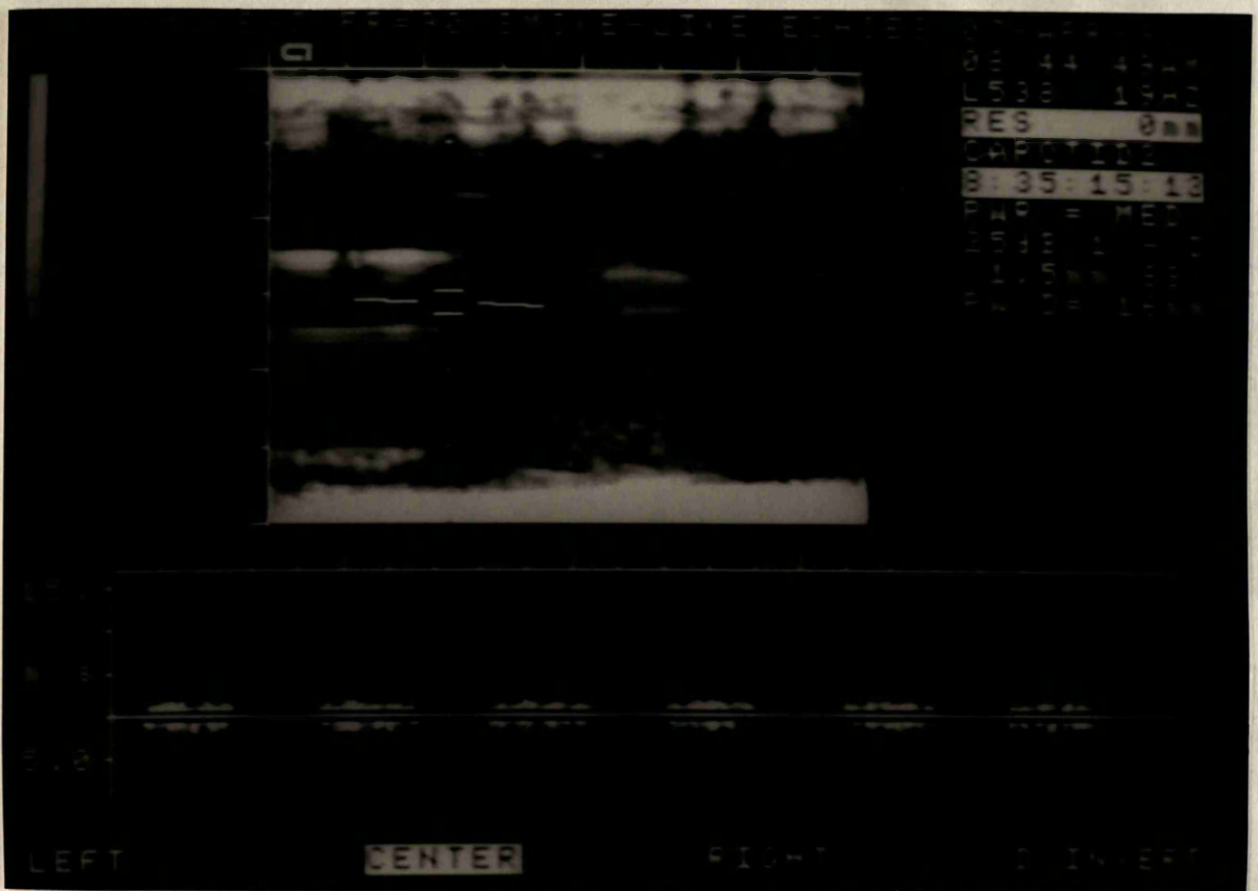
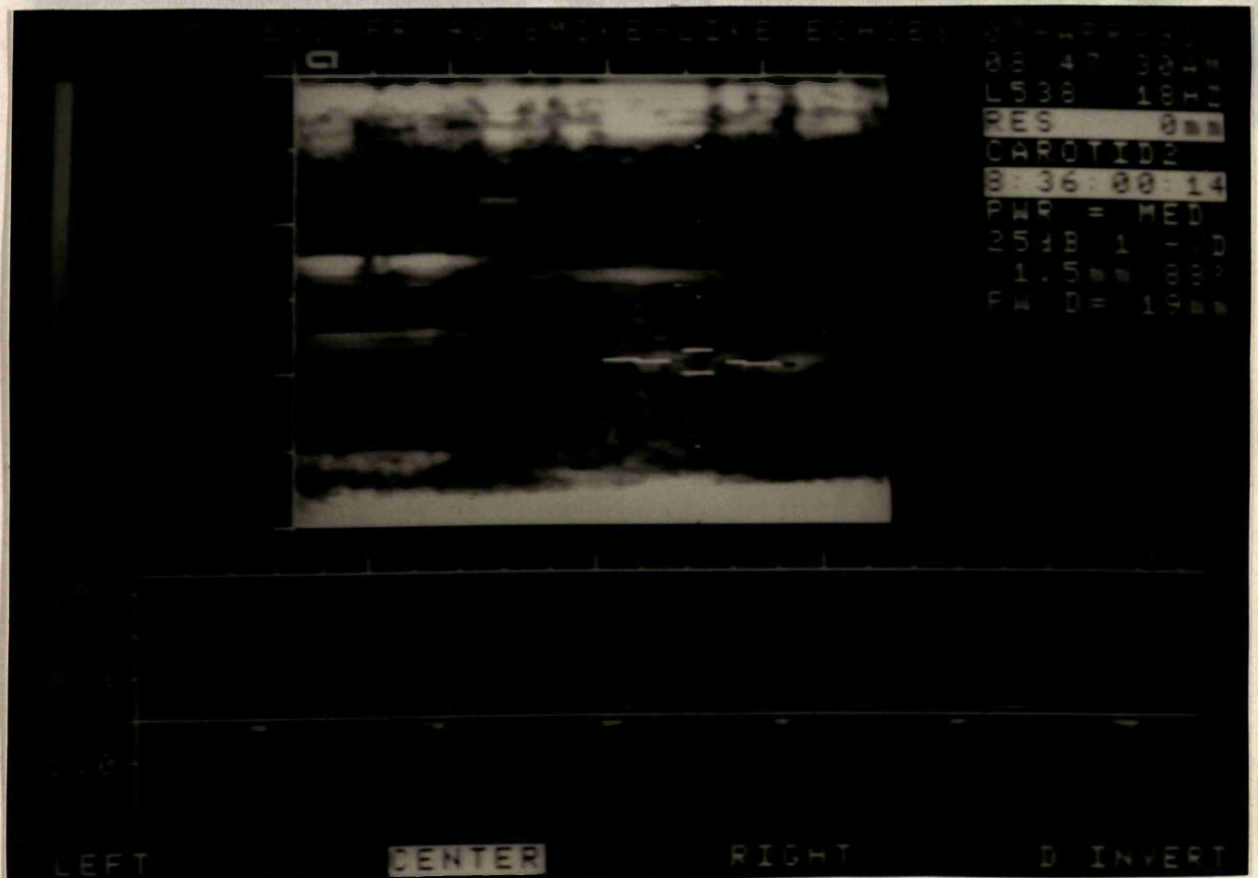


Figure 5.6 Average Doppler intensities of injection different materials. Compared to the control (non-injection), injection of whole blood clots, platelet-rich clots, and air bubbles caused an increase in an average Doppler signal intensity ($p < 0.001$, $p = 0.03$, $p = 0.001$). Air bubbles produced the highest average signal intensity among them. However, injection of normal saline did not cause significant change in average signal intensity ($p = 0.19$).

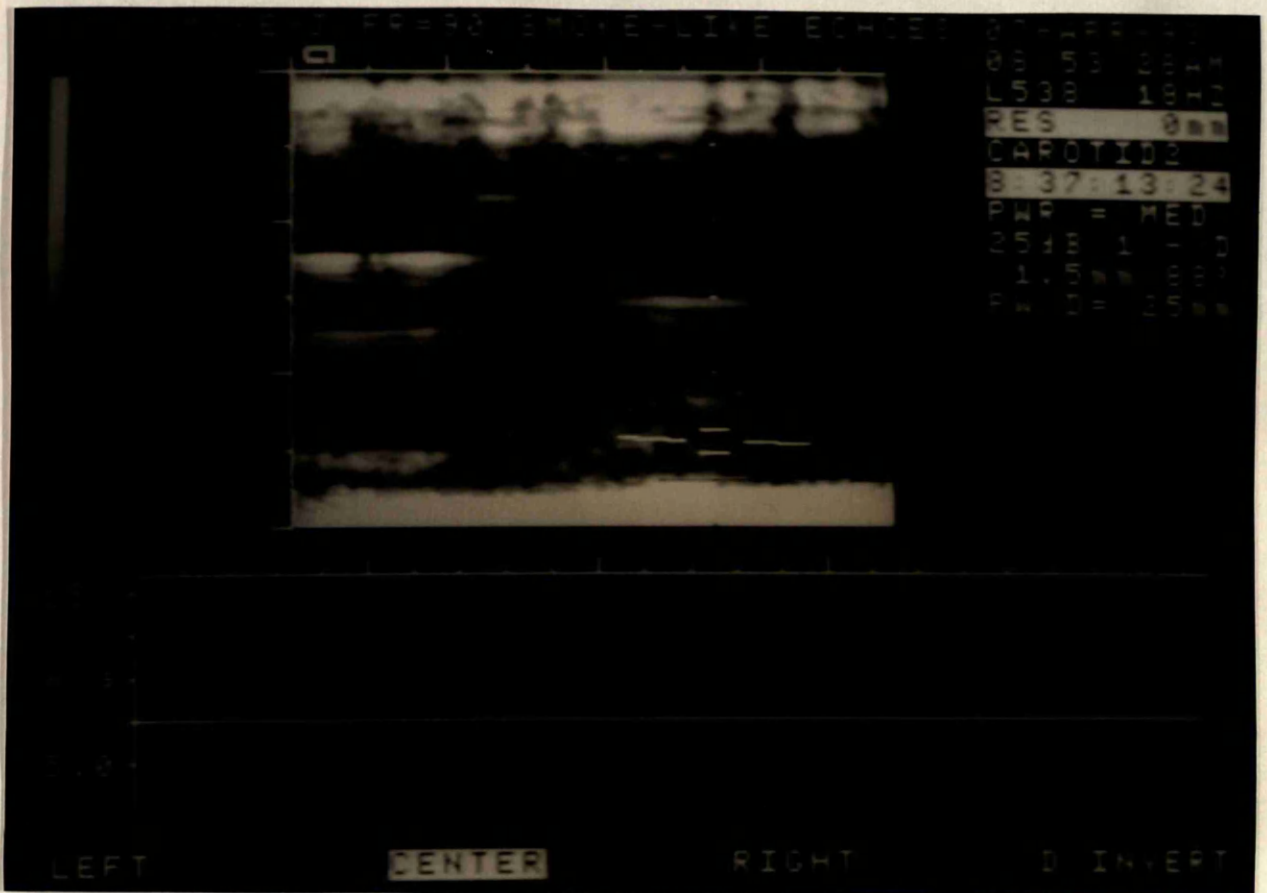
Note: * significant difference; NS, no significant difference.



a) Measurement in the centre



b) Measurement in the smoke echo area



c) Measurement near the side of the chamber

Figure 5.7 Doppler velocity related to smoke-like echo. Mean Doppler peak velocity in the centre of outflow stream was higher (148.7 ± 17.9 cm/sec) than that in the smoke-like signal area (32.8 ± 0.18 cm/sec) ($p < 0.01$). Both waveforms were in a biphasic wave pattern. The velocity in the area near the side of chamber was too low to be recorded.

6.1 INTRODUCTION

6.1.1 Definition of Turbulence Flow

Turbulent flow has been defined as flow in which pressure and velocity change constantly and erratically. Common examples are wind and water swirling around obstructions (Crystal et al, 1990). In the medical area, the phenomenon of turbulence is present with vessel stenosis and also occurs ex-vivo for example at connections of tubing systems including cardiopulmonary bypass systems (Stein et al, 1980).

CHAPTER SIX

ULTRASONIC QUANTIFICATION OF TURBULENCE AND DIFFERENTIATION OF EMBOLIC SIGNALS

The main features of asymmetric intermediate Reynolds's numbers have been described by Bascom et al (1993) (see Figure 6.1). There are four typical patterns: Zone I, laminar flow; Zone II, turbulent flow; Zone III, turbulent profile; and Zone IV, re-lamination. However, the dimensions of each of these zones and their detailed properties will depend on the Reynolds's number as well as the precise stenosis geometry.

6.1.2 Turbulence and Vessel Stenosis

Normally, turbulent flow is found to be present with a stenotic vessel, no matter whether it is a result or a cause of this vascular lesion (Rutzel et al, 1984). There is no doubt that stenosis can produce the turbulent flow but it is still controversial as to what degree of stenosis is needed to cause Doppler-detectable turbulence. Obviously, it is necessary to improve the understanding of the relationship between turbulence and stenosis because it may offer the hope of a criterion for the early development and detection of atherosclerotic plaques in humans (Giddens and Khalifa, 1982).

6.1.3 Detection of Turbulence with Doppler Ultrasound Technique

Although it has been proved that the accuracy of standard duplex ultrasonography is close to that of angiography of carotid artery through a non-invasive approach (De Bray et al, 1995), its efficiency may be limited in the situation of minor stenoses or existence of large plaques of calcification on the vessel walls, which may mask very

6.1 INTRODUCTION

6.1.1 Definition of Turbulence Flow

Turbulent flow has been defined as flow in which pressure and velocity change constantly and erratically. Common examples are wind and water swirling around obstructions (Crystal et al, 1990). In the medical area, the phenomena of turbulence is present with vessel stenosis and also occurs ex-vivo for example at connections of tubing systems including cardiopulmonary bypass systems (Stein et al, 1980).

The main features of asymmetric stenosis at intermediate Reynolds's numbers have been described by Bascom et al (1993) (see Figure 6.1). There are four typical patterns of flows in different zones distal to the stenosis. In order from the post-stenosis, there are: Zone I, Separation zone, Zone II, reattachment point, Zone III, Turbulent profile, and Zone IV, relamination. However, the dimensions of each of these zones and their detailed properties will depend on the Reynolds's number as well as the precise stenosis geometry.

6.1.2 Turbulence and Vessel Stenosis

Normally, turbulent flow is found to be present with a stenotic vessel, no matter whether it is a result or a cause of this vascular lesion (Ranval et al, 1994). There is no doubt that stenosis can produce the turbulent flow but it is still controversial as to what degree of stenosis is needed to cause Doppler-detectable turbulence. Obviously, it is necessary to improve the understanding of the relationship between turbulence and stenosis because it may offer the hope of a criterion for the early development and detection of atherosclerotic plaques in humans (Giddens and Khalifa, 1982).

6.1.3 Detection of Turbulence with Doppler Ultrasound Technique

Although it has been proved that the accuracy of standard duplex ultrasonography is close to that of angiography of carotid artery through a non-invasive approach (De Bray et al, 1995), its efficiency may be limited in the situation of minor stenoses or existence of large plaques of calcification on the vessel walls, which may mask very

segmental stenoses (De Bray et al, 1995). Doppler ultrasonography can supply haemodynamic information about a stenotic vessel by demonstration of turbulence, acceleration and backward flow and the detection of flow features is far less affected by calcification than for the ultrasound picture distortion which is caused for example by vessel wall calcification.

Doppler ultrasound has an established role in the non-invasive assessment of arterial disease since it can be commercially used to quantify the blood flow velocity, which is derived from the Doppler frequency shift. Previous turbulence studies involving the use of Doppler ultrasound have focused on attempting to establish spectral parameters that can be correlated to the size of the stenosis (Morin et al 1988 and Kaluzynski and Tedgui 1989). However, there are additional properties of the Doppler signal that are also influenced by the nature of the flow field and these may aid in characterising flow disturbances.

Generally, it has been assumed that the backscattered power is invariant over the flow cycle and is independent of the flow conditions (e.g. laminar vs. turbulent). In recent years, these assumptions have been questioned. For example, it has shown from *in vitro* studies that the backscattered intensity for normal haematocrit blood increases with the onset of turbulence (Shung et al 1984 and Bascom et al 1988). It has been demonstrated that the type of flow regime that is insonated may cause a change in the backscattered Doppler intensity (Bascom et al 1988 and 1993). The turbulence intensity was measured and found higher than that of normal flow in the centre of canine ascending aorta using a hot-film anemometer (Yamaguchi, 1980).

Turbulence phenomena may occur in the cerebral arteries when there is a severe cerebral artery stenosis or cerebral artery spasm or even cerebral collateralisation via the ipsilateral anterior and/or posterior cerebral communicating artery following carotid obstruction diseases (Rosenkranz et al, 1992). Turbulent flow detected in the intracranial arteries during compression of the ipsilateral common carotid artery was initially documented by Aaslid et al (1982) using transcranial Doppler ultrasonography. It showed up in the spectra as a brief period of low-frequency noise.

Transcranial Doppler has been further successfully used to detect turbulent flow in patients with stenosis or spasm of the cerebral artery or under conditions of collateral circulation (Rosenkranz et al, 1992 and Provinciali et al, 1992). But they did not supply any quantitative information about intracranial turbulence in blood flow. Quantitative study of the relationship between the Doppler signal intensity and intracranial cerebral artery stenosis using TCD has not yet been documented.

6.1.4 Turbulent Flow and Cerebral Embolism

Transcranial Doppler can be used to record flow velocity non-invasively in the major intracranial arteries (Aaslid et al, 1982). This technique has been also proved useful in detecting cerebral emboli characterised by abnormal transient Doppler signal with changed frequency/velocity and harmonic chirps (Spencer, 1992). Cerebral embolic signals, like turbulent flow signals, also show an increase in signal intensity (Russell et al 1991 and Markus et al, 1993b). As mentioned above, turbulent flow, which normally happens when there is a stenotic lesion in the basal arteries or when the collateral pathway through the anterior communicating artery is activated (Provinciali et al, 1992), may co-exist with cerebral embolism in the same patient during transcranial Doppler ultrasonography recording. This is particularly likely case of embolism into intracranial circulation from an ulcerative atheroma in the internal carotid artery or the middle cerebral artery (Spencer et al, 1990 and Barnett, 1991). An additional area where confusion between emboli and turbulence may arise is in shunting during carotid endarterectomy (Padayachee et al, 1986). Such Doppler signals were suspected to be due to turbulent blood flow or air bubbles. Differentiation is needed in this situation because the results and the preventive therapies are different with the different pathological mechanisms. However, so far such a study has not been reported either in intracranial or extracranial territory using the Doppler method.

6.1.5 Aims

In the present investigation, we aimed: 1) to reproduce turbulence in a short asymmetric stenosis middle cerebral artery model; 2) to evaluate the effect of the

stenosis degree on the average signal intensity of the backscattered Doppler ultrasound signal and mean velocity. To achieve this, we also examined any change of the average signal intensity in different flow fields prior or distal to the stenotic position. We hypothesised that the Doppler signal intensity of turbulent flow is distinguished from that of the normal blood flow and should be associated with degree of stenosis. 3) to compare embolic signals with turbulent flow signals using total Doppler signal intensity. For this purpose, we employed a method of quantitative signal intensity analysis which measured the change of total signal intensity caused by either embolic particles or turbulent flow and we also carried out a visual observation.

6.2 MATERIALS AND METHODS

6.2.1 Reproduction of Turbulent Flow in the MCA Stenosis Model

Turbulent flow was reproduced on the middle cerebral artery model, which was fully described in section 2.2.1 of Chapter Two and illustrated in Figure 2.1, by making an asymmetrical stenosis on a rabbit's thoracic aorta with an internal diameter of 5.0 mm. The modified part of the model was shown in Figure 6.2. All the tests in this study were conducted under a pulsatile flow conditions.

Out-dated packed human red blood cells were employed as circulating fluid in this study. 300 ml human red blood cells were suspended in 200 ml physiological saline to obtain a haematocrit of 35%, measured with a Sysmex NE 800 (TOA Medical Electronic, Japan). Then, the diluted red blood cells were degassed for 15 minutes with an ultrasonic basin (Transsonic T890/H, CAMLAB, UK) and circulated with the two pumps described in 2.2.1 of Chapter Two. The flow rate was monitored throughout the study using a calibrated electromagnetic flow meter. Initial flow rate was maintained at 80 ml/min. before narrowing the aorta.

6.2.2 The Degree of Stenosis and the Turbulence

In this study, the degree of stenosis was expressed as the percentage of reduced cross-sectional area. In order to examine the relationship between the degree of

stenosis and producibility of turbulent flow signals, a series of stenosis degrees (from 45%, 55%, 65%, 75%, 85% to 90% by reduced cross-sectional area) were prepared.

A short asymmetrical stenosis model was made for this study. The reason for choice of an asymmetrical stenosis was influenced by the fact that with a symmetrical stenosis problems would arise with refraction when attempting to obtain Doppler signals formed within the constricted region (Bascom et al, 1993). Additionally, clinical observations (Glagov et al, 1987) suggest that stenoses are generally asymmetric in shape especially in regions where the artery curves.

In order to make different degrees of asymmetrical stenosis of the aorta, firstly, metal bars with different corresponding diameters were prepared. For forming an asymmetrical stenosis, a 2/0 braided silk suture (©Ethicon Ltd. UK) was used to tie round the aorta enclosing the metal bar of a selected diameter and the metal bar was then gently withdrawn. The remaining cross-sectional area of stenotic aorta was equal to the area of the metal bar withdrawn. The cross-sectional area of the metal was calculated from its known diameter. As a result, a series of short asymmetrical stenoses (because they have a short length of the constricted region of stenosis) could be performed with bars of different diameters. The correspondence of the diameters of bars used in this study and the degrees of reduced cross-sectional area of the aorta was list as follows:

Diameter of Bar (mm)	Reduced Cross-sectional Area (%)	Remaining Cross-sectional Area (%)
1.60	≈90 (89.76)	≈10 (10.24)
2.00	85 (84.00)	15 (16.00)
2.57	75 (73.58)	25 (26.41)
2.97	65 (64.72)	35 (35.28)
3.40	55 (53.76)	45 (46.24)
3.74	45 (44.05)	55 (55.95)

- The internal diameter of the rabbit's aorta = 5 mm.
- Reduced cross-sectional area (%) = (Cross-sectional area of bar ÷ Cross-sectional area of aorta) x 100%

To confirm the change in a cross-sectional area after saturation, the stenotic artery was filled with paraffin wax and subsequently sectioned at different four sample zones with a blade after the experiment. The images of the resulting cross-sectional area of a 55% degree stenosis were shown in Figure 6.3.

6.2.3 Preparation and Injection of Embolic Materials

To compare the signal intensities of circulating embolic materials with those increased by turbulent flow, three types of commonly-found embolic materials, air bubbles, whole blood clots, and platelet-rich thrombus clots were injected into this system in the present study. The methods for preparation of all the three kinds of embolic materials were detailed in 2.4 of Chapter Two. Solid embolic materials (n=8 for each type) were injected individually but microbubbles (0.1 ml, 400 bubbles/ml in concentration) were injected as a solution. The methods to size embolic materials and to dilute and count the bubbles have been mentioned in Chapter Two and 3.2.4 of Chapter Three. Average size for the solid embolic materials was 100 μm and the mean size of microbubbles used in this study was $29 \pm 6 \mu\text{m}$. The solid embolic particles were suspended in 10 ml normal saline and each particle was introduced into the circulation system gently with a 1 ml plastic syringe in 1 ml saline. The air bubbles, suspended in Ultravist 370, were injected with a 0.1 ml glass syringe. Solid embolic materials were injected within 5 minutes and microbubbles were used within 30 seconds after preparation.

To avoid embolic signal overlap the turbulent flow, embolic materials were injected in unstenosed vessels.

6.2.4 TCD Recording and Off-line Signal Analysis

A 2-MHz probe of Transcranial Doppler ultrasonography (Nicolet, Warwick, UK) was employed in this study. The gain (2 units), power (75 watts), and other TCD settings were kept constant throughout the study. However, the insonation depth varied with focusing distance along the turbulent flow. In this study, Doppler signals were sampled from four zones along the stenosis. They comprised 1) pre-stenosis, 1

cm before stenosis (equivalent to upstream velocity profile); 2) on stenosis (equivalent to high jet velocity profile and separation zone); 3) post-stenosis I, 0.5 cm distal to stenosis (equivalent to turbulence profile); and 4) post-stenosis II, 2.5 cm distal to stenosis (equivalent to relaminarisation). To avoid possible overlapping between two sample areas, the sample volume of TCD was properly minimised (5 mm). Coupled with acoustic gel, the probe of TCD was allowed to slide up and down to insonate different zones along turbulent flow without changing the angle of ultrasound beams. The sample positions along the asymmetric stenosis are illustrated in Figure 6.2.

3. Comparison of the total signal intensity of turbulence with that of emboli

For off-line signal analysis, average signal intensity, total signal intensity and mean Doppler flow velocity were calculated and then compared in this study. The method for calculation of the average and total signal intensity was described in 2.3.2 of Chapter Two.

In addition to signal intensity analysis, the changes in the shape of the velocity waveform with distance from the stenosis were also studied by simultaneous flow visualisation, point velocity measurement and audio characterisation. The relationship between the transition of turbulence and the degree of stenosis of artery was examined visually from the image component of the Doppler velocity waveform.

6.2.5 Statistical Analysis

1. Comparison of average signal intensity in different sample positions

A stenosis of a degree of 65% reduced cross-sectional area was chosen for this comparison because turbulent flow was most typical and reproducible at this degree of stenosis. The average signal intensity was calculated from six frames of Doppler flow velocity waveform which were previously recorded at each of the above sample positions. The average signal intensities gained from pre-stenosis, on-stenosis, post-stenosis I, and post-stenosis II were compared with one another.

2. Correlation between the degree of stenosis and average signal intensity or mean flow velocity at post-stenosis I position

Six frames of Doppler flow velocity waveform were sampled and saved at the post-stenosis I position for every degree of stenosis from 45% to 90%. By means of intensity analysis software, the average signal intensities from the six frames at the post-stenosis were examined and correlated with the degrees of stenosis. The readings of mean flow velocity were calculated by the combination of manually marking the peak systolic velocity and early diastolic velocities and using built-in TCD calculation software. The six mean flow velocities at the post-stenosis were related to the degree of stenosis.

3. Comparison of the total signal intensity of turbulence with that of emboli

Total signal intensity of turbulence and emboli was measured over a period of 100 ms because that was the usual maximum duration of embolic signals in this study. A 65% degree of stenosis was used for this test. We chose the total signal intensity of turbulence at the position of post-stenosis to compare with embolic signals because the average signal intensity was higher here than at all other sample positions. The total signal intensity was calculated from eight turbulence signals recorded at the position mentioned above. The total signal intensity of embolic materials including whole blood clots (n=8), platelet-rich clots (n=8), and air bubbles (n=8) was calculated as mentioned in 2.3.2 of Chapter Two.

6.2.5 Statistical Analysis

All data in this study were expressed as mean \pm 1SD. One way ANOVA was used for comparison of the total signal intensity in the same sample position (post-stenosis I) between six different degrees of stenosis. The relationship between the total signal intensity increased by turbulence flow in the post-stenosis I zone and the degree of stenosis was evaluated by calculating the correlation coefficient. This statistical method was also used to investigate the relationship between the flow velocity in the post-stenosis I and the degree of stenosis. Logarithmic transformation was used to improve the relation study and regression analysis was applied in this situation. Student *t*-test was employed to examine the significance of the comparison of the mean between two groups. Results were considered significant if $p < 0.05$.

6.3 RESULTS

6.3.1 Turbulent Flow in Different Sample Positions

The Doppler velocity waveform in different sample positions (zones) (at stenosis degree = 65%) are shown in Figure 6.4. The diluted red blood cell concentrated flow demonstrated a normal Doppler velocity waveform in the zone of pre-stenosis. In the on-stenosis zone, the flow showed a sharp increase in systolic velocity (so-called jet flow or flow acceleration) and the colour-coded signal intensity started to intensify. In the post-stenosis zone, the systolic velocity tended to drop but a typical turbulence component was noted in the centre of the waveform, accompanied by a remarkable reverse flow and a loss of high frequency definition in the velocity waveform. Also a flood-like noise could be heard over the systolic period in both the on-stenosis and post-stenosis zones. The flow in the post-stenosis II tended to be normal but had lower flow velocity. The order of mean flow velocity from the low to the high was: post-stenosis II, pre-stenosis, post-stenosis I, and on-stenosis.

Analysis of average Doppler signal intensity showed that the average signal intensity started to rise in the on-stenosis zone (1004.00 ± 52.00 units) compared with that in the pre-stenosis zone (527.83 ± 12.25 units) ($p < 0.0001$). The average signal intensity reached a peak in the post-stenosis I zone (1480.70 ± 61.10 units) and went down significantly in the zone of post-stenosis II (1204.00 ± 13.10 units, $p < 0.0001$) (Figure 6.5). The order of average signal intensity was different from the order of mean flow velocity: pre-stenosis, on-stenosis, post-stenosis II, and post-stenosis I.

6.3.2 The Relationship between the Turbulence and the Degree of Stenosis of Artery

1. Turbulence and the degree of stenosis

Visual observation of the changes in flow pattern with the degree of stenosis was undertaken in this study. The transition of turbulence did not occur until the degree of stenosis increased to 55% but it was still in an immature shape. A typical turbulence became visible at 65% degree of stenosis and at 75%. Reversed flow went on in the same course. Turbulent flow became damped at 85% and 90% degree of stenosis.

However, the systolic velocity kept increasing from 65% to 90% degree of stenosis (Figure 6.6).

2. Average signal intensity and the degree of stenosis

The average signal intensity calculated in the post-stenosis region from different degree of stenosis was related to the degree of stenosis. There was a poor correlation between the average signal intensity at the post-stenosis region and the degree of stenosis of the artery ($y = 1102.53 - 4.69 x$, $r = -0.43$) (Figure 6.7).

6.4 DISCUSSION

3. Mean flow velocity and the degree of stenosis

The relationship between the mean flow velocities measured in the post-stenosis region from the all degrees of stenosis and the degree of stenosis was evaluated. The mean flow velocity was inversely proportional to the degree of stenosis but the relationship was nonlinear in the overall course (Figure 6.8a). It was studied whether the fit was improved by using logarithm of the mean velocity in the regression analysis. After a logarithmic transformation of the mean velocity readings from the stenosis degree of 45% to 85%, It was found that a linear fit was existed between the mean flow velocity and the selected degrees of stenosis [$y = 274.46 - 130.76 \times \log(x)$, $r = -0.91$, $p < 0.001$] (Figure 6.8b).

6.3.3 Comparison of Turbulence Signal with Embolic Signals

1. Visual comparison

Figure 6.9 comprises turbulent flow signals and embolic signals induced by injection of commonly-seen embolic materials. From the colour-coded intensity spectrum, turbulence flow signals are characterised as having a high-intensity core in the centre of the systolic period of the velocity waveform, accompanied with jet flow velocity, a consistent harsh noise, and reversed flow. But embolic signals were featured as a high intensity component point which randomly occurred at any time in the cardiac cycle, were brief in duration and accompanied with transient harmonic chirps. They were easily distinguished from each other according to these features.

2. Comparison of total signal intensity of turbulence with that of embolic signals

There was no significant difference between the total signal intensity of turbulence flow (3258 ± 900 units) and that of whole blood clots (2389 ± 1278 units) ($p = 0.14$). However, the total intensity of embolic signal increased by introduction of platelet-rich clots (23303 ± 9596 units) and air bubbles (39220 ± 14076 units) was significantly higher than that of turbulence flow signal (Turbulence vs. Platelet clot $p = 0.0003$, Turbulence vs. microbubbles, $p = 0.0001$) (Figure 6.10).

6.4 DISCUSSION

Turbulence has been successfully reproduced, detected and compared in an modified MCA model in this study. This colour Doppler imaging technique affords overall demonstration of turbulence on which signal intensity quantification and visual assessment are allowed. This may suggest that qualitative and quantitative assessment of turbulent flow in an *in vivo* situation should be possible.

It has been shown that average signal intensity increased significantly in the zone of turbulence in comparison to that from other flow zones. This and the average signal intensities distributed in the distance prior or distal to stenosis, is in good agreement with a recent result reported by Bascom et al (1993). The reason for this turbulence-induced signal intensity increase is not fully clear but a possible explanation was given by some previous investigators (Mo and Cobbold, 1992 and Bascom et al, 1993). As the flow changes from laminar to turbulent, fluctuations in the velocity field increase, resulting in an enhanced variance of the RBC distribution, which should cause the Doppler signal intensity to rise.

One of the purposes of the present study is to relate the occurrence of turbulence to the severity of stenosis. This observation was conducted on a series of short stenoses from 45% to 90%. It was shown that the transition to turbulence did not occur with 45% stenosis (a moderate degree of stenosis). The transition to an immature turbulence was only triggered with a 55% stenosis and a typical turbulence was

present when increasing the severity of the stenosis to 65%. This result is close to the previous finding by Ojha and Langille (1993). They formed a short stenosis *in vivo* model using the rabbit's common carotid artery and found that turbulence did not occur at 55% stenosis although such a severity of stenosis could cause post-stenotic dilatation. The development of turbulence did not happen until increasing the severity of a short stenosis to 70% on the rabbit carotid arteries. Other investigators concluded that mild stenosis showed flow acceleration but no flow turbulence (Fietsam et al, 1992) and even defined the degree of carotid stenosis up to 50% ~ 99% as haemodynamically relevant (Sterpetti et al, 1988). By contrast, it was reported that turbulent flow could be created by a mild stenosis of 30% in the dog aorta (Giddens and Khalifa, 1982) and 40% asymmetrically stenosed human carotid artery (Steinke and Hennerici, 1992). There is no general agreement about the stenosis degree in generation of turbulence. This is probably due to the fact that, in addition to the severity of stenosis, the occurrence of turbulence is also affected by other factors including flow rate, haematocrit of the flowing materials, the compliance of tube wall (Stein et al, 1980), and the sample distance distal to a stenosis. The difference in the sensitivity of Doppler devices used should be another source of the disagreement (Steinke and Hennerici, 1992). This limitation of ultrasound in enhancing detection of a mild degree of stenosis through turbulence measurements has to be recognised from our current study and the reported literature. But, on the other hand, our results also showed that the measurement of the change of flow velocity with the same device can compensate it.

It was also found that the Doppler signal recorded from the severe degree of stenosis (85% and 90%) was damped compared to moderate degree stenosis. This may be because, at a high-degree stenosis, the stenotic throat is too narrow to allow enough RBC flow to reach the post-stenotic regions. There are less RBC acting as ultrasound scatters as a result. This situation also has been reported in the intracranial circulation (the narrowed MCA) (Rosenkranz et al, 1992) as well as the extracranial circulation (the severely stenosed carotid artery) (Murie et al, 1984 and Steinke et al, 1992). This phenomena has a clinical significance since it is one of characteristics of stenosis.

We further investigated the effect of the degree of stenosis on average Doppler signal intensity and mean flow velocity to gain insight into the mechanisms of this phenomenon. The average intensity grows markedly in the zone of turbulence profile and then dissipates rapidly at the zone of relaminarisation. This behaviour is characteristic of post-stenotic flow as has been demonstrated in both animal (Giddens et al, 1976) and *in vitro* models (Giddens and Khalifa, 1982). However, it was observed unexpectedly that this increase at post-stenosis I seems to be independent to the change in degree of stenosis. This result is not in accord with the previous finding by Giddens and Khalifa's (1982). They reported that the intensity of turbulence was proportional to the reduction of cross-sectional area and therefore concluded that the signal intensity of turbulence could be used as a diagnostic indicator of assessment of the cross-sectional area of stenosis. However, the data from the present study seem to question this application. The additional influencing factors described above, and possibly also the use of temporal bone in this model may explain differences.

In contrast, mean flow velocity recorded at the zone of turbulence profile showed a different course. It demonstrated a quantitative relationship with the gradient of stenosis degree. A similar result was reported by Vattiyam et al (1992) in an *in vivo* model. This result implies that pathologic increases in velocity facilitate transcranial Doppler detection of luminal narrowing in the intracranial arteries, whether due to atherosclerotic stenosis, recanalisation or partial obstruction after embolisation.

In this study, although we have not directly correlated the average signal intensity to the mean velocity recorded at different sample positions, it is clear that the average signal intensity recorded at post-stenosis I did not accord with that of flow velocity sampled at the same region as the degree of stenosis increased. This differs from the conclusion of Chapter Seven (7.3.1). It should be pointed out, however, that the present average signal intensity was not collected from laminar flow (while this is the case in Chapter Seven) but from turbulence. It is well known that signal intensity is not only influenced by flow velocity but also by other haemodynamic factors.

Stenotic abnormalities are not only obstructive but also potentially emboligenic lesions (Bandyk et al, 1988). It is possible for turbulence and embolism to co-exist simultaneously in a clinical situation. In this study, we attempted to differentiate them not only by visual assessment but also by signal intensity analysis. It was found that turbulence and embolic signals are not difficult to distinguish by their own visual features and audio behaviour in the Doppler waveform. In contrast, there is some difficulty of differentiation using total signal intensity because both turbulence and emboli cause a marked increase in total signal intensity. However, this is not such a problem if air bubble emboli are involved or other kinds of involved solid emboli have a big size. Intensity analysis may become more important when an embolic signal superimposes on turbulence signal since visual identification may be difficult in this situation, but we did not address this in the current study.

In conclusion, distinctive patterns of fluid dynamic turbulence are detected and characterised in the *in vitro* MCA model. These findings may provide a more quantitative and reproducible method of interpreting flow patterns in the region of a stenosed cerebral artery. Each major flow area shows different Doppler characteristics. Turbulence is only detectable at moderate-to-high degrees of stenosis. Mean flow velocity is more sensitive to the degree of stenosis than average signal intensity, from measurement immediately distal to the stenosis, and this has a potential clinical application. Turbulence has a Doppler image quite distinct from embolic signals. Signal intensity analysis may help in this differentiation if air bubble emboli or solid emboli with a relatively large size are involved.

Figure 6.1. Showing the main features of the flow patterns in the stenosed cerebral artery. Zone I: The flow is laminar. Further downstream, in Zone II, the vortices generated within the shear layer of the jet begin to break down and the flow exhibits a transition to turbulence. Distal to this region, in Zone IV relaminarisation occurs and the velocity profile begins to return to the prestenotic state.

This illustration is modified from Bascom et al (1993).

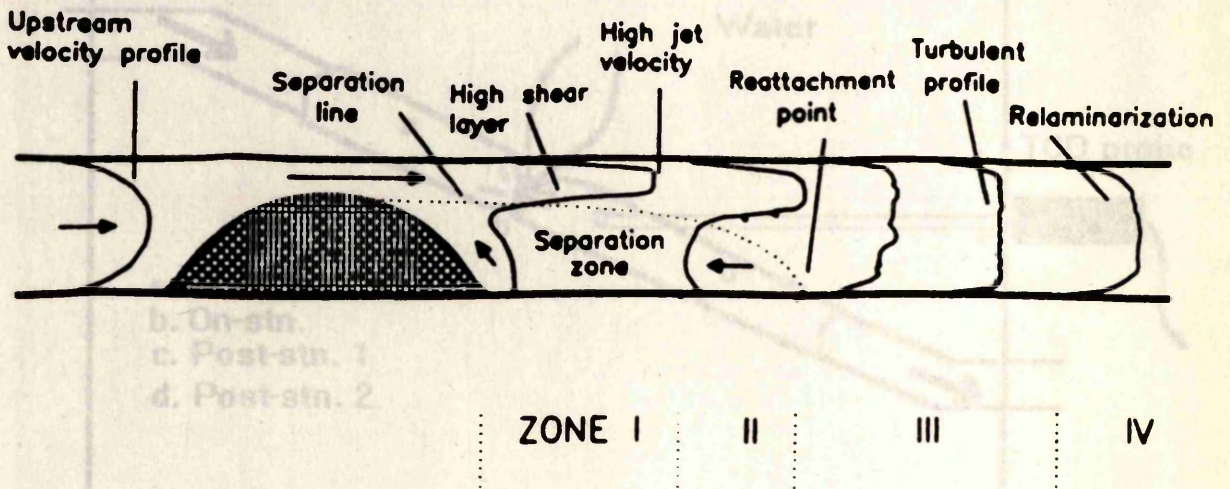


Figure 6.1 Showing the main features of the anticipated four zones distal to an asymmetric stenosis at a Reynolds's number of around 545. Just beyond the stenosis a stable jet is present together with a well-defined separation zone (Zone I). Further downstream, in Zone II, the vortices generated within the shear layer of the jet begin to break down and the flow exhibits a transition to turbulence. Distal to this region, in Zone IV relaminarisation occurs and the velocity profile begins to return to the prestenotic state.

This illustration is modified from Bascom et al (1993).

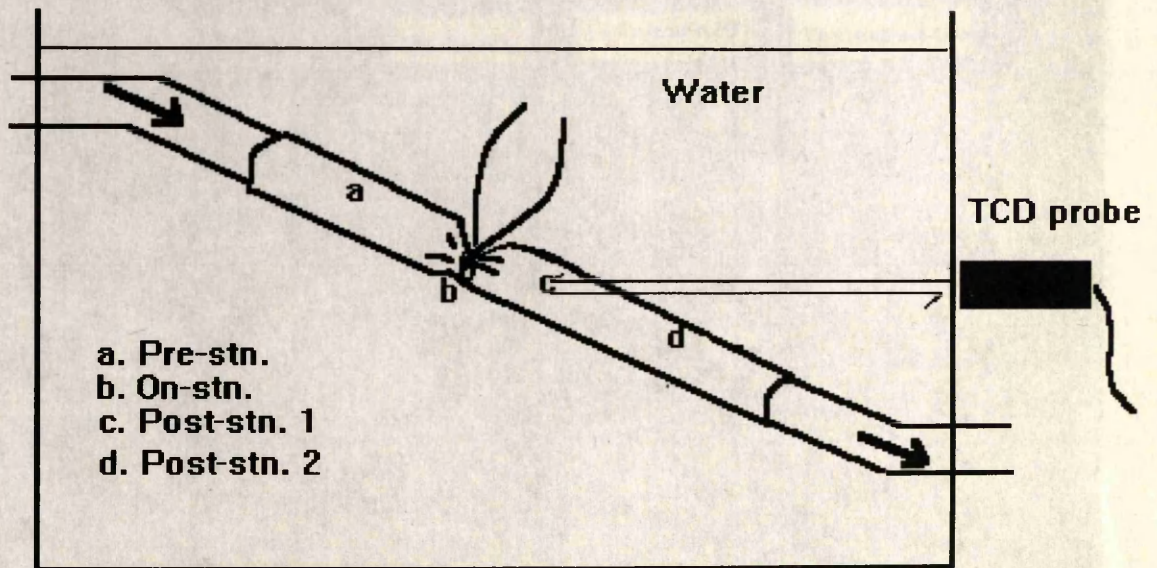


Figure 6.2 Illustration of the MCA stenosis model and the Doppler ultrasound sample positions.

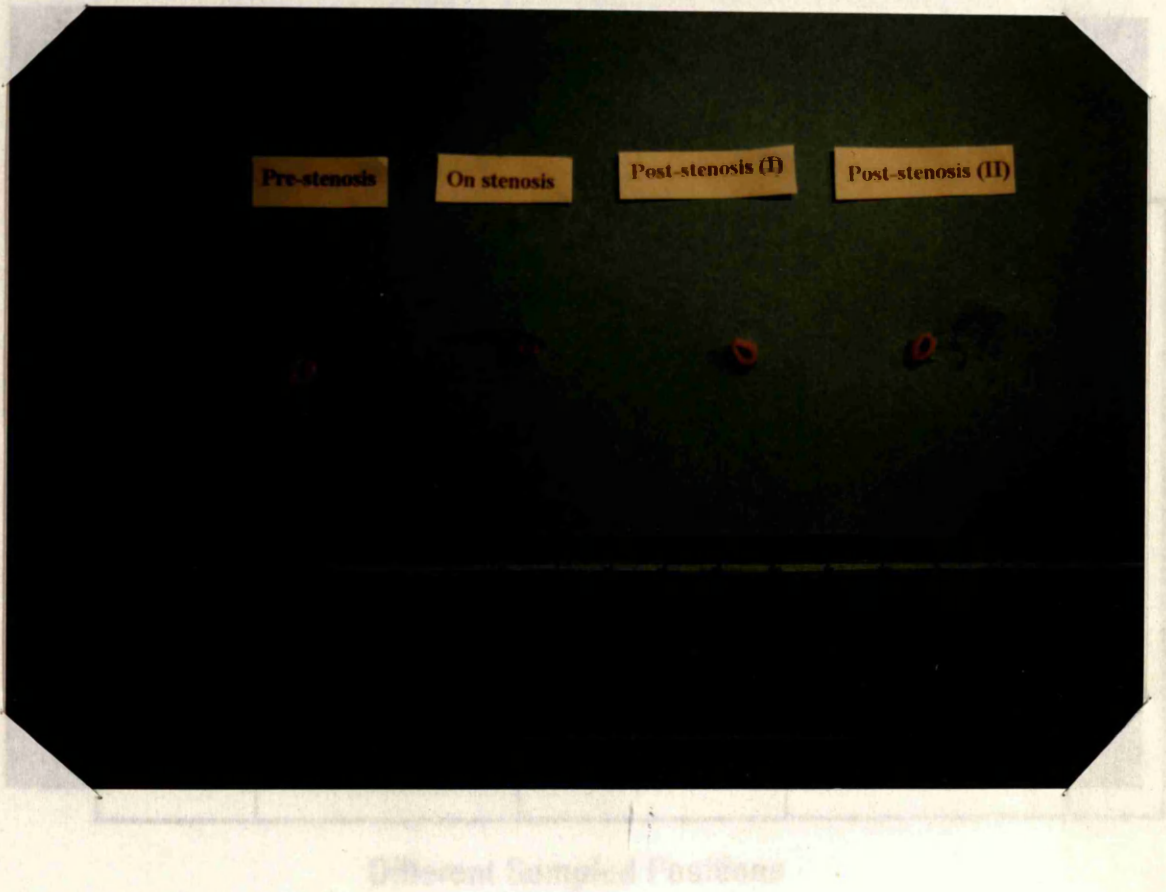
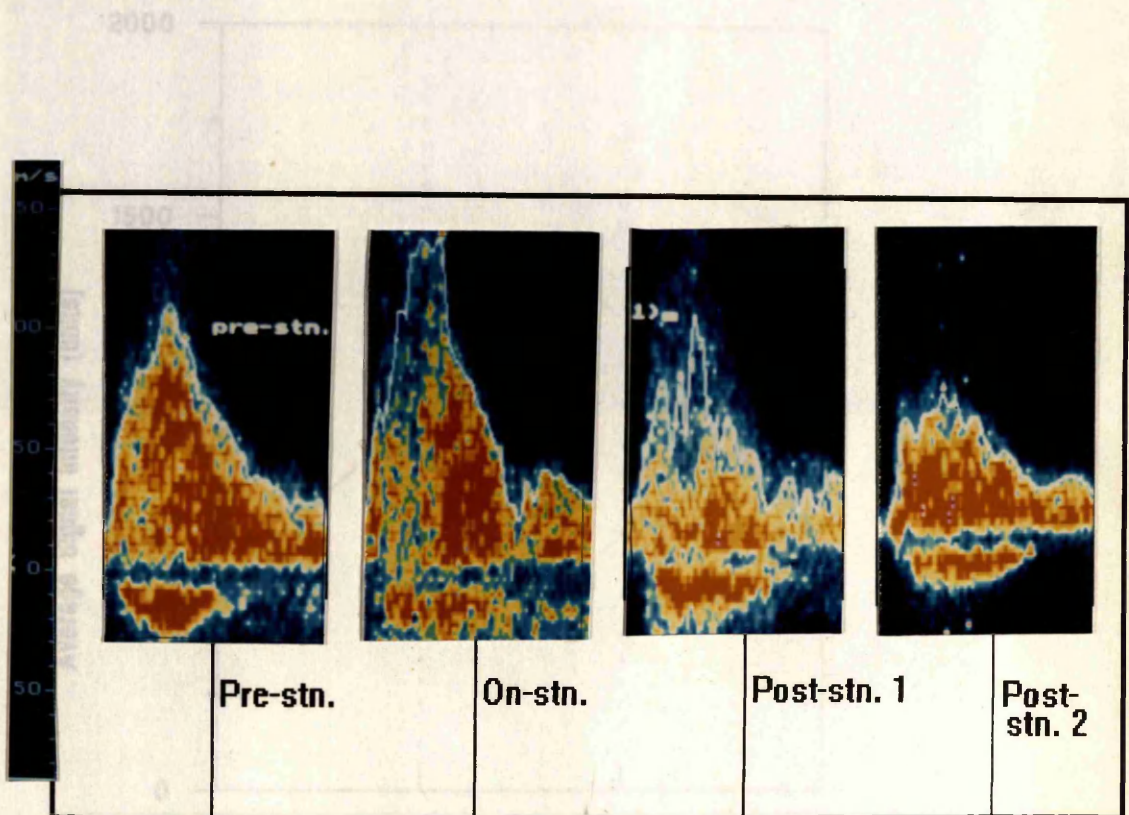


Figure 6.3 Photography of the different cross-sections along the stenosis aorta. The degree of stenosis in the above picture is 55 % by reduced cross-section area.

Figure 6.4 Doppler ultrasound waveforms registered at different positions along the stenosis aorta. RBC suspension flow velocity profiles are similar velocity waveforms in the position of pre-stenosis. At the stenosis, a turbulent flow is observed and the signal intensity is low. At the post-stenosis I position, the velocity tended to decrease, the flow is turbulent and the reverse flow becomes visible. At the post-stenosis II, the flow is back to normal but having a lower velocity. The degree of stenosis is 55% by reduced area.



Different Sampled Positions

Figure 6.3 Average Doppler signal intensity at five different sample positions along the stenosed aorta. There was an increase in average signal intensity at stenosis compared to that of pre-stenosis ($p < 0.001$). The average signal intensity reached the peak in the position of post-stenosis I and then was lower significantly at the position of post-stenosis II ($p < 0.0001$).

Figure 6.4 Doppler ultrasound waveform sampled in different positions along the stenosis aorta. RBC concentrate flow displayed a normal Doppler velocity waveform in the position of pre-stenosis; the flow show a sharp increase in systolic velocity and the signal intensity started to distribute unevenly; On the post-stenosis I position, the velocity tended to decrease but high intensity turbulent signal in the central waveform and reverse flow became notable; the flow on the post stenosis II came back to normal but having a lower velocity. (The degree of stenosis = 65% by reduced area).

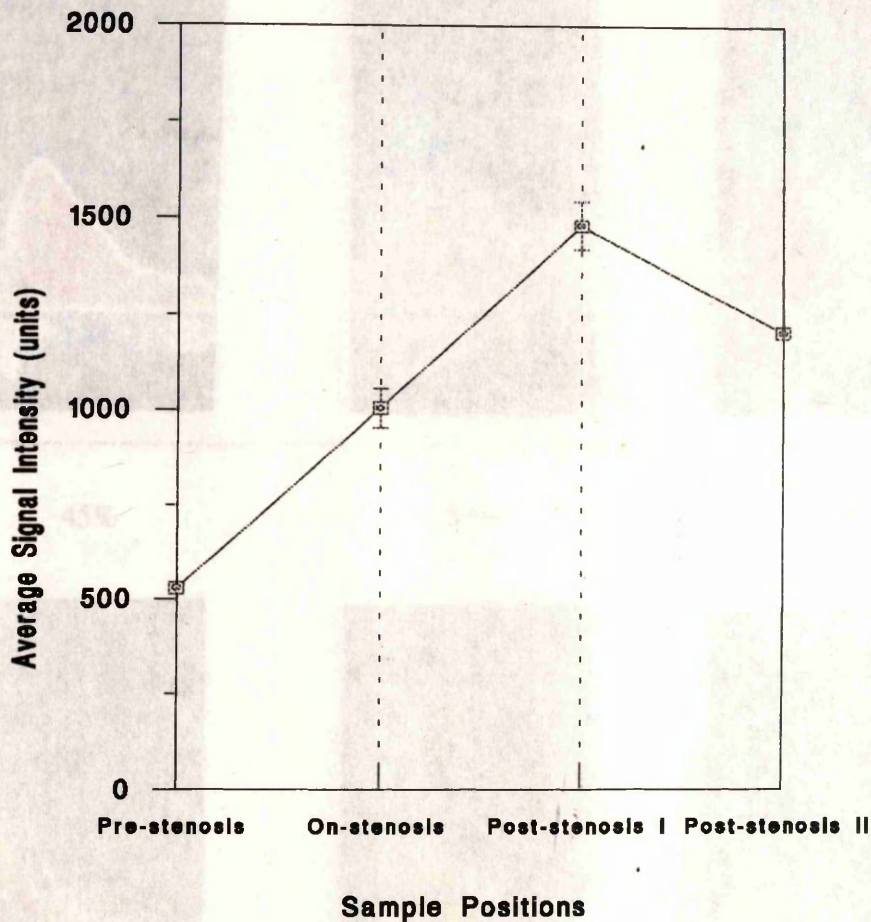
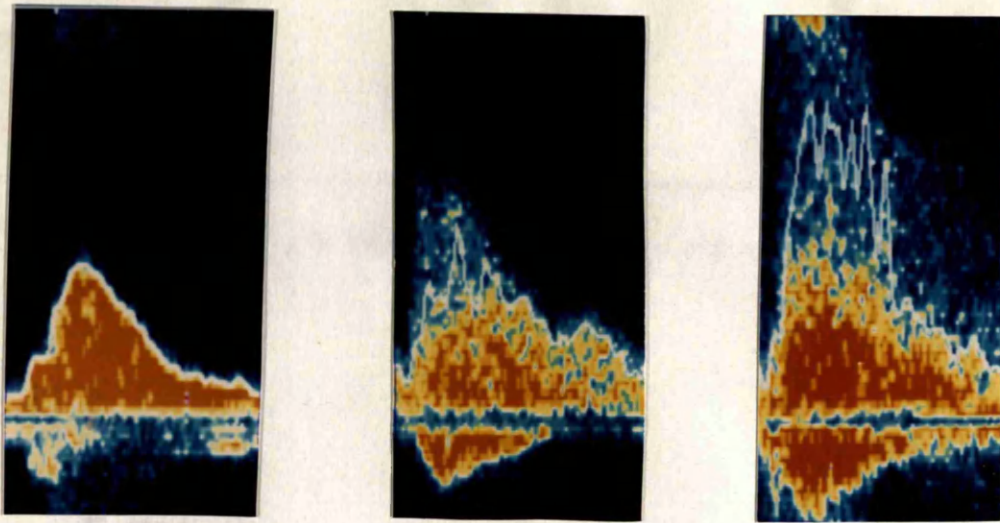


Figure 6.5 Average Doppler signal intensity in different sample positions along the stenosed aorta. There was an increase in average signal intensity at stenosis, compared to that of pre-stenosis ($p < 0.0001$). The average signal intensity reached the peak in the position of post-stenosis I and then went down significantly in the position of post-stenosis II ($p < 0.0001$).

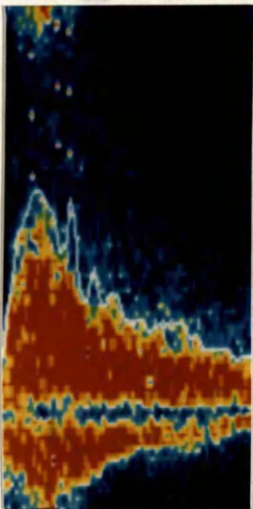
Figure 6.6 The change of Doppler signal intensity in different sample positions along the stenosed aorta with increasing degree of stenosis. The degree of turbulence did not occur until the degree of stenosis reached 50%. At 50% and 70% stenosis, turbulence started to appear and was associated with remarkable reversed flow. Turbulence started to appear at 50% and 70% degree of stenosis. Both systems had similar flow characteristics in association with the rising degree of stenosis but with different turbulence characteristics.



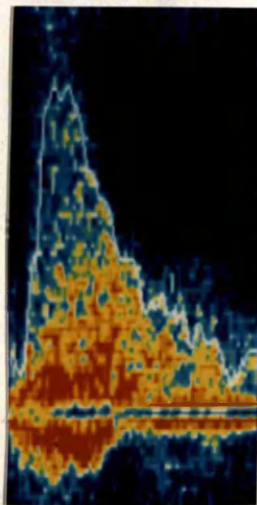
45%

55%

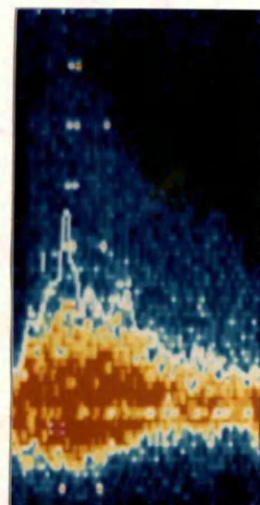
65%



75%



85%



90%

Percentage of Reduced Cross-section Area

Figure 6.6 The change of image components in Doppler velocity waveform at post-stenosis I with increasing degree of stenosis. The transition of turbulence did not occur until the degree of stenosis was arisen to 55%. At degree 65% and 75% stenosis, turbulence became most typical and was accompanied with remarkable reversed flow. Turbulence remained but became damped at 85% and 90% degree of stenosis. Both systolic and diastolic velocity increased in association with the rising degree of stenosis but systolic velocity changed more predominately.

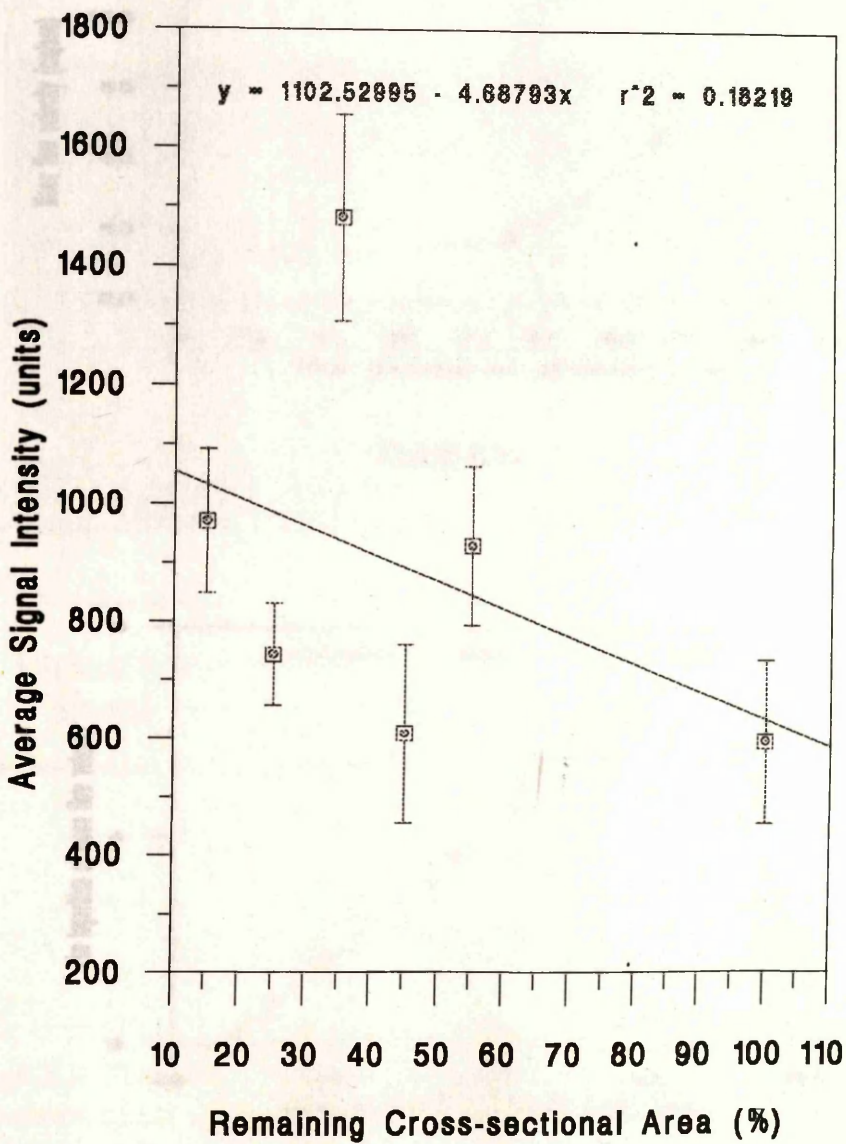


Figure 6.7 Correlation between the degree of stenosis and the average signal intensity at post-stenosis I. There was a poor correlation between the degree of stenosis and average signal intensity recorded in post-stenosis ($r = -0.426$).

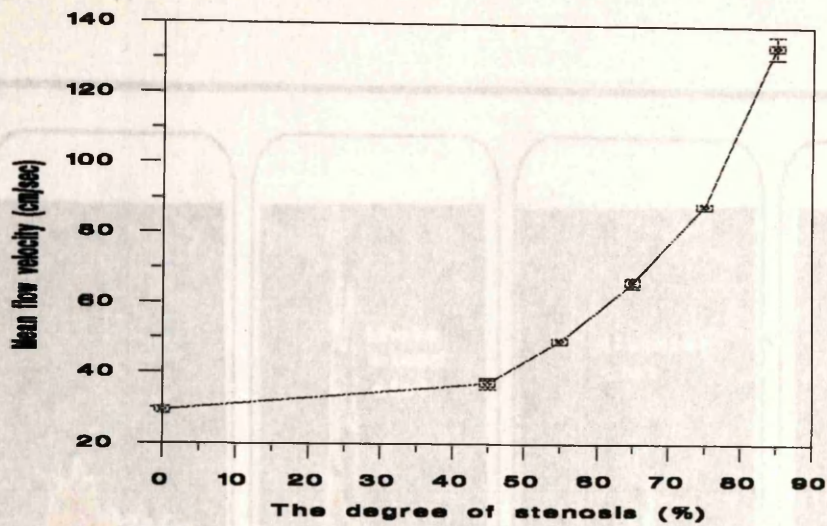


Figure 6.8a

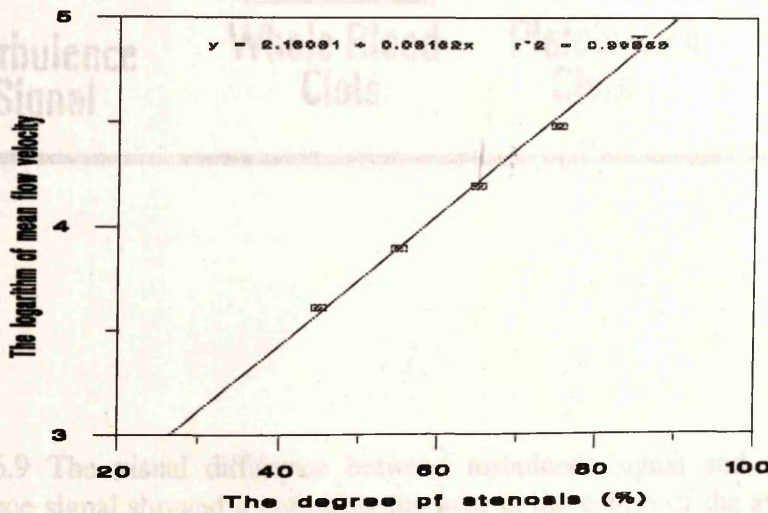


Figure 6.8b

Figure 6.8 Correlation between the degree of stenosis and the mean velocity at post-stenosis I. The mean velocity recorded at post-stenosis I was inversely proportional to the degree of stenosis but the relationship was nonlinear (Figure 6.8a). After logarithmic transformation of mean flow velocity, the relationship became linear ($r = 0.91$, $p < 0.001$) (Figure 6.8b).

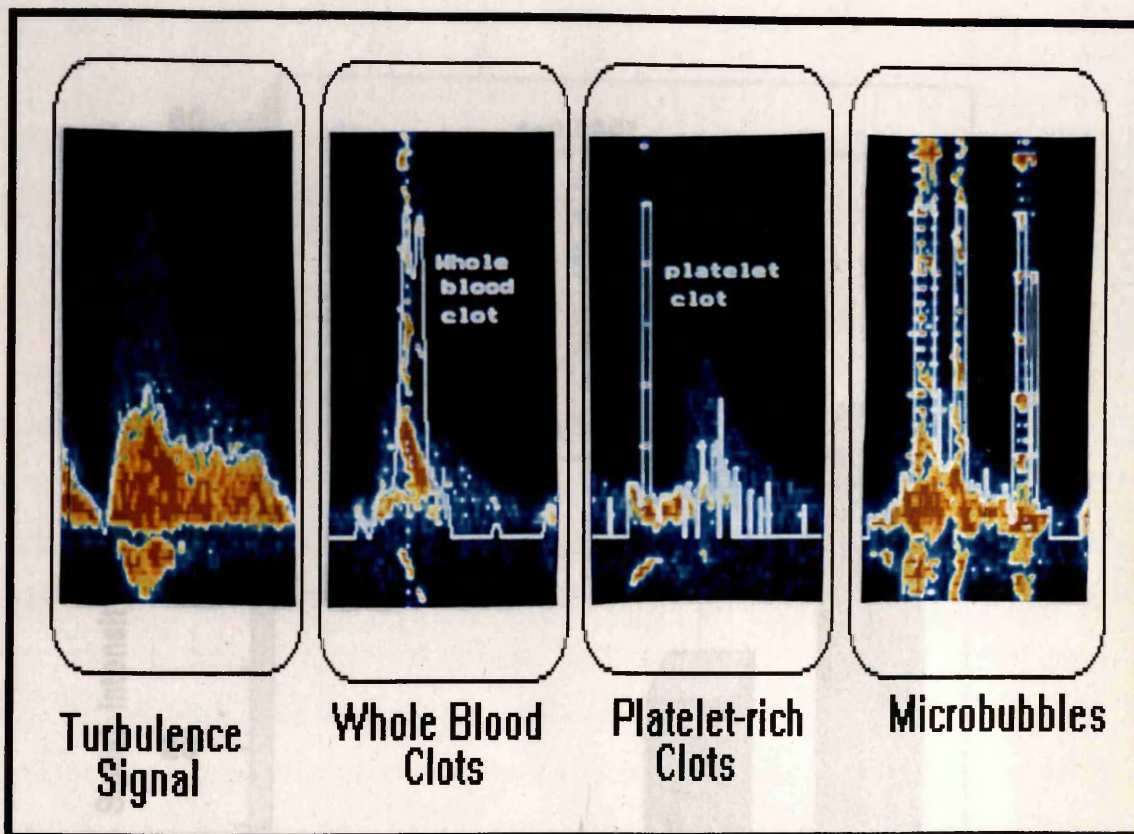


Figure 6.9 The visual difference between turbulence signal and embolic signals. Turbulence signal showed a high intensity area in the centre of the systolic period of the flow waveform and usually accompanied with a jet flow velocity, a harsh noise, and a reversed flow. However, embolic signals are featured as high intensity points which randomly superimposed on the flow waveform of either systolic or diastolic period, accompanied with harmonic chirps.

Figure 6.10 Comparison of the total signal intensity of turbulence and those of embolic materials. There was no significant difference in the total signal intensity between turbulence and embolic signal produced by injection of whole blood clots. However, the total signal intensities induced by introduction of platelet-rich clots as well as air bubbles were significantly greater than that of turbulence ($p = 0.0003$ and $p = 0.0001$ respectively).

(NS: no significant difference.)

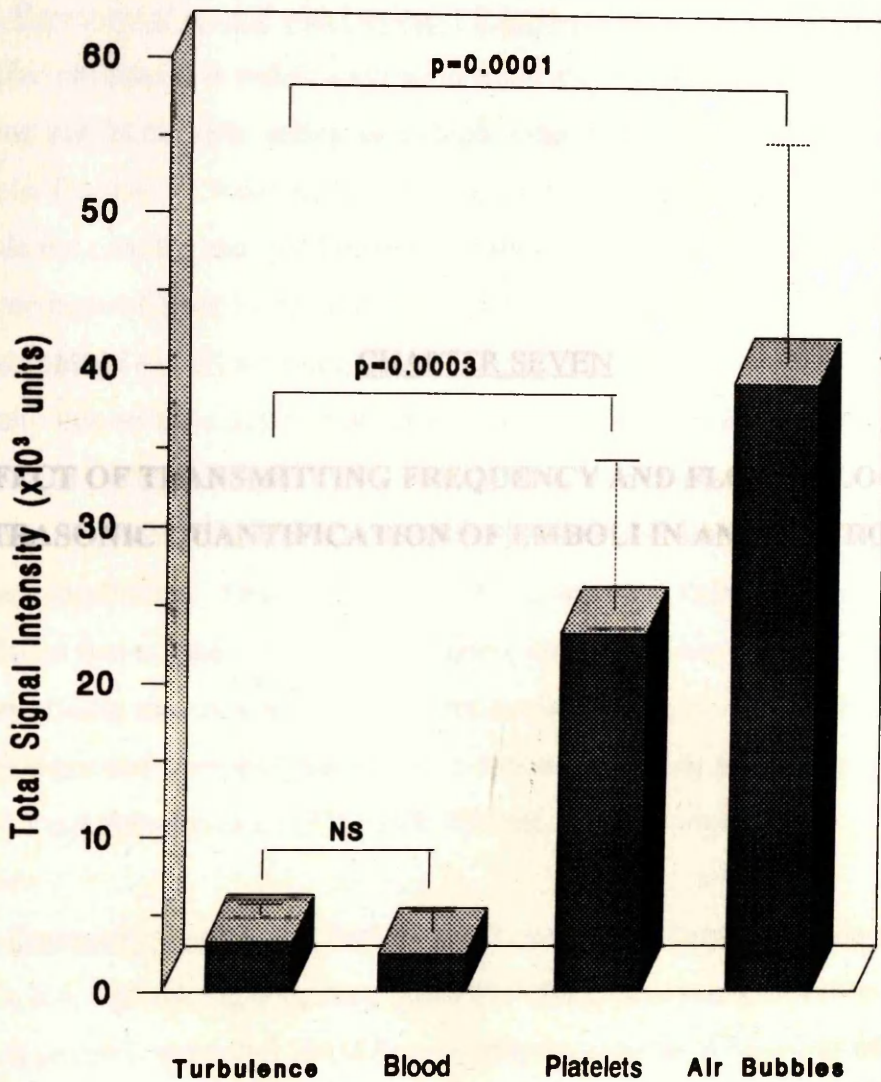


Figure 6.10 Comparison of the total signal intensity of turbulence and those of embolic materials. There was no significant difference in the total signal intensity between turbulence and embolic signal produced by injection of whole blood clots. However, the total signal intensities induced by introduction of platelet-rich clots as well as air bubbles were significantly greater than that of turbulence ($p = 0.0003$ and $p = 0.0001$ respectively).

(NS: no significant difference.)

7.1 INTRODUCTION

7.1.1 Detection of Emboli with Doppler Ultrasonography

Doppler ultrasound is mainly used to measure the velocity of blood flow since the flowing red blood cells, acting as multiple reflectors in motion, cause a change in Doppler frequency. However, Doppler signals recorded from the moving blood cells include not only the changed frequency of ultrasound but also information relating to the amplitude of Doppler signal intensity or power (Russell 1992). Particulate emboli and air bubble emboli emerging **CHAPTER SEVEN** as an increase in Doppler signal intensity due to their different acoustic impedance and different size from those of

EFFECT OF TRANSMITTING FREQUENCY AND FLOW VELOCITY ON ULTRASONIC QUANTIFICATION OF EMBOLI IN AN IN VITRO MODEL

in the bloodstream. Since as early as 1965, embolic signals in the extracranial circulation have been demonstrated during cardiopulmonary bypass (Lassen and Howry, 1965), then in animal models with decompression sickness (Coffin et al, 1968 and Spencer and Campbell, 1968) and in patients following bone fracture (Kelly et al, 1977 and Herndon et al, 1975) with different ultrasonic equipment.

7.1.2 Detection of Intracranial Emboli with Transcranial Doppler Ultrasonography

With a low transmitting frequency probe (2 MHz), transcranial Doppler (TCD) has made it possible to monitor blood flow velocity in intracranial basilar arteries through the natural bony windows (Aaslid, 1992) and detect cerebral emboli (Spencer et al, 1990, Padayachee et al, 1987 and Pugsley et al, 1990). Emboli are detectable with TCD as short-duration, high-intensity signals superimposed on the blood velocity spectrum. Recently, studies based on the calculation of intensity and/or duration of embolic signals, have attempted to quantify the size of detected emboli (Russell et al, 1991) and to differentiate the nature of emboli (Markus et al, 1993b).

7.1.3 Effect of Transmitting Frequency and Flow Velocity on the Quantification of Embolic Signal

Amongst the several factors affecting this quantification of emboli signals the transmitting frequency of ultrasound and the velocity of flow have received scant

7.1 INTRODUCTION

7.1.1 Detection of Emboli with Doppler Ultrasonography

Doppler ultrasound is mainly used to measure the velocity of blood flow since the flowing red blood cells, acting as multiple reflectors in motion, cause a change in Doppler frequency. However, Doppler signals recorded from the moving blood cells include not only the changed frequency of ultrasound but also information relating to the amplitude of Doppler signal intensity or power (Russell 1992). Particulate emboli and air bubble emboli emerging in vessels may induce an increase in Doppler signal intensity due to their different acoustic impedance and different size from those of blood cells. Doppler signals with high signal intensity may therefore represent the presence of emboli. This may theoretically allow Doppler ultrasound to detect emboli in the bloodstream. Since as early as 1965, embolic signals in the extracranial circulation have been demonstrated during cardiopulmonary bypass (Austen and Howry, 1965), then in animal models with decompression sickness (Gillis et al, 1968 and Spencer and Campbell, 1968) and in patients following bone fractures (Kelly et al, 1977 and Herndon et al, 1975) with different ultrasonic equipment.

7.1.2 Detection of Intracranial Emboli with Transcranial Doppler Ultrasonography

With a low transmitting frequency probe (2 MHz), transcranial Doppler (TCD) has made it possible to monitor blood flow velocity in intracranial basilar arteries through the natural bony windows (Aaslid, 1992) and detect cerebral emboli (Spencer et al, 1990, Padayachee et al, 1987 and Pugsley et al, 1990). Emboli are detectable with TCD as short-duration, high-intensity signals superimposed on the blood velocity spectrum. Recently, studies based on the calculation of intensity and/or duration of embolic signals, have attempted to quantify the size of detected emboli (Russell et al, 1991) and to differentiate the nature of emboli (Markus et al, 1993b).

7.1.3 Effect of Transmitting frequency and Flow Velocity on the Quantification of Embolic Signal

Amongst the several factors affecting this quantification of emboli signals the transmitting frequency of ultrasound and the velocity of flow have received scant attention. It has been suggested that Doppler ultrasound with higher frequency may facilitate the detection of emboli in the blood flow since ultrasound beams with higher frequency usually have shorter wavelength and, therefore, there is a greater possibility of reflection (Russell, 1992).

7.1.4 Aims

This study was designed to examine the influence of different Doppler transmitting frequency and alteration of flow velocity. To study this, transcranial Doppler examination of solid emboli was performed with alteration of these variables in an *in vitro* model simulating the human middle cerebral artery (MCA).

7.2 MATERIALS AND METHODS

7.2.1. *In Vitro* Models

1. A model for investigation of the effect of alteration in the velocity of flow

The *in vitro* model used in this study was previously described in section 2.3.1 of Chapter Two. Diluted human red blood cell (RBC) concentrate was used as a circulating material in this study. The haemodynamic parameters such as the concentration of RBC, haemoglobin (Hb) and haematocrit (HCT) were determined with a Sysmex NE 8000 (TOA Medical Electronic, Japan) within three hours of the TCD study. A magnetic flow meter was connected to monitor flow. Continuous monitoring of flow velocity and embolic signals was achieved by a 2 MHz pulsed Doppler probe which was coupled with acoustic gel to the temporal bone inlaid in the wall of model.

2. A model for investigation of the effect of alteration in the transmitting frequency of Doppler

This model was constructed with a section of human internal carotid artery (internal diameter 5 mm, length 8 cm) obtained from fresh post-mortem material, passing through the bottom of a plastic box as described previously. The Doppler signals

were recorded from a probe suspended at 30 degrees to the vessel. The model was filled with normal saline covering the surface of Doppler probe (Figure 7.1) The flow rate and mean flow velocity were kept constant during the study.

7.2.2 Preparation and Injection of Emboli

Platelet-rich thrombin was prepared by the method mentioned in section 2.5.1 Chapter 2. Embolus material was sliced into small cubes and the size of emboli was microscopically measured. The size of embolus used in this study was 2 x 2 x 2 mm for studies of flow velocity and 1 x 1 x 1 mm for studies of frequency effects. Emboli were introduced into the model from storage buffer (Dubecco's phosphate) and injecting via a three-way tap, taking care to exclude air bubbles. The injected clot was collected at the outlet for later recirculation. The clot was measured and weighed before and after repeated injections.

For investigation of the effect of changing flow velocity, the same platelet-rich clot was injected into the model twelve times at two mean flow velocity settings: 23 cm/sec (flow rate = 64 ml/min) and 40 cm/sec (100 ml/min). In addition, fifteen repeated injections were performed for each change in Doppler transmitting frequency, 2 MHz, 4 MHz and 8 MHz.

7.2.3. Ultrasound Doppler Equipment and Off-line Analysis

A pulsed transcranial Doppler system (Nicolet, TC2000, Warwick, UK) was employed in the study. In both of the investigations, Doppler signals were received and recorded at low gain setting to facilitate demonstration of embolus signal. For investigation of the effect of change in flow velocity, the parameters of TCD were kept constant through the study (gain 4, output power 36, insonation depth 78 mm, sample volume 10 mm, sweep speed 3). It was necessary to undertake the comparison of Doppler frequency probes in separate experiments, as interference prevented simultaneous use of one probe in close proximity to another. For this part of the study, TCD parameters were maintained constant as follows (gain 1, output power 22, insonation depth 68 mm, sample volume 6 mm, sweep speed 3).

Off-line analysis was based on six frames of Doppler spectral information recorded after each change in the studied variable.

The emboli within higher velocity flow were of a shorter duration than those in lower velocity flow. Intensity analysis software (section 2.4.2. Chapter Two) was used to measure the average intensity of the blood flow velocity waveform by calculating the total intensity over each frame. The total intensity for each embolic signal was also calculated. All signal intensities are described in relative units. The duration of embolic signals was estimated by converting signal length to time expressed as ms.

7.2.4. Statistical Analysis

Paired t-testing was used to study the effect of changes in velocity. One-way ANOVA was used to measure the changes from altering Doppler frequency. To test the effect of repeated injection of a single embolus, the precision of embolic signal intensity and duration was described as the coefficient of variation (CV) expressed as a percentage ($CV = SD/mean \times 100\%$). All data in this study were expressed as mean \pm 1SD.

7.3 RESULTS

7.3.1 Alteration of Flow Velocity

1. *Average signal intensity of flow waveform*

The average intensity of Doppler signals reflected from blood flow was significantly higher with flow at 40 cm/sec than flow at 23 cm/sec (228.7 ± 10.9 units vs. 68.7 ± 11.5 units, $p < 0.0001$) (Figure 7.2). The difference was also readily visible on colour-coded Doppler velocity waveforms (Figure 7.3a, b).

2. *Embolic signal intensity*

Emboli moving within blood flowing at a low velocity had a significantly higher signal intensity than those carried in the blood flow at a high velocity (23 cm/sec, $5.7 \times 10^4 \pm 2.2 \times 10^4$ units vs. 40 cm/sec, $3.3 \times 10^4 \pm 0.5 \times 10^4$ units, $p = 0.0006$) (Figure 7.4 and Figure 7.5a, b).

3. Embolic signal duration

The emboli within higher velocity flow were of a shorter duration than those in lower velocity flow (40 cm/sec, 73.8 ± 10.8 mS vs. 23 cm/sec, 139.7 ± 38.4 mS, $p < 0.0001$) (Figure 7.5a, b and Figure 7.6).

7.4 DISCUSSION

7.3.2. Alteration of Doppler Transmitting Frequency

The results relating to change of Doppler transmitting frequency are summarised in Table 1.

1. Average signal intensity of flow waveform

The average signal intensity of RBC flow decreased significantly with an increase in transmitting frequency of the probe ($p < 0.0001$).

2. Embolic signal intensity

Similarly, the intensity of embolic signals recorded from a probe with lower transmitting frequency was significantly higher than that by a probe with higher frequency ($p < 0.0001$).

3. Embolic signal duration

The duration of embolic signals was inversely proportional to the used transmitting frequency of the probe ($p < 0.0001$).

7.3.3 Precision of Repeated Measurement of Embolic Signals

The precision of repeated embolic signal measurement was 14.8% for flow velocity at 40 cm/sec and 38.3% for 23 cm/sec for signal intensity; and signal duration: 14.7% for 40 cm/sec and 27.5% for 23 cm/sec for signal duration.

No change was found in the size or weight of clot before and after the repeated injections. For example, for the clot with a size of 2 x 2 x 2 mm, the weight before injection was 0.0016 gram and it was 0.0015 gram after being injected 24 times. The overall weight change was below 1% (0.938%).

The circulating blood flow had a RBC count of $3.77 \times 10^{12}/l$, HB 11.6 g/dl, and HCT 40.8%, which were within the normal range (Williams, 1986).

7.4 DISCUSSION

As transcranial Doppler ultrasonography is increasingly used in detection of emboli in the cerebral circulation, it has become necessary to investigate the factors which may affect interpretation of findings from this application. With the use of intensity analysis software, we have examined the influence of two factors, flow velocity and the transmission frequency of probe. The first of them is encountered daily in clinical TCD application since the variability of blood flow velocity is notable in different individuals (normal MCA mean velocity varies from 41 ± 7 to 94 ± 10 cm/sec) (Adams et al, 1992). The second variable is important when comparing embolic signals detected in different arteries, for instance, the MCA from temporal 'window' approach to those in the internal carotid artery from an extracranial approach, which usually involves using probes with different transmitting frequencies.

It is clearly obvious that a change in bloodstream velocity causes a change in Doppler-detected flow velocity. We have examined this in relation to Doppler signal intensity to the velocity of blood flow, which has not been reported before. The data in this study demonstrated that blood cells moving at higher velocity also produced a higher signal intensity while the concentration of RBC was kept constant. Thus it suggests that Doppler signal intensity reflected from moving blood flow is not only dependent on the amount of red blood cells passing through the cross-sectional area of the vessel (Russell, 1992) but is also dependent on the velocity at which blood cells move. The intensity of the returned ultrasound depends on the proportion of the transmitted beam that is reflected. There are two main types of ultrasound reflection, specular and nonspecular reflection (scattering). Since the diameter of red blood cells (7-10 μm) is smaller than the wavelength of ultrasound (0.77 mm) transmitted from a 2 MHz probe (Aaslid, 1992), the reflection behaviour of red blood cells is mainly

scattering. A greater reflection of ultrasound produced by RBC moving at a higher velocity may explain our observation of increased signal intensity from higher velocity blood flow. Thus, blood flow at higher velocity produces more reflection since more RBC's transit through the sample volume during a certain time (Figure 7.8). This observation is of practical importance when attempting to estimate a change of diameter in a cerebral artery on the basis of changes in signal intensity (Aaslid et al, 1989 and Arts and Roelvros, 1972) since diameter changes will affect both velocity and signal intensity.

The acoustic features of emboli passing through a sample volume at different velocities has been described (Spencer 1992), in which a higher velocity embolus produced a clicking or snapping quality but a slower embolus produced a moaning quality to the sound. We have expanded this observation by quantifying the embolic signal intensity and duration. Our results show that the same embolus causes different signal intensity and signal duration depending on its velocity. However, the embolus in the bloodstream with lower flow velocity had a higher signal intensity as well as longer signal duration, which is the opposite of our results from background blood flow. It is of interest that the signal intensity and duration from lower velocity emboli were 1.7 times higher than those from the higher velocity embolus. This difference was very similar to the ratio of the flow velocities used in this study (40 cm/sec is 1.74 times faster than 23 cm/sec). It is probable that the reason for the increase in signal intensity of a slow velocity embolus is its longer duration in the sample volume of the ultrasound beam. This means that attempts to correlate embolic signal intensity and/or duration with embolus size should consider flow velocity information.

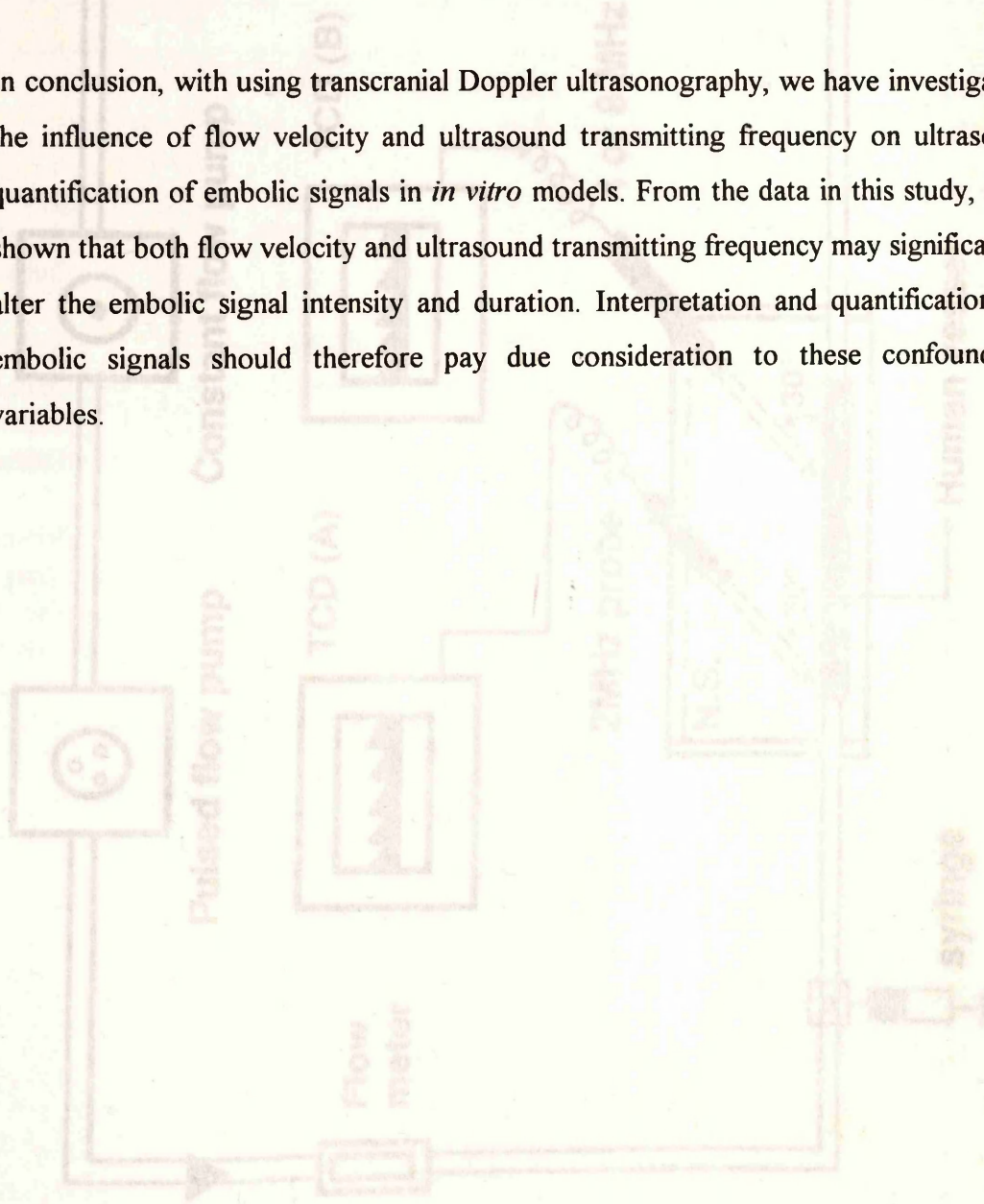
Since the velocity of sound is constant for a particular medium, the wavelength may be decreased by raising the ultrasound frequency. It is known that shorter wavelengths are associated with more specular reflection when the ultrasound beam reaches an acoustic interface. Increasing the ultrasound frequency may therefore at least theoretically facilitate detection of emboli since the emboli may then behave as specular rather than nonspecular reflectors (Russell 1992). Thus, the intensity of the ultrasound returning to the Doppler transducer will be higher when a higher

transmitting frequency is used. The embolus used in our study is 1 mm^3 which is longer than the wavelength (0.7 mm) of a standard 2 MHz probe. So, specular reflection is expected when ultrasonic detection of emboli was performed in this study. However, our result showed that average signal intensity of background blood flow and embolic signal intensity were both inversely proportional to the ultrasound frequency used. Similar results were found for embolic signal duration. This suggests that both specular reflection (from emboli) and scattering (from red blood cells) become weaker when higher ultrasound frequency is used. In fact, sound wave reflection has a multifactorial basis. On the one hand, a sound with high frequency has a shorter wavelength than that with lower frequency. But on the other hand, the higher frequency sound attenuates more readily when it travels in a medium (Tegeler and Eicke, 1993, Wells, 1983 and Powis et al, 1984). A parallel situation exists for different wavelengths of light. For example, infrared light with a low frequency and long wavelength reaches the earth more easily through the atmosphere than ultraviolet light which has a higher frequency and a shorter wavelength. In our study, the 2 MHz transducer would be expected to receive more reflected ultrasound than 4 MHz and 8 MHz transducers. So it is not surprising that the average signal scatter intensity of both background blood flow and embolic signal intensity recorded with the 2 MHz probe were higher than those recorded with higher ultrasound frequency probes, and that embolic signal duration becomes shorter with loss of reflection of the ultrasound signal.

It is well known that human skull, especially the diploe which forms the middle spiculate layer of the skull, plays a main role in attenuating TCD signals and this attenuation is acoustic frequency dependent (Eden and Halsey, 1994). From the present results, it seems that the hypothesis that Doppler ultrasound with high transmitting frequency may facilitate the detection of emboli can be established after the frequency-dependent acoustic attenuation factor is taken into account. To compensate the greater intensity loss with a increase in ultrasound transmitting frequency, an increase in the output of acoustic power may be required. The similar explanation may apply for soft tissues other than bone, for example, attenuation by muscle and skin for extracranial vessel examination.

In this study, we have also tested the variability in repeated injections of an individual embolus. The data from this study showed that the precision of ultrasound quantification is not very high, even though the same embolus was repeatedly tested and other settings were kept constant. This emphasises other potential variables, which would include the different position of embolus emerging in the sample volume, different reflecting interfaces and different embolus velocities.

In conclusion, with using transcranial Doppler ultrasonography, we have investigated the influence of flow velocity and ultrasound transmitting frequency on ultrasonic quantification of embolic signals in *in vitro* models. From the data in this study, it is shown that both flow velocity and ultrasound transmitting frequency may significantly alter the embolic signal intensity and duration. Interpretation and quantification of embolic signals should therefore pay due consideration to these confounding variables.



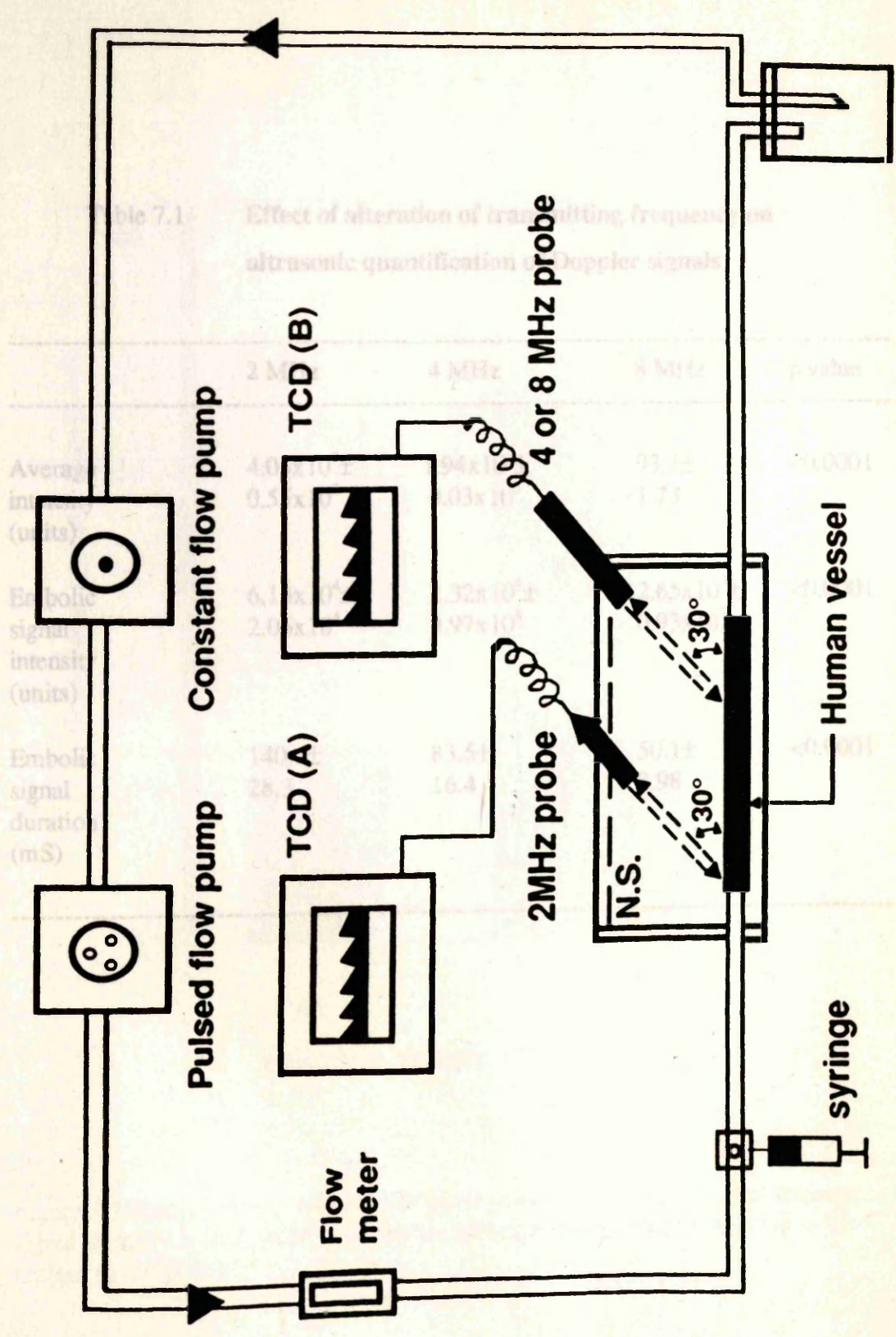


Figure 7.1 Diagrammatic illustration of the model for transmitting frequency test.

Table 7.1 Effect of alteration of transmitting frequency on ultrasonic quantification of Doppler signals

	2 MHz	4 MHz	8 MHz	p value
Average intensity (units)	$4.05 \times 10^3 \pm 0.55 \times 10^3$	$1.94 \times 10^3 \pm 0.03 \times 10^3$	93.3 ± 1.73	<0.0001
Emboic signal intensity (units)	$6.13 \times 10^4 \pm 2.06 \times 10^4$	$2.32 \times 10^4 \pm 0.97 \times 10^4$	$2.65 \times 10^3 \pm 0.93 \times 10^3$	<0.0001
Emboic signal duration (mS)	140.6 ± 28.3	83.5 ± 16.4	50.1 ± 8.98	<0.0001

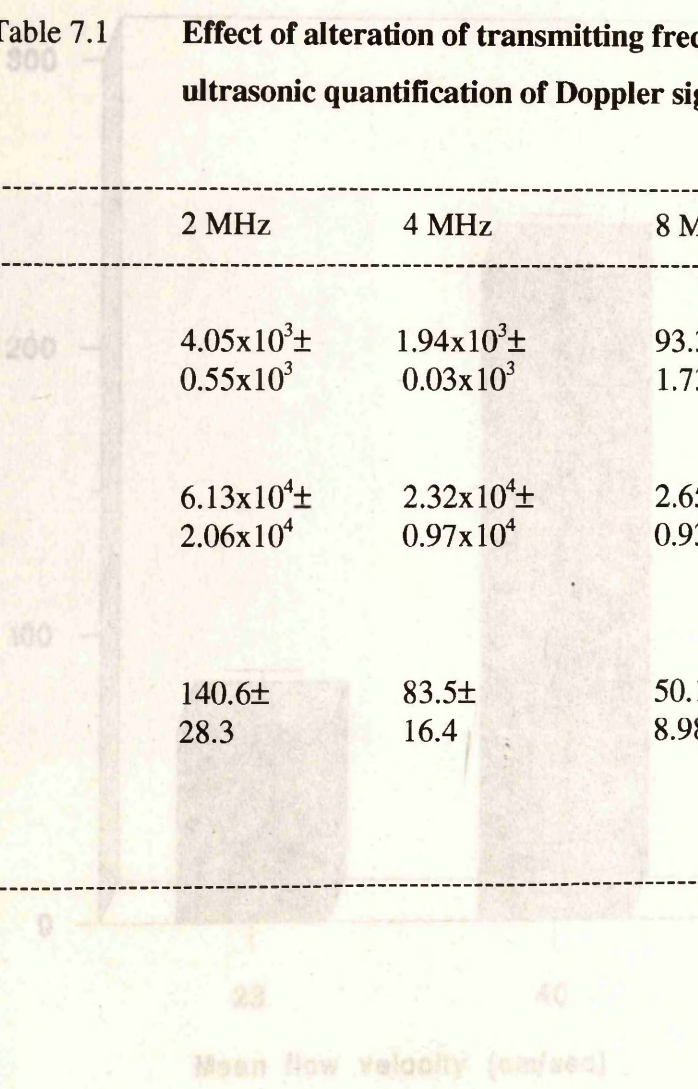


Figure 7.2 Signal intensity related to Doppler velocity of blood flow. The average signal intensity at flow velocity 40 cm/sec was significantly higher than that at 23 cm/sec (p < 0.0001).

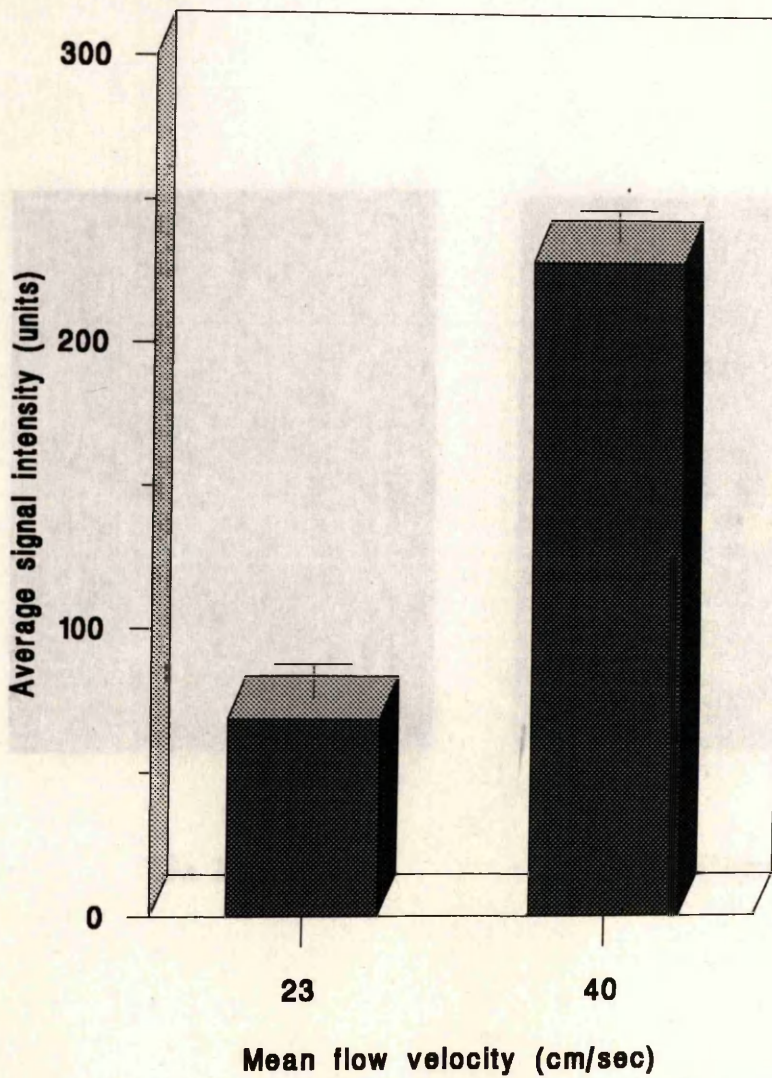
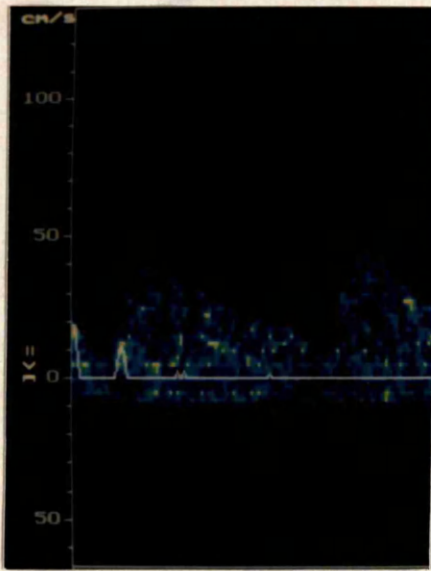
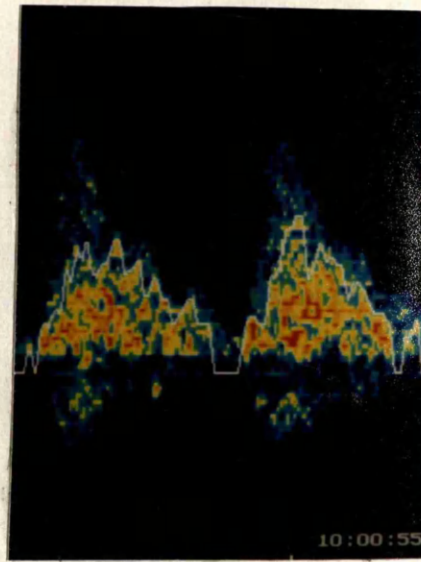


Figure 7.3 The background flow waveform was slightly more intense than the Doppler image of the flow at a mean velocity of 23 cm/sec (7.3a) and 40 cm/sec (7.3b) before injection of contrast medium.

Figure 7.2 Signal intensity related to Doppler velocity of blood flow. The average signal intensity at flow velocity 40 cm/sec was significantly higher than that at 23 cm/sec ($p < 0.0001$).



7.3a 23 cm/sec



7.3b 40 cm/sec

Figure 7.3 The background flow waveform. The pictures were taken from the Doppler images of the flow at a mean velocity of 23 cm/sec (7.3a) and 40 cm/sec (7.3b) before injection of embolic materials.

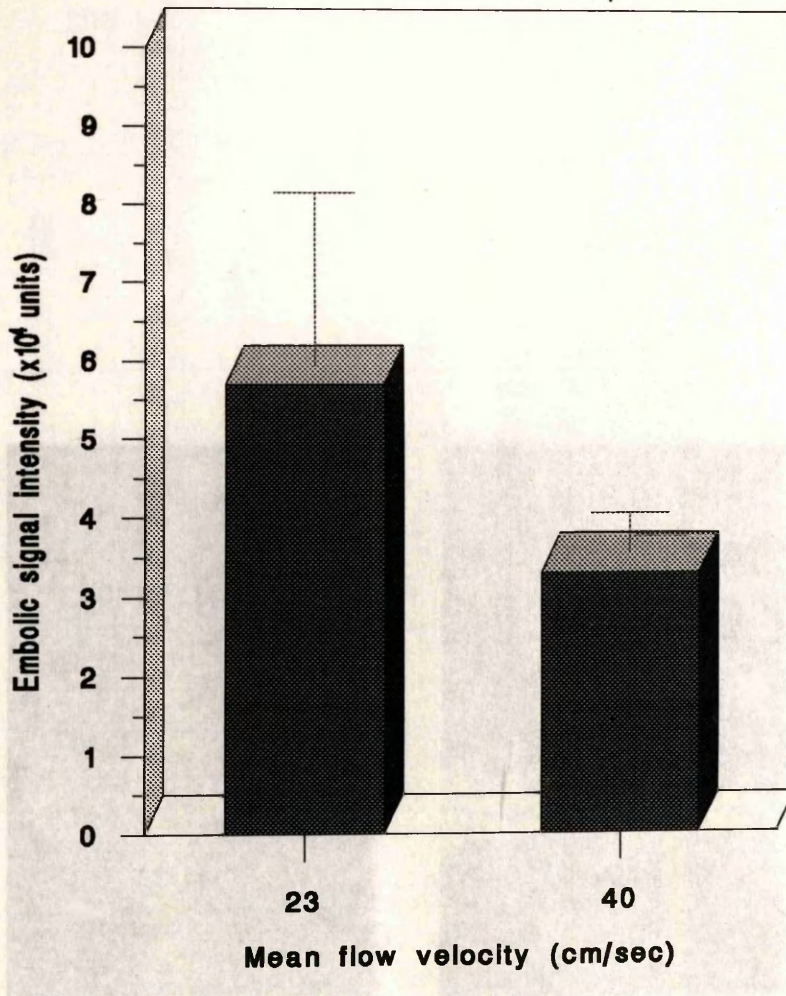
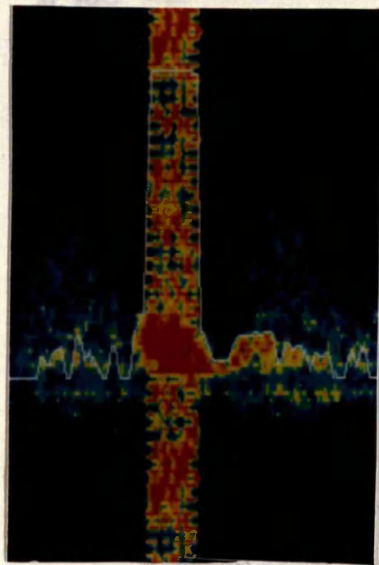
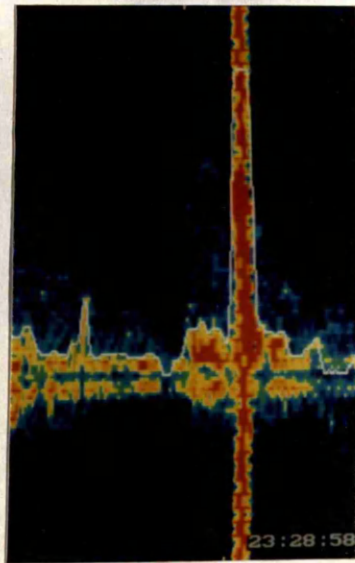


Figure 7.4 Embolic signal intensity related to Doppler velocity of blood flow. An increase in Doppler velocity of blood flow caused a decrease in embolic signal intensity ($p < 0.001$).

Figure 7.5 The mean embolic signal intensity versus the Doppler velocity.



a) 23 cm/sec



b) 40 cm/sec

Figure 7.5 The same embolus in the blood flow at different velocity.

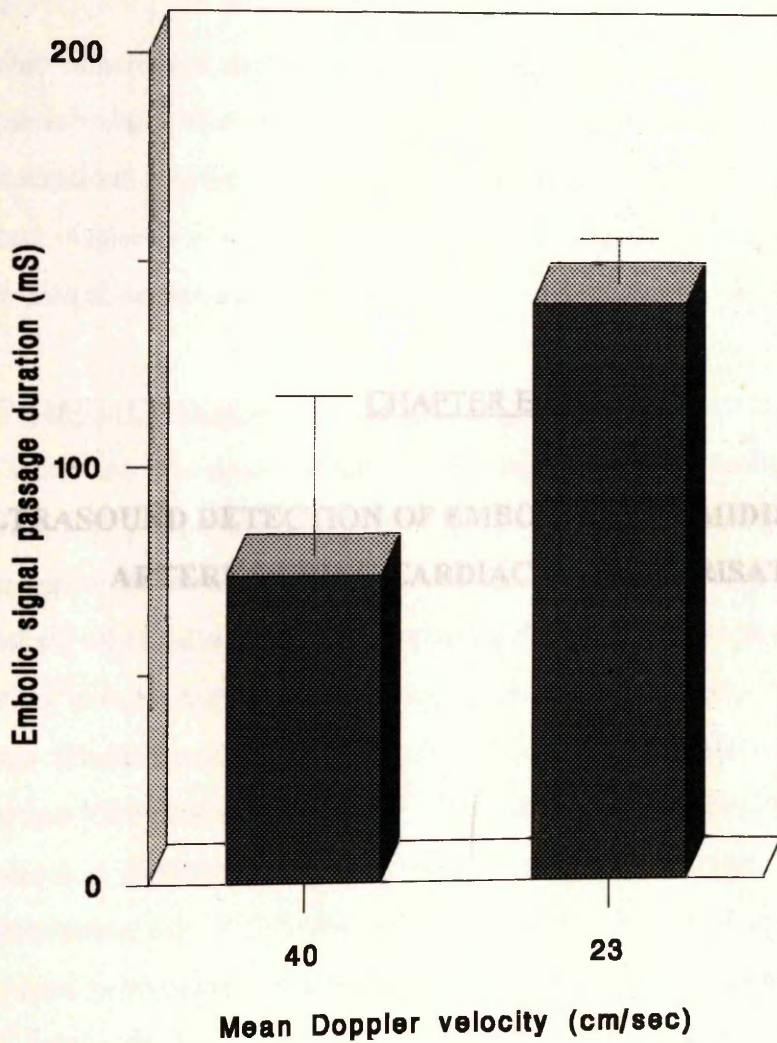


Figure 7.6 Embolic signal duration related to Doppler velocity of blood flow. An increase in Doppler velocity of blood flow caused an increase in embolic signal passage duration in the sample volume ($p < 0.0001$).

8.1 INTRODUCTION

Cardiac catheterisation is a well-established technique that is commonly used in the diagnosis and/or treatment of patients with congenital and acquired heart disease. Complications are rare but can be lethal. However, an early diagnostic test is lacking. Current diagnosis of the complication of cardiac catheterisation is usually dependent upon clinical examination and/or autopsy.

8.1.1 Cardiac Catheterisation **CHAPTER EIGHT**

The incidence of overall serious complications of cardiac catheterisation has been **ULTRASOUND DETECTION OF EMBOLI IN THE MIDDLE CEREBRAL ARTERY DURING CARDIAC CATHETERISATION** the cerebral embolism was localised to the middle cerebral artery (Ketyon et al, 1992). Recently, transient visual disturbance with normal fundus (Choi et al, 1986), neurological defects (Frink and Jellisch, 1987 and Longstreck and Smith, 1991), and lacunar infarction (Cacciatore and Russe Jr., 1991) during cardiac catheterisation have been documented. Lockwood et al (1984) reported 30 neurological complications during cardiac catheterisation over a five-year period and 40% of the patients (0.16%) developed neurological complications during cardiac catheterisation. Among them, insults involving the central nervous system occurred in thirty seven (0.12%). The incidence of the complications has been related to risk factors such as advanced age, smoking history, diabetes mellitus, hypertension, past strokes, cerebrovascular lesions, mild ventricular hypertrophy and peripheral arterial disease (Dawson and Fischer, 1977; Lockwood et al, 1984 and Cacciatore and Russe Jr., 1991). However, in many patients the exact cause of the complications is not precisely known (Dawson and Fischer, 1977) although cerebral atheromatous embolism (Winter, 1957; Lang, 1963; Fischer et al, 1970; Prender, 1978; Dross et al, 1984 and Grossman, 1986), air embolism (Charles et al, 1953; Galsbol et al, 1989; Moody et al, 1990 and Marikas et al, 1993a), and high osmolar ionic contrast (Adams et al, 1973; Levorstad et al, 1989 and Dastgheib et al, 1990) have been implicated.

8.1 INTRODUCTION

Cardiac catheterisation is a well-established technique that is commonly used in the diagnosis or/and treatment of patients with congenital and acquired heart disease. Complications are rare but can be lethal. However, an early diagnostic test is lacking. Current diagnosis of the complication of cardiac catheterisation is usually dependent upon clinical examination and/or autopsy.

8.1.1 Cardiac Catheterisation and Its Complications

The incidence of overall serious complications of cardiac catheterisation has been estimated as 1.5% (Adams et al, 1973). Less than a quarter of these reactions are neurological in nature (Dawson and Fischer, 1977) and a half of the cerebral embolism was localised to the posterior circulation (Keilson et al, 1992). Recently, transient visual disturbance with mental confusion (Vik-Mo et al, 1986), neurological defects (Frink and Ostrach, 1990 and Clements and Gatlin, 1991), and lacunar infarction (Cacciatore and Russo Jr., 1991) during cardiac catheterisation have been documented. Lockwood et al (1983) examined 30,000 cases who underwent cardiac catheterisation over a five-year period and found that forty one patients (0.16%) developed neurological impairment in the course of cardiac catheterisation. Among them, insults involving the central nervous system occurred in thirty seven (0.12%). The incidence of this complication has been also related to risk factors such as advanced age, smoking history, diabetes mellitus, hypertension, past strokes, cerebrovascular lesions, mild ventricular hypokinesia and peripheral arterial disease (Dawson and Fischer, 1977, Lockwood et al, 1983 and Cacciatore and Russo Jr., 1991). However, in many patients, the exact cause of the complications is not precisely known (Dawson and Fischer, 1977) although cerebral atheromatous embolism (Winter, 1957, Lang, 1963, Fischer et al, 1970, Prendes, 1978, Drost et al, 1984 and Grossman, 1986), air embolism (Charles et al, 1957, Ireland et al, 1989, Moody et al, 1990 and Markus et al, 1993a), and high osmolar ionic contrast (Adams et al, 1973, Levorstad et al, 1989 and Davidson et al, 1990) have been implicated.

occlusion with subsequent infarction of the tissue distal to the embolus. The other Pre-mortem diagnosis of neurological complication of cardiac catheterisation is important but difficult since it mainly depends on the clinical manifestations. Furthermore, none of the patients with neurological complications showed a change in vital signs or the electrocardiogram during cardiac catheterisation (Dawson and Fischer, 1977 and Cacciatore and Russo Jr., 1991). Additionally, the prognosis of atheromatous embolism is poor because current therapeutic interventions have been proved unsuccessful in altering the clinical course, which often results in irreversible renal failure, amputation of an extremity, or death (Colt et al, 1988 and Hendel et al, 1989).

8.1.2 Air Embolism and Catheterisation

It has been well documented that air emboli are often involved in the cerebral complications of diagnostic manoeuvres with catheterisation from different approaches such as central venous catheterisation (Ordway, 1974, Ploner et al, 1991 and Halliday et al, 1994), cerebral angiography (Hankey et al, 1990, Bachman, 1993 and Dunn, 1993), proximal aortography (Moody et al, 1990), and insertion of a Hickman line (Kilkes et al, 1991). Cerebral air embolism was suggested by the autopsy evidence of a number of empty sausage-like dilatations occurring in distended medium-sized cerebral arterioles (Moody et al, 1990).

8.1.3 Atheromatous Embolism and Catheterisation

Atheromatous embolisation is a rare complication of vascular catheterisation but has been recently emphasised amongst the causes of complications of cardiac catheterisation (Grossman, 1986). The incidence of this complication was reported to vary from 0.08% to 0.15% (Lang, 1963, and Drost et al, 1984). The confirmation of cerebral atheromatous embolism is often confirmed only by autopsy observation (Eker et al, 1994).

From the results described in Chapter Four, we found that Doppler signal intensity

It has been suggested that embolisation of atheromatous material may follow two distinct patterns. The first is the result of dislodgement of the material composing an atherosclerotic plaque, and is manifested by the signs and symptoms of arterial

occlusion with subsequent infarction of the tissue distal to the embolus. The other encountered pattern involves microembolisation of cholesterol crystals into smaller arteries usually less than 200 μm in diameter (Hendel et al, 1989). The dislodgement of atheromatous embolic materials from the irregular surface of an atherosclerotic aorta may be caused either by catheter manipulation or by the pressurised jet of contrast material (Cacciatore and Russo Jr, 1991).

8.1.4 Ultrasonic Detection of Emboli during Catheterisation

Since Doppler ultrasound was initially used to detect gas bubbles in the extracorporeal circuits (Austen and Howry, 1965), this technique has proved capable of detecting a variety of circulating embolic materials including fat emboli (Kelly et al, 1972 and Svartling, 1988), atheromatous material and blood clots (Russell et al, 1991) in different situations. Our initial results (see Section 4.3 of Chapter Four) also showed that air bubbles and atheromatous materials can be detected using TCD in a circulating model. Emboli usually appear as high intensity signals with harmonic chirps due to their different acoustic impedance from the blood cells. Such emboli have been related to the neurological impairment after cardiopulmonary bypass (Pugsley et al, 1990).

More recently, transcranial Doppler ultrasonography has been used to detect silent cerebral microemboli, which were assumed to be air emboli, in the middle cerebral artery with transcranial Doppler ultrasonography during carotid artery catheterisation with cerebral angiography and the relation of these events to different phases of this interventional procedure has been studied (Dagirmanjian et al, 1993 and Markus et al, 1993a) However, TCD test during the procedure of cardiac catheterisation has not been studied, despite its being a more frequent than cerebral angiography.

8.1.5 Aims

From the results described in Chapter Four, we found that Doppler signal intensity greatly increased after introduction of either air bubbles or atheromatous materials into an middle cerebral artery model and emboli of different sources appear to have different ultrasonic characteristics, which are likely to be based on composition and

size. Therefore, we hypothesise that TCD may detect atheromatous emboli as well as other kinds of emboli occurring in the middle cerebral artery and this may be used to identify patients at high risk of developing cerebral embolism. In this study, we aimed to use transcranial Doppler ultrasonography to: 1. detect cerebral microemboli which developed in the middle cerebral artery in the patients undergoing cardiac catheterisation and coronary angiography; 2. to relate the incidence of embolic signals to different phases of the catheterisation and coronary angiography; 3. to differentiate the types of emboli occurring during the catheterisation by comparison of the acoustic features of embolic signals recorded *in vivo* with those recorded *in vitro*.

for all the patients to receive coronary angiography was clinically diagnosed ischaemic heart disease. In addition to a routine recording, the history of risk factors, including diabetes mellitus, hypertension and peripheral disease was also registered.

8.2 METHODS

The same transcranial pulsed Doppler device with 2 MHz probe was used for all the following studies. It has a 128 point fast transform and employs a graded colour scale to display the intensity of the received Doppler signal. Doppler signals were recorded in an IBM compatible microcomputer to allow subsequent off-line analysis. An intensity analysis software (see Section 2.3.2 of Chapter Two) was used and all the recorded signals were quantitatively calculated by including each individual signal intensity and duration of high amplitude over the embolus passage of TCD sample volume. The sum of embolic signal intensities was calculated in each specific phase of cardiac catheterisation in each individual patient and mean embolic signal intensity during each specific phase was estimated from the sum of the data from all the patients for later comparison among different procedures.

Furthermore, in order to investigate the difference of embolic signal in some acoustic characteristics between certain phases and correlate the *in vitro* data to *in vivo* ones, the mean intensities of 98 embolic signals recorded at the time of insertion and manipulation catheter and 126 embolic signals at the time of injection of normal saline in aorta and left ventricle were also obtained using the same software.

Committee of Great Glasgow Health Board.

For estimation of the incidence of embolic signals, we summed up the events of the visibly high intensity signals recorded from individual patients, relating to different catheterisation phases.

The circulating model used in this study has been previously described in Section 2.2

8.2.1 Human studies

1. *Patient's information*

Seventeen patients (11 males - 6 females) undergoing cardiac catheterisation were continuously monitored with transcranial Doppler ultrasonography. The average age of the patients was 55 years (range of 29 to 65 years). The indication for all the patients to receive coronary angiography was clinically diagnosed ischaemic heart disease. In addition to a routine recording, the history of risk factors, including smoking, diabetes mellitus, hypertension and peripheral disease was also registered.

what described under Section 2.4 and 2.5

2. *Cardiac catheterisation*

Cardiac catheterisation was performed via the femoral approach. After the cardiac catheter was located in the left ventricle, 10 ml degassed normal saline and the same volume of contrast medium, (Ultravist 370, Schering Health Care Ltd. UK), were separately injected by hand into the left ventricle and supra aortic region, both within 2 seconds. The normal saline and contrast medium were degassed in a sonicating bath for 15 minutes before injection and sterilisation procedures were adopted.

over one minute. Doppler signal intensity of the blood flow velocity waveform over

3. *TCD monitoring*

Continuous middle cerebral artery Doppler monitoring was performed during cardiac catheterisation. To avoid the artifact signal which may be caused by movement of patient's head, the TCD probe was held in position with an elasticated headband. Insonation was performed at a depth of 45 - 58 mm using a sample volume of 9 mm. Abnormally high-pitched auditory and visual Doppler signals, representing emboli, were recorded throughout the cardiac catheterisation at a low gain setting.

Chapter Two

All patients gave written informed consent to a protocol approved by the West Ethics Committee of Great Glasgow Heath Board.

8.2.2 Experimental Study

1. *Study of the increased signal intensity of air bubbles, atheromatous material, and contrast medium in an in vitro model*

The circulating model used in this study has been previously described in Section 2.2 of Chapter Two. Red blood cell concentrates were diluted and used as the circulating material. Two types of embolic materials, air bubbles and atheromatous materials which have been mainly implicated in cerebral complication of vascular catheterisation, were prepared in the experimental study. The microbubbles were produced by agitation of 15 ml contrast medium with a polytron, and had a mean size of $29 \pm 2.3 \mu\text{m}$. Human atherosclerotic plaques, obtained from the carotid endarterectomy, were sliced into cubic particles with maximal dimension of $100 \mu\text{m}$. The procedure of preparation and measurement of embolic materials was the same as what described under Section 2.4 and 2.5 of Chapter Two. Bubble-rich contrast medium (2.5 ml) were injected into this circuit. Eight atherosclerotic emboli were injected into the circulating model, in single fashion, with a 2.5 ml syringe.

Moreover, to observe the effect of contrast medium and normal saline on the signal intensity, 2.5 ml degassed contrast medium and 2.5 ml degassed normal saline were also separately introduced into the circulating model. Doppler signals of circulating blood flow before injections were continually recorded for eight scanning screens over one minute. Doppler signal intensity of the blood flow velocity waveform over 0.2 mS was randomly sampled as control. Each above injection was completed within half a second.

2. *Off-line Doppler signal analysis*

Doppler signal analysis employed a 128-point fast-Fourier transform (FFT). Total signal intensity over the whole embolic passage duration in the sample volume was calculated. The principles for this estimation were described in Section 2.3.2 of Chapter Two.

8.2.3 Statistical analysis

A comparison of the emboli-induced signal intensity between two different catheterisation procedures and also between *in vitro* and *in vivo* control signal intensity was measured, using Student's *t* test. The possible relationship between the total events of emboli and embolus-increased intensities in different phases of catheterisation will be described as correlation coefficient (*r*). Significance level for this study is chosen at 0.05 (two-sided).

8.3 RESULTS

8.3.1 Human Studies

Continuous TCD monitoring was performed in all seventeen patients undergoing cardiac catheterisation. Embolic signals were recorded in each patient; these signals were characterised by TCD ultrasonography and were identified by both sharply audible sounds and visibly high intensity in Doppler velocity waveform. No neurological symptom was observed immediately after catheterisation. Since a limited number of patients were investigated, correlation of embolic signals with previously described risk factors was difficult. However, twelve out of the seventeen patients investigated (70.6%) were recorded as having a long history of smoking; four (33.3%) had well controlled hypertension, and two had diabetes mellitus.

The mean of total embolic signal intensity and embolic signal events recorded in 13 patients (Doppler waveform data of the remaining five was not successfully retrieved for the signal intensity calculation although all other Doppler readings were available) relating to different catheterisation procedures is summarised in Figures 8.1. Ventriculogram, changing guidewire, and catheter manipulation were most likely to cause embolic signals. The following readings were observed for the mean embolic signal intensities in different phases of cardiac catheterisation: ventriculogram ($20.9 \times 10^4 \pm 33.7 \times 10^4$ units), changing guidewire ($19.3 \times 10^4 \pm 41.1 \times 10^4$ units), manipulation of catheter ($17.9 \times 10^4 \pm 34.1 \times 10^4$ units), injection of normal saline at supra aorta level ($14.7 \times 10^4 \pm 10.2 \times 10^4$ units), injection of contrast medium in the left ventricle ($13.6 \times 10^4 \pm 21.7 \times 10^4$ units), injection of normal saline in the left

ventricle ($12.1 \times 10^4 \pm 10.1 \times 10^4$ units), injection of contrast medium in the supra aorta ($9.65 \times 10^4 \pm 10.1 \times 10^4$ units), coronary angiography ($7.03 \times 10^4 \pm 10.9 \times 10^4$ units), insertion of catheter ($0.74 \times 10^4 \pm 0.72 \times 10^4$ units). The first three in terms of embolic events were similar with the order of mean embolic signal intensities. The following readings were observed for the embolic signal events: changing guidewire (20.4 ± 29 events), ventriculogram (16.3 ± 15.8 events), manipulation of catheter (13.5 ± 15.9 events), normal saline (injected in left ventricle) (11.4 ± 7.4 events), contrast medium (injected in left ventricle) (10.58 ± 7.41 events), coronary angiography (8.67 ± 7.68 events), normal saline (injected in supra aorta) (7.83 ± 5.84 events), contrast medium (injected in supra aorta) (6.36 ± 3.26 events), insertion of catheter (2.0 ± 2.3 events).

We also found that the sum of embolic signal intensities corresponded well with embolus events during different procedures of cardiac catheterisation ($r = 0.78$, $p < 0.01$) (Figure 8.2).

It was observed that embolic signals occurred during catheter insertion and catheter manipulation often showed low intensities compared to those generated in the injection of normal saline at supra aortic level or within the left ventricle (Figure 8.3). Further off-line investigation indicated that embolic signals, occurring while inserting and manipulating the catheter, displayed lower signal intensities and longer signal duration (insertion and manipulation, the number of emboli ($n = 98$, $7.40 \times 10^3 \pm 10.2 \times 10^3$ -vs.- normal saline injection, $n = 126$, $17.8 \times 10^3 \pm 18.9 \times 10^3$ units, $p < 0.0001$; 0.25 ± 0.16 mS -vs.- 0.19 ± 0.11 mS, $p = 0.0014$) (see Figures 8.4 and 8.5).

8.3.2 Experimental Studies

Injection of 2.5 ml normal saline did not significantly increase signal intensity in the circulating model (normal saline, 329 ± 70 units -vs.- control, 323 ± 37 units, $p = 0.96$). However, injection of 2.5 ml contrast medium increased the signal intensity but behaved like high-intensity dye spreading out within the velocity waveform, which is distinct from embolic signals. Introduction of atherosclerotic plaques and micro-bubbles caused an increase in signal intensity (contrast, 1125 ± 775 units -vs.-

control, $p = 0.003$), but injection of microbubble-rich contrast medium caused over 100 times higher Doppler signal intensity than that from injection of contrast medium (bubbles, $16.47 \times 10^4 \pm 8.82 \times 10^3$ units -vs.- contrast, $p = 0.008$) (Figure 8.6).

8.3.3 Relation Studies

The *in vivo* embolic signals associated with inserting or manipulating the catheter ($n = 98$) and with injection of normal saline at the supra aortic level or within the left ventricle ($n = 126$), were compared with *in vitro* recordings from atherosclerotic material ($n = 8$) and microbubbles ($n = 8$) (Figure 8.7). There was no overall difference in signal intensity, but the catheter manipulation signals were close to in overall appearance to altheroma and for injection the signals resembled microbubble emboli (inserting and manipulating catheter, $7.40 \times 10^3 \pm 10.2 \times 10^3$ units -vs.- atherosclerotic material, $11.3 \times 10^3 \pm 14.7 \times 10^3$ units, $p = 0.48$; normal saline injection during catheterisation, $17.8 \times 10^3 \pm 18.9 \times 10^3$ vs. bubble injection, $16.5 \times 10^3 \pm 8.82 \times 10^3$ units, $p = 0.75$)

8.5 DISCUSSION

This study clearly demonstrates that emboli may occur in every patient undergoing cardiac catheterisation. Emboli in the middle cerebral artery during cardiac catheterisation have not previously been reported but would be anticipated from other angiographic studies. We found a correlation between embolic signal intensities and embolic signal events, suggesting that quantitative estimation of signal intensity from emboli is a reliable method to evaluate the degree of cerebral embolism and may prove more informative than counting only embolic signal peaks.

A higher incidence of embolic signals was demonstrated during active procedures, including ventriculogram, catheter manipulation and changing guidewire than during 'rest' phases of the catheterisation. This finding is partly in agreement with the previous clinical reports (Keilson et al, 1992, Dagirmanjian et al, 1993 and Markus et al, 1993a); Keilson et al (1992) suggested that most complications of the central

nervous system following cardiac catheterisation occur at the time of catheter manipulation; Dagirmanjian et al (1993) and Markus et al (1993a) reported that embolic phenomena occurred frequently during all phases of cerebral angiography but more embolic signals were recorded during catheter flushing and injection of contrast material than during manipulation of the catheter and guidewire.

In a sheep model by Markus and his colleagues (1993a) it was observed that air bubbles

Injection of contrast medium may cause an increase in signal intensity in an *in vitro* model, but not as high as that produced by injection of microbubbles. The acoustic features of injection of pure contrast medium were different from typical embolic signals. This may help to distinguish the contrast injection effect from real embolic signals during the clinical application of TCD. Additionally, we observed that embolic signals recorded at times of catheter insertion and manipulation were distinct in intensity and duration from those obtained at times of injection of normal saline in left ventricle and ascending aorta in both signal intensity and duration. This suggests either different types of emboli or alternatively the same type of emboli in different sizes. In order to clarify this, injections of embolic materials, thought to be related to neurological complications following cardiac catheterisation (Moody et al, 1990 and Pizzolitto et al, 1991), have been performed in the circulating model in this study. Our results showed no significant difference between *in vitro* and *in vivo* studies, suggesting that embolic signals, occurring at the time of catheter insertion or manipulation, may be related to dislodged atherosclerotic plaques or other formed-element embolic materials, and that the embolic signals at the time of injection with normal saline could be associated with micro-bubbles.

Earlier retrospective studies of aortopulmonary bypass demonstrated an incidence of

Now that contrast agents, which used to be the major hazard of angiography, have steadily declined in importance in causing the complication of cardiac catheterisation (Dawson and Fischer, 1977), embolism is of more interest. Solid emboli during cardiac catheterisation are usually believed to originate from the aorta, heart, neck vessels, or catheter (Dawson and Fischer, 1977). It has been suggested that atherosclerotic plaque in the carotid arteries can produce emboli by two mechanisms, by the rupture of its contents into the blood stream and by the breaking off of a thrombus formed on an ulcerated surface or in the blood stream when flow distal to

the plaque is slowed. (Spencer et al, 1990 and Farah et al, 1993). In these cases, catheter manipulation may act as a trigger. Moreover, the catheter itself may produce formed-element emboli by forming a catheter tip thrombus but this seems to happen easily in the venous system. The source of air bubbles which were introduced during angiography was examined in patients undergoing carotid artery catheterisation and a sheep model by Markus and his colleagues (1993a). It was observed that air bubbles can be introduced when contrast medium is drawn up or when the contrast medium is injected, due to the pressure changes with the formation of cavitation bubbles.

Embolic phenomena have been observed in all cases of cardiac catheterisation that we monitored, but none of our patients developed a focal neurological deficit. This is in accordance with the findings from the patients who underwent carotid angiography (Markus et al, 1993a) and other silent embolism investigations using TCD (Grosset et al, 1993b and Siebler et al, 1993). This may suggest that in most cases cerebral embolism does not result in a focal neurological deficit although the embolisation events occurring during cardiovascular catheterisation in the present study are undoubtedly high. A recent experimental observation by Johnston et al (1993) demonstrated that both global and regional brain perfusion was not adversely affected by gaseous microemboli which occurred during cardiopulmonary bypass. This result, combined with an experimental result showing that arterial gaseous emboli can be detected in venous drainage (Spencer et al, 1990), suggests that bubble emboli probably can pass through the vasculature of the brain. However, asymptomatic cerebral embolism does not mean that there is no deterioration in neurological status. Earlier retrospective studies of cardiopulmonary bypass demonstrated an incidence of altered mental state of only 3% (Coffee et al, 1983), but subsequent prospective studies with full neuropsychological assessment revealed the true incidence of neurological deficit or neuropsychological dysfunction to be over 50% (Shaw et al, 1986). Another retrospective analysis of 71 patients who died within six months of aortography or cardiac catheterisation disclosed that 25% to 30% had evidence of atheromatous emboli as compared with 4.3% in a historically matched control group (Ramirez et al, 1978). It has been suggested that a patient may experience asymptomatic cerebral embolism if the small infarct is located in a clinically silent area

of the brain (Petersen et al, 1987 and Kempster et al, 1988). However, emboli may have a cumulative detrimental effect on neuropsychological function, especially in the elderly (Ratcliffe et al, 1985). These facts suggest that asymptomatic cerebral embolism should not be ignored.

Besides the possible reasons mentioned above, the fact that none of patients with TCD-recorded cerebral emboli developed a neurological defect in this study also leads us to consider the hypothesis that embolism is not the sole pathophysiological mechanism involved in cerebral complications of cardiac catheterisation (Keilson et al, 1992). Alternative causes include toxic reactions to contrast medium (Lockwood et al, 1983), dehydration (Dawson and Fischer, 1977), and arterial spasm (Brown, 1992).

Percutaneous transluminal angioplasty (PTA) has recently become an established treatment for peripheral, renal, coronary and internal carotid vascular disease (Brown, 1992 and Koike et al, 1992). As a result, the number of related catheterisation and associated embolic complications has become of greater concern. Most recently, intraoperative transoesophageal echocardiography was used to visualise protruding aortic atheromas (Marshall et al, 1989 and Tunick and Kronzon, 1990, 1993), and a relationship between the protruding atheroma and perioperative cerebral embolism has been suggested (Katz et al, 1992). However, identification of the severely atherosclerotic aorta arch using transoesophageal echocardiography only supplies indirect information related to the potential source of atheromatous cerebral embolism. Our findings demonstrate that transcranial Doppler monitoring from the middle cerebral artery may have an advantage in increasing the ascertainment of diagnosis by giving information regarding cerebral emboli in the target organ.

In conclusion, transcranial Doppler examination was performed in the patients undergoing cardiac catheterisation and emboli were discovered in the middle cerebral artery of every patient. A higher incidence of embolic signals was recorded at times of ventriculography, catheter manipulation and changing guidewires. There is a significant difference in embolic signal intensity and duration between the time of

insertion or manipulation of catheter, and the time of injection of normal saline in the ascending aorta or left ventricle. The former signals may be related to dislodged atheromatous material and the latter may be associated with microbubbles. Transcranial Doppler ultrasonography may supply an early indication of embolism during cardiac catheterisation.

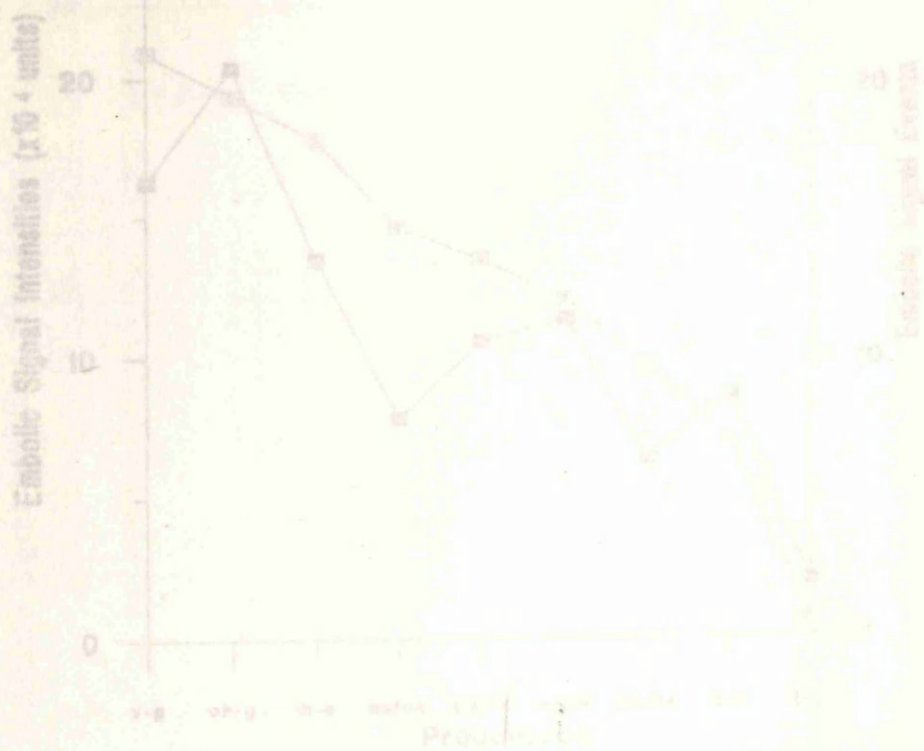


Figure 8.1 Embolic signal intensities and embolic signal events relating to different phases of cardiac catheterisation. Ventriculogram, changing guidewire, and catheter manipulation caused more signal intensities and higher number of embolic signals than other phases of cardiac catheterisation.

(Notes: v-g: ventriculogram; ch-g: changing guidewire; n-a: manipulation of catheter; ns/sa: injection of normal saline in supra aorta; cv/lv: injection of contrast medium in left ventricle; ns/ra: injection of normal saline in left ventricle; c-w: coronary angiography; i-c: inserting catheter.)

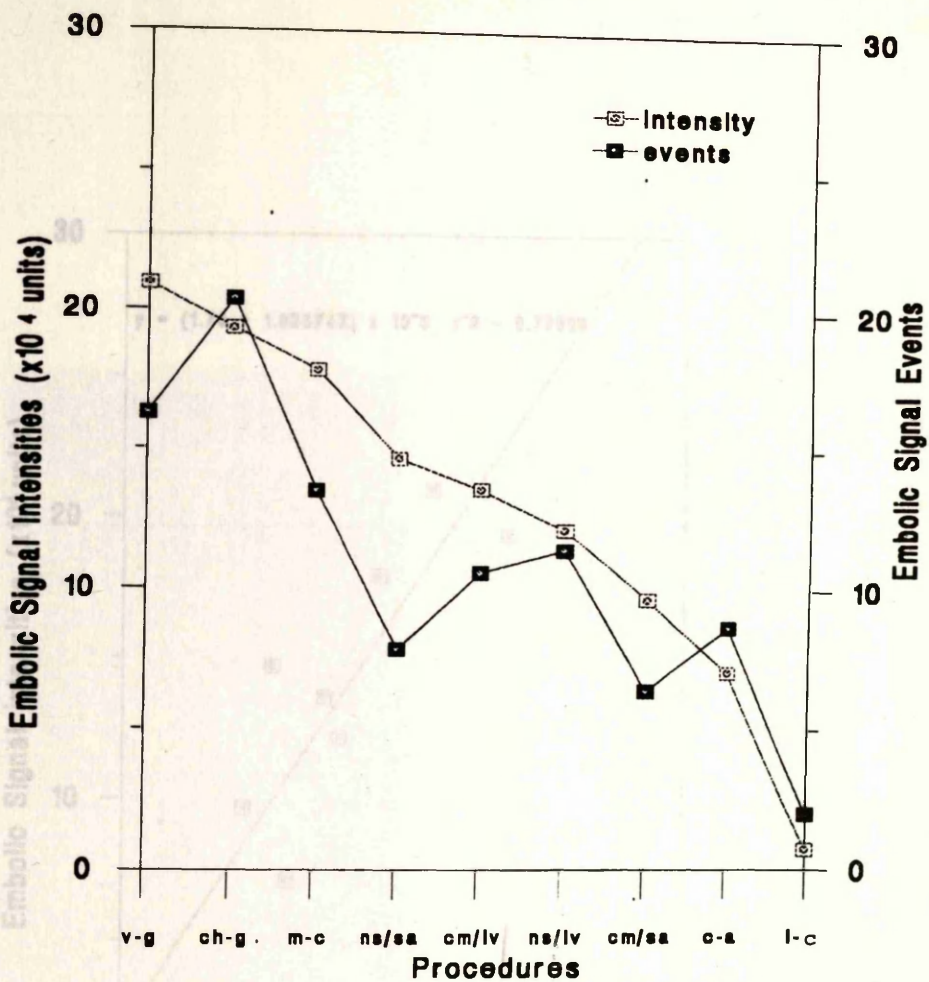


Figure 8.1 Embolic signal intensities and embolic signal events relating to different phases of cardiac catheterisation. Ventriculogram, changing guidewire, and catheter manipulation caused more signal intensities and higher incidence of embolic signals than other phases of cardiac catheterisation.

Figure 8.2 The correlation of embolic signal intensity and embolic signal events. There
 (Notes: v-g: ventriculogram; ch-g: changing guidewire; m-c: manipulation of catheter; ns/sa: injection of normal saline in supra aorta; cm/lv: injection of contrast medium in left ventricle; ns/lv: injection of normal saline in left ventricle; cm/sa: injection of contrast medium in supra aorta; c-a: coronary angiography; i-c: inserting catheter.)

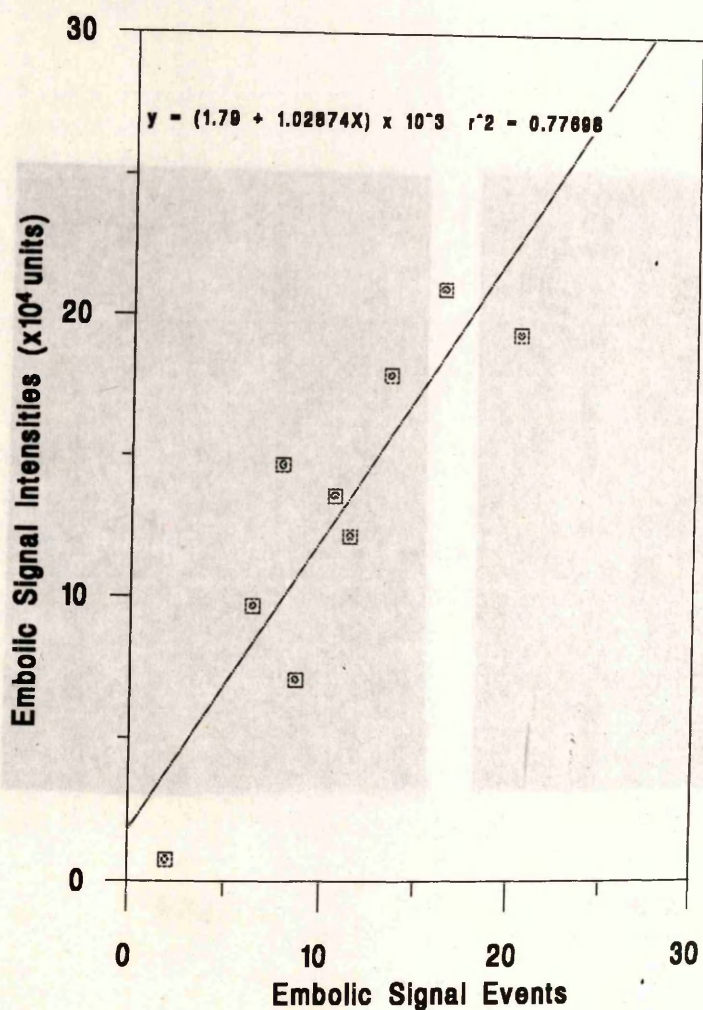
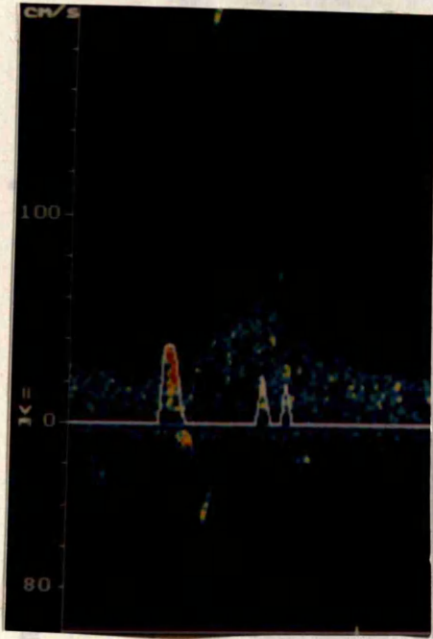
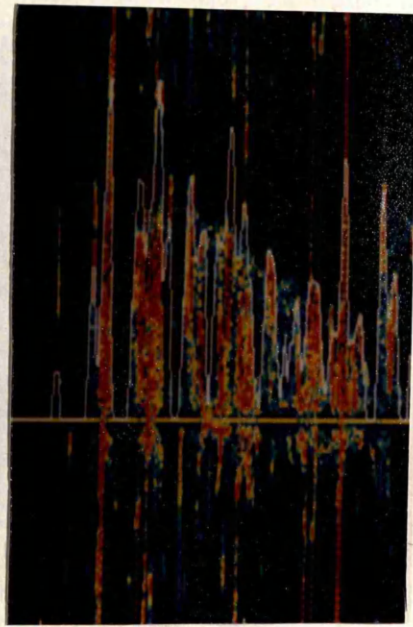


Figure 8.2 The correlation of embolic signal intensity and embolic signal events. There was a significantly relationship between embolic signal intensity and the incidence of embolic signals in different phases of cardiac catheterisation ($p < 0.01$).



8.3a



8.3b

Figure 8.3 Acoustic characteristics of embolic signals relating to the phases of cardiac catheterisation. Different appearance of embolic signals in different phases of cardiac catheterisation. Figure 8.3a showed a embolic signal suggesting atheromatous embolus with a longer sample duration and superimposed in the blood velocity waveform; figure 8.3b demonstrated a series of embolic signals with higher intensities (even overloaded) as well as increased Doppler frequencies, suggesting air emboli.

Figure 8.4
catheterisation
At supra aortic
time of catheter

(Notes: flow
signals due to

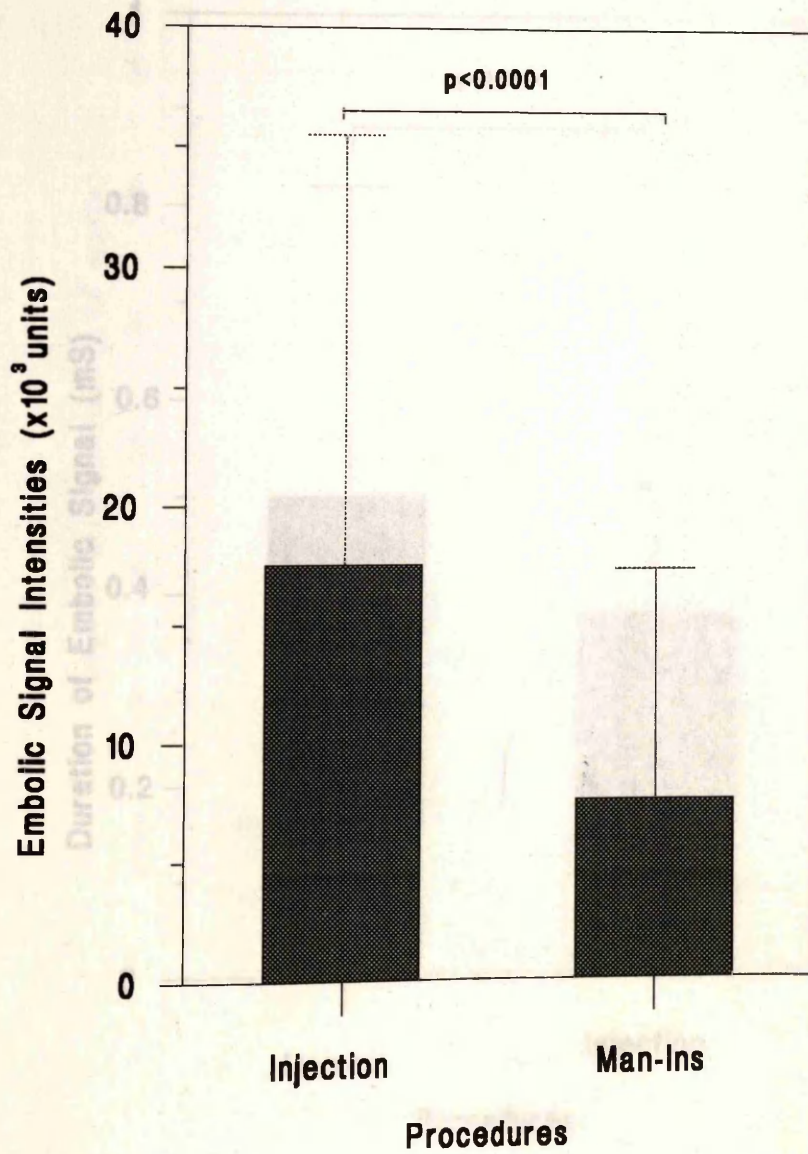


Figure 8.4 Comparison of embolic signal intensities at different phases of cardiac catheterisation. The embolic signal intensity recorded at time of normal saline injection at supra aortic region and into the left ventricle was significantly higher than that at time of catheter insertion or manipulation.

(Notes: *Injection*: embolic signals due to injection of normal saline; *Man-Ins*: embolic signals due to manipulation and insertion of catheter.)

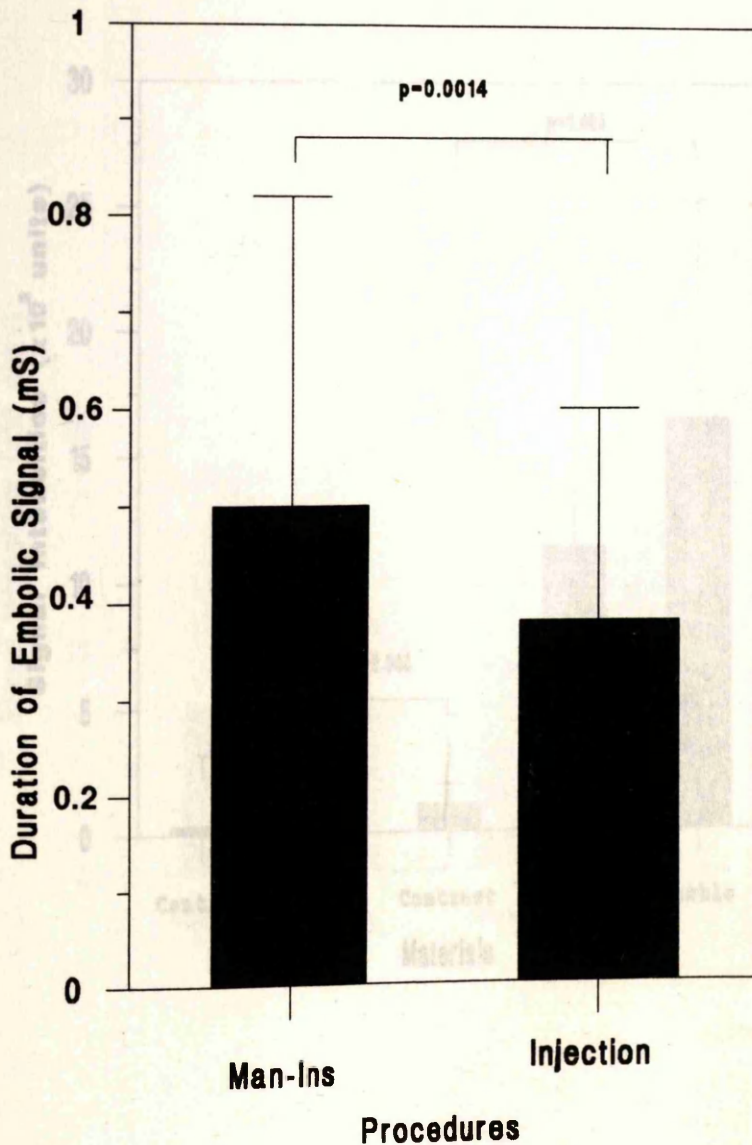


Figure 8.5 Comparison of embolic signal duration during different phases of cardiac catheterisation. Embolic signals recorded during catheter insertion and manipulation were of longer duration than those during injection of normal saline in supra aortic region and left ventricle.

Figure 8.6 Doppler signal intensities relating to description of different materials. Injection of contrast medium, atheromatous material, and microbubble-rich contrast caused an increase in Doppler intensity, but injection of normal saline did not.

Man-Ins: manipulation of catheter; N.S.: injection of normal saline (2.5 ml); Contrast: injection of contrast medium (2.5 ml); Atheroma: atheromatous material (100 μ m); Bubble: air bubbles in contrast medium mixture (average 30 μ m in diameter).

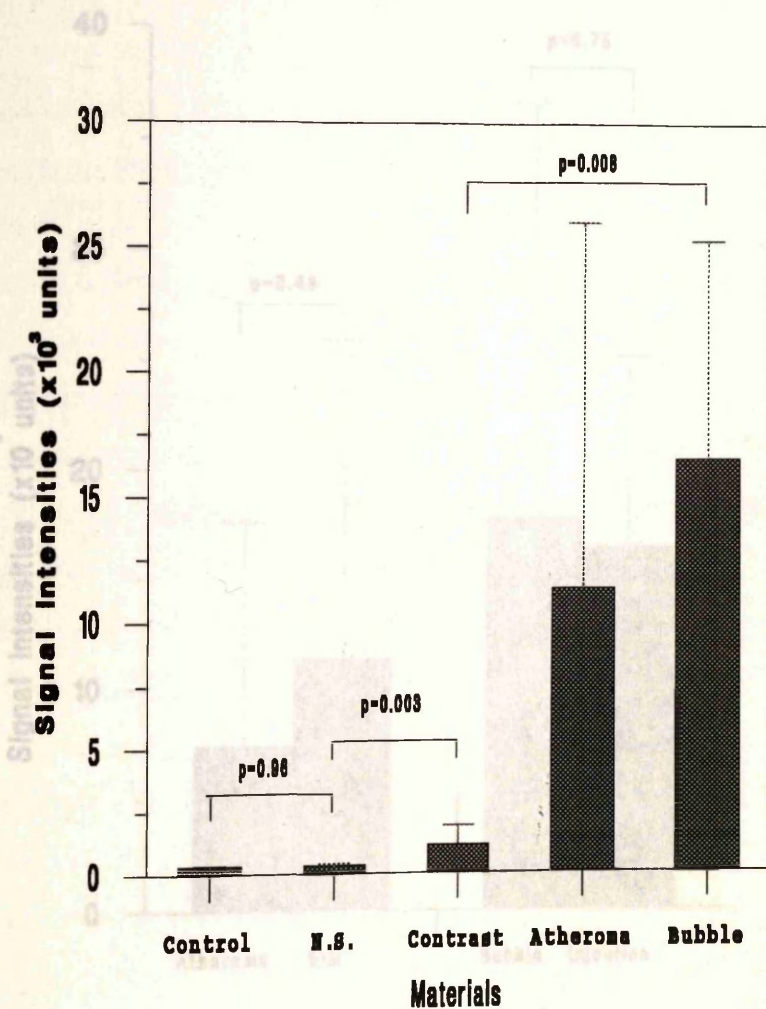


Figure 8.6 Doppler signal intensities relating to injection of different materials. Injection of contrast medium, atheromatous material, and microbubble-rich contrast caused an increase in Doppler intensity, but injection of normal saline did not significantly change the signal intensity. Among all the injections, microbubbles produced the highest signal intensity.

(Notes: *Control*: without injection; *N.S.*: injection of normal saline (2.5 ml); *Contrast*: injection of contrast medium (2.5 ml); *Atheroma*: atheromatous materials (100 μm); *Bubble*: air bubbles in contrast medium mixture (average 30 μm in diameter).

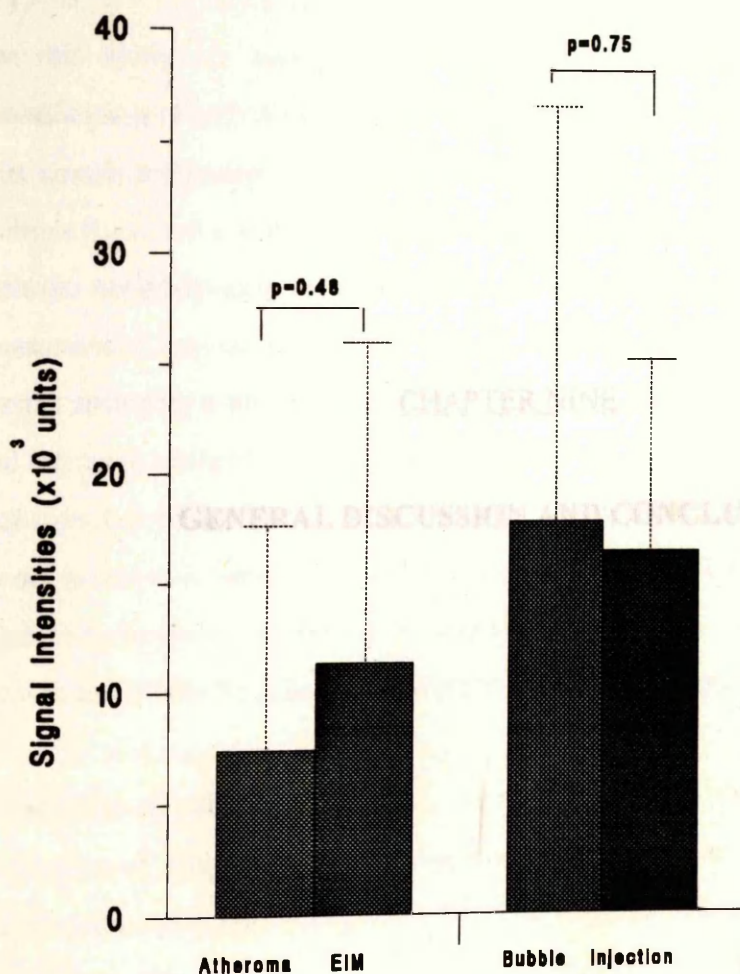


Figure 8.7 Correlation of embolic signal intensities in vitro with those in vivo. No significant difference was found between the signal intensities.

(Notes: *Atheroma*: embolic signal due to injection of atheromatous materials in vitro; *EIM*: embolic signals occurring during insertion and manipulation of catheter; *Bubble*: Embolic signals due to injection of microbubbles in vitro; *Injection*: embolic signals occurring at the time of injection of normal saline.)

9.1. General Discussion

For this study we have developed an *in vitro* circulating system with which quantification of embolic signals and other abnormal flow situations become possible. This circulation system played an important part in the present study because of its multiple functions and adaptability, including supplementation of steady pulsatile flow with the haemodynamic features close to physiological conditions, on-line flow rate measurement, and easy access for introduction of embolic materials and other test agents. Including a simulated MCA model was a key part in this system, and the result allowed a comparison of Doppler images from the *in vitro* model with that from the clinical setting. The MCA model acted as a basic bench on which other specific models, such as the smoke-produced chamber and the MCA stenosis model, were modified. This model is flexible and ready for future experimental Doppler investigations.

GENERAL DISCUSSION AND CONCLUSIONS

In addition to the bench models, circulating materials had an critical role in production of Doppler signals in this study. They acted as ultrasound scatters and supplied the necessary background information in the Doppler waveform. To our knowledge, this study is the first to describe Signacell solution as a replacement for blood material as a circulating fluid. We have observed that 0.03% Signacell solution can demonstrate a satisfactory Doppler ultrasound flow image which shows no significant difference from the clinical setting. The advantages of using Signacell are its economy and freedom from contamination. However, this solution may be not suited when a high haematocrit is desired for the circulating fluid. Furthermore, since the effects of aggregation were eliminated in our most of experiments by using diluted RBC concentrated or Signacell solution, some caution should be exercised in extrapolating our results to whole blood.

A major problem with any flow system used for Doppler ultrasound experiments may arise from the presence of air bubbles in the circulating fluid. Since they can radically

9.1. General Discussion

In this study, all circulating fluids and the solution used to store emboli were degassed before injection into the model. Moreover, the system

For this study we have developed an *in vitro* circulating system with which quantification of embolic signals and other abnormal flow situations become possible. This circulation system played an important part in the present study because of its multiple functions and adaptability, including supplementation of steady pulsatile flow with the haemodynamic features close to physiological conditions, on-line flow rate measurement, and easy access for introduction of embolic materials and other test agents. Including a simulated MCA in the bench model was a key part in this system, and the result allowed a comparison of Doppler images from the *in vitro* model with that from the clinical setting in more detail than ever previously reported. The MCA model acted as a basic bench on which other specific models, such as the smoke-produced chamber and the MCA stenosis model, were modified. This model is flexible and ready for future experimental Doppler investigations.

In addition to the bench models, circulating materials had an critical role in production of Doppler signals in this study. They acted as ultrasound scatters and supplied the necessary background information in the Doppler waveform. To our knowledge, this study is the first to describe Sigmacell solution as a replacement for blood material as a circulating fluid. We have observed that 0.03% Sigmacell solution can demonstrate a satisfactory Doppler ultrasound flow image which shows no significant difference from the clinical setting. The advantages of using Sigmacell are its economy and freedom from contamination. However, this solution may be not suited when a high haematocrit is desired for the circulating fluid. Furthermore, since the effects of aggregation were eliminated in our most of experiments by using diluted RBC concentrated or Sigmacell solution some caution should be exercised in extrapolating our results to whole blood.

A major problem with any flow system used for Doppler ultrasound experiments may arise from the presence of air bubbles in the circulating fluid. Since they can radically

affect the measured results and then cause misunderstanding and misinterpretation of the results, great care should be taken to ensure that none of the flow connections induce bubble formation. In this study, all circulating fluids and the solution used to store emboli were degassed before injection into the model. Moreover, the system was run for a short period before any test was conducted which largely removed intrinsic gas from the system. The other problem which may arise with embolus detection is artifact contamination. The common causes of the artefacts include the movement of probe, electrical interference, and various patient activities. However, these problems were avoided by fixation of probe, avoidance of unnecessary movement, and deleting waveforms marred by artifact.

For this study, Doppler signal intensity was chosen as a criteria to evaluate various aspects of emboli such as quantification of embolus size and differentiation between the embolic materials of different types. Two kinds of signal intensity indices, average signal intensity and total signal intensity, were introduced for the quantification of Doppler ultrasound signal in this study. The former was mainly used to quantify flow and the latter was applied to assess any definably-sized Doppler signals such as embolic signals. The need for such quantitative assessment of Doppler ultrasound flow images is based on the requirement for standardisation of methods of interpretation. Doppler signal intensity was chosen as an interpreting standard in this study due to the two facts: 1) it was a quantitative method available; and 2) increasing Doppler signal intensity is one of most important features of an embolic signal. The suitability of this method was proved in the early stages of this study when a relationship between the total signal intensity of embolic signal and the number of emboli introduced was defined.

In the next stage of this study, the relationship between signal intensity, and size of emboli was examined to assess suitability for differentiating emboli. The good correlation between intensity of embolic signals and embolus size suggests that, using signal intensity analysis, TCD may supply additional information about cerebral emboli by sizing them, down to as small as 35 μm for whole blood clots. However, signal intensity analysis could not differentiate embolic signals other than gas versus

solid. It was observed that an assigned signal intensity can be produced by a small, highly reflective target or a larger, less reflective target. As a result, we concluded that estimation of embolus size become possible only when the source of embolism is definite. More recently, Doppler frequency analysis has been reported as helpful in distinguishing different emboli, and this may enhance the technique in the future. The further design of pick up on-line automatic embolic signal detection may reach routine clinical practice.

In the study of the nature of spontaneous contrast (smoke-like echo), an echo phenomenon in enlarged hearts or vessel with regional blood stasis, spontaneous contrast was successfully reproduced in an expansion chamber which was set in the circulation system. In addition to TCD, spontaneous contrast signals were examined using two-dimensional ultrasonography. Both Doppler signal intensity analysis and visual assessment were performed in this study. Air bubbles and solid emboli injected into this chamber showed distinct ultrasonic images from smoke-like signals. The difference was also existed in TCD waveform. Furthermore, signal intensity analysis showed that there was no change in average signal intensity in the presence of spontaneous contrast whereas there was a significant increase in average signal intensity with introduction of emboli. Interestingly, it was observed that injection of normal saline also produced smoke-like echoes for a while. This finding further confirms our conclusion that spontaneous contrast is a special echo phenomenon caused by static whole blood in certain slow flow conditions.

We have made a qualitative interpretation of colour Doppler images of turbulence and a quantitative evaluation of the relationship between signal intensity, flow velocity and the degree of stenosis using an stenosed MCA model. To our knowledge the data presented in Chapter Six are the first to quantitatively study turbulent flow in an intracranial circulation setting. Additionally, since a stenosed lesion is not only an obstructing but also an emboligenic vessel abnormality, turbulence and embolic signal may co-exist simultaneously. So the study in Chapter Six was designed to answer three questions: 1) at which degree of stenosis dose a transition of turbulence occur; 2) how dose changing stenotic areas affect Doppler signal intensity and mean flow

velocity; 3) dose turbulence differ from embolic signals. A pulsatile flow model with short asymmetrical stenoses was used to answer question one and two. Visual and audible assessment, combined with signal intensity analysis was used to answer question three. It was shown that the characteristics of the Doppler signals measured at each site along the stenosis provide information on the nature of the insonated flow field and distinct morphologic features. Doppler signal sampled at the zone of turbulence profile showed a significant increase in average signal intensity. Our data support the haemodynamic concept that turbulence is usually detectable at moderate-to-high degrees of stenosis and a mild degree of stenosis normally involves a flow acceleration. A linear relationship was found between mean velocity and the degree of stenosis. Average signal intensity seemed to change independently to the changing reduction area of stenosis. It was found that embolic signals presented different visual image as well as audio character compared to turbulence. Difference in signal intensity between the two pathological signals become marked with air bubbles and platelet-rich emboli but not whole blood clots.

In the late stage of this study, as TCD is widely used to detect cerebral emboli, investigation of the possible factors which may affect such application was undertaken. The study in Chapter Seven was designed to examine the effect of two commonly encountered factors, ultrasound transmitting frequency and flow velocity, on quantification of embolic signal using signal intensity analysis. The MCA model was modified to meet the requirement of the study. The same embolic particle was repeatedly injected into the circulating system in different test settings. It was found that an embolus within higher velocity flow produced lower total signal intensity because of a shorter passage duration compared to the embolus at lower flow velocity. Similarly, the signal intensity of an embolus recorded from a probe with a lower transmitting frequency was significantly higher than that by a probe with a higher frequency. The data from this study supply the information which may be helpful in proper interpretation of embolic signals collected from different TCD settings or different clinical conditions.

Finally, the clinical interest in detecting and quantifying embolic signals was extended from the *in vitro* model. It has been well documented that emboli, especially air emboli, are often involved in cerebral complication of diagnostic catheterisation from different approaches. In this study, seventeen patients undergoing cardiac catheterisation were monitored using TCD. The incidence of embolic signals was recorded at different phases of the catheterisation. The signal intensity of recorded embolic signals was calculated off-line and compared with the signal intensities produced by introduction of different kinds of embolic materials in the *in vitro* model. Two types of emboli, air bubbles and atherosclerotic emboli, which were thought possibly involved in cardiac catheterisation procedure, were prepared and injected into the MCA model. In terms of both embolic incidence and the amplitude of increased average signal intensity, it was observed that the manoeuvres of ventriculography, change of guidewire, and manipulation of catheter were a major cause of cerebral emboli. With a correlation between the results from *in vitro* and from *in vivo*, the result suggests that embolic signals occurred during supra aortic and ventricle injection may be related to microbubbles and those happened during insertion and manipulation of catheter may be associated with dislodged atheromatous material.

9.2. Conclusions

It has been proved that the MCA model and related circulation system used in current study are suitable for a variety of TCD studies. Up to seven kinds of emboli were detected in this study. Signal intensity analysis is a sensitive and convenient method in quantification of embolic and non-embolic signals. Embolic signal intensity is proportional to the number and the size of emboli. However, sizing emboli according to the total intensity of embolic signals becomes possible if the nature of emboli is known. Differentiation of different emboli using embolic signal intensity is not possible because of the non-specific nature of signal intensity. Spontaneous contrast is not an embolic phenomenon but a kind of abnormal flow appearance.

Transcranial Doppler ultrasonography can facilitate the diagnosis of the stenotic lesions by means of the immediate identification of turbulence. With regard to estimation of the degree of stenosis using transcranial Doppler ultrasonography, mean flow velocity recorded in the post-stenosis zone is more reliable than the signal intensity collected in the same region. Similarly, in terms of differentiation between turbulence and embolic signals, the difference of visual characteristics and audible components of the Doppler signals are considered to be essential criteria. On the other hand, however, the signal intensity analysis may be helpful to this application when air emboli are involved or embolic signals overlap turbulence signals.

Both ultrasound transmitting frequency of the probe and flow velocity can significantly affect the signal intensity quantification of embolic signals. These factors need to be considered when trying to interpret embolic signals collected from different settings. Quantification of signal intensity of embolic signals recorded from cardiac catheterisation can not only show the distribution of embolic incidence of cerebral embolism but also may relate nature of emboli involved. The data from this study has proved that identification and quantification of embolic signals using TCD may provide more precise information than the usual clinical methods for understanding stroke mechanism, verification of high-risk subgroups, and evaluation of the effect of preventive therapies.

**PRESENTATIONS AND PUBLICATIONS CONTAINING THE WORK
UNDERTAKEN FOR THIS THESIS**

Yi, Y., Grosset, D.G., Kelman, A., Lees, K.R., Reid, J.L. (1993): Quantitative detection of embolic materials in the MCA model using transcranial ultrasonography. 1st British Transcranial Doppler Conference. Glasgow, UK.

Yi, Y., Grosset, D.G., Kelman, A., Lees, K.R., Reid, J.L. (1993): Ultrasonic characteristics of embolic particles in an in vitro model. 2nd International Conference on Stroke, Geneva, Switzerland.

Georgiadis, D., Grosset, D.G., Yi, Y., Kelman, A., Lees, K.R. (1994): Power Analysis of emboli signals helps in detection of the nature of the embolic material. 1994 Symposium on Cerebral Hemodynamics: Transcranial Doppler, Cerebral Blood Flow, and Other Modalities. San Diego, California, USA.

Yi, Y., Grosset, D.G., Kelman, A., Lees, K.R. (1994): Ultrasound Detection of Circulating Emboli in the MCA during Cardiac Catheterisation. Joint XII World Congress of Cardiology and XVIth Congress of the European Society of Cardiology. Berlin, Germany.

Grosset, D.G., Yi, Y., Lees, K.R., Kelman, A., Hillis, W.S. (1993): Cardiac source embolism is detectable by Doppler Ultrasound in patients and in an experimental model. (Abstract) Circulation 1993;88 (suppl.): I-579.

Yi, Y., Grosset, D.G., Kelman, A., Lees, K.R. (1995) Identification of echocardiographic 'smoke' in a bench model with Doppler ultrasound (submitted to Journal American College of Cardiology for publication).

Yi Yang, Grosset, D.G., Kelman, A., Lees, K.R. (1995) Cerebral Embolization During Cardiac Catheterisation. (submitted to British Heart Journal for publication).

REFERENCES

- Adams, R. J., Nichols, F. T., and Hess, D. C. (1992). *Normal values and physiological variables. Transcranial Doppler*. Raven Press, New York 41-48.
- Aguilar, M. J., Gerbode, F., and Hill, J. D. (1971) Neuropathologic complications of
- Aaslid, R. (1986). *Transcranial Doppler examination techniques*, Springer-Verlag, Wien, Austria.
- Antarengo, P., Cohen, A., Baudrimont, M., and Bouvier, M. G. (1992)
- Aaslid, R. (1992). Developments and principles of transcranial Doppler. *Transcranial Doppler*, Raven Press Ltd., New York, U.S.A..1-8.
- Aaslid, R., Lindegaard, K. F., Sorteberg, W., and Nornes, H. (1989) Cerebral autoregulation dynamics in humans. *Stroke*,**20**, 45-52.
- Aaslid, R., Markwalder, T-M., and Nornes, H. (1982) Noninvasive transcranial Doppler ultrasound recording of flow velocity in basal cerebral arteries. *J. Neurosurg.*,**57**, 769-774.
- Aaslid, R., Newell, D. W., Stooss, R., Sorteberg, W., and Lindegaard, K. F. (1991) Assessment of cerebral autoregulation dynamics from simultaneous arterial and venous transcranial Doppler recordings in humans. *Stroke*,**22**, 1148-1154.
- Abts, L. R., Beyer, R. T., Galletti, M., Richardson, P. D., Karon, D., Massimino, R., and Karlson, K.E. (1978) Computerized discrimination of microemboli in extracorporeal circuits. *Am. J. Surg.*,**135**, 535-538.
- Adams, D. F., Fraser, D. B., and Abrams, H. L. (1973) The complications of coronary arteriography. *Circulation*,**48**, 609-618.
- Adams, J. H. and Graham, D. I. (1988). *An Introduction to Neuropathology*, Churchill Livingstone, Edinburgh.
- Bachman, D. M. (1993) Microscopic air embolism during cerebral angiography. *Lancet*,**341**, 1537-1538.

Adams, R. J., Nichols, F. T., and Hess, D. C. (1992). *Normal values and physiological variables. Transcranial Doppler*, Raven Press, New York. 41-48.

Agular, M. J., Gerbode, F., and Hill, J. D. (1971) Neuropathologic complications of cardiac surgery. *J. Thorac. Cardiovasc. Surg.*, **61**, 676-685.

Amarenco, P., Cohen, A., Baudrimont, M., and Bousser, M. G. (1992)

Transesophageal echocardiographic detection of aortic arch disease in patients with cerebral infarction. *Stroke*, **23**, 1005-1009.

Archer, S. L., Kvernern, L. R., James, K., Ezekowitz, M., and Gornick, C. (1991)

Does Warfarin reduce the prevalence of left atrial thrombus in chronic atrial fibrillation? - a double blind, placebo-controlled study. *Circulation*, **84** (Suppl. II), II-693.

Armstrong, W. F., Mueller, T. M., Kinney, E. L., Tickner, E. G., Dillon, J. C., and Feigenbaum, H. (1982) Assessment of myocardial perfusion abnormalities with contrast-enhanced two-dimensional echocardiography. *Circulation*, **66**, 166-173.

Arts, M. G. J. and Roevros, J. M. J. G. (1972) On the instantaneous measurement of blood by ultrasonic means. *Med. Biol. Eng.*, **10**, 23-34.

Aschenberg, W., Schlutter, M., Kremer, R., Schroeder, E., Siglow, V., and Bleifeld, W. (1986) Transesophageal two-dimensional echocardiography for the detection of left atrial appendage thrombus. *J. Am. Coll. Cardiol.*, **7**, 163-166.

Austen, W. G. and Howry, D. H. (1965) Ultrasound as a method to detect bubbles or particulate matter in the arterial line during cardiopulmonary bypass. *J. Surg. Res.*, **5**, 283.

Bachman, D. M. (1993) Microscopic air embolism during cerebral angiography. *Lancet*, **341**, 1537-1538.

Ballot, B. (1845) Akustische Versuche auf der Niederlandische Eisenbahn nebst gelegentlichen Bemerkungen zur Theorie des Hr. prof. Doppler. *Pog. Ann.*,**66**, 321-351.

Bamford, J. M. (1990) The incidence and natural history of stroke: which patients might benefit from new treatment. *New Drug Strategies in the Prevention and Treatment of Stroke. An International Conference.* Jan. 1990. London.

Bandyk, D. F., Kaebnick, H. W., Adams, M. B., and Towne, J. B. (1988) Turbulence occurring after carotid bifurcation endarterectomy: A harbinger of residual and recurrent carotid stenosis. *J. of Vasc. Surg.*,**7**, 261-274.

Barnett, H. J. M. (1991) North American symptomatic carotid endarterectomy trial: Methods, patients characteristics, and progress. *Stroke*,**22**, 711-720.

Barnett, H. J. M. (1991) Clinical trials in stroke prevention. *Drug Res.*,**41**, 340-344.

Bascom, P. A. J. and Cobbold, R. S. C. (1990) Effects of transducer beam geometry and flow velocity profile on the Doppler power spectrum: a theoretical study. *Ultrasound in Med. & Biol.*,**16**, 279-295.

Bascom, P. A. J., Cobbold, R. S. C., Routh, H. F., and Johnston, K. W. (1993) On the Doppler signal from a steady flow asymmetrical stenosis model: effects of turbulence. *Ultrasound in Med. & Biol.*,**19**, 197-210.

Bascom, P. A. J., Routh, H. F., and Cobbold, R. S. C. (1988) Interpretation of power changes in Doppler signals from human blood - in vitro studies. *IUSP*, 985-988.

Beppu, S., Nimura, Y., Sakakibara, H., Nagata, S., Park, Y-D., and Izumi, S. (1985) Smoke-like echo in the left atrial cavity in mitral valve disease: its features and significance. *J. Am. Coll. Cardiol.*,**6**, 774-779.

Berger, M., Davis, D., lolley, D., Rams., and Spencer, M. P. (1990) Detection of subclinical microemboli in patients with prosthetic valves (abstract). *J. Cardiovasc. Tech.*,**9**, 282-283.

Brass, L. M. and Fayad, P. B. (1993) Intraoperative monitoring with transcranial
Berger, M. P. and Tegeler, C. H. (1993) Embolus detection using Doppler ultrasonography. *Transcranial Doppler Ultrasonography*, edited by Babikian and Wechsler. Mosby, St. Louis, USA.,232-241.

Brennan, R. W., Patterson, R. H., and Kessler, B. A. (1971) Cerebral blood flow and
Besouw, J-P. Van. and Hinds, C. J. (1989) Fat embolism syndrome. *Brit.J. Hosp. Med.*,**42**, 304-311.

Black, I. W., Hopkins, A. P., Lee, L. C. L., Walsh, W. F., and Jacobson, B. M. (1991) Left atrial spontaneous echo contrast: A clinical and echocardiographic analysis. *J. Am. Coll. Cardiol.*,**18**, 398-404.

Brucher, R. and Russell, D. (1993) Automatic embolus detection with artifact
Blauth, C. I., Arnold, J. V., Schulenber, W. E., McCartney, A. C., and Taylor, K. M. (1988) Cerebral microembolism during cardiopoulmonary bypass. *J. Thorac. Cardiovasc. Surg.*,**95**, 668-676.

Blauth, C. I., Cosgrove, D. M., Webb, B. W., Ratliff, N. B., Boylan, M., Piedmonte, M. R., Lytle, B. W., and Loop, F. D. (1992) Atheroembolism from the ascending aorta: An emerging problem in cardiac surgery. *J. Thorac. Cardiovasc. Surg.*,**103**, 1104-1111.

Blauth, C. I., Smith, P. L., Arnold, J. V., Jagoe, J. R., Wootton, R., and Taylor, K. M. (1990) Influence of oxygenator type on the prevalence and extent of microembolic retinal ischemia during cardiopulmonary bypass. Assessment by digital image analysis. *J. Thorac. Cardiovasc. Surg.*,**99**, 61-60.

Butler, B. D. and Kurusz, M. (1985) Guest editorial. Gaseous microembolism-
Boyle, R. (1670a) New pneumatical experiments about respiration. *Philos. Trans.*,**5**, 2046.

- Cacciatori, A. and Russo, L. S. (1991) Lacunar infarction as an embolic complication
- Boyle, R. (1670b) On the observation produced in a animal in changes as to rarity and density made in the self same air. *Trans. R. Soc. (London)*, **16**, 34.
- Caguin, F. and Carter, M. G. (1963) Fat embolization with cardiotomy with the use
- Brass, L. M. and Fayad, P. B. (1993). Intraoperative monitoring with transcranial Doppler ultrasonography during cardiac surgery and interventions. *Transcranial Doppler Ultrasonography*, Mosby, St. Louis, U.S.A., 222-231. Variation of Doppler ultrasound spectral width in the post-stenotic velocity field. *Ultrasound in Med. &*
- Brennan, R. W., Patterson, R. H., and Kessler, B. A. (1971) Cerebral blood flow and metabolism during cardiopulmonary bypass evidence of microembolic encephalopathy. *Neurology*, **21**, 665-673.
- Yagana, R. G. (1985) Comparison of Doppler echocardiographic peak frequency and turbulence parameters in the quantification of
- Brown, M. M. (1992) Balloon angioplasty for cerebrovascular disease. *Neurol. Res.*, **14**(2 suppl), 159-163.
- Caplan, L. R., O'Conn, L., Hier, D. B., Reddy, H., and Shah, S. (1986) Atrial size,
- Brucher, R. and Russell, D. (1993) Automatic embolus detection with artifact suppression. *J. Neuroimag.*, **3**, 77 (abstract).
- Caplan, L. R., Hier, D., and O'Conn, L. (1983) Cerebral embolism in the Michael
- Bruning, E. J. (1955) Origin and significance of intra-arterial foreign body emboli in lungs of children. *Virchows. Arch (Pathol. Anat.)*, **327**, 460.
- Castello, R., Pearson, A. C., Labowitz, A. J., and Lenzen, P. (1990) Prevalence and
- Bunegin, L., Wahl, D., and Albin, M. S. (1991) Estimation of embolic air volume in the middle cerebral artery (MCA) using transcranial sonography. *J. Neurosurg. Anesth.*, **3**, 205.
- Charles, C. F., Bernard, L., Sheldon, A., Albert, W. C., Karl, E. K., and Clarence, D.
- Bunegin, L., Wahl, D., and Albin, M. S. (1994) Detection and volume estimation of embolic air in the middle cerebral artery using transcranial Doppler sonography. *Stroke*, **25**, 593-600.
- 1) Anatomical and experimental observations on air embolism. *Surg. Gynec. & Obst.*, **59**, 569.
- Butler, B. D. and Kurusz, M. (1985) Guest editorial: Gaseous microembolism-sources and controversies. *Med. Instrum.*, **2**, 52.

- Cacciatore, A. and Russo, L. S. (1991) Lacunar infarction as an embolic complication of cardiac and arch angiography. *Stroke*,**22**, 1603-1605.
- Caguin, F. and Carter, M. G. (1963) Fat embolization with cardiectomy with the use of cardiopulmonary bypass. *J. Thoracic. Cardiovas. Surg.*,**46**, 665-672.
- Campbell, J. D., Hutchison, K. J., and Karpinski, E. (1989) Variation of Doppler ultrasound spectral width in the post-stenotic velocity field. *Ultrasound in Med. & Biol.*,**15**, 611-619.
- Cannon, S. R., Richards, K. L., and Morgann, R. G. (1985) Comparison of Doppler echocardiographic peak frequency and turbulence parameters in the quantification of aortic stenosis in a pulsatile flow model. *Circulation*,**71**, 129-135.
- Caplan, L. R., D'Cruz, I., Hier, D. B., Reddy, H., and Shah, S. (1986) Atrial size, atrial fibrillation and stroke. *Ann. Neurol.*,**19**, 158-161.
- Caplan, L. R., Hier, D., and D'Cruz, I. (1982) Cerebral embolism in the Michael Reese Stroke Registry. *Stroke*,**14**, 534-537.
- Castello, R., Pearson, A. C., Labovitz, A. J., and Lenzen, P. (1990) Prevalence and clinical implications of atrial spontaneous contrast in patients undergoing transesophageal echocardiography. *Am. J. of Cardiol.*,**65**, 1149-1153.
- Charles, C. F., Bernard, L., Sheldon, A., Albert, W. C., Karl, E. K., and Clarence, D. (1957) Experimental cerebral gas embolism. *Ann. of Surg.*,**145**, 641-670.
- Chase, W. H. (1934) Anatomical and experimental observations on air embolism. *Surg. Gynec. & Obst.*,**59**, 569.

Chimowitz, M. I., Nemecek, J. J., Marwick, T. H., Lorig, R. J., Furlan, A. J., and Salcedo, E. E. (1991) Transcranial Doppler ultrasound identifies patients with right-to-left cardiac or pulmonary shunts. *Neurology*,**41**, 1902-1904.

Clark, R. E. (1985) Microemboli: an overview. *Med. Instrum.*,**2**, 54-55.

Clarke, C. R. A. (1987). *Clinical Medicine*, 3rd edition. Bailliere Tindall, East Sussex, U.K.

(1993) Silent cerebral microemboli occurring during carotid angiography. Frequency

Clements, S. D. and Gatlin, S. (1991) Outpatients cardiac catheterization: a report of 3,000 cases. *Clin. Cardiol.*,**14**, 477-480.

Dahl, A., Russell, D., Nyberg-Hansen, R., and Rootwelt, K. (1983) Effect of

Coffee, C. E., Massey, E. W., and Roberts, K. B. (1983) Natural history of cerebral complications of coronary bypass graft surgery. *Neurology*,**33**, 1416-1421.

Colt, H. G., Begg, R. J., Saporito, J. J., Cooper, W. M., and Shapiro, A. P. (1988) Cholesterol emboli after cardiac catheterization. Eight cases and a review of the literature. *Medicine Baltimore*,**67**, 389-400.

Cardiol.,**11**, 1204-1211.

Cowburn, P. J., Grosset, D. G., Squire, I. B., Morris, A. D., Northridge, D., Lees, K. R., Dargie, H. J., and Reid, J. L. (1992) Doppler ultrasound detection of cerebral emboli in patients with mechanical heart valves: Correlation with neurological deficit. *Clin. Sci.*,**82(suppl.26)**, 1.

Am. J. of Cardiol.,**22**, 1481-1484.

Crystal, D. (1990). *Cambridge Encyclopedia*, Cambridge University Press, 1st edition. 1237.

Am. J. Hosp. Pharm.,**3**, 53-54.

Cujec, B., Polasek, P., Voll, C., and Shuaib, A. (1991) Transesophageal echocardiography in the detection of potential cardiac source of embolism in stroke patients. *Stroke*,**22**, 727-733.

Cunning, A. J., Pickering, G. W., Robb-Smith, A. E. T., and Russel, R. R. (1964) Mural thrombus of the internal carotid artery and subsequent embolism. *Q. J. Med.*,**33**, 155-195.

D'Arrigo, J. S., Simon, R. H., and Ho, S. Y. (1991) Experimental laboratory research. *J. Neuroimag.*,**1**, 134-139.

Dagirmanjian, A., Davis, D. A., Rothfus, W. E., Deeb, Z. L., and Goldberg, A. L. (1993) Silent cerebral microemboli occurring during carotid angiography: Frequency as determined with Doppler sonography. *Am. J. of Roentgenol.*,**161**, 1037-1040.

Dahl, A., Russell, D., NybergHansen, R., and Rootwelt, K. (1989) Effect of nitroglycerin on cerebral circulation measured by transcranial Doppler and SPECT. *Stroke*,**20**, 1733-1736.

Daniel, W. G., Nelessen, U., Schroder, E., Nonnast-Daniel, B., Bendenarski, P., Nikutta, and Lichtlen, P. R. (1988) Left atrial spontaneous echo contrast in mitral valve disease: An indicator for an increased thromboembolic risk. *J. Am. Coll. Cardiol.*,**11**, 1204-1211.

Davidson, C. J., Mark, D. B., Pieper, K. S., Kisslo, K. B., Hlatky, M. A., Gabriel, D. A., and Bashore, T. M. (1990) Thrombotic and cardiovascular complications related to nonionic contrast media during cardiac catheterization: Analysis of 8,517 patients. *Am. J. of Cardiol.*,**22**, 1481-1484.

Davis, N. M., Turco, S., and Sively, E. (1970) A study of matter in IV infusion fluid. *Am. J. Hosp. Pharm.*,**2**, 53-54.

Dawson, D. M. and Ficher, E. G. (1977) Neurologic complications of cardiac catheterization. *Neurology*,**27**, 496-497.

Edmonds-Seal, J. and Maroon, J. C. (1969) Air embolism diagnosed with pitzrecund. *Ann.*,**34**, 438-440.

De Bray, J. M., Galland, F., Lhoste, P., Nicolau, S., Dubas, E., Emile, J., and Pillet, J. (1995) Color Doppler and duplex sonography and angiography of the carotid artery bifurcations. Propective, double-blind study. *Neuroradiology*,**37**, 219-224.

Dietz, D., Heyman, J. S., and Clark, R. E., Hallenbeck, J. M., and Warner, D. S. (1974) Continuous wave ultrasonic micro emboli monitor for use in extracorporeal perfusion. *Proc 27 ACEMB.*,188.

Doppler, C. A. (1842) Uber das farbige Licht der Doppelsterne und einiger anderer Gestirne des Himmels. *Abhandl. Konigl. Bohm.*,

Drost, H., Buis, B., Haan, D., and Hillers, J. A. (1984) Cholesterol embolism as a complication of left heart catheterization. Report of seven cases. *Br. Heart. J.*,**52**, 339-342.

Duft, F., Greenfield, A. D. M., and Whelan, R. F. (1954) Observations on the mechanism of the vasodilation following arterial gas embolism. *Clin. Sci.*,**13**, 364.

Dunn, G. D. (1993) Microscopic air embolism and cerebral angiography. *Lancet*,**341**, 1215-1216.

Dutka, A. J., Mink, R., Mcdermott, J., Clark, J. B., (1992) Effect of Lidocaine on somatosensory evoked reponse and cerebral blood flow after canine cerebral air embolism. *Stroke*,**23**, 1515-1521.

Eden, A., Itoh, T., and Matsumoto, M. (1994) Effect of emitted power on waveform intensity in transcranial Doppler (5). *Stroke*,**25**, 523-524.

Editorial.(1975) Brain damage after open heart surgery. *Lancet*,**2**, 399.

Edmonds-Seal, J. and Maroon, J. C. (1969) Air embolism diagnosed with ultrasound. *Anes*,**24**, 438-440.

- coronary arteriography in humans: perfusion and anatomic studies. *J. Am. Coll. Surg.*, **117**, 100-104.
- Eker, A., Jegaden, O., Montagna, P., Ossete, J., Douieb, A., and Mikaeloff, P. (1994) Possible cholesterol crystal embolisation following coronary surgery: discussion of one such patient. *Lyon Chirurgical*, **90**, 49-51.
- Erbel, R., Stern, H., Ehrental, W., Schreiner, G., Treese, N., Kramer, G., Thelen, M., Schweizer, P., and Meyer, J. (1986) Detection of spontaneous echogenic contrast within the left atrium by transesophageal echocardiography: Spontaneous echocardiographic contrast. *Clin. Cardiol.*, **9**, 245-252.
- Evans, D. H., McDicken, W. N., Skidmore, R., and Woodcock, J. P. (1989): *Doppler Ultrasound: Physics, Instrumentation and Clinical Applications*, John Wiley & Sons, Inc, Chichester.
- Fabian, T. C., Hoots, A. V., Stanford, D. S., Patterson, C. R., and Mangiante, E. C. (1990) Fat embolism syndrome: Prospective evaluation in 92 fracture patients. *Critical. Care. Med.*, **18**, 42-46.
- Farah, M. G. and Hawawini, H. (1993) Thrombus of the ascending aorta as a source of cerebral embolism. *Chest*, **104**, 1604-1605.
- Fazio, C. and Sacchi, U. (1954) Experimentally produced red softening of the brain. *J. Neuropath. Exper. Neurol.*, **13**, 476.
- Feigenbaum, H. (1976). *Echocardiography*, 2nd edition. Philadelphia Lea and Febiger,
- Feinstein, S. B. (1991) Symposium: Contrast echocardiography. Editorial: The ongoing development of contrast echocardiography: Its promise for myocardial perfusion assessment. *Am. J. Cardiac. Imaging*, **5**, 188-191.
- Feinstein, S. B., Lang, R. M., Dick, C., Neumann, A., Alsaadir, J., Chua, K.G., Carroll, J., Feldman, T., and Borow, K. M. (1988) Contrast echocardiography during

coronary arteriography in humans: perfusion and anatomic studies. *J. Am. Coll. Cardiol*, **11**, 59-65.

Feinstein, S. B., Ten Cate, F. J., Zwehl, W., Ong, K., Mauver, G., Tei, C., Shah, P. M., Meerbaum, S., and Corday, E. (1984) Two-dimensional contrast echocardiography. I. In vitro development and quantitative analysis of echo contrast agents. *J. Am. Coll. Cardiol.*, **3**, 14-20.

Fietsam, R., Ranval, T., Cohn, S., Brown, O. W., Bendick, P., and Glover, J. L. (1992) Hemodynamic effects of primary closure versus patch angioplasty of the carotid artery. *Ann. of Vasc. Surg.*, **6**, 443-449.

Fischer, W. M., Gottschalk, P. G., and Browell, J. N. (1970) Transient cortical blindness. An unusual complication of coronary arteriography. *Neurology*, **20**, 353-355.

Fisher, C. M. (1965) Lacunes: small deep cerebral infarcts. *Neurology*, **15**, 774-784.

Fisher, C. M. (1978) Thalamic pure sensory stroke: a pathological study. *Neurology*, **28**, 1141-1144.

Fisher, E. A., Stahl, J. A., Budd, J. H., Goldman, R. A., Klapper, A., Lee, Y., and Goldman, M. E. (1991) Left atrial 'smoke' is a major risk factor for thrombus formation. *Circulation*, **84** (suppl.II), II-692.

Forbes, C. D. and Jackson, W. F. (1993). *A Colour Atlas and Text of Clinical Medicine*, Wolfe Publishing, London, U.K..

Fries, C. C., Levowitz, B., Adler, S., Cook, A. W., Karlson, K. E., and Dennis, C. (1957) Experimental cerebral gas embolism. *Ann. Surg.*, **145**, 461-470.

Frink, R. J. and Ostrach, L. H. (1990) Streptokinase in the treatment of an acute cerebral embolus - A case report. *Angiology*,**41**, 66-69.

Furlan, A. J., Craciun, A. R., Salcedo, E. E., and Mellino, M. (1984) Risk of stroke in patients with mitral annulus calcification. *Stroke*,**15**, 801-803.

Furness, A. and Wright, G. (1985) Microbubble detection during cardiopulmonary bypass for open-heart surgery. *Life Support Syst.*,**3**, 103-109.

Gallagher, E. G. and Pearson, D. T. (1973) Ultrasonic identification of sources of gaseous microemboli during open heart surgery. *Thorax.*,**28**, 295-309.

Garcia-Fernandez, M. A., Torrecilla, E. G., Roman, D. S., Azevedo, J., Bueno, H., Moreno, M. M., and Delcan, J. L. (1992) Left atrial appendage Doppler flow patterns: implications on thrombus formation. *Am. Heart J.*,**124**, 955.

Garvan, J. M. and Gunner, B. W. (1964) The harmful effects of particles in intravenous solutions. *Med. J. Aust.*,**2**, 1.

Georgiadis, D., Grosset, D. G., and Lees, K. R. (1993) Transhemispheric passage of microemboli in patients with unilateral internal carotid artery occlusion. *Stroke*,**24**, 1664-1666.

Gibo, H., Carver, C. C., Rhoton, A. L., Lenkey, C., and Nitchell, R. J. (1981) Microsurgical anatomy of the middle cerebral artery. *J. Neurosurg.*,**54**, 151-169.

Giddens, D. P. and Khalifa, A. M. A. (1982) Turbulence measurements with pulsed Doppler ultrasound employing a frequency tracking method. *Ultrasound in Med. & Biol.*,**8**, 427-437.

Giddens, D. P., Mabon, R. F., and Cassanova, R. A. (1976) Measurements of disordered flows distal to subtotal vascular stenoses in the thoracic aortas of dogs. *Circulation Res.*,**39**, 112-119.

Giller, C. A., Bowman, G., Dyer, H., Mootz, L., Krippner, W., Loftus, C. M., and Muizelaar, J. P. (1993) Cerebral arterial diameters during changes in blood pressure and carbon dioxide during craniotomy. *Neurosurgery*,**32**, 737-742.

Giller, C. A. and et al. (1990) Diameter changes in cerebral arteries during craniotomy. *J. Cardiovasc. Technol.*,**9**, 301.

Gillis, M. F., Karagianes, M. T., Peterson, P. L. (1968) Bends: Detection of circulating gas emboli with external sensor. *Science.*,**161**, 579.

Gilston, A. (1986) Brain damage after cardiac surgery. *Lancet*,**1**, 1323.

Glagov, S., Weisenberg, E., Zarins, C. K., Stankunavicius, R., and Kolettis, G. J. (1987) Compensatory enlargement of human atherosclerotic coronary arteries. *N. Engl. J. Med.*,**316**, 1373-1375.

Goldberg, S. J., Kececioglu-Draeos, Z., Sahn, D. J., Valdes-Cruz, L. M., and Allen, H. D. (1982) Range gated echo-Doppler velocity and turbulence mapping in patients with valvular aortic stenosis. *Am. Heart J.*,**103**, 858-863.

Grosset, D. G., Georgiadis, D., Abdullah, I., Bone, I., and Lees, K. R. (1994) Doppler emboli signals vary according to stroke subtype. *Stroke*,**25**, 382-384.

Grosset, D. G., Georgiadis, D., Kelman, A. W., and Lees, K. R. (1993b) Quantification of ultrasound emboli signals in patients with cardiac and carotid disease. *Stroke*,**24**, 1922-1924.

Grosset, D. G., Straiton, J., Du Trevou, M., and Bullock, R. (1992) Prediction of symptomatic vasospasm after subarachnoid hemorrhage by rapidly increasing transcranial Doppler velocity and cerebral blood flow changes. *Stroke*,**23**, 674-679.

J. Neurosurg., **68**, 745-751.

Grosset, D. G., Straiton, J., McDonald, I., and Bullock, R. (1993a) Angiographic and Doppler diagnosis of cerebral artery vasospasm following subarachnoid haemorrhage. *Brit. J. of Neurosurg.*,**7**, 291-298.

Angiography on the management of patients admitted with focal cerebral ischemia. Circulation,**84** (Suppl. II), II-693.

Grossman, W. (1986). *Cardiac catheterization and angiography*, 3rd edition. Lea and Febiger, Philadelphia.

D. W., Rolly, P. L., and Gorman, D. F. (1990) The effect of gas emboli on rabbit cerebral blood flow. *Stroke*,**21**, 94-99.

Grulke, D. C., Marsh, N. A., and Hills, B. A. (1973) Experimental air embolism: measurement of microbubbles using the Coulter counter. *Brit. J. Exp. Path.*,**54**, 684-691.

air emboli syndrome. Bowel infarction after retrograde angiography. Arch. Intern. Med., **149**, 2371-2374.

Gurd, A. R. (1970) Fat embolism: An aid to diagnosis. *J. Bone. Joint. Surg.*,**52B**, 732-736.

L., Hjeltnes, E., and Lindeburgh, T. (1983) Brain hyperperfusion during cardiac operations (Cerebral blood flow measured in man by intra-arterial injection of

Halliday, P., Anderson, D. N., Davidson, A. I., and Page, J. G. (1994) Management of cerebral air embolism secondary to a disconnected central venous catheter. *Bri. J. of Surg.*,**81**, 71.

Hamdon, J. H., Hechtol, C. O., Dallas, P., and Crickenberger, D. P. (1973) Use of

Hankey, G. J., Warlow, C. P., and Sellar, R. J. (1990) Cerebral angiographic risk in mild cerebrovascular disease. *Stroke*,**21**, 209-222.

Harders, A. G. and Gilsbach, J. M. (1987) Time course of blood velocity changes related to vasospasm in the circle of Willis measured by transcranial Doppler ultrasound. *J. of Neurosurgery*,**66**, 718-728.

Ireland, M. A., Davis, M. J., Hockings, B. E., and Gibbons, P. (1959) Safety and

Harrison, M. J. G., Pugsley, W., Newman, S., Paschalis, C., Klinger, L., Treasure, T., and Aspey, B. (1990) Detection of middle cerebral emboli during coronary artery bypass surgery using transcranial Doppler sonography. *Stroke*,**21**, 1512.

Johanson, W. E., Stump, D. A., DeWitt, D. S., Vinten-Johansen, J., O'Steen, W. K., Hassler, W., Steinmetz, H., and Gawlowski, J. (1988) Transcranial Doppler ultraonography in raised intracranial pressure and in intracranial circulatory arrest. *J. Neurosurg.*, **68**, 745-751.

Jolly, N., Mohan, J. C., and Arora, R. (1993) Transesophageal Doppler pulmonary
Hata, J. S., Biller, J., Stuhlmuller, J. E., Kerber, R. E., and Vandenberg, B. F. (1991) Impact of transesophageal echocardiography on the management of patients admitted with focal cerebral ischemia. *Circulation*, **84 (Suppl. II)**, II-693.

Kalendovsky, Z., Austin, J., and Steel, P. (1975) Increased platelet aggregability in
Helps, S. C., Parsons, D. W., Reilly, P. L., and Gorman, D. F. (1990) The effect of gas emboli on rabbit cerebral blood flow. *Stroke*, **21**, 94-99.

Kaluzynski, K. and Tedgui, A. (1989) Asymmetry of Doppler spectrum in stenosis
Hendel, R. C., Cuenoud, H. F., Giansiracusa, D. F., and Alpert, J. S. (1989) Multiple cholesterol emboli syndrome. Bowel infarction after retrograde angiography. *Arch. Intern. Med.*, **149**, 2371-2374.

Kaluzynski, K. and Tedgui, A. (1989) Prevalence of ultra stokes in patients
Henriksen, L., Hjelms, E., and Lindeburgh, T. (1983) Brain hyperperfusion during cardiac operations (Cerebral blood flow measured in man by intra-arterial injection of xenon 133: Evidence suggestive of intraoperative microembolism). *J. Thorac. Cardiovasc. Surg.*, **86**, 202-208.

Kaluzynski, K. and Tedgui, A. (1989) Prevalence of ultra stokes in patients
Herndon, J. H., Bechtol, C. O., Dallas, P., and Crickenberger, D. P. (1975) Use of ultrasound to detect fat emboli during total hip replacement. *Acta Orthop Scand.*, **46**, 108-118.

G. R., Schwartz, W. J., and Recht, L. D. (1992) The preponderance of posterior circulatory events is independent of the route of cardiac catheterization.
Hess, D. C., Krauss, J. S., and Rardin, D. (1991) Stroke in a young adult with fletcher trait. *Southern Medical Journal*, **84**, 507-508.

Keller, M. W. and Feinstein, S. B. (1986) Automated production and analysis of
Ireland, M. A., Davis, M. J., Hockings, B. E., and Gibbons, F. (1989) Safety and convenience of a mechanical injector pump for coronary angiography. *Cathet. Cardiovasc. Diagn.*, **16**, 199-201.

Johnston, W. E., Stump, D. A., DeWitt, D. S., VintenJohansen, J., OSteen, W. K., James, R. L., and Prough, D. S. (1993) Significance of gaseous microemboli in the cerebral circulation during cardiopulmonary bypass in dogs. *Circulation*,**88**, 319-329.

Jolly, N., Mohan, J. C., and Arora, R. (1992) Transoesophageal Doppler pulmonary venous flow pattern and left atrial spontaneous contrast in mitral stenosis. *Int. J. Cardiol.*,**36**, 357-360.

Kalendovsky, Z., Austin, J., and Steel, P. (1975) Increased platelet aggregability in young patients with strokes. *Arch. Neurol.*,**32**, 12-20.

Kaluzynski, K. and Tedgui, A. (1989) Asymmetry of Doppler spectrum in stenosis differentiation. *Med. Biol. Eng. Comput.*,**27**, 456-462.

Kase, C. S., Wolf, P. A., Chodosh, E. H., Zacher, B., KellyHayes, M., Kannel, W. B., Dagostino, R. B., and Scampini, L. (1989) Prevalence of silent stroke in patients presenting with initial stroke. The Framingham Study. *Stroke*,**20**, 850-852.

Katz, E. S., Tunick, P. A., Rusinek, H., Ribakove, G., Spencer, F. C., and Kronzon, I. (1992) Protruding aortic atheromas predict stroke in elderly patients undergoing cardiopulmonary bypass: Experience with intraoperative transesophageal echocardiography. *J. Am. Coll. Cardiol.*,**20**, 70-77.

Keilson, G. R., Schwartz, W. J., and Recht, L. D. (1992) The preponderance of posterior circulatory events is independent of the route of cardiac catheterization. *Stroke*,**23**, 1358-1359.

Keller, M. W. and Feinstein, S. B. (1986) Automated production and analysis of surfactant stabilized echo contrast agents for use in clinical imaging. *J. Ultrasound Med.*,**4**, 493-498.

Keller, M. W., Feinstein, S. B., and Watson, D. D. (1987) Successful left ventricular opacification following peripheral venous injection of sonicated contrast agent: an experimental evaluation. *Am. Heart J.*, **114**, 570-575.

Keller, M. W., Glasheen, W., Teja, K., Gear, A., and Kaul, S. (1988) Myocardial contrast echocardiography without significant hemodynamic effects or reactive hyperemia: a major advantage in the imaging of regional myocardial perfusion. *J. A. C. C.*, **12**, 1039-1047.

Kelly, G. L., Dodi, G., and Eiseman, B. (1972) Ultrasound detection of fat emboli. *Orthopedic Surg.*, **23**, 459-461.

Kelly, G. L., Dodi, G., and Eiseman, B. (1977) Ultrasound detection of fat emboli. *Surgical Forum*, **23**, 459-461.

Kempster, P. A., Gerraty, R. P., and Gates, P. C. (1988) Asymptomatic cerebral infarction in patients with chronic atrial fibrillation. *Stroke*, **19**, 955-957.

Kessler, C., Kelly, A. B., Suggs, W. D., and Harker, L. A. (1992) Production of transient ischaemic events by platelet emboli in baboons. *Neurol. Res.*, **14(suppl.)**, 187-189.

Kessler, J. and Patterson, R. H. (1970) The production of microemboli by various blood oxygenators. *Ann. Thorac. Surg.*, **9**, 221.

Kilkes, M. G., Dunwoody, G., Bull, T. M., Eppel, B., and Barrett, N. J. (1991) A case of intracerebral air embolism secondary to the insertion of a hickman line. *J. Parent. Enter. Nutri.*, **15**, 488-490.

Kistler, J. P., Ropper, A. H., and Martin, J. B. (1988). *Harrison's Principles of Internal Medicine*, 11th edition. McGraw-Hill Book Co., New York. 261, 281-286.

Koike, T., Minakawa, T., Abe, H., Takeuchi, S., Sasaki, O., Nishimaki, K., and Tanaka, R. (1992) PTA of supra-aortic arteries with temporary balloon occlusion to avoid distal embolism. *Neurol. Med. Chir. Tokyo*,**32**, 140-147.

Kumar, P. J., Clark, M. L., and Jackson, W. F. (1990). *Clinical Medicine: a textbook for medical students and doctors*, 2nd edition. Bailliere Tindall, London.

Lang, E. K. (1963) A survey of the complications of percutaneous retrograde arteriography: Seldinger technique. *Radiology*,**81**, 257-263.

Laub, D. R. Jr. and Laub, D.R. (1990) Fat embolism syndrome after liposuction: a case report and review of the literature. *Ann. Plast. Surg.*,**25**, 48-52.

Leahy, A. L., McCollum, P. T., Feeley, T. M., Sugrue, M., Grouden, M. C., O'Connell, D. J., Moore, D. J., and Shanik, G. D. (1988) Duplex ultrasonography and selection for carotid endarterectomy: plaque morphology or luminal narrowing? *J. of Vasc. Surg.*,**8**, 558-562.

Lechat, P. H., Nas, J. L., Lascault, G., Loron, P. H., Theard, M., Klimczac, M., Drobinski, G., Thomas, D., and Grosgeat, Y. (1988) Prevalence of patients foramen ovale in patients with stroke. *N. Engl. J. Med.*,**318**, 1148-1152.

Lequire, V. S., Shapiro, J. L., Lequire, C. B., Cobb, C. A., and Fleet, W. F. (1959) A study of the pathogenesis of embolism based on human necropsy material and animal experiments. *J. Bone & Joint Surg.*,**35**, 999-1009.

Levorstad, K., Vatne, K., Brodahl, U., Laake, B., Simonsen, S., and Aakhus, T. (1989) Safety of the nonionic contrast medium omnipaque in coronary angiography. *Cardiovasc. Intervent. Radiol.*,**12**, 98-100.

Levy, D. (1990) The fat embolism syndrome. A review. *Clin. Orthop.*,**261**, 281-286.

Lisovoski, F. and Rousseaux, P. (1991) Cerebral infarction in young people. A study of 148 patients with early cerebral angiography. *J. Neuro. Neurosurg. Psych.*,**54**, 576-579.

Lockwood, K., Capraro, J., Hanson, M., Conomy, J., and Oh, C. (1983) Neurologic complications of cardiac catheterization (abstract). *Neurology*,**33(suppl.2)**, 147.

Lord Rayleigh(Stutt, F. W.)(1945). *The Theory of Sound*, Dover, U.S.A..

Lundar, T., Lindgaard, K-F., Froysaker, T., and et al., (1985) Cerebral perfusion during nonpulsatile cardiopulmonary bypass. *Ann. Thorac. Surg.*,**40**, 144-150.

Mahony, C., Ayappa, I. A., Ferguson, J., Brown, L. V., and Lai-Fook, S. J. (1991) Spontaneous contrast (SC) in the rabbit. *Circulation*,**84 (Suppl. II)**, II-692.

Marcus, R. H., Weinert, L., Neumann, A., Borow, K. M., and Lang, R. M. (1991) Venous air embolism. Diagnosis by spontaneous right-sided contrast echocardiography. *Chest*,**99**, 784-785.

Markus, H. (1993d) Transcranial Doppler detection of circulating cerebral emboli: A review. *Stroke*,**24**, 1246-1250.

Markus, H., Loh, A., and Brown, M. M. (1993c) Computerized detection of cerebral emboli and discrimination from artifact using Doppler ultrasound. *Stroke*,**24**, 1667-1672.

Markus, H., Loh, A., Israel, D., Buckenham, T., Clifton, A., and Brown, M. M. (1993a) Microscopic air embolism during cerebral angiography and strategies for its avoidance. *Lancet*,**341**, 784-787.

Markus, H. S. and Brown, M. M. (1993b) Differentiation between different pathological cerebral embolic materials using transcranial Doppler in an in vitro model. *Stroke*,**24**, 1-5.

Maroon, J. C., Edmonds-Seal, J., and Campell, R. L. (1969) An ultrasonic method for detecting air embolism. *Neurosurg.*,**31**, 196-201.

Marshall, W. G. Jr., Barzilai, B., Kouchoukos, N. T., and Saffitz, J. (1989) Intraoperative ultrasonic imaging of the ascending aorta. *Ann. of Thorac. Surg.*,**48**, 339-344.

Meltzer, R. S., Tickner, E. G., Sahines, T. P., and Popp, R. L. (1980) The source of ultrasound contrast effect. *J. of Clin. Ultrasound*,**8**, 121.

Merino, A., Hauptman, P., Badimon, L., Badimon, J. J., Cohen, M., Fuster, V., and Goldman, M. (1992) Echocardiographic 'smoke' is produced by an interaction of erythrocytes and plasma proteins modulated by shear forces. *J. Am. Coll. Cardiol.*,**20**, 1661-1668.

Merino, A., Hauptman, P. J., Badimon, L., Badimon, J. J., and Goldman, M. E. (1991) Echogenic smoke is shear rate dependent. *Circulation*,**84** (Suppl. II), II-692.

Mikell, F. L., Asinger, R. W., Elsperger, K. J., Aderson, W. R., and Hodges, M. (1982) Regional stasis of blood in the dysfunctional left ventricle: Echocardiographic detection and differentiation from early thrombosis. *Circulation*,**66**, 755-763.

Millikan, C. H., McDowell, F., and Easton, J. D. (1987). *Stroke*, Philadelphia.

Mitzel, H., Albin, M. S., and Cosstellio, R. (1991) Neuropsychological change and statistical artifact. *J. Neurosurg. Anesth.*,**3**, 241.

Mo, L. Y. L. and Cobbold, R. S. C. (1992) A unified approach to modeling the backscattered Doppler ultrasound from blood. *IEEE Trans. Biomed. Eng.*,**39**, 450-461.

Mohr, J. P., Caplan, L. R., Melski, J. W., Goldstein, R. J., Duncan, G. W., Kistler, J. P., Pessin, M. S., and Bleich, H. L. (1978) The Harvard Cooperative Stroke Registry: a prospective registry. *Neurology*,**28**, 745-762.

Moody, D. M., Bell, M. A., Challa, V. R., Johnston, W. E., and Prough, D. S. (1990) Brain microemboli during cardiac surgery or aortography. *Ann. Neurol.*,**28**, 477-486.

Morin, J. F., Johnston, K. W., and Law, Y. F. (1988) Factors affecting the continuous wave Doppler spectrum for the diagnosis of carotid arterial disease. *Ultrasound in Med. & Biol.*,**14**, 175-189.

Mortensen, J. D. (1978) Safety and efficacy of blood oxygenators: a review. *Med. Instrum.*,**12**, 128-134.

Mortensen, J. D., Yates, W. G., Schoenberg, A. A. (1981) Final Report: Cardiopulmonary bypass systems: A study of safety and performance. *TR5534-010. Utah Biomedical Test Laboratory/FDA Contrast 223-80-5081*,105-347.

Moylan, J. A., Birnbaum, M., Katz, A., and Everson, M. A. (1976) Fat emboli syndrome. *J. Trauma.*,**16**, 341-347.

Muge, A., Daniel, W. G., Hausmann, D., Godke, J., Wagenbreth, I., and Lichtlen, P. R. (1990) Diagnosis of left atrial appendage thrombi by transesophageal echocardiography: clinical implications and follow-up. *Am. J. Cardiac. Imaging*,**4**, 173-179.

Muller, C., Rahn, B. A., and Pfister, U. (1992) Fat embolism and fracture, a review of the literature. *Aktuelle Traumatologie*,**22**, 104-113.

Padayachee, T. S., Gosling, R. G., Bishop, C. C., Burnand, K., Brown, N. L. (1986)

Muller, H. R., Lampl, Y., and Haefele, M. (1991) A TCD test for clinical assessment of cerebral autoregulation. *Ultraschall in der Medizin*,**12**, 218-221.

Plum, F.

Murie, J. A., Sheldon, C. D., and Quin, R. Q. (1984) Carotid artery bruit: association with internal carotid stenosis and intraluminal turbulence. *Br. J. Surg.*,**71**, 50-52.

ultrasound. *Perfusion*,**2**, 213.

Naylor, A. R., Wildsmith, J.A.W., McClure, J., Jenkins, A. M. L., and Ruckley, C. V. (1991) Transcranial Doppler monitoring during carotid endarterectomy. *Br. J. Surg.*,**78**, 1264-1268.

Effect of arterial filtration on reduction of gaseous microemboli in the middle cerebral artery during cardiopulmonary bypass. *Annals of Thoracic*

Nishi, R. Y. (1972) Ultrasonic detection of bubbles with Doppler flow transducers. *Ultrasonics*,**10**, 173-179.

Padayachee, T. S., Parsons, S., Theobald, P., Janley, J., Gosling, R. G., and Devereux,

Nishide, M., Irino, T., Gotoh, M., Naka, M., and Tsuji, K. (1983) Cardiac abnormalities in ischaemic cerebrovascular disease studied by two-dimensional echocardiography. *Stroke*,**14**, 541-545.

Njemanze, P. C. (1991) Transcranial Doppler evaluation of syncope: An application in aerospace physiology. *Aviation Space and Environmental Medicine*,**62**, 569-572.

Ojha, M. and Langille, B. L. (1993) Evidence that turbulence is not the cause of poststenotic dilatation in rabbit carotid arteries. *Arteriosclerosis and Thrombosis*,**13**, 977-984.

Pearson, D. T., Poelad, S. J., Murray, A., and Clayton, R. (1987) Extracorporeal

Ophir, J. and Parker, K. (1989) Contrast agent in diagnostic ultrasound. *Ultrasound in Med. & Biol.*,**4**, 319-333.

Petersen, P., Madsen, B. B., Brun, B., and Pedersen, P. (1987) Silent cerebral

Ordway, C. B. (1974) Air embolus via CVP catheter without positive pressure: Presentation of case and review. *Ann. Surg.*,**176**, 479-481.

Petty, G. W., Massaro, A. R., Tatemichi, T. K., Mohr, J. P., Hilal, S. K., Stein, B.

M., Solomon, R. A., Duterte, D. I., and Sacco, R. L. (1990) Transcranial Doppler

Padayachee, T. S., Gosling, R. G., Bishop, C. C., Burnand, K., Browse, N. L. (1986) Monitoring MCA blood velocity during carotid endarterectomy. *Br. J. Surg.*,**73**, 98-100.

Philp, R. B., Inwood, M.J., and Warren, B. A. (1972) Interaction between gas bubbles
Padayachee, T. S., Parsons, S., Theobald, R., and et al., (1987) Computerised techniques for detecting gaseous microemboli in blood using pulsed Doppler ultrasound. *Perfusion*,**2**, 213.

Pizzolitto, S., Rocco, M., Antonucci, F., and Antoci, B. (1991) Atheroembolism: a
Padayachee, T. S., Parsons, S., Theobald, R., Gosling, R. G., and Deverall, P. B. (1988) The effect of arterial filtration on reduction of gaseous microemboli in the middle cerebral artery during cardiopulmonary bypass. *Annals of Thoracic Surgery*,**45**, 647-649.

Padayachee, T. S., Parsons, S., Theobald, R., Linley, J., Gosling, R. G., and Deverall, P. B. (1987) The detection of microemboli in the middle cerebral artery during cardiopulmonary bypass: A transcranial Doppler ultrasound investigation using membrane and bubble oxygenators. *Ann. of Thorac. Surg.*,**44**, 298-302.

Powis, F. L. and Powis, W. J. (1984) *A clinician's guide to ultrasonic imaging*, Urban
Parkes, D. (1987). *Treatment in Clinic Medicine: Neurological Disorders*, Springer-Verlag, Berlin, Germany.

Prender, J. L. (1978) Transient cortical blindness following vertebral angiography
Pearson, D. T., Carter, R. F., and Hammo, M. B. (1981). *Techniques in Extracorporeal Circulation*, Butterworths, London, 1st edition, 25-50.

Provinciali, L., Minciotti, P., Cravolo, M. G., Chiaramoni, L., Maricotti, M., Mastro
Pearson, D. T., Poslad, S. J., Murray, A., and Clayton, R. (1987) Extracorporeal circulation material evaluation: microemboli. *Life. Support. Syst.*,**5**, 53-67.

Petersen, P., Madsen, E. B., Brun, B., and Pedersen, F. (1987) Silent cerebral infarction in chronic atrial fibrillation. *Stroke*,**18**, 1098-1100.

Eur. Neurol.,**30**, 98-103.
Petty, G. W., Massaro, A. R., Tatemichi, T. K., Mohr, J. P., Hilal, S. K., Stein, B. M., Solomon, R. A., Duterte, D. I., and Sacco, R. L. (1990) Transcranial Doppler

ultrasonographic changes after treatment for arteriovenous malformations. *Stroke*,**21**, 260-266.

Philp, R. B., Inwood, M.J., and Warren, B. A. (1972) Interaction between gas bubbles and components of the blood: implications in decompression sickness. *aerospace Med.*,**43**, 946-953.

Pizzolitto, S., Rocco, M., Antonucci, F., and Antoci, B. (1991) Atheroembolism: a form of systemic vascular disease. *Pathologica*,**83**, 147-158.

Ploner, F., Saltuari, L., Marosi, M. J., Dolif, R., and Salsa, A. (1991) Cerebral air emboli with use of central venous catheter in mobile patient. *Lancet*,**338**, 1331.

Pollick, C. and Taylor, D. (1991) Assessment of left atrial appendage function by transesophageal echocardiography: Implications for the development of thrombus. *Circulation*,**84**, 223-230.

Powis, R. L. and Powis, W. J. (1984). *A thinker's guide to ultrasonic imaging*, Urban & Schwarzenberg, Baltimore, U.S.A., 1st edition, 9-14.

Prendes, J. L. (1978) Transient cortical blindness following vertebral angiography. *Headache*,**18**, 222-224.

Provinciali, L., Minciotti, P., Ceravolo, M. G., Chiaramoni, L., Maricotti, M., Mauro, A., and Salvolini, U. (1992) Haemodynamic changes following carotid occlusion: MRI angiography and transcranial Doppler patterns. *Neurol. Res.*,**14**, 208-210.

Provinciali, L., Minciotti, P., Geravolo, G., Angeleri, F., and Sanguinetti, C. M. (1990) Transcranial Doppler sonography as a diagnostic tool in vascular dementia. *Eur. Neurol.*,**30**, 98-103.

Pugsley, W. (1989) The use of Doppler ultrasound in the assessment of microemboli during cardiac surgery. *Perfusion*,**4**, 115-122.

Pugsley, W., Klinger, L., Paschalis, C., Aspey, B., Newman, S., Harrison, M., and Treasure, T. (1990) Microemboli and cerebral impairment during cardiac surgery. *Vasc. Surg.*,**24**, 34-43.

Ramirez, G., O'Neill, W. M., Lambert, R., and Bloomer, A. (1978) Cholesterol embolization: a complication of angiography. *Arch. Intern. Med.*,**138**, 1430-1432.

Ranval, T. J., Solis, M. M., Barnes, R. W., Vitti, M. J., Gange, P. J., Eidt, J. F., Barone, G. W., Harshfield, D. L., Schaefer, R. F., and Read, R. C. (1994) Isolated symptomatic midcervical stenosis of the internal carotid artery. *Am. J. Surg.*,**168**, 171-174.

Ratcliffe, P. J. and Wilcock, G. K. (1985) Cerebrovascular disease in dementia: the importance of atrial fibrillation. *Postgrad. Med. J.*,**61**, 201-204.

Richardson, P. D. (1985) Qualitative and quantitative methods for investigation gas emboli in blood. *Med. Instrum.*,**2**, 55-56.

Ries, F., Kaal, K., Schultheiss, R., Solymosi, L., and Schilef, R. (1991) Air microbubbles as a contrast medium in transcranial Doppler sonography. *J. Neuroimag.*,**1**, 173-178.

Ries, F., Schultheiss, R., Eichelkraut, W., Junker, W., Solymosi, L., and Kaal, K. (1988) Air microbubbles as a simple enhancing agent for transcranial Doppler examination. *J. Cardiovasc. Ultrasonogr.*,**7**, 82 (abstract).

Ringelstein, E. B., Richert, F., Bardos, S., and et al., (1985) Transkraniell-sonographisches Monitoring des Blutflusses der A. cerebri media wahrend

rehanalisierender Operationen an der extrakraniellen A. carotis interna. *Nervenarzt*,**56**, 423-430.

Rizzo, S., Cardia, G., Fullone, M., and Regina, G. (1993) Noninvasive preoperative evaluation of carotid atheroma: Echo-color-Doppler versus duplex scanning. *Vasc. Surg.*,**27**, 357-362.

Rohmann, S., Erbel, R., Darius, H., Makowski, T., Jensen, P., Fisher, T., and Meyer, J. (1992) Spontaneous echo contrast imaging in infective endocarditis: a predictor of complication. *Int. J. of Cardiac Imaging*,**8**, 197-207.

Rosenkranz, K., Langer, R., Cordes, M., and Felix, R. (1992) Transcranial Doppler ultrasound in internal carotid artery and middle cerebral artery disease. *Neurosurgical Review*,**15**, 37-44.

Rovai, D., Nissen, S., Elion, J., Smith, M., L'Abbate, A., and Kwan, O. L. (1987) Contrast echo washout curves from the left ventricle: Application of basic principles of indicator-dilution theory and calculation of ejection fraction. *J. Am. Coll. Cardiol.*,**10**, 125-134.

Russell, D. (1992). The detection of cerebral emboli using Doppler ultrasound. *Transcranial Doppler*, Raven Press Ltd., New York, U.S.A., 1st edition, 207-230.

Russell, D., Madden, K. P., Clark, W. M., Sandset, P. M., and Zivin, J. A. (1991) Detection of arterial emboli using Doppler ultrasound in rabbits. *Stroke*,**22**, 253-258.

Sadler, D., Brown, J., Islam, M., Patel, P., and Prothro, D. (1991) Left atrial thrombi in no-rheumatic atrial fibrillation: assessment of prevalence by transesophageal echocardiography. *Circulation*,**84 (Suppl. II)**, II-693.

Saito, T., Terada, Y., Suma, H., Takayama, T., Fukuda, S., Wanibuchi, Y., and Furuta, S. (1992) The calcified ascending aorta-preoperative evaluation and intraoperative management. *Nippon. Kyobu. Geka. Gakkai. Zasshi.*,**40**, 1189-1194.

Event rates before and after carotid endarterectomy. *Brain*,**116**, 1005-1015.

Sarrat, S. and Nezelof, C. (1960) A complication of intravenous therapy: giant cellular macrophatic pulmonary arteries. *Presse. Med.*,**68**, 357.

transcranial emboli in patients with symptomatic atherosclerotic carotid artery disease. *Stroke*,**23**, 1652-1654.

Saunders, F. W. and Cledgett, P. (1988) Intracranial blood velocity in head injury. A transcranial ultrasound Doppler study. *Surg. Neurol.*,**29**, 401-409.

J. J. Kasprzak, D. G., Nyhus, L. M., and Capeo, V. (1981) Ultrasonography of blood during stasis and

Schwarz, K. Q., Bezante, G. P., Chen, X., and Schlieff, R. (1993) Quantitative echo contrast concentration measurement by Doppler sonography. *Ultrasound in Med. & Biol.*,**19**, 289-297.

Gaire, C., Lichti, E., Helvey, W. and Almond, C. (1972) A comparison of the microparticles produced when two disposable-bag oxygenators

Sevitt, S. (1977) The significance and pathology of fat embolism. *Ann. Clin. Res.*,**9**, 173-180.

Shaw, P. J., Bates, D., and Cartlidge, N. E. F. (1986) Early intellectual dysfunction following coronary bypass surgery. *Q. J. Med.*,**58**, 59-68.

high-grade internal carotid stenosis with color Doppler-assisted duplex imaging. *Stroke*,**25**, 385-389.

Shaw, P. J., Bates, D., Cartlidge, N. E. F., French, J. M., Heaviside, D., Jalian, D. G., and Shaw, D. A. (1987) Neurologic and neuropsychological morbidity following major surgery: comparison of coronary artery bypass and peripheral vascular surgery. *Stroke*,**18**, 700-707.

graphy in the diagnosis of vasospasm following subarachnoid hemorrhage. *Neurology*,**39**, 1514-1518.

Shimon, A. R., Ling, S. O., Gerson, S. L., Reiser, S. A., Ong, L. S., Lichtenberg, G. S., Amico, A. S., Shapiro, J. R., Allen, M. N., and Meltzer, R. S. (1989) Myocardial perfusion imaging by contrast echocardiography with use of intracoronary sonicated albumin in humans. *J. A. C. C.*,**14**, 660-665.

Shung, K. K., Yuan, Y. W., and Fei, D. Y. (1984) Effect of flow disturbance on ultrasonic backscatter from blood. *J. Acoust. Soc. Am.*,**75**, 1265-1272.

Siebler, M., Sitzer, M., Rose, G., Bendfeldt, D., and Steinmetz, H. (1993) Silent cerebral embolism caused by neurologically symptomatic high-grade carotid stenosis. Event rates before and after carotid endarterectomy. *Brain*, **116**, 1005-1015.

Siebler, M., Sitzer, M., and Steinmetz, H. (1992) Detection of intracranial emboli in patients with symptomatic extracranial carotid artery disease. *Stroke*, **23**, 1652-1654.

Sigel, B., Coelho, J. C. U., Spigos, D. G., Flanigan, D. P., Schuler, J. J., Kasprisin, D. O., Nyhus, L. M., and Capek, V. (1981) Ultrasonography of blood during stasis and coagulation. *Invest. Radiol.*, **16**, 71.

Simmons, E., MaGuire, C., Lichti, E., Helvey, W., and Almond, C. (1972) A comparison of the microparticles produced when two disposable-bag oxygenators and a disc oxygenator are used for cardiopulmonary bypass. *J. Thorac. Cardiovasc. Surg.*, **63**, 613-721.

Sitzer, M., Furst, G., Siebler, M., and Steinmetz, H. (1994) Usefulness of an intravenous contrast medium in the characterization of high-grade internal carotid stenosis with color Doppler-assisted duplex imaging. *Stroke*, **25**, 385-389.

Sloan, M. A., Haley, E. C., Jr., Kassel, N. F., Henry, M. L., Stewart, S. R., Beskin, R. R., Sevilla, E. A., and Torner, J. C. (1989) Sensitivity and specificity of transcranial Doppler ultrasonography in the diagnosis of vasospasm following subarachnoid hemorrhage. *Neurology*, **39**, 1514-1518.

Sloan, M. A., Mueller, J. D., Adelman, L. S., and Caplan, L. R. (1991) Fatal brainstem stroke following internal jugular vein catheterization. *Neurology*, **41**, 1092-1095.

Smith, P. L. (1988) The cerebral complication of coronary artery bypass surgery. *Ann. R. Coll. Surg. Engl.*, **70**, 212-216.

Spencer, M. P., Lawrence, G. H., Thomas, G. I., and Sauvage, L. R. (1965) The use of extracorporeal bypass. *Ann. N.Y. Acad. Sci.*, **129**, 1-12.

Smith, P. L. C., Treasure, T., Newman, S. P., Joseph, P., Ell, P. J., Schneidan, A., and Harrison, M. J. G. (1986) Cerebral consequences of cardiopulmonary bypass. *Lancet*, **1**, 823-825.

Spencer, M. P. and Reid, J. M. (1979) Quantitation of carotid stenosis with Doppler ultrasonography. *Stroke*, **10**, 103-107.

Sorteberg, W., Lindegaard, K-F., Rootwelt, K., Dahl, A., NybergHansen, R., Russell, D., and Nornes, H. (1989) Effect of acetazolamide on cerebral artery blood velocity and regional cerebral blood flow in normal subjects. *Acta. Neurochir.*, **97**, 139-145.

Spencer, M. P. (1976) Decompression limits for compressed air determined by ultrasonically detected blood bubbles. *J. Appl. Physiol.*, **40**, 229-235.

Spencer, M. P. (1977) The use of Doppler ultrasonography in the diagnosis of cerebral artery stenosis. *Stroke*, **8**, 103-107.

Spencer, M. P. (1992). *Transcranial Doppler*, Raven Press, New York, 1st edition, 215-230.

Spencer, M. P. and Campbell, S. D. (1968) Development of bubbles in venous and arterial blood during hyperbaric decompression. *Bull. Mason. Clin.*, **22**, 26-32.

Spencer, M. P. and Campbell, S. D. (1972a) Decompression venous gas emboli. *Proceedings of the 5th Symposium on Underwater Physiology. August 21-25.*, **47**.

Spencer, M. P. and Campbell, S. D. (1994) Bubbles in the blood during hyperbaric decompression. *Proc. Int. Union. Physiol. Sci.*, Raven Press, Ltd., New York, U.S.A., 1st edition, 197-205.

Spencer, M. P., Campbell, S. D., Sealey, J. L., Henry, F. C., and Lindbergh, J. (1969a) Experiments on decompression bubbles in the circulation using ultrasonic and electromagnetic flowmeters. *J Occup Med.*, **11**, 238-244.

Spencer, M. P., Campbell, S. D., Sealey, J. L., Henry, F. C., and Lindbergh, J. (1969b) The effect of decompression on the circulation of gas emboli. *J. Appl. Physiol.*, **27**, 275-281.

Spencer, M. P. and Clarke, H. F. (1972b) Precordial monitoring of pulmonary gas embolism and decompression bubbles. *Aerospace Med.*, **43**, 762-767.

Spencer, M. P. and Reid, J. M. (1979) Quantitation of carotid stenosis with Doppler ultrasonography. *Stroke*, **10**, 103-107.

Spencer, M. P., Lawrence, G. H., Thomas, G. I., and Sauvage, L. R. (1969b) The use of ultrasonics in the determination of arterial atheroembolism during open heart surgery. *Ann. Thorac. Surg.*,**8**, 489-497.

Neurology,**42**, 131-134

Spencer, M. P. and Reid, J. M. (1979) Quantitation of carotid stenosis with continuous-wave (C-W) Doppler ultrasound. *Stroke*,**10**, 326-330.

Farina, C., and Hunter, W. J. (1988) Ultrasonographic features of carotid plaque and

Spencer, M. P., Reid, J. M., Hileman, R., and Cairo, J. (1980) On line dual-directional spectral display in Doppler diagnosis of stenotic and nonstenotic plaques. *Proceedings of the 25th Annual Meeting of the American Institute of Ultrasound in Medicine*. New Orleans. September 15-19.,**704**,

J. Neuroimaging,**3**, 18-22

Spencer, M. P., Thomas, G. I., Nicholls, S. C., and Sauvage, L. R. (1990) Detection of middle cerebral emboli during carotid endarterectomy using transcranial Doppler ultrasonography. *Stroke*,**21**, 415-423.

Spencer, M. P. and Whisler, D. (1986) Transorbital Doppler diagnosis of intracranial arterial stenosis. *Stroke*,**17**, 916-921.

728

Stehbens, W. E. (1972). *Pathology of cerebral blood flow vessels*, Mosby, St. Louis, U.S.A., 1st edition. 131-206.

Tex. Heart Inst. J.,**13**, 91-96

Steiger, H. J. (1992). *Transcranial Doppler*, Raven Press, Ltd., New York, U.S.A., 1st edition, 197-206.

Sharma, M. K. (1991) Detection of paradoxical cerebral echo

Stein, P. D., Walburn, F. J., and Blick, E. F. (1980) Damping effect of distensible tubes on turbulent flow: Implications in the cardiovascular system. *Biorheology*,**17**, 275-281.

graphy, Transcranial Doppler ultrasonography, Mosby, St. Louis 5-27

Steinke, W., Els, T., and Hennerici, M. (1992) Comparison of flow disturbances in small carotid atheroma using a multi-gate pulsed Doppler system and Doppler color flow imaging. *Ultrasound in Med. & Biol.*,**18**, 11-18.

Ten Cate, F. J., Feinstein, E. B., Zverev, W., Meckbaum, S., Fainstein, M., Shah, M., Steinke, W., Hennerici, M., Rautenberg, W., and Mohr, J. P. (1992) Symptomatic and asymptomatic high-grade carotid stenoses in Doppler color-flow imaging. *Neurology*,**42**, 131-138.

Thiel, A., Russ, W., Kaps, M., Naeck, G. P., and Hempelmann, G. (1988) Sterpetti, A. V., Schultz, R. D., Feldhaus, R. J., Davenport, K. L., Richardson, M., Farina, C., and Hunter, W. J. (1988) Ultrasonographic features of carotid plaque and the risk of subsequent neurologic deficits. *Surgery*,**104**, 652-660.

Thompson, J. E. (1979) Complications of carotid endarterectomy and their Stump, D. A., Stein, C. S., Tegeler, C. H., Hitchings, L. P., Hager, R., Eicke, M., and Burke, G. (1991) Validity and reliability of an ultrasound device for detecting carotid emboli. *J. Neuroimag.*,**1**, 18-22.

Timmerman, S., Schneider, A., Joseph, P., Fu, P., and Harrison, M. J. (1988) Impairment of cerebral function following cardiac and other Svartling, N. (1988) Detection of embolized material in the right atrium during cementation in hip arthroplasty. *Acta Anaesthesiol. Scand.*,**32**, 203-208.

Tunick, P. A. and Kronzon, I. (1990) Protruding atherosclerotic plaque in the aortic Swank, R. L. (1961) Alteration of blood on storage: measurement of adhesiveness of 'aging' platelets and leukocytes and their removal by filtration. *N. Engl. J. Med.*,**26**, 728.

Tunick, P. A. and Kronzon, I. (1983) Protruding atheromas in the thoracic aorta. A Taylor, K. M. (1986) Pathophysiology of brain damage during open-heart surgery. *Tex. Heart. Inst. J.*,**13**, 91-96.

Teague, S. M. and Sharma, M. K. (1991) Detection of paradoxical cerebral echo contrast embolization by transcranial Doppler ultrasound. *Stroke*,**22**, 740-745.

Circulation,**34** (Suppl.D), II-692

Tegeler, C. H. and Eicke, M. (1993). Physics and principles of transcranial Doppler ultrasonography. *Transcranial Doppler ultrasonography*, Mosby, St. Louis. 5-27.

of liver with and without particulate contrast agents. *Ultrasound in Med. & Biol.*,**17**,

Tegeler, C. H., Hitchings, L. P., Eicke, M., and et al., (1990) Microemboli detection in stroke associated with atrial fibrillation (abstract). *J. Cardiovasc. Tech.*,**9**, 283-284.

Ten Cate, F. J., Feinstein, S. B., Zwene, W., Meebaum, S., Fishbein, M., Shah, M., and Corday, E. (1984) Two-dimensional contrast echocardiography. II. Transpulmonary studies. *J. Am. Coll. Cardiol.*,**3**, 21-27.

Thiel, A., Russ, W., Kaps, M., Marck, G. P., and Hempelmann, G. (1988) Transcranial Doppler sonography monitoring during aortocoronary bypass operations. *Anaesthesist*,**37**, 256-260.

Thompson, J. E. (1979) Complications of carotid endarterectomy and their prevention. *World J. Surg.*,**3**, 155-165.

Treasure, T., Smith, P. L., Newman, S., Schneidan, A., Joseph, P., Eu, P., and Harrison, M. J. (1989) Impairment of cerebral function following cardiac and other major surgery. *Eur. J. Cardiothorac. Surg.*,**3**, 216-221.

Tunick, P. A. and Kronzon, I. (1990) Protruding atherosclerotic plaque in the aortic arch of patients with systemic embolization: A new finding seen by transesophageal echocardiography. *Am. Heart J.*,**120**, 658-660.

Tunick, P. A. and Kronzon, I. (1993) Protruding atheromas in the thoracic aorta: A newly recognized source of cerebral and systemic embolization. *Echocardiography*,**10**, 419-428.

Turakhia, A. K., Teague, S. M., Lawler, B., and Harris, J. (1991) Hemorrhologic determinants of the echocardiographic 'smoke' phenomenon: an in vitro simulation. *Circulation*,**84 (Suppl.II)**, II-692.

Tuthill, T., Baggs, R., Violante, M., and Parker, K. (1991) Ultrasound properties of liver with and without particulate contrast agents. *Ultrasound in Med. & Biol.*,**17**, 231-237.

van der Linden, J. and Casimir-Ahn, H. (1991) When do cerebral emboli appear during open heart operations? A transcranial Doppler study. *Ann. Thorac. Surg.*,**51**, 237-241.

Vattiyam, H. M., Shu, M. C. S., and Rittgers, S. E. (1992) Quantification of Doppler color flow images from a stenosed carotid artery model. *Ultrasound in Med. & Biol.*,**18**, 195-203.

Vik-Mo, H., Todnem, K., Flling, M., and Rosland, G. A. (1986) Transient visual disturbance during cardiac catheterization with angiography. *Cathet. Cardiovasc. Diagn.*,**12**, 1-4.

Vuilliomenet, A., Bertel, O., and Kaufmann, U. (1992) Spontaneous left atrial echo contrast in transesophageal echocardiography. *Schweizerische Medizinische Wochenschrift*,**122**, 549-553.

Wareing, T. H., DailaRoman, V. G., Barzilai, B., Murphy, S. F., and Kouchoukos, N. T. (1992) Management of the severely atherosclerotic ascending aorta during cardiac operations: A strategy for detection and treatment. *J. Thorac. Cardiovasc. Surg.*,**103**, 453-462.

Watanabe, T., Shimasaki, T., Kuraoka, S., Abe, H., Iijima, Y., and Washio, M. (1992) Retrograde cerebral perfusion against massive air embolism during cardiopulmonary bypass (letter). *J. Thorac. Cardiovasc. Surg.*,**104**, 532-533.

Webster, M. W. I., Smith, H. J., Sharpe, D. N., Chancellor, A. M., Swift, D. L., Bass, N. M., and Glasgow, G. L. (1988) Patent foramen ovale in young stroke patients. *Lancet*,**2**, 11-12.

Weinfeld, F. D. (1981) National survey of stroke. *Stroke*,**12**(suppl. I), I1-I15.

Wells, P. N. T.(1983). *Ultrasonics in Clinical Diagnosis*, Churchill Livingstone ,
Edinburgh, U.K., 3rd edition, 1-12.

Wenda, K., Ritter, G., Ahlers, J., and von.Issendorff, W. D. (1990) Detection and
effects of bone marrow intravasations in operations in the area of the femoral marrow
cavity. *Unfallchirurg*,**93**, 56-61.

Wessler, S. and Stehbens, W. E.(1971). *Thrombosis. In thrombosis and bleeding
disorders*, Academic Press, New York, 1st edition, 489.

Wilson, B., Shung, K. K., Hete, B., Levene, H., and Barnhart, J. L. (1993) A
feasibility study on quantitating myocardial perfusion with albunex, an ultrasonic
contrast agent. *Ultrasound in Med. & Biol.*,**19**, 181-191.

Winter, W. J. (1957) Atheromatous emboli: A cause of cerebral infarction. Report of
two cases. *Arch. Pathol.*,**64**, 189-196.

Wolf, P. A., Kannel, W., McGee, D. L., Meeks, S. L., Bharucha, N. E., and
McNamara, P. M. (1983) Duration of atrial fibrillation and imminence of stroke: The
Framingham Study. *Stroke*,**14**, 664-667.

Wright, E. S., Sarkozy, E., Dobell, A. R. C., and Murphy, D. R. (1963) Fat
globulemia in extracorporeal circulation. *Circulation*,**53**, 500.

Yamaguchi, T. (1980) Turbulence intensity measured in the center of canine
ascending aorta with a hot-film anemometer. *J. Tokyo Women's Med. Coll.*,**50**, 177-
190.

Yasaka, M., Yamaguchi, T., Oita, J., Sawada, T., Shichiri, M., and Omae, T. (1993)
Clinical features of recurrent embolization in acute cardioembolic stroke. *Stroke*,**24**,
1681-1685.